Regulation of sterol regulatory element binding protein (SREBP) by the PI3-kinase/Akt pathway and its role in the regulation of cell growth

Thomas Porstmann

A thesis submitted toward the degree of

Doctor of Philosophy

September 2007

CANCER RESEARCH UK

Gene Expression Analysis Laboratory,
Cancer Research UK – London Research Institute,
44 Lincoln's Inn Fields, London.

UCL

Department of Biochemistry and Molecular Biology,
University College London,
Gower Street, London.

ProQuest LLC
789 East Eisenhower Parkway
P.O. Box 1346
Ann Arbor, MI 48106-1346

Declaration

I, Thomas Porstmann, confirm that the work presented in this thesis is my own. Where information has been derived from other sources, I confirm that this has been indicated in this thesis.

London, September 2007

Abstract

Protein kinase B (PKB/Akt) is a central component of intracellular signaling pathways. It becomes activated downstream of growth factor receptors and has been implicated in cell growth, proliferation and protection from apoptosis. Akt is also a mediator of metabolic insulin action, and stimulates glucose uptake, glycogen synthesis and lipogenesis.

Activation of Akt resulted in induction of expression of several enzymes involved in cholesterol and fatty acid biosynthesis. These genes are transcriptional targets of the family of sterol regulatory element-binding proteins (SREBP). Induction of fatty acid synthase and HMG-CoA synthase, two key enzymes of the sterol and fatty acid biosynthesis pathway, by Akt requires SREBP. In addition, activation of Akt results in rapid accumulation of mature SREBP1 in the nucleus. This process was independent of activation of glycogen synthase kinase 3 (GSK3) but required active complex 1 of the mammalian target of rapamycin (mTOR/TORC1). Analysis of cellular metabolites by NMR revealed that induction of glucose and amino acid uptake, lactate production as well as fatty acid and phosphoglyceride biosynthesis by Akt also requires TORC1 activity. Thus it can be postulated that induction of expression of lipogenic genes through activation of SREBP is part of an anabolic response to activation of the PI3K/Akt/mTOR pathway and may be required for the induction of lipid biosynthesis during cell growth and proliferation.

The PI3K/Akt pathway has been implicated in regulation of cell and organ size in *Drosophila melanogaster*. Several transgenic fly lines carrying an RNAi construct targeting dSREBP expression were generated. Silencing of dSREBP resulted in a significant developmental delay as well as a profound loss of viability. Tissue specific silencing of dSREBP in the wing resulted in a reduction in cell and organ size suggesting that activation of dSREBP by the PI3K/Akt pathway could be involved in cell growth control in flies.

Acknowledgements

I am very thankful to my supervisor Almut Schulze for giving me the opportunity to work in her laboratory, for her excellent scientific training and inspiring enthusiasm. Almut has always assisted me both scientifically and non-scientifically, for which I am very grateful.

I would like to thank Beatrice Griffiths for her technical and intellectual advice as well as for her patience and support during writing the thesis. Thanks to Oona Delpuesh and Claudio Santos for scientific discussions and making my research a much more enjoyable experience. Additional thanks to Claudio for critical reading of my thesis.

I would like to thank Julian Downward for his support and advice and the opportunity to join his lab-meetings and retreats. Thanks to all the past and present members of the Signal Transduction Laboratory for scientific and social contribution, especially Megan Cully for a very fruitful fly collaboration and critical reading of my thesis and Kristina Klupsch for her friendship.

I would also like to thank my co-supervisors Richard Treisman and Ian Tomlinson for very informative and critical committee meetings.

Special thanks to Sally Leevers and Nic Tapon and their past and present lab members, in particular Steven Marygold, for their introduction into the fly world and keeping my fly project running. Many thanks to Y.-L. Chung and J.R. Griffiths (CRUK Magnetic Resonance Group, St. Georges Hospital and Molecular Imaging, CRUK Cambridge Research Institute) for a very successful collabarotion. Furthermore, I would like to thank Subham Basu (Barts Hospital, CRUK) for providing the RPE myrAkt-ER and U2OS myrAkt-ER cell lines and Hugo Stocker (ETH Zurich, Switzerland) for providing me with fly stocks.

Many thanks to the staff of the excellent research services of the Equipment Park, the Bioinformatics group, the FACS Laboratory, the Protein Analysis Laboratory and Fly Facility. I thank Cancer Research UK for providing funding and an optimal research environment.

Finally, I would like to thank my family, for quiescent but very important support wherever I am.

Table of Contents

List of Figures

List of Tables

Abbreviations

AA	arachidonic acid (LXR antagonist)
ACC	acetyl-CoA carboxylase
AEL	after egg laying
AICAR	AMPK agonist
ALLN	N-Acetyl-Leu-Leu-Nle-CHO
AMPK	AMP-activated kinase
APS	ammonium persulphate
ATP	adenosine-5-triphosphate
ACL	ATP-citrate lyase
BCR domain	breakpoint cluster region homology domain
bHLH-Zip	basic helix-loop-helix-leucine zipper
bp	base pair(s)
ß-ME	ß-mercaptoethanol
BSA	bovine serum albumin
bZIP	basic leucine zipper
cpm	counts per minute
cDNA	complementary DNA
CPRG	Chlorophenolred-ß-D-galactopyranoside
C-terminus	carboxy-terminus
CTMP	carboxy-terminal modulator protein
CHX	cycloheximide
da-GAL4	daughterless-GAL4
DMEM	Dulbecco's modified Eagle medium
DMSO	dimethyl sulphoxide
DNA	desoxyribonucleic acid
dNTP	desoxyribonucleosidtriphosphate
Dpp	decapentaplegic
dsRNA	double-stranded RNA
dsRNAi	dsRNA-mediated interference (of gene expression)
DTT	dithiothreitol
eIF2α	eukaryotic translation initiation factor 2α
4E-BP	4E-binding protein
ECL	enhanced chemiluminescence
E.coli	Escherichia coli
EDTA	ethylenediaminetetraacetic acid

EGF	epidermal growth factor
EGFR	EGF receptor
en-GAL4	engrailed-GAL4
ER	endoplasmic reticulum
ERK	extracellular signal-regulated kinase
LY294002	PI3K inhibitor
FA	fatty acid
FAS	fatty acid synthase
FACS	fluorescence activated cell sorting
FCS	foetal calfe serum
F12	Ham's nutrient mixture
GAPDH	glyceraldehyde-3-phosphate dehydrogenase
GSK3	glycogen synthase kinase-3
HEPES	N-[2-hydroxyethyl]piperazine-N-[2-ethanesulphonic acid]
HK	hexokinase
HMGR	3-hydroxy-3-methylglutaryl coenzyme A reductase
HMGS	3-hydroxy-3-methylglutaryl coenzyme A synthase
HRP	horseradish peroxidase
h / hrs	hours
4-OHT	4-hydroxytamoxifen
IGF-1	insulin-like growth factor-1
IgG	immunoglobulin G
INSIG	insulin-induced gene
IRS1/2	insulin receptor substrate
kb	kilobase
kDa	kilo Dalton
LDL	low density lipoprotein
LPDS	lipoprotein deficient serum
LXR	liver X-activated receptor
MAPK	mitogen-activated protein kinase
MEF	mouse embryonic fibroblast
mins	minutes
N-terminus	amino-terminus
OD	optical density
ORF	open reading frame
PBS	phosphate-buffered saline
PCR	polymerase chain reaction
PD98059	MEK inhibitor

PFK2	phospho-fructo kinase 2
PDK1	3-phosphoinositide-dependent protein kinase-1
PH-domain	pleckstrin homology domain
PI3K	phosphoinositide-3-kinase
PKB	protein kinase B
PI	phosphatidylinositol
PtdIns(3,4)P2/PIP2	phosphatidylinositol-3,4-bisphosphate
PtdIns(3,4,5)P3/PIP3	phosphatidylinositol-3,4,5-trisphosphate
PC	phosphatidylcholine
PE	phosphatidylethanolamine
PS	phosphatidylserine
PTEN	phosphatase and tensin homologue deleted on chromosome ten
PUFA	polyunsaturated fatty acid
q-rtPCR	semiquantitative real-time PCR
siRNA	small interference RNA
RBD	Ras binding domain
RPE	retinal pigment epithelial cell line
rpm	rotations per minute
rpS6	ribosomal protein S6
RT	room temperature
rt-qPCR	reverse transcriptase quantitative PCR
RTK	receptor tyrosine kinase
RXR	retinoic acid receptor
S1P and S2P	site 1 and site 2 protease
SCAP	SREBP cleavage-activating protein
SD	standard deviation
SEM	standard error of the mean
SDS	sodium dodecyl sulphate
SDS-PAGE	SDS-polyacrylamide gel electrophoresis
SGK	serum and glucocorticoid activated kinase
SH2 domain	SRC homology 2 domain
SH3 domain	SRC homology 3 domain
SRE	sterol regulatory element
SREBP	sterol regulatory element-binding protein
CA-SREBP	constitutive active SREBP
DN-SREBP	dominant negative SREBP
flSREBP	full length SREBP
mSREBP	mature SREBP

T0901317	LXR agonist
TCA cycle	tricarboxylic acid cycle
TEMED	N,N,N,N-tetramethylenediamine
Tm	melting Temperature
TOP	5' tract of oligopyrimidine
TORC1	target of rapamycin complex 1 (contains raptor)
TORC2	rapamycin insensitive complex 2 (contains rictor)
TOS	TOR signal sequence
TRIS	tris[hydroxymethyl]aminomethane
TSS	transcriptional start site
UO126	MEK1/2 inhibitor
UPS	ubiquitin proteasome sytsem
UTR	untranslated region
U2OS	osteosarcoma cell line
WT /wt	wild type

1 Chapter 1: Introduction

1.1 Signalling

Cells coordinate cell growth, metabolism and proliferation in response to environmental cues including growth factor availability. The Ras/PI3K/mTOR signalling pathways are among the most frequently targeted pathways in all sporadic cancer and when mutated, drive cell growth independently of environmental cues. Growth factors acting through receptor tyrosine kinases (RTKs), which then activate the key signalling-transducer, the small GTPase Ras (see chapter 1.2) and the phosphatidylinositol-3-OH kinsase (PI3K) (see chapter 1.3). Both proteins activate a number of downstream effectors such as Raf and protein kinase B/Akt (see chapter 1.4). One effector critical for cell growth is the mammalian target of rapamycin (mTOR) kinase (see chapter 1.5). mTOR is activated by both Ras and PI3K, but its activity is also controlled by the availability of nutrients. Several tumour suppressors have been identified to attenuate Ras/PI3K/mTOR signalling. The phosphatase and tensin homologue (PTEN) (see chapter 1.3.3) terminates PI3K signalling, while under nutrient-poor conditions the tuberous sclerosis complex 1 (TSC1, also know as hamartin), TSC2 (tuberin) or the protein kinase 11 (LKB1) inhibit mTOR activity (see chapter 1.5.1). This network ensures that cell growth and proliferation only take place under favourable environmental conditions (Luo et al., 2003; Shaw and Cantley, 2006; Wullschleger et al., 2006).

1.2 Ras

Ras family proteins are small membrane-bound proteins that belong to the large superfamily of low-molecular-weight guanine nucleotide-binding proteins (small GTPases). They act as a molecular switch linking receptor tyrosine kinase (RTK) activation to downstream signalling. Small GTPases can be divided into five families that are important for different cellular processes. Members of the Rho family control gene expression and modulate the cytoskeleton while the Rab and the Sar1/Arf families regulate intracellular vesicle transport. Proteins of the Ras family have been shown to be important in cell growth, proliferation, differentiation, apoptosis, cell-cell contact and cell motility (Takai et al., 2001).

The Ras gene was first discovered as a 21 kDa protein encoded by the oncogene of rat sarcoma viruses. Searches in the human genome identified H-ras as the cellular homologue. The four Ras isoforms are H-Ras, N-Ras, K-Ras4A and K-Ras4B, which are widely expressed and show tissue specific expression profiles (Lowy and Willumsen, 1993; Schubbert et al., 2007). Ras

proteins undergo post-translational modifications, which result in localisation to the plasma membrane. A C-terminal C-A-A-X motif (C=Cysteine, A=aliphatic, X=any amino acid) becomes farnesylated, the initial step in a series of alterations (Basso et al., 2006; Hancock et al., 1989; Sebti, 2003).

The diverse biological effects of Ras proteins place them at a central position among many signal transduction pathways. The importance of Ras proteins as key mediators of cellular growth control makes constitutively activated Ras such a potent transforming oncogene. Ras has been found to be mutational activated in about 30% of all malignancies (Malumbres and Barbacid, 2003).

1.2.1 Ras signaling pathway

Ras activation has been demonstrated in response to stimulation with a number of growth factors like platelet-derived growth factor (PDGF) (Arvidsson et al., 1994), nerve growth factor (NGF) (Basu et al., 1994), hepatocyte growth factor (HGF) (Graziani et al., 1993), insulin (Burgering et al., 1991) and epidermal growth factor (EGF) (Buday and Downward, 1993).

Epidermal Growth Factor (EGF) mediated Ras activation is the best-studied activation mechanism and will be used as a model. Ligand binding to the EGF receptor (EGFR) induces dimerisation and auto-phosphorylation on tyrosine residues, which leads to the recruitment of the adaptor protein Shc to the intracellular domain of EGFR. SHC is activated by tyrosine phosphorylation, which enables the binding of growth-factor-receptor-bound protein 2 (GRB2) via its SH2 (src-homology) domain. The SHC-GRB2 complex interacts via the SH3 domain of GRB2 with a proline-rich region of son of sevenless (SOS), which results in recruitment of SOS to the plasma membrane. (Blaikie et al., 1994; Harmer and DeFranco, 1997; Sasaoka et al., 1994). (SH2 domains recognize phosphorylated tyrosine residues while SH3-domains have a high affinity towards proline rich motifs, which exist in proteins such as SOS, Ruk and Cbl.)

SOS has been identified as a guanine nucleotide exchange factor (GEF) for Ras (Li et al., 1993). GEFs catalyse the exchange of GDP with GTP and convert Ras from an inactive to an active form (Boriack-Sjodin et al., 1998; Margarit et al., 2003). Conversely, to transfer Ras into its inactive state GTPase activity of Ras can be activated by GTPase-activating-proteins (Ras-GAPs), including p120GAP and neurofibromin 1 (NF1) (Martin et al., 1990; Scheffzek et al., 1997; Takai et al., 2001).

1.2.2 Ras downstream effectors

GTP-bound Ras activates more than 20 effector enzymes; including the serine/threonine kinases Raf, the lipid kinases, phosphoinositide 3-kinases (PI3K), the Rac exchange factor Tiam1, phosholipase Cε and the guanine nucleotide exchange factor Ral-GDS (Mitin et al., 2005; Repasky et al., 2004).

Among the Ras effector pathways, the Raf-MEK-ERK cascade is the best characterised. Activated Raf phosphorylates and thus activates the dual specificity kinases MEK1 and MEK2, which phosphorylate and activate MAP kinases ERK1 and ERK2 (Kolch, 2000). ERK1 and ERK2 translocate to the nucleus where they activate a number of transcription factors, including Ets family transcription factors, SRF, ATF2 and Jun (Treisman, 1996). Among the genes regulated by these transcription factors are key cell-regulatory proteins, such as cyclin D1, promoting cell cycle progression (Pruitt and Der, 2001). Activation of the ERK1/2 pathway also leads to inactivation of TSC1/TSC2, as a result of phosphorylation of TSC2 (Ma et al., 2005b; Roux et al., 2004). Inhibition of TSC2 leads to activation of TORC1, thereby ERK1/2 may stimulate protein translation and ribosome biosynthesis (Mayer and Grummt, 2006).

Ras-GTP has also been shown to interact with the p110 catalytic subunit of class I PI3K (Rodriguez-Viciana et al., 1994). PI3K is a lipid kinase that phosphorylates the 3'-position of phosphoinositides resulting in the generation of the second messenger PIP3 (see chapter 1.3). PIP3 mediates activation of downstream kinases such as Akt/PKB and PDK1 (Bader et al., 2005; Downward, 2004). The Ras-p110 interaction itself is not sufficient for PI3K membrane localization (Suire et al., 2002), suggesting that RAS-dependent activation of PI3K may necessitate active growth factor receptor signalling. The *in vivo* function of Ras binding to PI3K p110α has recently been described to be required for normal growth factor signalling and oncogenic Ras-mediated tumorigenesis in mice (Gupta et al., 2007).

Ras induced activation of Ral is thought to be involved in the control of vesicle transport and cell morphology as well as to have a fundamental function in Ras-driven transformation of human cells (Lim et al., 2005). A model of the Ras pathway is illustrated in Figure 1-1.

1.3 PI3K signalling pathway

The phosphatidylinositol-3-kinases (PI3K) include a large and complex family, which is involved in various cellular processes such as cell growth, proliferation, survival, cell motility and metabolism (Engelman et al., 2006).

PI3Ks are heterodimeric lipid kinases composed of a regulatory and catalytic subunit that catalyze the phosphorylation of inositol-containing lipids at the 3'-hydroxyposition. The products (phosphatidylinositol-3,4-bisphosphate and phosphatidylinositol-3,4,5-trisphosphate) are second messengers that interact with pleckstrin homology domain (PH-domain) containing proteins and mediate downstream functions of PI3Ks.

1.3.1 Classification of PI3K family members

The PI3K family contains three classes with multiple isoforms with different substrate specificities and sequence homology (Cantley, 2002). The class 1 PI3Ks consists of two subgroups, 1A and 1B. Class 1A PI3Ks, consisting of PI3Kα and β, are activated by growth factor receptor tyrosine kinases (RTK), whereby class1B PI3Ks are activated by G-protein-coupled receptors (GPCRs) (Katso et al., 2001). Class I PI3Ks are the best-characterised isoforms, which regulate cell growth, glucose homeostasis, proliferation and migration.

Three isoforms are found in mammalian class 2 PI3Ks, PI3KC2 α, β and γ (Domin et al., 1997; Ono et al., 1998; Rozycka et al., 1998). PI3KC2β contributes to stem cell factor (SCF) stimulated protein kinase B (PKB) activity (Arcaro et al., 2002), while PI3KC2α regulates clathrin-mediated membrane trafficking and receptor internalization (Gaidarov et al., 2001).

Class 3 PI3Ks consist of a single member, vacuolar protein-sorting defective 34 (hVps34) protein. hVps34 was originally identified in regulating endocytosis and vesicular trafficking (Simonsen et al., 2001). Recently, hVps34 has been shown to be required for insulin and nutrient-mediated activation of the mTOR (mammalian target of rapamycin) targets S6K1 (S6 kinase 1) and 4EBP1, indicating that hVps34 might also be involved in cell growth control (Byfield et al., 2005; Nobukuni et al., 2005). In response to nutrient starvation, Vps34 is required for the induction of autophagy (Eskelinen et al., 2002; Kihara et al., 2001).

Since the specific function of class 2 and class 3 PI3Ks are less well characterized, only the cellular importance of class 1 PI3K to the cell and in oncogenesis will be discussed in more detail. It has been shown that the PI3K inhibitors wortmannin and LY294002 inhibit class 1 and class 3 and to a lesser extent class 2 PI3Ks (Stein, 2001).

1.3.2 Class 1 PI3K and signal transduction

The class IA heterodimeric enzymes consist of a regulatory subunit p85 and a catalytic subunit p110. There are three mammalian p110 proteins, p110α, 110ß and 110δ. All consist of a catalytic domain, a p85-binding domain, a Ras binding domain (RBD) and a C2 domain that may be essential for membrane anchoring. There are also three isoforms of the p85 regulatory subunit, p85α, p85ß and p85γ. p85 proteins contain two SH2 domains, an inter-SH2 domain that binds constitutively to the p110 subunit, an SH3 domain and a BCR (breakpoint cluster region)-homology domain that negatively regulate the catalytic activity of p110. These domains allow indirect interaction between receptor tyrosine kinases (RTKs) and PI3K through intermediate phosphoproteins, i.e. the insulin receptor substrates IRS1/IRS2. Phosphorylated tyrosine residues on RTKs interact with the SH2 domain of the p85 subunit and cause recruitment of the inactive cytoplasmic p110-p85 complex to the plasma membrane. The interaction between p85 and RTKs reduces the inhibitory effect of p85 on p110 (Yu et al., 1998) and brings the p110 catalytic subunit into close proximity to its phospholipid substrate in the membrane. Both insulin and insulin growth factor 1 (IGF1) receptors use the insulin receptor substrate (IRS) family of adaptor molecules to engage class IA PI3Ks, which is the canonical pathway of PI3K activation. IRS proteins also relay signals from growth factor receptors to Ras, resulting in pathway activation (Pawson and Nash, 2003). Interestingly, the p110ß isoform can also be regulated by heterotrimeric G proteins, indicating that the class 1 p110ß isoform might integrate signals from RTKs and GPRCs (Engelman et al., 2006). PI3Ks can also be activated by oncogenic Ras via the RBD in the p110 subunit (Rodriguez-Viciana et al., 1994).

In contrast to the class 1A activation by tyrosine-phosphorylated RTKs, stimulation of G-protein-coupled receptors (GPCR) transmit signals to the class 1B p110γ/p101-PI3Kγ. The Gßγ subunit recruits PI3Kγ from the cytosol to the membrane by interaction with its non-catalytic p110γ subunit and further direct stimulation of Gßγ with the catalytic subunit p110γ contributes to activation of PI3Kγ. Recently, two additional p110 homologue regulatory subunits p84 and p87PIKAP (Suire et al., 2005; Voigt et al., 2006), were described.

1.3.3 PTEN, a negative regulator of PI3K

PTEN (phosphatase and tensin homologue) is a dual-specifity phosphatase that has activity towards lipid and protein substrates (Gu et al., 1999; Tamura et al., 1998). The main physiological lipid substrate of PTEN is PtdIns(3,4,5)P3 (PIP3) (Haas-Kogan et al., 1998; Maehama and Dixon, 1998; Wu et al., 1998). PTEN controls the activity of Akt by limiting the lipid substrate PtdIns(3,4,5)P3 necessary for its activation. Mutation or deletion of PTEN leads

to the loss of reduced lipid phosphatase activity and allows unregulated Akt activity and uncontrolled cell proliferation (Ali et al., 1999). Mice with a homozygous deletion of PTEN die during embryogenesis (day E7.5-8.5) and cell lines from these mice show increased Akt activation. Heterozygous PTEN knock-out mice show increased tumour formation in different tissues (Di Cristofano et al., 1998; Myers et al., 1998; Stambolic et al., 1998).

1.3.4 Akt-independent pathways downstream of PI3K

In addition to regulation of Akt, which will be discussed in chapter 1.4, PI3K activation leads to induction of several downstream effectors (outlined in Figure 1-2). Many of these, such as the small GTPases CDC42 and RAC1are involved in tumourigenesis (Jiang et al., 2000; Liliental et al., 2000; Welch et al., 1998) can be activated by PIP3-sensitive GEFs, such as VAV1 (Han et al., 1998) and PREX1 (Welch et al., 2002). However, CDC42 activation can also occur in the absence of PI3K catalytic activity through direct association with p85 (Jimenez et al., 2000). RAC1 and CDC42, together with PI3K, are involved in cell motility and polarity by controlling cytoskeleton dynamics (Van Haastert and Devreotes, 2004) and there is evidence that both have transforming capacity in fibroblasts. It is possible that activation of RAC1 and CDC42 by PI3K provides a link between PTEN loss and tumour invasion (Liliental et al., 2000).

Although the serum and glucocorticoid-inducible kinase (SGK) has a high homology to Akt and may have an overlapping role in the induction of survival pathways (Brunet et al., 2001b), the activation mechanism by PI3K differs from that of Akt. SGKs are serine/threonine kinases that do not contain a PH-domain, which is necessary for recruitment of Akt to the plasma membrane. SGKs are activated by PDK1 in a PI3K-dependent manner (Park et al., 1999).

The atypical PKCλ/ξ isoform are the only PKC, which are activated by insulin. Activation of PKCλ/ξ requires PI3K input and involves phosphorylation of threonine 410 by PDK1 (Bandyopadhyay et al., 1997; Standaert et al., 2001). Mouse embryonic stem cells and adipocytes deficient in PKCλ/ξ show impaired insulin-mediated glucose transport. This can be rescued by over-expressed PKCλ/ξ (Bandyopadhyay et al., 2004).

1.4 Akt/PKB

Akt, also known as protein kinase B (PKB) belongs to the AGC (protein kinase A (PKA)/ protein kinase G/ protein kinase C-like) family of protein kinases. All AGC kinase family members show extensive homology within their kinase domain.

Akt was first identified as the cellular homologue of the transforming oncogene v-Akt (AKT8) in a mouse T-cell lymphoma retrovirus (Staal, 1987). Three closely related isoforms of PKB/Akt have been identified in the mammalian genome: Akt1/PKBα, Akt2/PKBβ and Akt3/PKBγ (Bellacosa et al., 1991; Coffer and Woodgett, 1991; Jones et al., 1991), which all contain a highly conserved kinase domain.

Growth factors, cytokines and other growth promoting stimuli activate PI3K to initiate Akt signalling. Akt contributes to diverse cellular processes including cell proliferation, survival, metabolism and growth (Manning and Cantley, 2007). The physiological functions for the three isoforms have been determined in mouse knockout models. Akt1 is important in development, Akt2 in glucose homeostasis and Akt3 in brain development (Dummler and Hemmings, 2007).

1.3.1 Activation and regulation of Akt

Akt are serine/threonine kinases with a molecular weight of 57 kDa. They contain an N-terminal pleckstrin-homology (PH) domain that interacts with the lipid second messenger phosphatidylinositol-3,4,5-trisphosphate (PIP_3). In response to PI3K activation, PI3Ks generate PIP_3, which leads to plasma membrane recruitment of inactive Akt (Andjelkovic et al., 1997; Bellacosa et al., 1998). This translocation brings it into close proximity to another PH domain-containing protein kinase, PDK1 (3-phosphoinositide-dependent kinase). PDK1 phosphorylates Akt on a threonine residue within the protein kinase T-loop (T308 in Akt1) (Alessi et al., 1997). This phosphorylation results in conformational changes and facilitates access of the modified T-loop to ATP and substrates (Stephens et al., 1998; Vanhaesebroeck and Alessi, 2000). For Akt to become fully activated, a second phosphorylation step has to occur on a serine residue that is located in a hydrophobic motif proximal to the carboxyl terminus (S473 in Akt1). Several kinases have been implicated in phosphorylating Akt S473 such as ATM, DNA-PK and ILK (Woodgett, 2005). The mTOR-rictor kinase complex 2 (TORC2) has been shown to phosphorylate S473 in Akt (Hresko and Mueckler, 2005; Sarbassov et al., 2005). However, residual S473 phosphorylation was detected in TORC2 deficent mice (Shiota et al., 2006), indicating that TORC2 is not the only S473 kinase. Although both phosphorylations act in synergy to fully activate the protein kinase, these two residues are phosphorylated independently (Jacinto et al., 2006; Williams et al., 2000). Upon S473 phosphorylation, Akt can shuttle to different cellular compartments such as the nucleus (Jacinto et al., 2006). Therefore phosphorylation status and cellular localization might determine Akt substrate specificity.

Akt can be inactivated by the phosphatase PP2A (Brazil and Hemmings, 2001), which dephosphorylates threonine and serine and returns Akt to its inactive conformation. The PH domain leucine-rich repeat protein phosphatases (PHLPPs) selectively dephosphorylate serine 473 and terminate Akt signalling, and this may affect its target specificity (Brognard et al., 2007; Gao et al., 2005). Two other negative modulators act via binding to Akt. The carboxy-terminal modulator protein (CTMP) (Maira et al., 2001) and TRB3 (Du et al., 2003), a mammalian homologue of Drosophila tribbles, both prevent phosphorylation of Akt and thus block downstream signalling.

1.4.1 Survival and proliferation

Peptide library screening has been used to determine the optimal Akt peptide substrate motif, which has a serine as the phospho-acceptor site, a bulky hydrophobic amino acid at +1, a serine or threonine at the -2 position and two highly conserved arginine residues at -5 and -3 (Hutti et al., 2004; Obata et al., 2000). The consensus sequence for Akt phosphorylation consists of R-X-R-X-X-S/T [using the one-letter amino-acid code, where X represents any amino acid] (Chan et al., 1999). Over 100 Akt substrates have been reported so far, of which approximately 25% do not display the consensus sequence (Manning and Cantley, 2007). The quantity and variety of Akt target proteins explain the biological diversity in response to Akt activation (Figure 1-3).

Among the first Akt targets to be identified were glycogen synthase kinase-3α (GSK3α) and -3ß (GSK3β). Akt phosphorylates GSK3α on serine 21 and GSK3β on serine 9. Phosphorylation by Akt results in inhibition of their kinase activity (Cross et al., 1995). The role of GSK3 in proliferation and regulation of apoptosis can be explained by its substrates (Cohen and Frame, 2001). GSK3 phosphorylates and inhibits the prosurvival Bcl-2 family member MCL-1 (Maurer et al., 2006) and regulates the stability of a number of proteins including cyclin D1, Jun and c-myc (Diehl et al., 1998; Wei et al., 2005; Yeh et al., 2004). GSK3β dependent phosphorylation results in degradation of cyclin D1 (Diehl et al., 1998) and inhibition of GSK3 by Akt allows the accumulation of cyclin D1, which is required for G1/S transition.

Programmed cell death (apoptosis) is a normal cellular function that controls excessive proliferation by eliminating cells. Akt protects cell from apoptosis by different mechanisms. It directly phosphorylates several components of the cell death machinery. Akt phosphorylates the proapoptotic Bcl-2 family member BAD, which causes binding of 14-3-3 proteins and sequesters Bad away from its target proteins (Datta et al., 2000). BAD binds and inhibits the prosurvival protein BCL_{XL} (Datta et al., 1997; del Peso et al., 1997). Akt also phosphorylates and inhibits the protease caspase-9, which is a key effector of the apoptotic process (Cardone et

al., 1998). Akt can protect cells from oxidative stress-induced cell death through inhibiting the apoptosis signal-regulating kinase 1 (ASK1) (Downward, 2004; Nagai et al., 2007).

One of the best-characterised Akt targets are the members of the O subfamily of forkhead-domain containing transcription factors (FoxO) (Tran et al., 2003). FoxO proteins control transcription of target genes involved in apoptosis, cell cycle, stress tolerance and metabolism (van der Horst and Burgering, 2007). They contain three conserved Akt phsophorylation sites and phosphorylation of theses sites creates a binding site for 14-3-3 proteins. Binding of 14-3-3 causes nuclear export and hence functional inactivation of the FoxO proteins (Brunet et al., 1999; Kops et al., 1999). FOXO regulated genes include several pro-apoptotic factors such as the BCL-2 family member BIM and FAS ligand (Brunet et al., 1999; Dijkers et al., 2002). FoxOs induce expression of the cyclin-dependent kinase (CDK) inhibitor $p27^{Kip1}$, which inhibits cell-cycle progression (Medema et al., 2000), and suppress expression of the cyclins D1 and D2, which drive progression from G_1 to S phase (Schmidt et al., 2002).

Other transcription factors that are regulated by Akt are CREB and NF-κB (Pugazhenthi et al., 1999; Romashkova and Makarov, 1999). However, the *in vivo* evidence for their regulation is limited. *In vitro*, Akt activates NF-κB by phosphorylation and activation of IκB kinase (IKK). IKK induces degradation of the NF-κB inhibitor IκB (Ozes et al., 1999; Romashkova and Makarov, 1999). Degradation of IκB releases NF-κB, allowing its translocation to the nucleus and expression of anti-apoptotic target genes, like those of IAPs (inhibitors of apoptosis) (Wang et al., 1999; Wang et al., 1998).

Phosphorylation of MDM2 by Akt leads to its translocation to the nucleus, where it binds p53 and causes its degradation (Mayo and Donner, 2001; Zhou et al., 2001b). p53 controls cell-cycle progression and is involved in the induction of apoptosis in response to DNA damage. It also has been shown that p53 positively regulates the PTEN promoter (Graff et al., 2000). p53 and its homologue p73 regulate pro-apoptotic genes such as PUMA, BAX and NOXA (Villunger et al., 2003). The Yes-associated protein (YAP) regulates p73 transcriptional activity. Phosphorylation of YAP by Akt creates a 14-3-3 binding site, resulting in cytosolic retention and prevention of p73 transcriptional activity (Basu et al., 2003).

In addition, Akt has been implicated in the regulation of a specific form of apoptosis, which is induced when epithelial cells are deprived of adhesion to components of the basement membrane (Khwaja et al., 1997). The three primary integrin signalling molecules that have been linked to cell survival are FAK (focal adhesion kinase), Shc and ILK (integrin-linked kinase) (Aplin et al., 1999; Giancotti and Ruoslahti, 1999). ILK activates Akt activity either directly or indirectly (Attwell et al., 2000; Persad et al., 2000). FAK may also activate Akt through direct

PI3K activation as well as indirectly through a p130Cas/CRKII/DOCK180/Rac pathway (Kiyokawa et al., 1998; Sonoda et al., 2000). Although Shc is thought to activate the MAP kinase pathway through Grb2, data indicate that Shc is also a potent PI3K/Akt activator (Gu et al., 2000).

Finally, there is evidence for the involvement of Akt in controlling the cell cycle. Akt inhibits the cell-cycle inhibitory proteins $p21^{cip1}$ and $p27^{Kip1}$. Phosphorylation of $p21^{Cip1}$ at threonine 145 abolishes the inhibitory effect of $p21^{Cip1}$ on CDK2 and CDK4 (Zhou et al., 2001a). Akt phosphorylates $p27^{Kip1}$ on threonine 157, causing cytosolic sequestration via 14-3-3 binding (Sekimoto et al., 2004).

Among other proteins reported to be phosphorylated by Akt are the C-Raf-1 and B-Raf kinases (Guan et al., 2000; Zimmermann and Moelling, 1999), and the endothelial nitric oxide synthase (eNOS) (Fulton et al., 1999). The diversity of substrates of Akt demonstrates that this kinase is not only involved in apoptosis and cell proliferation, but also in the control of metabolism and protein translation as illustrated in Figure 1-3.

1.4.2 Metabolism

The overall function of insulin is to inform the organism about nutrient abundance, to induce glucose conversion into glycogen and fatty acids in the liver and to promote uptake and storage of glucose, amino acids and fat in muscles and adipocytes. It is thought that the PI3K/Akt pathway mediates the insulin responsive energy and nutrition homoeostasis by regulating glucose transport, glycolysis, protein synthesis, lipogenesis, glycogen synthesis and gluconeogenesis in a highly cell-type and cell-context specific manner (Manning and Cantley, 2007).

Insulin binds to its receptor and causes autophosphorylation on consensus tyrosine residues. The activated receptor phosphorylates tyrosines on the insulin receptor substrates (IRS1,2,3,4) that recruit downstream effector PI3K to the membrane and activates Akt and PDK (Katso et al., 2001). Inhibition of PI3K using the inhibitor LY294002 or wortmannin blocks insulin-mediated glucose uptake and translocation of the glucose transporter Glut 4 to the plasma membrane in adipocytes and myocytes (Thong et al., 2005). Mice deficient in PI3K signalling in muscle exhibit decreased muscle size, impaired insulin-stimulated glucose uptake and elevated levels of circulating lipids (Luo et al., 2006), while liver specific deletion of PI3K results in increased expression of gluconeogenic genes, hyperinsulinemia and hypolipidemia (Taniguchi et al., 2006). The two downstream effectors of the insulin/PI3K-mediated glucose and lipid

homeostasis are Akt/PKB and two atypical forms of protein kinase C (PKCλ/ξ). In a PI3K impaired signalling background, Akt seems to be more important in regulating hepatic glucose, while PKCλ/ξ are required for lipid metabolism (Taniguchi et al., 2006).

1.4.2.1 Glucose homeostasis

Akt2 is the most important isoform involved in glucose homeostasis, particular in mediating glucose uptake and glycolysis in insulin-responsive tissues (Dummler and Hemmings, 2007). Akt induces glucose uptake by inducing translocation of the glucose transporter type 4 (GLUT4) to the plasma membrane and by increasing expression of GLUT1 (Kohn et al., 1996; Welsh et al., 2005). However, Akt seems not to be the only effector of insulin mediated glucose transport. The atypical protein kinase C (PKCλ/ζ) (Kotani et al., 1998) and p38 mitogen-activated protein kinase (Sweeney et al., 1999) have a function parallel with Akt in glucose uptake. In addition to glucose uptake, Akt also induces expression of surface transporters, ion channels and receptors for the uptake of other nutrients, such as amino acid, iron and low-density lipoprotein (Edinger and Thompson, 2002; Palmada et al., 2005).

Akt stimulates the association of hexokinase with the mitochondrial membrane, which has been shown to be required for inhibition of apoptosis (Gottlob et al., 2001), but also promotes the conversion of glucose into glucose-6-phosphate (G6P) (Robey and Hay, 2006). G6P can either be stored as glycogen or catabolised via the glycolytic pathway. Glycogen synthesis is controlled by the allosterically regulated glycogen synthase (GS). Glycogen synthase kinase 3 (GSK3) phosphorylates GS and leads to its inhibition. Akt mediated inactivation of GSK3 contributes to an activation of GS (Cross et al., 1995). Akt also activates glycolysis by increasing expression of glycolytic enzymes via HIF-1α (Lum et al., 2007; Semenza et al., 1996). In addition, Akt inactivates gluconeogenesis via inhibition of FoxO1. FoxO1 transcriptionally regulates phosphoenolpyruvate carboxykinase (PEPCK) and glucose-6-phosphatase (G6Pase), the main enzymes promoting hepatic glucose production (Accili and Arden, 2004).

1.4.2.2 Lipid biosynthesis

Akt is also involved in insulin-mediated regulation of lipid biosynthesis. The net result of Akt activation is an increase in lipid biosynthesis. Akt directly phosphorylates and inhibits the hepatic transription factor PGC-1α (Li et al., 2007). PGC-1α activates transcription of genes encoding enzymes involved in ß-oxidation and gluconeogenesis in the liver (Puigserver, 2005). Akt also suppresses expression of genes coding for ß-oxidation enzymes by phosphorylating

and inhibiting the transcription factor FoxA2 (Wolfrum et al., 2004). Furthermore, Akt regulates insulin-mediated conversion of glucose into fatty acids. Akt phosphorylates and activates the enzyme ATP-citrate lyase (ACL) (Berwick et al., 2002). ACL catalyses the conversion of mitochondrial citrate to cytoplasmic acetyl-CoA, the precursor for lipid biosynthesis. Fatty acid synthase (FAS) is a multifunctional enzyme that catalyses the condensation of long chain fatty acids from acetyl-CoA and malonyl-CoA. It has been shown that Akt increases FAS transcription and fatty acid synthesis in adipocytes (Wang and Sul, 1998). Hepatic Akt activation even leads to hypertriglyceridemia with the involvement of sterol-regulatory element-binding proteins (SREBPs) (Ono et al., 2003). SREBPs are a family of transcription factors that regulate the expression of genes involved in fatty acid and cholesterol synthesis as well as several genes required for gluconeogenesis and glycogenesis (Horton et al., 2003). SREBPs expression is induced by insulin in nutritional regulation and it has been shown that activated Akt increases SREBP1c mRNA in hepatocytes. In addition, the PI3K-inhibitors wortmannin and LY294002 abolish insulin/Akt dependent accumulation of SREBP1c mRNA (Fleischmann and Iynedjian, 2000). The SREBPs will be discussed in more detail in chapter 1.6.

1.5 mTOR signalling pathway

The target of rapamycin (TOR) is an evolutionary conserved serine/threonine kinase that regulates cell growth and metabolism in response to nutrient availability and growth factor signalling. TORs are large proteins (~280 kDA) that belong to the phosphatidylinositol kinase-related kinase (PIKK) family. They contain a catalytic serine/threonine kinase domain, a FKB12-rapamycin binding domain (FRB), FAT and FATC domains, which are essential for TOR kinase activity and multiple tandem HEAT repeats (Liu and Zheng, 2007; Wullschleger et al., 2006).

The mammalian TOR is part of two distinct multiprotein complexes. mTORC1 is a complex of mTOR with mLST8 and raptor and is sensitive to the fungal antibiotic rapamycin, while mTORC2 is resistant to rapamycin and is a complex containing mTOR with mLST8, rictor and SIN1 (Bhaskar and Hay, 2007). The functions of the two complexes were first characterized in *Saccharomyces cerevisiae* (Loewith et al., 2002). They show that complex 1 regulates protein synthesis and cell growth by linking cell size to cell cycle progression whereas complex 2 is involved in cell-cycle-dependent actin cytoskeleton polarisation (Loewith et al., 2002). Genetic studies in *Drosophila*, as well as in yeast and mammals found the TOR protein complexes are only active in a dimeric form as part of the multiprotein complexes (Wang et al., 2006; Wullschleger et al., 2005; Zhang et al., 2006).

1.5.1 Regulation of mTOR signalling

Unlike the regulation of mTORC2, where little is known about upstream activators, several signals have been implicated in mTORC1 activation. mTORC1 responds to growth factor stimuli, cellular energy status, nutrient availability (mainly amino acids), and environmental stresses (Bhaskar and Hay, 2007). The main signalling pathway that regulates mTORC1 signalling by growth factors is the PI3K/Akt pathway (Manning and Cantley, 2003).

1.5.1.1 Upstream Signalling regulators

Activation of mTORC1 by Akt occurs via several indirect mechanisms (Figure 1-4 A). Firstly, in response to isulin, Akt phosphorylates and inhibits the tuberous sclerosis complex 2 protein (TCS2) of the heterodimer hamartin/tuberin (TSC1/TSC2) complex (Inoki et al., 2002). The TSC1/TSC2 complex operates as a GTPase-activating protein (GAP) for the small GTPase Rheb (Ras homologue enriched in brain). GTP-bound Rheb binds directly to mTORC1 and stimulates its activity (Castro et al., 2003; Garami et al., 2003; Inoki et al., 2003a). Therefore inhibition of TSC2 by Akt allows Rheb to activate mTORC1. In addition, TSC2 can be phosphorylated by several growth factor-stimulated kinases such as the p38-activated kinase MK2 (Li et al., 2003), ERK2 (Ma et al., 2005b) and p90 ribosomal S6 kinase 1 (RSK1) (Roux et al., 2004). However, only the Akt phosphorylation sites serine 939 and threonine 1462 are conserved in fly. The *in vivo* significance of these sites is debatable. In *Drosophila*, a TSC2 construct lacking the Akt phosphorylation sites rescues the lethality of *TSC2* mutant flies (Dong and Pan, 2004), indicating that TSC2 might not be a critical substrate for Akt during fly development.

Recently, the proline-rich Akt substrate of 40 kDa (PRAS40) has been found to bind to the mTORC1 complex and negatively regulate mTORC1 signalling (Vander Haar et al., 2007, Sancak, 2007 #630). Akt phosphorylates PRAS40 and consequently stimulates mTORC1 signalling (Vander Haar et al., 2007). The *Drosophila* genome also encodes a PRAS40 homologue termed Lobe (Sancak et al., 2007). In *Drosophila* S2 cells, silencing of *Lobe* results in activation of TORC1 signalling and increased cell size, independent of TSC2 (Sancak et al., 2007). Therefore Akt might activate TORC1 via two parallel mechanisms with redundant function. Two recent publications placed PRAS40 as a target of mTORC1 (Fonseca et al., 2007; Oshiro et al., 2007). It was concluded that PRAS40 associates with 14-3-3 in an insulin- and amino acid-induced manner mediated by Akt and mTORC1 dependent phosphorylation at T246 and S183, respectively (Fonseca et al., 2007).

A third mechanism suggests that Akt activates mTOR by maintaining a high ATP level in the cell (Hahn-Windgassen et al., 2005). mTOR senses the cellular energy status via the AMP-activated protein kinase (AMPK). In response to energy depletion (high AMP/ATP ratio) by glucose deprivation or under hypoxic conditions, AMP binds AMPK causing a conformational change that exposes the threonine 172 in the activation loop, which is phosphorylated by the tumour suppressor protein kinase 11 (LKB1). This phosphorylation is required for AMPK activation (Hardie, 2005). Activated AMPK phosphorylates TSC2 at serine 1364 resulting in enhanced TSC2-GAP activity (Inoki et al., 2003b) and inactivation of mTORC1 signalling. High ATP levels lead to a concomitant decrease in the AMP/ATP ratio and inhibit AMPK-mediated phosphorylation and activation of TSC2 (Hahn-Windgassen et al., 2005). Akt might maintain a high energy level partly through the continuation of nutrient uptake and activation of glycolysis (Edinger and Thompson, 2002; Lum et al., 2007).

TSC2 is also positively targeted by kinases, which activate TSC2 GAP function leading to inhibition of mTORC1 signalling. The phosphorylation and activation of TSC2 by AMPK was already discussed above. It has recently been shown that phosphorylation by AMPK could also prime GSK3 to phosphorylate TSC2, which integrates Wnt signalling into cell growth control (Inoki et al., 2006). The sequential phosphorylation by both kinases might be essential to fully activate TSC2 and inhibit mTORC1 (Inoki et al., 2006). Taken together, TSC2 integrates several inputs from growth factors via Akt, ERK and RSK, cellular energy levels via AMPK and Wnt signalling via GSK3 to regulate mTORC1 activity (Figure 1-4 B).

1.5.1.2 Regulators of upstream environmental cues (nutrients, energy, stress)

mTORC1 regulates energetically demanding processes like protein synthesis. Sufficient supply of nutrients (amino acids) and energy (ATP) is required for mTORC1 activity. mTORC1 itself and upstream regulators sense cellular energy and nutrient availability. The nutrient and energy status is communicated to TORC1 leading to its activation or inhibition and subsequently determines which metabolic pathways are switch on or off (Figure 1-4 B).

Amino acid starvation results in a rapid inhibition of mTORC1 activity, whereas readdition of amino acids restores mTORC1 signalling (Hay and Sonenberg, 2004). There are conflicting data regarding whether amino acid concentration affects mTORC1 activity directly or indirectly. However, there is evidence that it requires the presence of Rheb but is independent of TSC2 (Kim et al., 2002; Nobukuni et al., 2005; Smith et al., 2005).

AMPK independent transducers of cellular energy-depletion on the TSC-dependent TORC1 regulation are REDD1 and REDD2 (Sofer et al., 2005). The *Drosophila* genome codes for two orthologues of REDD1 and 2 termed *Scylla* and *Charybdis* and genetic studies suggest that they function in a similar way to their mammalian homologues in activating TSC2 (Reiling and Hafen, 2004). In addition, under low oxygen conditions (hypoxia) REDD1/2 is transcriptionally upregulated in a hypoxia-inducible transcription factor (HIF-1) –dependent manner (Brugarolas et al., 2004; Shoshani et al., 2002). Hypoxia also activates AMPK, presumably by ATP depletion due to reduced oxidative phosphorylation, and thereby activates TSC2 and inhibits mTORC1 (Liu et al., 2006).

Another mechanism suggests that the endocytic regulator Vps34 PI3K signals amino acid availability to mTORC1, although it is not known whether the effect is exerted directly or via Rheb (Byfield et al., 2005; Nobukuni et al., 2005).

1.5.1.3 Localization

mTORC1 has been found to be localised in both the nucleus (Drenan et al., 2004; Kim and Chen, 2000; Zhang et al., 2002) and the cytoplasm (Desai et al., 2002; Drenan et al., 2004) as well as being present at the endoplasmatic reticulum (ER) and Golgi apparatus (Drenan et al., 2004). In addition, TSC2 and Rheb are also found associated with the ER and Golgi (Buerger et al., 2006; Jones et al., 2004; Wienecke et al., 1996). Recent findings in yeast suggests that TORC1 and/or Rheb sense nutrients at the Golgi and endosomal membranes by monitoring the flux through endocytotic and secretory pathways (Neufeld, 2007). The Golgi specific ion pump Pmr1 has been identified as a TORC1 signalling regulator in yeast (Devasahayam et al., 2006). PMR1 encodes a Ca^{2+}/Mn^{2+} -ATPase, which is involved in the modification, degradation and sorting of amino acid permeases (Durr et al., 1998; Rudolph et al., 1989). Deletion of the Golgi and ER localisation motifs causes delocalisation of mTORC1 and inhibition of mTORC1-dependent ribosomal S6 kinase (S6K) phosphorylation (Liu and Zheng, 2007). In addition, Rheb association with the Golgi is required for its ability to activate mTOR signalling. Brefeldin A treatment abolishes the transmission of Rheb signals to S6K (Buerger et al., 2006). Brefeldin A inhibits the anterograde ER/Golgi protein transport. These findings suggest that endomembrane compartments are anchors for TORC1 signalling components and their localization is an important regulator of TORC1 pathway activity.

1.5.2 Downstream targets

mTORC1 regulates several growth-related processes such as protein biosynthesis and cellular metabolic processes including glucose homeostasis and lipid biosynthesis (Wullschleger et al., 2006). The best studied targets of mTORC1 signalling are S6K1/2 and 4E-binding protein (4E-BP) (Tee and Blenis, 2005). Phosphorylation of both proteins by mTORC1 requires interaction between raptor and a conserved TOR signalling sequence (TOS) in S6K and 4E-BP (Nojima et al., 2003; Schalm et al., 2003). Only two additional mTORC1 targets, PRAS40 and HIF-1α contain TOS motifs (Land and Tee, 2007; Oshiro et al., 2007). Activation of mTORC1 directly enhances the transcriptional activity of HIF-1α (Land and Tee, 2007).

1.5.2.1 The PI3K-S6K negative-feedback loop

It has been shown that persistent activation of TORC1 diminishes PI3K activity, indicating a negative-feedback mechanism (Radimerski et al., 2002a) (Figure 1-4 A). The TORC1 complex attenuates PI3K signalling via its effector S6K (Harrington et al., 2004; Radimerski et al., 2002b). S6K phosphorylates IRS proteins, targeting them for proteasomal degradation. Activation of S6K also results in transcriptional repression of IRS proteins (Gual et al., 2003; Harrington et al., 2005). The inhibitory effects of S6K on IRS signalling are reversible by treatment with the TORC1 inhibitor rapamycin.

1.5.2.2 Protein translation

The major targets of mTORC1 involved in protein translation are S6K1/2 and 4E-binding protein (4E-BP) (Tee and Blenis, 2005). mTORC1 phosphorylates S6K within its hydrophobic motif while PDK1 is responsible for phosphorylation of the T-loop. Activated S6K phosphorylates the ribosomal protein S6 (rpS6), which is reported to regulate translation of mRNAs that contain a 5' tract of oligopyrimidine (5'TOP mRNAs). However, it remains to be resolved how mTORC1 and S6K control 5'TOP dependent translation, since two studies in S6K1/2 double knockout mice show that phosphorylation of rpS6 is dispensable for 5'TOP translation (Pende et al., 2004; Ruvinsky et al., 2005). mTORC1 initiates CAP-dependent protein translation through phosphorylation and inactivation of the repressors of mRNA translation 4E-BPs (Tee and Blenis, 2005). 4E-BPs prevent the association of the initiation factor complex that mediate CAP-dependent translation by binding to the eukaryotic initiation factor 4E (eIF-4E).

1.5.2.3 Transporters

Nutrient uptake is regulated by the surface expression of several transporters in the plasma membrane. The PI3K/TORC1 pathway regulates both transcription and surface localisation of nutrient transporters (Edinger, 2007). In yeast, TORC1 activates surface localization of specific amino acid permeases such as Tat2 and Hip1, whereby the general amino acid permease GAP1 is degraded (De Virgilio and Loewith, 2006). TORC1 also prevents the turnover of glucose and amino acid transporters (Schmelzle et al., 2004). In mammals, mTORC1 promotes the surface localization of transporters required for glucose, amino acid, iron and lipoprotein uptake (Edinger and Thompson, 2002). In addition to the regulation of amino acid transporter trafficking, mTORC1 also activates expression of at least five amino acid transporters as shown in a human lymphoma cell line (Peng et al., 2002).

1.5.2.4 Metabolism

mTORC1 regulates glucose homeostasis at least in part via S6K-dependent phosphorylation of rpS6 (Ruvinsky and Meyuhas, 2006). Both S6K1 deficient and $rpS6^{P-/-}$ knock-in mice, where all serine phosphorylation sites are substituted by alanine, show impaired glucose uptake due to insufficient insulin secretion caused by diminished ß-cell mass (Pende et al., 2000; Ruvinsky et al., 2005). mTORC1 signalling also controls fat metabolism. mTORC1 activity is important for lipid accumulation during adipogenesis, presumably due to inhibition of ß-oxidation of fatty acids by regulating the activity of the nuclear receptor PPARγ (Kim and Chen, 2004) Furthermore, *S6K* mutant mice have reduced lipid levels due to increased ß-oxidation in adipocytes (Um et al., 2004) and impaired TORC1 signalling in *Drosophila* leads to a lean phenotype due to less fat in the animal (Teleman et al., 2005).

1.6 The PI3K and mTOR signalling pathways in cancer

The activity of the PI3K/Akt/mTORC1 pathway is altered by a number of different mechanisms and accounts for up to 30% of all human cancers (Luo et al., 2003). Ras, which directly activates PI3K, is a dominant acting oncogene that is frequently implicated in human malignancies (Shaw and Cantley, 2006). The PI3K catalytic p110α subunit is found mutated in ovarian, cervical and lung carcinomas (Ma et al., 2000; Massion et al., 2002; Shayesteh et al., 1999) and the regulatory p85 subunit of PI3K is mutated in human colon and ovarian cancer (Jimenez et al., 1998; Philp et al., 2001). Activating mutations in RTKs provide evidence for the importance of the PI3K/Akt pathway in human cancer. For example, a truncated variant of the EGFR that lacks the extracellular domain (EGFR viii) potently activates the PI3K/Akt pathway,

but not the RAS/MAPK pathway (Moscatello et al., 1998). Beside the high rate of activating mutations in p110α, the most common mechanism of activation of the PI3K/Akt pathway in human cancer is through loss of PTEN (Brugge et al., 2007; Shaw and Cantley, 2006). PTEN acts as a haploinsufficient tumour suppressor in the prostate and its dose dictates tumour progression in mice (Di Cristofano et al., 1998; Trotman et al., 2003). PTEN is found mutated in a wide range of malignancies, including breast, ovarian and colon cancers and is the second most mutated tumour suppressor in human cancers, after p53 (Cantley and Neel, 1999; Shaw and Cantley, 2006). Akt is frequently activated through gene amplification and mutation (Brugge et al., 2007). Recently, a somatic mutation in the PH-domain of Akt1 was observed in human breast, colorectal and ovarian cancers that result in PI3K-independent membrane recruitment and constitutive activation (Carpten et al., 2007). This Akt mutant functions similarly to myristoylated Akt or its retroviral homologue, where membrane targeting is critical for Akt-mediated transformation (Ahmed et al., 1993; Mirza et al., 2000; Sun et al., 2001).

There is both direct and indirect evidence for the involvement of the TSC1&2/mTORC1 pathway in PI3K-mediated tumourigenesis. Inhibition of mTOR activity prevents tumour progression in both mice and humans. Rapamycin derivates have been used in several clinical trials and show anti-tumour activity for many different tumour types, including breast cancer and non-small-cell lung cancer (Chan, 2004; Chan et al., 2005). Germline mutations of the tumour suppressors TSC1 or TSC2 lead to tuberous sclerosis, a hamartoma syndrome that is linked to malignant predisposition (Li et al., 2004). mTORC1 activity is also regulated through AMPK, which is activated by the tumour suppressor LKB1. Mutations in LKB1 are found in the familial cancer disorder Peutz-Jeghers syndrome and in a high percentage of sporadic lung adenocarcinomas (Hemminki et al., 1998; Sanchez-Cespedes et al., 2002). Interestingly, germline mutations in PTEN (Cowden's disease), LKB1 (Peitz-Jeghers syndrome) and TSC1 or TSC2 (tuberous sclerosis) show overlapping clinical symptoms of histologically similar hamartomas. Although these syndromes occur in different tissues, the common link between these three diseases is that the loss of function mutation of these tumour suppressors results in activation of mTORC1 (Shaw and Cantley, 2006). These findings indicate the important role of mTORC1 activity in growth control and in promoting tumourigenesis.

1.7 Sterol Regulatory Element-binding Proteins (SREBPs)

SREBPs belong to the family of basic helix-loop-helix-leucine zipper (bHLH-Zip) transcription factors. There are two mammalian genes encoding three SREBP proteins, designated SREBP1a, SREBP1c (alternatively known as adipocyte determination and differentiation factor-1 ADD1) (Brown and Goldstein, 1997) and SREBP2 (Hua et al., 1995). The human SREBP2 gene is

located on chromosome 22q13. Human SREBP1a and SREBP1c are encoded by the same gene on chromosome 17p11.2 through the use of alternative transcription start sites that result in different forms of exon 1.

All SREBPs consist of an N-terminal transcription activating and basic helix-loop-helix leucine-zipper (bHLH-Zip) for DNA binding and dimerization, two hydrophobic transmembrane-spanning segments and a C-terminal regulatory domain. They are synthesized as inactive, 125-kDa precursor proteins localised in the ER-membrane (Brown and Goldstein, 1997; Horton et al., 2002). In the ER, SREBP forms a complex via their regulatory domain with the SREBP cleavage-activating protein (SCAP) (Sato et al., 1994). SCAP is a polytopic ER-membrane protein, which consists of multiple WD repeats that mediate protein-protein interaction and a sterol-sensing domain (SSD). The WD repeats mediate the interaction between SREBP and SCAP (Sakai et al., 1997).

Several bHLH-Zip transcription factors like Myc and Max contain an arginine residue within their DNA binding domain, which permits binding to E-boxes in target promoters. SREBPs contain a unique tyrosine instead of the arginine, which allows binding not only to classic palindromic E-boxes but also to nonpalindromic SRE and SRE-like sequences. Substitution of the tyrosine with arginine abolishes trans-activation of SRE motifs for all SREBPs, while increasing activity of SREBP1, but not SREBP2, towards E-boxes (Amemiya-Kudo et al., 2002). A total loss of SREBP DNA-binding activity can be achieved by substitution of the tyrosine with alanine (Kim and Spiegelman, 1996).

Mature SREBPs can enter the nucleus and form dimers that bind to DNA elements containing direct repeats of 5'-PyCAPy-3', termed sterol regulatory elements (SRE), but also SRE-like and E-box sequences in the promoter/enhancer regions of several target genes, activating their transcription. SREBPs target genes are responsible for cholesterol synthesis (HMG-CoA reductase and synthase) and uptake (LDL receptor), fatty acid synthesis (FAS), phospholipid and triglyceride production (GPAT), and generation of the cofactor NADPH, required for the synthesis of these molecules. This indicates that SREBPs are global regulators of cholesterol and lipid homeostasis (Horton, 2002).

1.7.1 SREBP isoforms and their functions

The specific trans-activation of nuclear mSREBPs on SREBP-target promoters depends on their DNA binding preferences. Cholesterogenic genes, containing classical SRE motifs in their promoters, are strongly and efficiently activated by both SREBP1a and SREBP2, but not by

SREBP1c. Promoters of lipogenic enzymes, containing variations of SRE, SRE-like and E-box sequences, are strongly activated by SREBP1a, but only modestly by SREBP1c and SREBP2 (Amemiya-Kudo et al., 2002). SREBPs target gene promoter analysis using chromatin IP showed that SREBP1a but not SREBP1c can bind to SREs in the HMG-CoA reductase and fatty acid synthase promoters resulting in the recruitment of histone acetylase (HAT) (Bennett et al., 2004). SREBP1a and SREBP1c also differ in their binding to transcriptional coactivators such as CBP/p300 and the mammalian Mediator complex, which may explain the low transcriptional activity of SREBP1c (Toth et al., 2004). However, all SREBP-dependent transcription requires recruitment of the ARC105/MED15 subunit of the Mediator complex to target genes (Yang et al., 2006b). Diet dependent SREBP1c-mediated gene expression also requires binding to the co-activator PGC-1ß in hepatic tissue (Lin et al., 2005). PGC-1ß belongs to the PGC-1 family of co-activators involved in the control of liver metabolism (Lin et al., 2002; Puigserver, 2005). Interestingly, SREBP isoforms can form homo and heterodimers, resulting in different transcriptional activities (Datta and Osborne, 2005). Therefore the abundance of one isoform may influence the target gene expression of the other ones (Datta and Osborne, 2005).

The function of mature SREBP *in vivo* was examined in livers of transgenic and knockout mice. Consistent with *in vitro* promoter analysis, data from knockout and transgenic mice shows that SREBP1c preferentially enhances transcription of genes involved in fatty acids synthesis, while SREBP2 activates cholesterol biosynthesis genes and SREPB1a activates genes that mediate synthesis of cholesterol, fatty acids and triglycerides (Figure 1-5). At non-physiological levels, each SREBP isoform can activate all SREBP-regulated genes (Horton et al., 2003). Furthermore, over-expression of mSREBP1a in livers of transgenic mice results in overproduction of cholesterol and fatty acids and causes the development of fatty livers in these animals (Shimano et al., 1996). Overexpression of mSREBP1c causes triglyceride enriched fatty livers with no increase in cholesterol (Shimano et al., 1997a). Mice lacking the SREBP1c isoform are viable, whereas deletion of both SREBP1 isoforms leads to 50% to 85% reduction in offspring (Shimano et al., 1997b). Although, SREBP1a is able to activate expression of genes encoding enzymes involved in cholesterol synthesis, deletion of SREBP2 in mice is embryonic lethal (Shimano et al., 1997b). These results indicate that SREBP1a and SREBP1c have overlapping function and that SREBP2 can compensate, at least in part, for the loss of both SREBP1 isoforms (Eberle et al., 2004).

SREBP1a and SREBP2 are the predominant isoforms in most cultured cell lines, whereas SREBP1c and SREBP2 are predominantly expressed in liver and adipose tissue (Shimomura et al., 1997b). SREBP1c mediates the lipogenic action of insulin in the liver, resulting in the conversion of glucose into triglycerides in the presence of excess carbohydrates. SREBP1c

mediates this effect by inducing the expression of FAS and glucokinase (Foretz et al., 1999a) and by suppressing phosphoenolpyruvate carboxykinase, the rate-limiting enzyme in gluconeogenesis (Chakravarty et al., 2001). SREBP1c may also affect glucose homeostasis by inducing glucose uptake (Becard et al., 2001; Chakravarty et al., 2001).

Recently, it has been reported that SREBPs activate expression of genes encoding proteins unrelated to lipid synthesis. SREBP1 may play a role in cell cycle progression since SREBP1a induces expression of the CDK inhibitor p21 (Inoue et al., 2005). p21 is a transcriptional target of p53 and induces cell cycle arrest in response to a number of stimuli (Beuvink et al., 2005). Furthermore, *in vitro* and *in vivo* studies showed that SREBP1 induces expression of the PI3K regulatory subunit p55γ, heme oxygenase 1 (HMOX1), plasma glutathione peroxidase, synaptic vesicle glycoprotein 2A and COTE1 (Kallin et al., 2007). This suggests that SREBP1 may also contribute to stress and growth factor-induced signalling.

1.7.2 Regulation of SREBP

Regulation of SREBP transcription factors is very tight and integrates availability of nutrients and metabolic substrates, cellular energy status and mitogenic stimuli (Eberle et al., 2004). They are regulated at the transcriptional and posttranscriptional level, including sterol-controlled proteolytic cleavage of full length SREBP and posttranslational modification of mature SREBP. Although the three isoforms share most of the regulatory mechanism, there are significant differences. SREBP1c is mainly transcriptionally regulated, whereas SREBP1a and SREBP2 may be principally regulated at the posttranscriptional level (Eberle et al., 2004).

1.7.2.1 Transcriptional Regulation

A number of studies have addressed the regulation of SREBP gene expression *in vivo* and *in vitro*. Expression of SREBP1c and SREBP2 seems to be subject to distinct regulation in vivo. Both genes contain SREs in their promoter region (Amemiya-Kudo et al., 2000; Sato et al., 1996) and regulation through a feed-forward loop has been described in transgenic animals over-expressing the different SREBP proteins (Horton et al., 2003).

Studies in mice show that SREBP1c transcription is controlled by changes in the nutritional status of the liver (Horton et al., 1998). Subsequent experiments i*n vitro*, in hepatocytes and adipocytes showed that insulin stimulates expression of SREBP1c (Foretz et al., 1999a; Kim et al., 1998), which also leads to an increase in full length and mature forms of the transcription factor (Azzout-Marniche et al., 2000). In contrast, glucagon inhibits SREBP1c transcription

(Foretz et al., 1999a). The PI3K pathway has been reported to mediate the effect of insulin on SREBP1c transcription (Fleischmann and Iynedjian, 2000), via activation of the downstream effector Akt (Fleischmann and Iynedjian, 2000; Ribaux and Iynedjian, 2003) and PKCλ (Matsumoto et al., 2003). Atypical PKC activity is also necessary for insulin-mediated lipid homeostasis via regulation of SREBP1c expression (Matsumoto et al., 2003). Loss of PI3K results in decreased PKCλ/ξ activity associated with reduced SREBP1c expression level and hypolipidemia in livers of transgenic mice (Taniguchi et al., 2006).

The rat SREBP1c promoter is induced by insulin in hepatocytes through a 149bp fragment containing two insulin-response elements, an SRE complex (SRE, E-box, NF-Y, and SP1 binding sites) and two liver X receptor (LXR)-response elements (LXREs). Mutation of the SREs completely abolishes the response of the SREBP1c promoter to insulin (Cagen et al., 2005; Deng et al., 2002). Furthermore, the Sp1 binding sites are important for the basal and insulin induced expression of SREBP1c (Deng et al., 2007). In addition, the promoter of the SREBP1a gene also contains several SP1 sites (Zhang et al., 2005). Deng et al. (2007) proposed a mechanistic model suggesting that insulin-induced SREBP1 gene expression is mediated via enhanced association of Sp1 with transcription factors (i.e. LXRα, NF-Y), a distinct coactivator complex called ARC/Mediator (Yang et al., 2006b), and coactivators such as SRC-1 and p300, which concomitantly increase the transactivating capacity of Sp1 (Deng et al., 2007). However these data have to be considered carefully with regard to the human homologue, because SREBP promoter sequences differ between mammalian species, which suggests that they may be regulated distinctly from each other. Comparison of the human and mouse promoters showed that only the human SREBP1c promoter is regulated by two tissue-specific transcription factors, PDX-1 and HNF-4 (Tarling et al., 2004).

SREBP1c transcription is also regulated by the liver X receptor α (LXRα). LXRα belongs to the LXR nuclear hormone receptor family that coordinates cholesterol homeostasis in the liver, by regulating lipid metabolism (Steffensen and Gustafsson, 2004). A variety of oxysterols (cholesterol derivates) activate LXRs, whereas polyunsaturated fatty acids (PUFA) such as arachidonic acid inhibit their transcriptional activities (DeBose-Boyd et al., 2001; Janowski et al., 1999; Repa et al., 2000). One product of the SREBP1 regulated fatty acid pathway is oleate, the fatty acid required for the synthesis of cholesteryl-esters, which are necessary for the transport and the storage of cholesterol.

The SREBP1c promoter contains two LXR-response elements (LXREs) (Cagen et al., 2005). Thus, treatments with the synthetic LXR agonist T0901317 and oxysterol induces up-regulation of SREBP1c mRNA and increase the amount of the mature protein, leading to expression of

lipogenic target genes and enhance fatty acid synthesis (Repa et al., 2000; Schultz et al., 2000). In contrast, polyunsaturated fatty acids (e.g. arachidonic acid) inhibit SREBP1 expression and lipid synthesis by antagonising LXR-dependent activation of SREBP1 (Hannah et al., 2001; Ou et al., 2001; Yoshikawa et al., 2002). The LXREs in the SREBP1c promoter are required for complete insulin-mediated SREBP1c expression and fatty acid synthesis in the liver, as mutations of these binding sites significantly reduce the insulin response (Cagen et al., 2005; Chen et al., 2004). These data suggest a model in which LXR mediates the insulin effect on SREBP1c transcription (Chen et al., 2004). In addition, LXR directly activates expression of lipogenic genes such as FAS (Joseph et al., 2002).

It has recently been published that LXRs also sense glucose availability (Mitro et al., 2007). D-Glucose and D-glucose-6-phosphate have been found to act as agonists of LXRα and LXR. They bind directly to LXRs and induce expression of LXR target genes in hepatocytes, e.g. SREBP1c and FAS (Mitro et al., 2007). One of the most important physiological functions of insulin is to stimulate glucose uptake and it has been shown that LXRs are required for full induction of SREBP1c by insulin (Chen et al., 2004). This suggests the hypothesis that insulin-mediated uptake of glucose activates LXR and leads to transcription of SREBP1.

Furthermore, Zhou et al. (2001) showed that metformin or AICAR-mediated activation of AMPK blocks insulin induced SREBP1c mRNA and protein expression. The same study showed a down-regulation of the target genes FAS and S14 as well as inhibition of ACC activity, which resulted in decreased triglyceride content and increased ß-oxidation (Zhou et al., 2001c). Finally, androgens and progesterone have been shown to induce SREBP1c expression resulting in activation of lipogenic pathways (Heemers et al., 2001; Lacasa et al., 2001).

1.7.2.2 Posttranslational Regulation

A sterol-controlled processing machinery regulates the proteolytic cleavage of full length SREBPs. Several posttranslational modifications are regulating stability and transcriptional activity of mature SREBPs, including phosphorylation, ubiqitination, acetylation and sumoylation.

Activation of SREBP requires SCAP-dependent ER-Golgi translocation. Under sterol-depleted conditions, the SCAP hexapeptide-sorting motif (MELADL) is accessible for Sec24 binding. Sec 24 is a member of the COPII protein complex, which selects the cargo and clusters them into budding vesicles (Sun et al., 2007). Following incorporation into COPII-coated vesicles, the SREBP/SCAP complex translocates to the Golgi (Sun et al., 2007), where SREBP

undergoes a two-step cleavage process called regulated intramembrane proteolysis (RIP) (Brown et al., 2002). In the Golgi, the site1 (S1P) and site 2 protease (S2P) act sequentially to release the N-terminal part of the protein from the membrane (Brown and Goldstein, 1999; Goldstein et al., 2002). The 66 kDa fragment is designated mature SREBP (mSREBP). In the presence of sterols, INSIG, an intrinsic membrane protein of the ER blocks SREBP/SCAP translocation to the Golgi (Yabe et al., 2002; Yang et al., 2002a) Recently, it has been shown that cholesterol and its derivates oxysterol (e.g. 25-hydroxycholesterol) inhibit SREBP processing via two different mechanisms. Cholesterol acts by binding to SCAP, inducing a conformational change that is recognized by INSIG (Sun et al., 2007). In contrast, oxysterols bind to INSIG and initiate formation of the INSIG-SCAP complex (Radhakrishnan et al., 2007). However, both ligands trigger INSIG-SCAP complex formation, thereby abrogating COPII-protein binding to SCAP and inhibiting the ER-Golgi transport of SREBP (Sun et al., 2007) (Figure 1-6).

The transcriptionally active forms of SREBP in the nucleus become rapidly degraded in an ubiquitin-dependent manner, which results in a decrease in the expression of SREBP target genes (Wang et al., 1994). It has been shown that GSK3ß phosphorylates mSREBP1c, resulting in inhibition of its target genes expression (Kim et al., 2004). DNA binding enhances the GSK3-dependent phosphorylation in the C-terminus of nuclear mSREBP1 (Punga et al., 2006). The phosphorylated residues are recognized by the specific SCF ubiquitin ligase Fbw7, which leads to ubiquitination and proteasomal degradation of mSREBP1 (Sundqvist et al., 2005). Silencing of Fbw7 or mutation of the GSK3ß phosphorylation sites in SREBP1 prevents its rapid degradation and leads to enhanced SREBP-dependent transcription (Sundqvist et al., 2005).

The Erk family of MAP kinases phosphorylates mSREBP1 and mSREBP2. The phosphorylation is thought to be involved in transcriptional activation by insulin and platelet-derived growth factor (PDGF) (Kotzka et al., 1998; Kotzka et al., 2000; Roth et al., 2000). Furthermore, PKA phosphorylation attenuates DNA-binding of mSREBP1 and the resulting target gene expression (Lu and Shyy, 2005).

As described above, SREBP processing is regulated by the intracellular level of sterols (Brown and Goldstein, 1999). High sterol concentration suppresses proteolytic processing of SREBPs, which effects the amount of mature SREBP (Hirano et al., 2001). In contrast, low sterol-levels lead to processing and activation of SREBPs. In response to acute insulin exposure, hepatic SREBP1 is rapidly cleaved in a PI3K-dependent manner (Hegarty et al., 2005; Yellaturu et al., 2005), whereas overexpression of dominant negative Akt blocks mSREBP accumulation in the nucleus by inhibiting ER to Golgi translocation (Du et al., 2006). Another report suggests a mechanism in which insulin induces processing of SREBP1c in the liver by down-regulating

expression of INSIG2a (Yabe et al., 2003). In contrast, the INSIG1 isoform is up-regulated in response to insulin stimulation (Attie, 2004). SREBP1c directly induces expression of INSIG1. INSIG1, together with sterols, act in a convergent manner, as both are required to fully block SREBP processing (Gong et al., 2006).

However, other mechanisms of SREBP processing have been reported. During early apoptosis, activated caspase 3 cleaves SREBPs in the ER and releases the N-terminal fragment to be translocated to the nucleus (Pai et al., 1996). It has been suggested that SREBP1c functions as a pro-apoptotic gene in pancreatic ß-cells, possibly through suppressing CDK4 expression and by promoting expression of $p21^{WAF1/CIP1}$, APO-1/FAS/CD95 and BAX (Wang et al., 2003).

1.7.3 SREBP homologues

SREBP homologues have been identified and characterized in the fly *Drosophila melanogaster* (see chapter 1.9.3), the worm *C. elegans* and the fission yeast *S. pombe*. In *C. elegans*, SREBP activates expression of lipogenic enzymes and is required for fat production, primarily in the intestine (McKay et al., 2003). Silencing of *SREBP* leads to impaired intestinal fat storage, infertility and a decrease in organismal size. This phenotype could be prevented by supplementation of oleic acid to the diet (McKay et al., 2003). However, the mechanism of the regulation of SREBP in *C. elegans* is not known.

The yeast SREBP orthologue Sre1 is proteolytically processed under sterol-depleted conditions and activates genes required for adaptation to hypoxia and anaerobic growth (Hughes et al., 2005; Todd et al., 2006). The yeast genome also contains a functional orthologue of SCAP, Scp1. The Sc1-Sre1 complex senses oxygen availability by monitoring oxygen-dependent sterol synthesis.

1.8 Lipid metabolism and cancer

Cancer cells differ from normal cells in their signalling as well as in their growth and metabolic programmes. Tumours consist of highly proliferating and rapidly growing cells with a high demand on energy and metabolites for the biosynthesis of macromolecules. In order to fulfil these demands, many tumour cells increase glycolysis as the main source for ATP production even in the presence of sufficient oxygen. This phenotype is known as aerobic glycolysis or "Warburg effect" (Warburg, 1956) and the increased glucose uptake is the molecular basis for tumour imaging using PET as a diagnostic tool (Weber and Wieder, 2006). An increased glucose uptake and glycolysis allows faster energy production and provides cells with

metabolites for the synthesis of macromolecules required for cell growth and proliferation. In contrast to normal cells, cancer cells obtain most of their fatty acids from glucose-derived *de novo* lipid synthesis despite an abundant supply of extracellular lipids. This is reflected in an elevated activity of lipogenic enzymes such as ACL and FAS (Kuhajda, 2000; Turyn et al., 2003). There are several observations that implicate activation of cholesterol and fatty acid synthesis in cell transformation and tumour development (Hager et al., 2006). The high rate of glycolysis and lipid biosynthesis is driven by oncogenic activation of the PI3K/Akt/TORC1 pathway (Bui and Thompson, 2006; Menendez and Lupu, 2006).

1.8.1 Cellular functions of cholesterol and fatty acids

Cholesterol and intermediates of the cholesterol biosynthesis pathway have many biological functions in different compartments of the cell. Cholesterol functions as a structural lipid in the plasma membrane of most eukaryotic cells (except plant cells) and is the precursor for a variety of metabolites (Bittman, 1997). All steroid hormones are derived from cholesterol and it can also be converted into Vitamin D, bile acids and cholesteryl-esters. Bile acids help lipid digestion and cholesteryl-ester is the form in which cholesterol can be transported to other tissues and stored in the liver. Isoprene derivatives of the cholesterol pathway have an important role in protein prenylation (Basso et al., 2006). The maturation of small GTPases, such as Ras and Rho, heterotrimeric G-proteins (γ subunits), nuclear lamins A and B and other proteins require covalent attachment of farnesyl or geranylgeranyl isoprenoids (Perez-Sala, 2007; Resh, 1999). It has been shown that Ras farnesylation is required for its localisation to the inner side of the plasma membrane and for interaction with PI3Kγ (Rubio et al., 1999).

Cholesterol is a major component of specialised membrane microdomains, such as membrane rafts and caveolae, which are involved in cellular processes like membrane protein segregation and concentration, signal transduction, protein and lipid sorting as well as virus assembly and release (Hanzal-Bayer and Hancock, 2007; Simons and Vaz, 2004). Membrane rafts are thought to resemble small platforms composed of sphingolipids and cholesterol in the outer leaflet of the plasma membrane and phospholipids with saturated fatty acids and cholesterol in the inner leaflet (Simons and Vaz, 2004). Another subset of lipid structures are cell surface invaginations called caveolae. They are formed by polymerization of caveolins and a subset of lipid-raft components, including cholesterol and sphingolipids (Parton and Simons, 2007). One important role of membrane rafts and caveolae may be their function in signal transduction processes. Rafts form areas of high concentration of growth factor receptors such as the EGFR (Miljan and Bremer, 2002; Waugh et al., 1999), the estrogen receptor (Marquez et al., 2006) and the insulin receptor (Mastick et al., 1995) and include adaptor proteins, scaffolding proteins and signalling

molecules such as Ras (Roy et al., 1999). However a recent review invokes doubt regarding linking caveolae to specific signalling pathways due to conflicting data (Parton and Simons, 2007); which show that adipocyte-derived caveolae do not contain insulin receptors (Souto et al., 2003).

Lipids have several functions in the organism. They are the main form of stored energy (triacylglycerol) and major constituents of cellular membranes. Specialised lipids like phosphatidylinositol derivates serve as intracellular second messengers. Phospholipids are the most abundant membrane lipids. They are amphipathic molecules containing hydrophobic (nonpolar) tails that consist of saturated and unsaturated fatty acids (FA), and a hydrophilic (polar) head group containing glycerol, phosphate and a specific organic group (alcohol). The common alcohol moieties are serine, ethanolamine, choline, glycerol and inositol. In mammalian cells, four major phospholipids are present in the plasma membrane: phosphatidylserine (PS), phosphatidylethanolamine (PE), phosphatidylcholine (PC) and sphingomyelin. Sphingomyelin is a derivative of sphingosine and co-localizes with cholesterol to lipid rafts. The membrane composition in terms of the proportion of these phospholipids determines its functional specialisation.

De novo fatty acid synthesis is essential during embryogenesis (Chirala et al., 2003). In adult tissue, *de novo* synthesis of fatty acids occurs nearly exclusively in liver, lactating breast and cycling endometrium, and in adipose tissue. All other tissues derive the lipids they require from the circulatory system. Under physiological conditions, fatty acids are synthesized in the liver and exported to metabolically active tissue for energy conversion, for storage in adipocytes or are converted into PUFAs, triglycerides, or lipids (Weiss et al., 1986). The latter is particularly important in highly proliferating cells and tissues that need circulating lipids for the synthesis of new structural lipids. Consequently, expression of lipogenic enzymes and *de novo* lipogenesis is low in most adult tissues (Menendez and Lupu, 2006; Swinnen et al., 2006). In contrast, many cancers obtain the bulk of FA from *de novo* lipid synthesis, irrespective of the availability of extracellular lipids (Swinnen et al., 2006). The carbon source for *de novo* lipid synthesis is cytosolic acetyl-CoA. The TCA cycle metabolite citrate is transported from the mitochondria to the cytosol where it used for the synthesis of acetyl-CoA by ATP-citrate lyase (ACL). The committed step in FA synthesis is the carboxylation of acetyl-CoA to malonyl-CoA. This irreversible reaction is catalysed by acetyl-CoA carboxylase (ACC). Therefore ACL and ACC provide glucose-derived carbon units for lipid and sterol biosynthesis. Fatty acid synthase (FAS) is the enzyme that catalyses the synthesis of saturated FA from acetyl-CoA and malonyl-CoA. Acetyl-CoA can also be converted into acetoacetyl-CoA, the precursor metabolite for *de novo* isoprenoid and cholesterol synthesis. HMG-CoA reductase (HMGR) and HMG-CoA synthase (HMGS) are the key-regulatory enzymes in the cholesterol biosynthesis pathway, also

termed the mevalonate pathway (Figure 1-7). Intermediates of the cholesterol pathway are required for prenylation of small GTPases like Rho and K-Ras. Cholesterol is also derived from circulating low-density lipoproteins (LDL) via LDL-receptor (LDLR) mediated endocytosis and lysosomal processing (Allayee et al., 2000; Goldstein and Brown, 1990).

1.8.2 Fatty acids and cholesterol in cancer

Clinical and biochemical studies have reported extremely high levels of FA synthesis in many human epithelial cancers including breast, ovarian and prostate (Kuhajda et al., 2000; Menendez and Lupu, 2004). The increase in lipogenesis is reflected by an elevated expression level of lipogenic genes and significantly elevated activity of lipogenic enzymes. FAS, ACC and ACL have been shown to be over-expressed in various cancer types (Kuhajda, 2000; Menendez and Lupu, 2004; Yahagi et al., 2005). ACL was found to be significantly up-regulated in breast and bladder carcinomas and inhibition by RNAi or chemical inhibitors induced a decline in glucose-dependent lipid synthesis, and limited proliferation and survival in tumour cells *in vitro*. The same treatment also reduced tumour growth *in vivo* (Bauer et al., 2005; Hatzivassiliou et al., 2005). In addition, SREBPs have been found deregulated in several tumours such as prostate (Ettinger et al., 2004), breast (Martel et al., 2006) and glioblastoma (Ma et al., 2005a) and could thus contribute to cell transformation and tumour development (Swinnen et al., 2004). Some studies suggest that upregulation of growth factor signalling pathways drives expression of lipogenic enzymes via activation of SREBPs (Swinnen et al., 2006). H-Ras transformed MCF-10A breast epithelial cells show upregulation of MAP-kinase and PI3K pathways as well as elevation of SREBP1c activity, resulting in upregulation of its target gene FAS (Yang et al., 2002b; Yang et al., 2003). In prostate cancer cell lines, EGF and androgens were found to stimulate SREBP expression, leading to FAS over-expression and elevated fatty acid synthesis (Swinnen et al., 2000). Accordingly, activation of FAS expression and fatty acid synthesis has been linked to malignant transformation (Menendez and Lupu, 2006; Rashid et al., 1997) and FAS has been termed a "metabolic oncogene" (Baron et al., 2004). In addition, deregulation of SREBP has been proposed to contribute to tumour formation (Swinnen et al., 2004).

It has been demonstrated that many tumours show an accumulation of cholesterol (Pizer et al., 1998). Acute myeloid leukaemia cells show enhanced cholesterol synthesis and LDL processing via deregulated transcription of HMGR and LDLR (Banker et al., 2004). Statins are inhibitors of the rate-limiting enzyme of cholesterol synthesis, HMGR, and have been used as cholesterol lowering drugs in the clinic for several years. Interestingly, several clinical studies indicate a therapeutic benefit of statin treatment in cancer prevention (Demierre et al., 2005) and the use of statins as cytostatic drugs for some tumour types has been discussed (Brower, 2003).

However, the anticancer effect of statins is likely to be via the inhibition of G-protein activation through a lack of geranylgeranyl isoprenoids (Demierre et al., 2005). In a human prostate cancer cell line (LNCaP), cholesterol-rich lipid rafts mediate enhanced EGF signalling and Akt activation. Thus Akt activates several metabolic pathways and inhibits pro-apoptotic factors in LNCaP cells (Zhuang et al., 2002). Mice xenografts derived from this cell line show upregulation of SREBP expression and elevated cholesterol levels (Ettinger et al., 2004).

These findings suggest that oncogenic signalling affects lipogenesis in cancer, linking tumour-associated glycolysis to lipid and sterol synthesis, which may contribute to cell transformation and tumour development. Therefore interference with metabolic pathways is considered as a potential therapeutic approach to induce a metabolic catastrophe that kills tumour cells (Jin et al., 2007; Swinnen et al., 2006).

1.9 *Signalling and metabolism in Drosophila melanogaster*

The fruit fly *Drosophila melanogaster* is a well-established model for insulin/IGF and TSC/TOR -regulated cell and organ size (Leevers and Hafen, 2004).

1.9.1 Fly development

Flies do not grow once they have reached the adult, reproductive form. Therefore, the size of the fly is determined by both the larval growth rate as well as the duration of the larval stages, termed instars (Edgar, 2006). After larval development is complete, flies undergo pupation and metamorphosis during which larval tissues are remodelled to generate the adult fly. Imaginal discs start as very small structures in initial larvae instars but gradually grow and replace almost all larval tissues during development, giving rise to most of the adult structures (Cohen et al., 1993). As an example, imaginal discs can grow from 5 to 50,000 cells during larval development (Bryant and Simpson, 1984). However, the number of cells in the imaginal discs is not the only determinant of final organ size. Disc size is sensed and controlled by final organ size sensing mechanisms during larval growth that can also modulate cell size, in order to reach the correct organ size with a different number of cells (Day and Lawrence, 2000; Neufeld et al., 1998).

1.9.2 IIS/dTOR signalling

The insulin/PI3K pathway is highly conserved between vertebrates and flies and involves regulation of cell growth and metabolism (Guarente and Kenyon, 2000). In *Drosophila* the insulin/insulin-like growth factor signalling (ISS) system comprises seven insulin-like peptides (dILP1-dILP7), a single insulin receptor (InR), the IRS protein called chico, a class 1A PI3K (dPI3K), the negative regulator dPTEN and the kinases dAkt and dPDK1 (Oldham and Hafen, 2003). The *Drosophila* class 1A PI3K consists of a catalytic subunit (Dp110) and a p55-like regulatory subunit (p60). The InR and its downstream effectors are expressed ubiquitously; the ILPs are expressed in a tissue-specific manner and thus relay different inputs into cellular effects by regulation of the ISS (Brogiolo et al., 2001; Ikeya et al., 2002).

The ISS-TOR cascade in flies also affects carbohydrate metabolism (Rulifson et al., 2002) and lipid homeostasis (Broughton et al., 2005) in a cell type specific and nutrient dependent manner. The signalling pathway mediates glucose uptake and nutrient storage in the fat body, thereby regulating feeding behaviour, lifespan and reproduction (Broughton et al., 2005; Shingleton et al., 2005). Reduction of dTOR function by the hypomorphic $dTOR^{7/p}$ mutant causes a decrease in lipid levels in the fat body. This could be explained by an increased utilization of lipids and their conversion into ketone bodies (Luong et al., 2006). In contrast, activated dAkt results in accumulation of enlarged lipid-droplets in *Drosophila* nurse cells via activation of the conserved lipid-storage protein, LSD2/perilipin (Vereshchagina and Wilson, 2006). Furthermore, *melted* mutant flies produce 40% less fat than normal, due to lowered triglyceride production, which mimics the effect of nutrient deprivation. Melted protein can recruit dFoxO and the dTSC1/2 complex to the plasma membrane, leading to increased dTOR activity and inhibition of dFoxO function (Teleman et al., 2005).

1.9.3 dSREBP

In contrast to vertebrates where there are three SREBP isoforms, the genome of *Drosophila melanogaster* encodes a single SREBP homologue, dSREBP (HLH106 or CG8522) (Theopold et al., 1996). The *Drosophila* genome also contains genes for the dSREBP processing factors dS1P, dS2P and dSCAP, but not the negative regulator INSIG (Seegmiller et al., 2002). In *Drosophila* Schneider S2 cells, dSREBP requires dSCAP for ER to Golgi translocation and dS1P and dS2P for cleavage. Processing releases transcriptionally active mature dSREBP that can enter the nucleus and regulate expression of its target genes, i.e. dFAS (Seegmiller et al., 2002). However, phosphatidylethanolamine, a phospholipid, mediates the feedback regulation of dSREBP cleavage in fly cells (Dobrosotskaya et al., 2002). Flies cannot synthesize

cholesterol, but obtain it exclusively from food. Mutant *dSREBP* flies are fatty acid auxotroph suggesting that the main function of dSREBP in flies is the maintenance of fatty acid homeostasis (Kunte et al., 2006).

1.10 The PI3K and TOR signalling pathways in growth control in mammals and flies

The PI3K/Akt/TOR pathway has been implicated in cell growth in mammalian cells (Kozma and Thomas, 2002) and the regulation of cell and organ size in *Drosophila melanogaster* (Leevers and Hafen, 2004) through activating anabolic pathways for *de novo* protein and lipid biosynthesis as well as synthesis of nucleic acids. These macromolecules provide the essential building blocks required for cell growth (Plas and Thompson, 2005).

1.10.1 Mammals

In mammals, two of the main biological functions of the class 1 PI3K signalling pathway are regulation of cell metabolism and cell growth downstream of insulin and insulin-like growth factor-1 (IGF-1) (Saltiel and Kahn, 2001). Mice deficient in PI3K signalling in muscle exhibit decreased muscle size, impaired insulin-stimulated glucose uptake and elevated levels of circulating lipids (Luo et al., 2006). In addition, activation of PI3K by insulin, IGF-1, PDGF and EGF promote cell growth and proliferation. Over-expression of a constitutively active form of p110α in the heart results in increased cell and organ size (Shioi et al., 2002), whereas dominant negative p110α suppresses IGF-1 induced increase in organ size (McMullen et al., 2004).

The function of Akt in promoting cell growth (i.e. increase in cell mass) is conserved among species. Mice deficient for Akt1 and Akt2 exhibit severe growth deficiency (Peng et al., 2003). Deletion of PTEN leads to enhanced insulin sensitivity and Akt activity in adipose tissue (Kurlawalla-Martinez et al., 2005) resulting in increased cell size in these tissues (Crackower et al., 2002; Kwon et al., 2004). Akt stimulates cell growth predominantly through activation of mTORC1. Akt promotes increased cell size by increasing nutrient uptake via activating surface localisation of amino acids, glucose, LDL and iron transporters as well as stimulating protein synthesis in an mTORC1 dependent manner (Edinger and Thompson, 2002; Faridi et al., 2003). In addition, Akt regulates *de novo* lipid synthesis required for cell growth through activating ACL. Inhibition of ACL blocks cell growth and prevents tumour formation (Bauer et al., 2005; Hatzivassiliou et al., 2005).

TORC1 is essential for normal growth in yeast, *Drosophila*, and mammals (Wullschleger et al., 2006). It has been shown that inhibition of mTORC1 by rapamycin treatment decreases cell size (Fingar et al., 2002; Ohanna et al., 2005; Ruvinsky et al., 2005). The main effectors in mTORC1-mediated cell growth control are S6K and rpS6. Depletion of these proteins is equivalent to mTORC1 inhibition, and rapamycin does not further decrease the small cell size phenotype in those mice (Ohanna et al., 2005; Ruvinsky et al., 2005).

1.10.2 *Drosophila melanogaster*

In *Drosophila melanogaster* cell growth regulation by the IIS system has been studied intensively. Genetic studies show that this pathway regulates cell growth during development, cell size and cell number as well as organ size in the fly. Many IIS components are sufficient for cell autonomous growth control (Edgar, 2006).

Elevated expression of several dILPs increases larval growth rates and adult size (Brogiolo et al., 2001; Ikeya et al., 2002). Hypomorphic *InR* mutants and mutation of *chico* show a dramatic decrease in cell, organ and body size due to reduced growth and proliferation (Bohni et al., 1999; Stocker and Hafen, 2000). Activation or block of dPI3K activity effects cell and organ growth in the *Drosophila* wing and eye tissue (Leevers et al., 1996; Weinkove et al., 1999). Over-expression of the dPI3K catalytic subunit Dp110 results in increased wing size, while over-expression of a dominant negative Dp110 construct results in the opposite phenotype (Weinkove and Leevers, 2000). These phenotypes are due to changes in cell size (Weinkove and Leevers, 2000). In contrast, the *Drosophila* homologue of the tumour suppressor PTEN (dPTEN) antagonizes the Chico/dPI3K signalling dependent cell growth effect. *dPTEN* suppresses hyperplastic growth in flies by reducing cell size and cell number (Bohni et al., 1999; Goberdhan et al., 1999).

dAkt seems to be the central player in controlling growth and body size in response to insulin. dAkt controls cell number by phosphorylation and inhibition of dFoxO (Junger et al., 2003) and controls cell size by activating the dTORC1/dS6K pathway (Potter et al., 2002). However the relevance of the Akt phosphorylation sites at dTSC2 for dTORC1 activation has been questioned (Dong and Pan, 2004). Furthermore, in contrast to findings in mammals, the *Drosophila* PI3K and S6K do not seem to be in a linear pathway (Radimerski et al., 2002b). Interestingly, the dAkt-dependent growth effect does not rely on dTORC2 activity, although dTORC2-stimulated serine 505 phosphorylation is required for dAkt-induced hyperplasia in a *dPTEN* mutant background (Hietakangas and Cohen, 2007). Furthermore, dTORC2 is also

important for the dAkt-mediated inhibition of FoxO signalling *in vivo* (Hietakangas and Cohen, 2007; Lee and Chung, 2007).

dTORC1 protein kinase is one of the most important growth control regulators in flies (Oldham and Hafen, 2003; Oldham et al., 2000; Zhang et al., 2000). Mutations in d*TSC1* and d*TSC2*, which results in activation of dTORC1 signalling, cause strong overgrowth of the eye (Gao and Pan, 2001; Potter et al., 2001; Tapon et al., 2001). Overexpressed dRheb also has positive growth effects (Patel et al., 2003; Stocker et al., 2003). dTORC1 activates proteins involved in growth and translation, including dS6K. Mutation of *S6K* affects cell size but not cell number and the insulin-dependent activation of dS6K occurs through dPI3K, dAkt, dPDK1, as well as dTORC1 both in cell culture and *in vivo* (Lee and Chung, 2007; Lizcano et al., 2003; Radimerski et al., 2002b). In *Drosophila* S2 cells, dRheb/TORC signalling controls growth by promoting protein synthesis, but not glucose or amino acid import (Hall et al., 2007).

1.11 Outline of the thesis

During tumour development, cells require a set of essential alterations in cell physiology that collectively enable malignant growth. Resistance to programmed cell death (apoptosis) and proliferation in the absence of growth factors or in the presence of anti-proliferative signals are among the hallmarks of cell transformation. It has been demonstrated that activated Akt protects cells from apoptosis (Frisch and Screaton, 2001). Constitutive activation of PI3K and its effector Akt is a frequent event in human cancer. Such activation can occur through oncogenic activation of Ras or mutational loss of the tumour suppressor PTEN.

Cells need a sufficient supply of nutrients, metabolic intermediates and precursors for the synthesis of proteins, nucleotides and membrane components to increase in size, which is essential for cell division. Intracellular signalling pathways, which are activated by hormones and growth factors, are involved in the regulation of cell growth. Akt is the major enzyme, which controls insulin-mediated metabolism, such as induction of protein synthesis, lipogenesis, glucose uptake and conversion of glucose into fatty acids and cholesterol (Manning and Cantley, 2007). Sterol regulatory element binding proteins (SREBPs) are the major transcription factors that regulate genes involved in fatty acid and cholesterol synthesis. It has been postulated that a constitutively active PI3K-Akt pathway may be involved in fatty acid and cholesterol accumulation in many solid tumours. Akt appears to have a key role in tumourigenesis, by providing metabolic resources for cell growth and proliferation as well as facilitating escape from apoptosis. Akt has been shown to modulate the activity of several transcription factors and it is likely that regulation of gene expression by Akt plays an important role in its cellular functions.

To improve the understanding of Akt regulated gene expression, an inducible version of the Akt-kinase (myrAkt-ER) was used, which can be activated by treatment with 4-hydroxy-tamoxifen (4-OHT). Human retinal ephithelial cells (RPE) have been generated to stably express the myrAkt-ER construct and have been used in a cDNA based microarray experiment. By comparing mRNA abundance in cells before and after myrAkt-ER activation, several enzymes involved in fatty acid synthesis and cholesterol synthesis have been identified as transcriptional targets for Akt. Expression of these enzymes is controlled by the SREBP-family of transcription factors.

The aim of this thesis was to analyse the involvement of Akt in SREBP regulated lipid-biosynthesis and the potential result of this regulation on the cellular phenotype *in vitro* and *in vivo*. In chapter 3, the role of SREBP in regulating the expression of genes encoding rate

limiting enzymes for fatty acid and cholesterol synthesis by Akt was studied by silencing SREBP or co-expression of dominant negative SREBP constructs. The data indicate that SREBP is required for Akt-induced expression of lipogenic genes. Chapter 4 addresses the mechanism of regulation of SREBP by Akt. Experiments were performed to address whether the observed rapid accumulation of SREBP by Akt may involve downstream effectors of Akt. Findings suggest a GSK3 independent mechanism, however activity of the mTOR complex is required for accumulation of mSREBP and expression of SREBP target genes in response to Akt activation. Furthermore, activation of SREBP by Akt requires ER to Golgi translocation as well as glucose availability, whereas inhibition of glycolysis blocks SREBP activation. In chapter 5, the metabolite profile of RPE cells in response to activated Akt is analysed by nuclear magnetic resonance (NMR). Akt induces glucose and amino acid uptake, lactate production and increased levels of fatty acids and phosphoglycerides. The majority of changes in metabolite concentrations induced by Akt are blocked in the presence of the mTOR inhibitor rapamycin. Furthermore, the contribution of activation of Akt and SREBP in the regulation of mammalian cell growth is investigated. Akt-induced increase in cell size is mTOR dependent and ectopic expression of mature SREBP results in increased cell size. The involvement of SREBP in cell and organ size regulation was studied *in vivo*, using *Drosophila melanogaster* as a model system. The results of this study are described in chapter 6. Silencing of dSREBP in fly causes developmental delay and lethality in a dose dependent manner. Tissue specific silencing of dSREBP causes a reduction in organ size due to a decrease in cell size. Furthermore, results in *Drosophila* tissue culture cells as well as *in vivo* data indicate that the PI3K pathway can induce dSREBP activity and that dSREBP is required for PI3K-induced increased wing size.

These results presented here increase understanding of the regulation between Ras/PI3K/mTOR signalling pathways and lipid biosynthesis pathways via activation of SREBP in the regulation of cell growth, which may provide a novel target for tumour therapy.

Figure 1-1 The Ras signalling pathway

Growth factor binding to receptor tyrosine kinases on the cell surface results in activated receptor complexes, which contain adaptors such as SHC, GRB2 and Gab proteins. These proteins recruit SHP2 and SOS. SOS increases Ras–GTP levels by catalysing nucleotide exchange on Ras. The protein GAP protein neurofibromin (NF1) binds to Ras–GTP and accelerates the conversion of Ras–GTP to Ras–GDP, which terminates signalling. The B-Raf/MEK/ERK cascade regulates the activity of several transcription factors involved in proliferation. Ras also activates the PI3K/PDK1/Akt pathway that frequently determines cellular survival. TIAM1 is an exchange factor of Rac. Rac regulates actin dynamics and, therefore, the cytoskeleton. RALGDS, RALGDS-like gene (RGL) and RGL2 are exchange factors of Ral. Among the effectors of Ral is phospholipase D (PLD) an enzyme that regulates vesicle trafficking. Ras also binds and activates the enzyme phospholipase C epsilon (PLCε), the hydrolytic products of which regulate calcium signalling and the protein kinase C (PKC) family. P, phosphate; Y, receptor tyrosine. Adapted from (Schubbert et al., 2007).

Figure 1-1

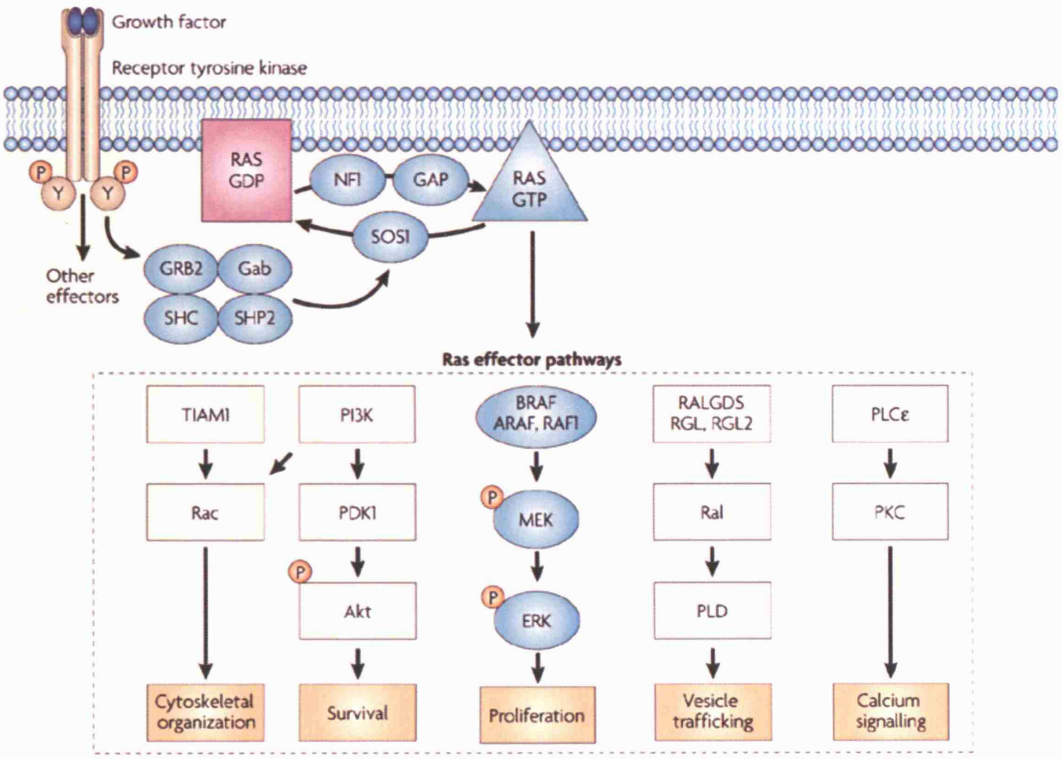

(from Schubbert, 2007) **Nature Reviews** | Cancer

Figure 1-2 The PI3K signalling pathway

Activated RTKs activate class I PI3K through direct binding or through tyrosine phosphorylation of scaffolding adaptors, such as IRS1, which then bind and activate PI3K. The complexes localise at the membrane where the p110 subunit of PI3K catalyses the conversion of PIP2 to PIP3, in a reaction that can be reversed by the PIP3 phosphatase PTEN. PIP3 serves as a second messenger that results in activation of Akt. PI3K has also been shown to regulate the activity of other cellular targets, such as SGK, the small GTP-binding proteins Rac1 and CDC42, and PKC, in an Akt-independent manner. The activation of these targets contributes to survival, cytoskeletal rearrangement and transformation. Adapted from (Vivanco and Sawyers, 2002).

Figure 1-2

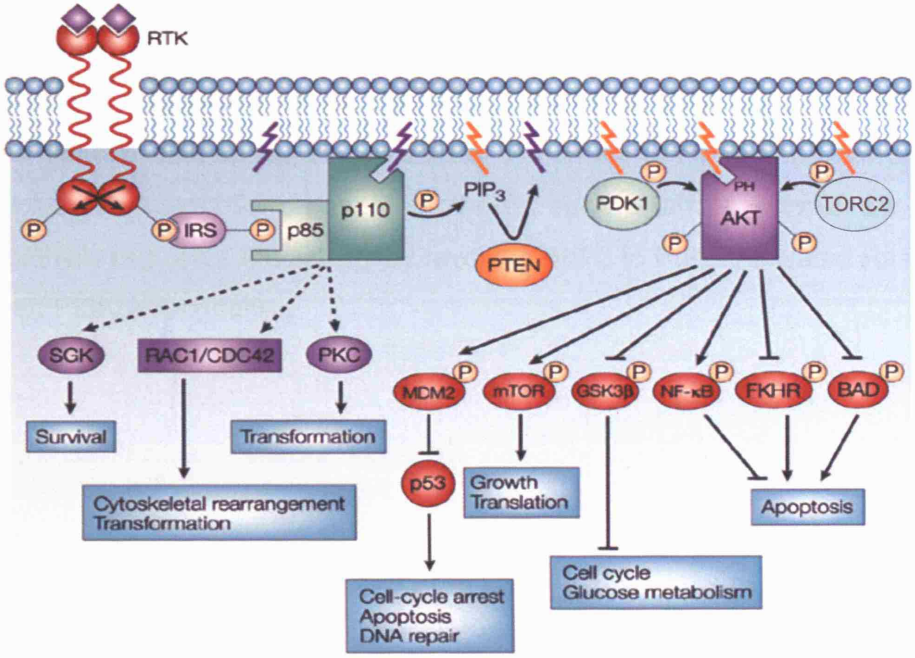

(adapted from Vivanco, 2002) **Nature Reviews** | Cancer

Figure 1-3 The PI3K/Akt signalling pathway

Akt and PDK1 bind to PIP3 at the plasma membrane via their PH domains. PDK1 phosphorylates the activation loop of Akt at threonine 308. RTK signalling also activates TORC2 through a currently unknown mechanism, and TORC2 phosphorylates Akt on serine 473 in the hydrophobic motif. Both phosphorylations are required for full activation of Akt kinase activity. A number of direct and indirect targets of Akt involved in metabolism, protein synthesis, survival and cell cycle are shown. PTEN negatively regulates Akt activity by reversing PIP3 to PIP2. Activated Ras results in enhanced PI3K/Akt signalling.

Figure 1-3

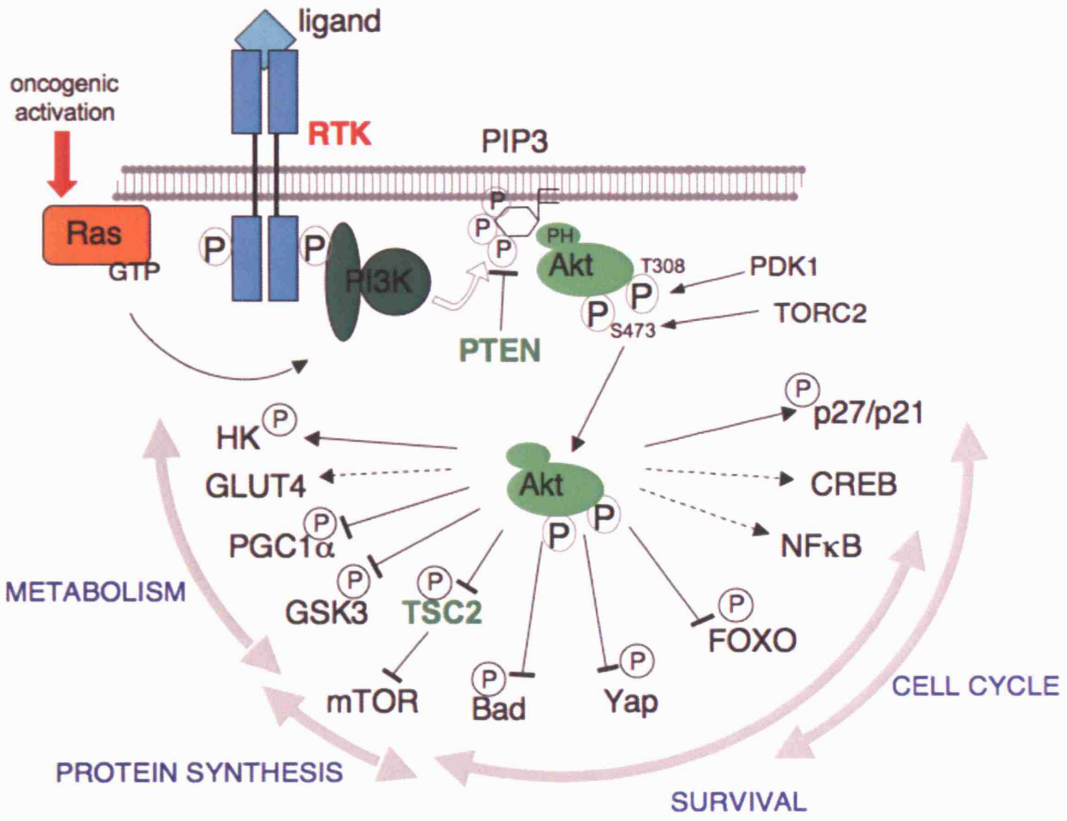
ligand
oncogenic activation
RTK
PIP3
Ras
GTP
PI3K
PH
Akt
T308
PDK1
S473
TORC2
PTEN
HK
GLUT4
PGC1α
GSK3
TSC2
mTOR
Bad
Yap
FOXO
p27/p21
CREB
NFκB
METABOLISM
CELL CYCLE
PROTEIN SYNTHESIS
SURVIVAL

Figure 1-4 The Akt/mTOR signalling pathway

(A) PDK1 phosphorylates Akt at T308 and mTORC2 phosphorylates Akt at S473, which can be dephosphorylated by the S473 phosphatase PHLPP. Akt activates mTORC1 through multisite phosphorylation of TSC2 within the TSC1-TSC2 complex, and this blocks the ability of TSC2 to act as a GAP for Rheb, thereby allowing Rheb-GTP to accumulate. Rheb-GTP activates mTORC1, which phosphorylates downstream targets 4E-BP1 and S6 kinases. Akt can also activate mTORC1 by phosphorylating PRAS40, thereby relieving the PRAS40-mediated inhibition of mTORC1. Once active, both mTORC1 and S6K can phosphorylate serine residues on IRS1, which targets IRS1 for degradation. This induces a negative feedback mechanism and attenuates PI3K/Akt signalling. Adapted from (Manning and Cantley, 2007).

(B) The mTOR signaling network consists of two major branches, each mediated by a specific mTOR complex (mTORC). Rapamycin-sensitive mTORC1 controls several pathways that collectively determine the mass (size) of the cell such as translational initiation, ribosome biogenesis, metabolism and inhibition of autophagy. Rapamycin-insensitive mTORC2 controls the actin cytoskeleton. mTORC1 and possibly mTORC2 respond to growth factors (insulin/IGF). mTORC1 activity is also sensitive to cellular levels of amino acids and ATP:ADP ratio, which is an index of cellular energy levels. mTORC1 senses energy levels through AMPK, which is activated by the LKB1 protein kinase, and inhibits the TSC1–TSC2 complex. It remains elusive how mTORC1 senses amino-acid levels. mTORC1 (and likely mTORC2) are multimeric, although drawn as monomers for simplicity. Adapted from (Wullschleger et al., 2006).

Figure 1-4

A)

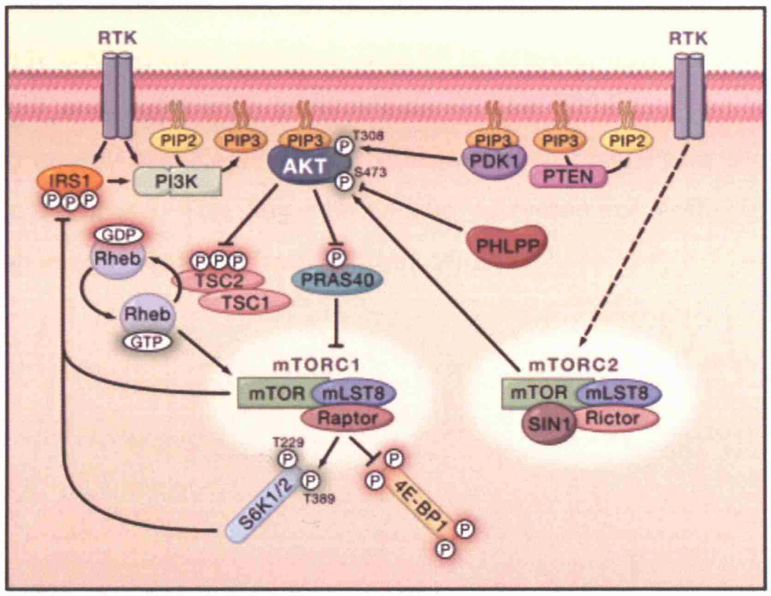

(adapted from Manning, 2007)

B)

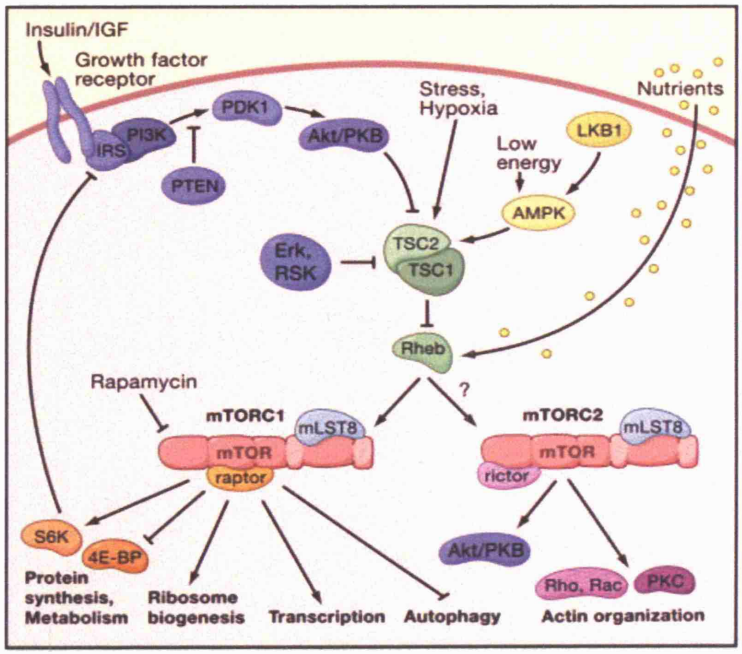

(from Wullschleger, 2006)

Figure 1-5 Genes regulated by SREBPs

The diagram shows the major metabolic intermediates in the pathways for synthesis of cholesterol, fatty acids, and triglycerides. *In vivo*, SREBP2 preferentially activates genes for cholesterol biosynthesis, whereas SREBP1c preferentially activates genes involved in fatty acid and triglyceride biosynthesis. These pathways use ATP as a source of metabolic energy and NADPH as a reducing power. NADPH is the electron carrier for anabolic reactions. The key rate-limiting enzymes for both biosynthetic pathways are shown in bold. Adapted from (Horton, 2002).

Figure 1-5

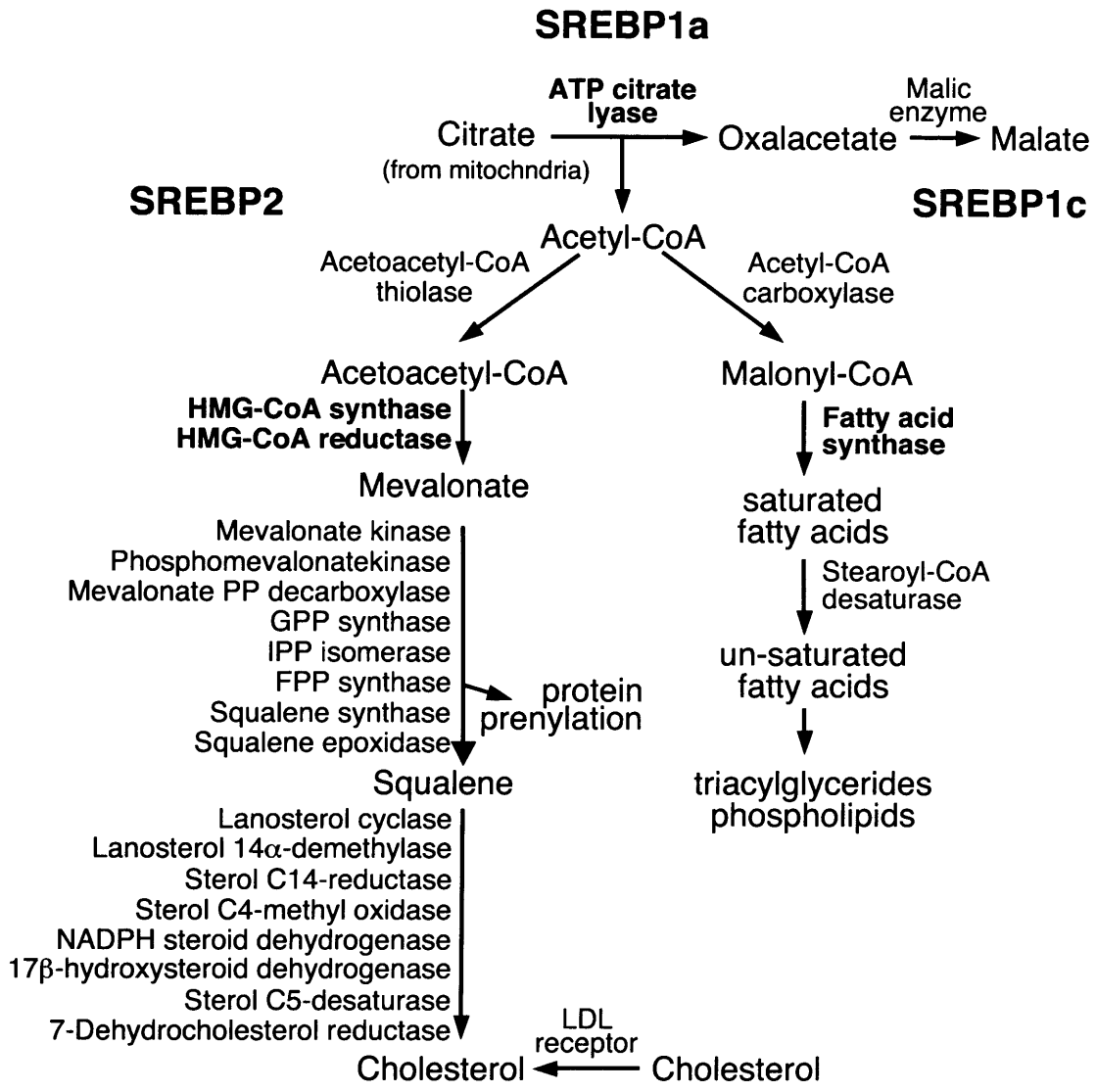

(adapted from Horton, Goldstein and Brown, 2002)

Figure 1-6 Sterol regulated intramembrane processing (RIP) of SREBP proteins

Full length SREBP proteins reside in the ER membrane in a complex with the SREBP cleavage activating protein SCAP. Under low sterol conditions, the SREBP/SCAP complex can bind to COPII proteins and translocate to the Golgi. SREBP is cleaved by site1 and site2 proteases and the N-terminal part of the protein can enter the nucleus. Under saturating sterol conditions, SCAP binds to INSIG and undergoes a conformational change, which masks the COPII binding site. The SREBP/SCAP/INSIG complex is retained in the ER. DNA-bound mSREBP1 can be phosphorylated by GSK3. As a result, the ubiquitin ligase Fbw7 is recruited and induces ubiquitination and degradation of mSREBP1.

Figure 1-6

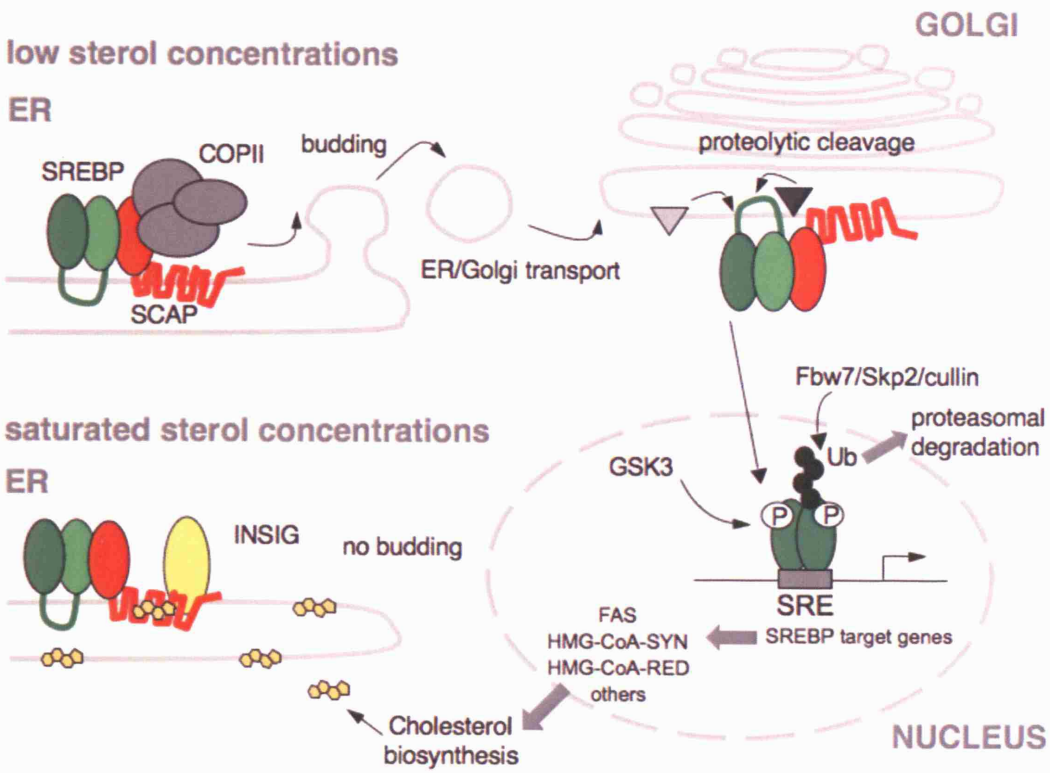
GOLGI
low sterol concentrations
ER
SREBP
COPII
budding
SCAP
ER/Golgi transport
proteolytic cleavage
Fbw7/Skp2/cullin
proteasomal degradation
Ub
saturated sterol concentrations
ER
INSIG
no budding
GSK3
P
P
SRE
FAS
HMG-CoA-SYN
HMG-CoA-RED
others
SREBP target genes
Cholesterol biosynthesis
NUCLEUS

Figure 1-7 Model of *de novo* lipid biosynthesis

Activation of glucose uptake and induction of glycolysis is required for the generation of mitochondrial citrate. Phosphorylation and activation of ATP-citrate lyase (ACL) increases the production of cytoplasmic Acetyl-CoA, which is the substrate for Acetyl-CoA carboxylase (ACC) and fatty acid synthase (FAS) as well for HMG-CoA synthase (HMGS) and HMG-CoA reductase (HMGR).

Figure 1-7

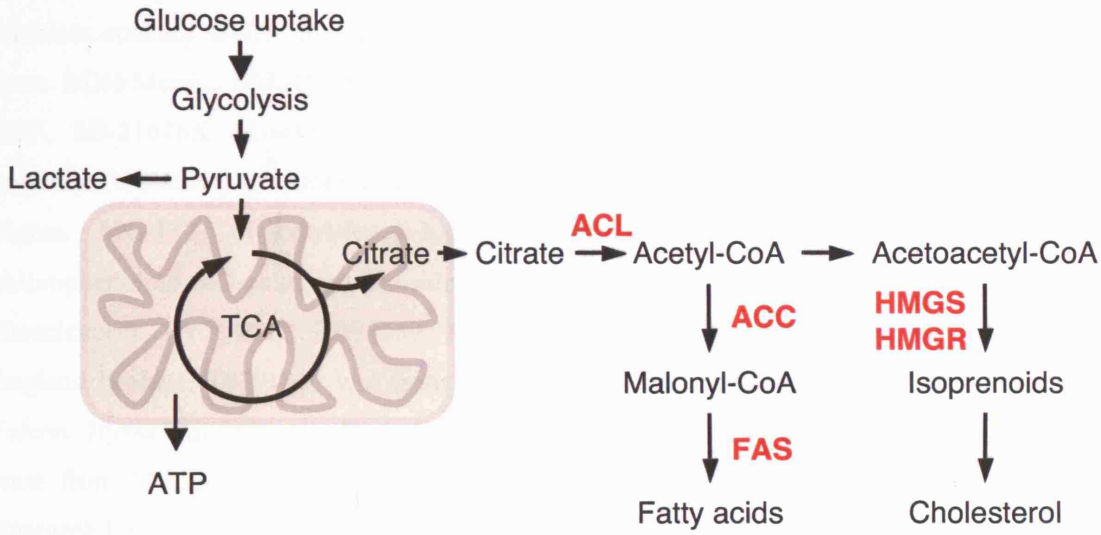
Glucose uptake
Glycolysis
Lactate
Pyruvate
TCA
ATP
Citrate
Citrate
ACL
Acetyl-CoA
Acetoacetyl-CoA
ACC
HMGS
HMGR
Malonyl-CoA
Isoprenoids
FAS
Fatty acids
Cholesterol

2 Chapter 2: Materials and Methods

2.1 Chemicals and enzymes

Lipoprotein deficient serum (LPDS) was from Autogen Bioclear (Intracel), foetal calf serum was from PAA Laboratories, HAMS F12 and polyHEMA were from Sigma-Aldrich. Protease inhibitor cocktail tablets (Complete, EDTA-free) were purchased from Roche. Ethanol was from BDH/Merck. DMSO, BSA, 4-hydroxy-tamoxifen, 25-hydroxycholesterol, cholesterol, EGF, SB-216763, SB-415286, LiCl, 2-deoxy-D-glucose, 5-thio-glucose, actinomycin D, brefeldin A, insulin, arachidonic acid, cycloheximide and methyl pyruvate were obtained from Sigma. MG-132, N-acetyl-leucyl-leucyl-norleucinal (ALLN), rapamycin, AICAR and chlorophenolred-ß-D-galactopyranoside were purchased from Calbiochem (Merck Biosciences). LY294002, PD98059, UO126 and all restriction enzymes were from New England Biolabs. T0901317 was from Cayman Chemical. Plasticware was from Corning and Falcon. Hyperfilm ECL was from Amersham. Filter units and PVDF membrane (Immobilon) were from Millipore. The following sterile buffers and solutions were provided by Cancer Research UK central services: deionised water, phosphate buffered saline PBS (±Ca2+/Mg2+), LB medium, LB-agar, E4 (Dulbecco's modified Eagle medium) medium, trypsin/versene, glutamine, sodium bicarbonate.

2.2 Cell lines

2.2.1 Bacterial strains

strain:	used for:
XL1-Blue (Stratagene)	cloning
XL10-Gold (Stratagene)	site-directed mutagenesis

2.2.2 Mammalian cell lines

RPE myrAkt-ER and U2OS myrAkt-ER cells were originally developed by Dr. S. Basu (CRUK, Bart's hospital). U2OS cells were obtained from ATCC. hTERT-RPE1 (RPE) cell line was originally purchased from BD Biosciences. RPE mSREBP1a-ER and RPE mSREBP2-ER cell lines were developed by Beatrice Griffiths (GEA, CRUK-LRI) by retroviral transduction.

2.3 DNA

2.3.1 Plasmid constructs

The fatty acid synthase promoter constructs pGL2-FAS -150 to -73 (NEG) and pGL2-FAS -150 to -43 (WT) were a gift from Dr. T. Osborne, UC Irvine, Irvine, CA. pCMV-SREBP-1a, -1c, -2 were a gift from Dr. Shimano, OKINAKA Memorial Institute of Medical Research, Tokio, Japan. Dominant negative SREBP proteins, SREBP1a (m1aYA), SREBP1c (m1cYA) and SREBP2 (m2YA) were generated by site-directed mutagenesis using the QuickChange Kit from Stratagene by replacing the conserved tyrosine residue in the DNA binding domain (EKRY) with an alanine residue (EKRA). The HMG-CoA synthase promoter constructs pGL3-SYNwt-luc, pGL3-SYNmutSRE1 and pGL3-SYNmutSRE2 were a gift from Dr. J. Swinnen (Catholic University of Leuven, Leuven, Belgium). pcDNA3 was obtained from J. Downward (CRUK-LRI). CMV-ß-Gal (LacZ) was obtained from R. Treisman (CRUK-LRI), pRL-CMV (Renilla Luciferase) was obtained from Promega. The Fbw7-RNAi construct (pSuper-Fbw7-RNAi, pSuper is based on BlueScript-KS) and pIRES2-EGFP-Fbw7-Flag tagged construct were a gift from Dr. A. Behrens (CRUK-LRI).

The rat mTOR construct pcDNA3-AU1-mTORwt was a gift from Dr. G. Chiang (Burnham Institute for Medical Research, USA). The pCMV-INSIG2-myc construct was obtained from the ATCC (No. MBA-12). The hamster SCAP construct pCMV-SCAP was obtained from the ATCC (No. 63366).

2.3.2 Primers

All primers are 5' - 3'.

2.3.2.1 Cloning primers

Oligonucleotides were synthesised and purified by the Oligonucleotide Synthesis Service, Cancer Research UK, Clare Hall.

SREBP1 forward 5' CCACAACGCCATTGCGGCGCTCGCCCTCTCCTCCATCAATG 3'

SREBP1 reverse 5' CATTGATGGAGGAGAGGGCGAGCGCCGCAATGGCGTTGTGG 3'

Nterm-SREBP1 seq 5' CTGCCCCACTCCCAGCATAG 3'

dnSREBP1 forward 5' GCCATTGAGAAGCGCGCCCGCTCCTCCATCAATG 3'

dnSREBP1 reverse 5' CATTGATGGAGGAGCGGGCGCGCTTCTCAATGGC 3'

SREBP1 seq 5' GTGCAGACAGGGCCTTTGCC 3'

dnSREBP2 forward

5'CCCATAATATCATTGAGAAACGAGCTCGCTCCTCCATCAATGAC 3'

dnSREBP2 reverse 5'

GTCATTGATGGAGGAGCGAGCTCGTTTCTCAATGATATTATGGG 3'

SREBP2 seq 5' CCTGGTGGGCAGCAGTGGGACC 3'

2.3.2.2 Reverse transcription gene specific primers

SREBP1 5' GACTCTTCCTTGATACCAGGCC 3'

SREBP2 5' TCGATGCCCTTTAGAAGCTTG 3'

GAPDH 5' ATGGCATGGACTGTGGTCAT 3'

2.3.2.3 Real-time PCR primers

Human:

HMG-CoA synthase, forward 5' GGACACCCATCATTTGGTCAA 3'

reverse 5' CGAGCGTAAGTTCTTCTGTGCT 3'

HMG-CoA reductase, forward 5' TGGACAGGATGCAGCACAGAA 3'

reverse 5' TGGCATGGTGCAGCTGATAT 3'

fatty acid synthase, forward 5' GAAACTGCAGGAGCTGTC 3'

reverse 5' CACGGAGTTGAGCCGCAT 3'

SREBP1a, forward 5' GCGAGCCGTGCGATCTG 3'

reverse 5' GGCTTCAAGAGAGGAGCTCAA 3'

SREBP1c, forward 5' GGAGGGGTAGGGCCAACGGCCT 3'

reverse 5' CATGTCTTCGAAAGTGCAATCC 3'

SREBP2, forward 5' GAAAGGCGGACAACCCATAAT 3'

reverse 5' AGAACGCCAGACTTGTGCATC 3'

INSIG1, forward 5' CACGCCAGTGCTAAATTGGAT 3'

reverse 5' AAGGCCACTTCTGGAACGATC 3'

INSIG2, forward 5' CATGCCAGTGCTAAAGTGGATT 3'

reverse 5' CAAGGCCAAAACCACTTCTAGA 3'

GAPDH, forward 5' ACAGCCTCAAGATCATCAGCAA 3'

reverse 5' ATGGCATGGACTGTGGTCATG 3'

GAPDH (sequence specific cDNA), forward 5' GTCGGAGTCAACGGATTTGGT 3'

reverse 5' CGGTGCCATGGAATTTGC 3'

Fly:

dfatty acid synthase, forward 5' CCCCAGGAGGTGAACTCTATCA 3'
reverse 5' GACTTGACCGATCCGATCAAC 3'
dSREBP, forward 5' GGCAGTTTGTCGCCTGATG 3'
reverse 5' CAGACTCCTGTCCAAGAGCTGTT 3'
dactin 5C, forward 5' CACCCTGAAGTACCCCATTGAGCAC 3'
reverse 5' CAGACGCAGGATGGCATGGGGAAGG 3'

2.3.2.4 RNAi templates (fly cell culture)

Primers contained 5'T7 RNA polymerase-binding sites preceded by a GAA overhang and followed by sense (forward) or antisense (reverse) sequence.
dAkt, forward 5' GACCGTTTGTTCTTCAGCGGCG 3'
reverse 5' TCCGGAATCGTGTGTAGGGGC 3'
Dp110, forward 5' CGCGCTCGAAGAAATCGTCC 3'
reverse 5' TCAGAAAGTGTAAGCACCGG 3'
dfatty acid synthase, forward 5' CATTCCCGGTAACTTGCACT 3'
reverse 5' GTTTTCGAAGCTCTTGTCCG 3'
dPTEN, forward 5' CATGCCCAGCATTACAAA 3'
reverse 5' TATATATTTGTTAACTGT 3'
dSREBP, forward 5' GCTACAATTGTCCCCAGCAACAGCCG 3'
reverse 5' GCCCAGCTGAAGTAAATCCTTCACC 3'
dTSC2, forward 5' AATGTGCTGACAGCCTTCCT 3'
reverse 5' GGCACACTCGACTCCAGATGA 3'
gfp, forward 5' CGACGGCCAGTGAATTGTAATACGACTC 3'
reverse 5' TACGCCAAGCTCATAATACGACTCACTAT 3'

2.3.3 siRNA oligos

2.3.3.1 Ambion

Silencer Negative Control, catalogue number 4615
GFP, catalogue number 16106, 5' GACCCGCGCCGAGGUGAAGtt 3'
SREBP1, sense: 5' GGAAGAGUCAGUGCCACUGtt 3'
antisense: 5' CAGUGGCACUGACUCUUCCtt 3'
SREBP2, sense: 5' GGUCACAUUACCUUCCUUCtt 3'
antisense: 5' GAAGGAAGGUAAUGUGACCtg 3'

2.3.3.2 Dharmacon

siCONTROL Non-Targeting siRNA SmartPool, catalogue number 001206
Human GAPDH SmartPool, catalogue number 004253,
oligo 1: 5' CAACGGAUUUGGUCGUAUUUU 3'
oligo 2: 5' GACCUGACCUGCCGUCUAGUU 3'
oligo 3: 5' CAAUAUGAUUCCACCCAUGUU 3'
oligo 4: 5' GCGAUGCUGGCGCUGAGUAUU 3'
Human FRAP1Smart pool, catalogue number 003008,
oligo 1: 5' GGCCAUAGCUAGCCUCAUAUU 3'
oligo 2: 5' CAAAGGACUUCGCCCAUAAUU 3'
oligo 3: 5' CAGAAUUGUCAAGGGAUAUU 3'
oligo 4: 5' CCAAAGCACUACACUACAAUU 3'

2.4 Antibodies

Actin, C-11, goat polyclonal, Santa Cruz Biotechnology
P-Akt (Ser/Thr) substrate, rabbit polyclonal, Cell Signaling
P-Akt (Ser473), rabbit polyclonal, Cell Signaling
P-Akt (Thr308), rabbit polyclonal, Cell Signaling
ATP-citrate lyase, rabbit polyclonal, Cell Signaling
P-ß catenin (Ser33/37/Thr41, rabbit polyclonal, Cell Signaling
DP-1, 1DP06, mouse monoclonal, Stratech Scientific
ERα, polyclonal, Santa Cruz Biotechnology
Fatty acid synthase, mouse monoclonal, Cell Signaling
GAPDH, 9484 (HRP-conjugated), mouse monoclonal, Abcam
GSK3α, rabbit polyclonal, Upstate
P-GSK3α/β, rabbit polyclonal, Cell Signaling
Lamin B1, C-20, goat polyclonal, Santa Cruz Biotechnology
P-s6rb, rabbit polyclonal, Cell Signaling
SREBP2, IgG-1C6, mouse monoclonal, BD Biosciences
SREBP1, IgG-2A4, mouse monoclonal, BD Biosciences
TOR, rabbit polyclonal, Cell Signaling

All primary antibodies were used at dilutions recommended by the manufacturer's, unless otherwise indicated. Secondary anti-mouse, anti-rabbit antibodies (Amersham) and anti-goat (Dako) coupled to horseradish peroxidase (HRP) were used at a dilution of 1:2000.

2.5 Tissue culture techniques

Media and solutions:

PBSA: 137 mM NaCl, 3.35 mM KCl, 10 mM Na2HPO4, 1.84 mM KH2PO4, pH 7.2; trypsin/versene: 0.05% trypsin (w/v), 0.02% EDTA (w/v), 1% phenol red in PBSA;

E4-medium (DMEM); glutamine stock 250 mM; sodium bicarbonate stock 7.5%; lipoprotein deficient serum (LPDS); foetal calf serum (FCS); HAMS F12; polyHEMA;

ethanol; 4-hydroxy-tamoxifen (4-OHT); BSA; DMSO

2.5.1 Preparation of polyHEMA plates

To maintain suspension cell cultures, plates were coated twice with 0.2 ml/cm^2 of polyHEMA dissolved in ethanol at a concentration of 10 mg/ml. After the ethanol had evaporated the plates were washed twice with PBS.

2.5.2 Maintenance of mammalian cells

RPE myrAkt-ER cells were maintained in DMEM/HAMS F12 medium (1:1) supplemented with 10% FCS, 2 mM L-glutamine, and 0.348% sodium bicarbonate in humidified incubators at 37°C and 5% CO2. U2OS and U2OS myrAktER cells were maintained in DMEM medium supplemented with 10% FCS, 2-4 mM L-glutamine in humidified incubators at 37°C and 10% CO2. For passaging, the media were removed; cells were washed in PBS and incubated in trypsin-versene. To inactivate the trypsin, the cells were diluted into growth medium. Cells were then plated onto new dishes at a dilution of 1:2 to 1:10.

2.5.3 Cryopreservation of cells

Solution:

Freezing mix: 10% sterile DMSO, 40% FCS plus 50% culture media

For cryopreservation, media were removed; cells were washed in PBS and incubated in trypsine-versene. To stop the reaction, cells were diluted into growth media and centrifuged at 1000 rpm for 5 mins. The cell pellet was resuspended in freezing mix containing 10% sterile DMSO, 40% FCS and 50% media and transferred in 1 ml aliquots into cryovials (Nunc). The

cryovials were transferred into a freezing chamber, which is filled with isopropanol for gradual temperature adjustment and maintained at -70°C overnight. Cells were stored in liquid nitrogen.

For recovery from nitrogen, cells were quickly thawed at 37°C, diluted into growth medium, centrifuged at 1000 g for 5 mins, resuspended in fresh medium and plated. The medium was changed the next day.

2.5.4 Plating of cells for adherent and suspension experiments

Media were removed; cells were washed in PBS and incubated in trypsine-versene. To stop the reaction, cells were diluted in growth media and transfer into a 50 ml tube. Cells were counted using a Neubauer chamber and $3x10^5$ cells per 10 cm or $7.5x10^5$ cells per 15 cm plate were centrifuged for 5 mins at 1000 rpm at room temperature (RT). The cell pellet was resuspended in media containing 10% or 0.5% FCS. Cells were then plated on normal or polyHEMA coated plates and treated with 4-hydroxy-tamoxifen (4-OHT) or solvent (ethanol) or other drugs for 24 or 48 hours.

2.5.5 Mammalian cell size estimation

Cell size was assessed either by measuring cell volume using a Z2 Coulter Counter (Multisizer II, Beckman-Coulter) or by measuring forward light scatter (FSC) in a fluorescence-activated cell sorter (Becton Dickinson LSRII Flow cytometer). These analyses were carried out by Beatrice Griffiths (GEA, CRUK-LRI).

2.5.5.1 Coulter Counter

Cells were harvested by trypsinisation and resuspended in PBS. Cell size was analysed by measuring cell volume using a Z2 Coulter Counter (Multisizer II, Beckman-Coulter).

2.5.5.2 FACS

Cells were harvested by trypsinisation and washed in PBS. Each sample was then treated with 20 μg/ml cell-permeant DNA dye Hoechst 33342 and 200 μl of 50 μg/ml propidium iodide (PI). Cells were then analysed by FACS using a Becton Dickinson LSRII Flow cytometer as previously described (Darzynkiewicz and Bedner, 2000). Debris and cell doublets were excluded from the analysis and only PI-negative cells were analysed to avoid distractive effects

of cell death on cell size. For each sample at least 10,000 events were acquired. Forward light scatter as an indication for cell size was measured and data analysis was performed using FloJo software (TreeStar).

2.6 Protein techniques

2.6.1 Preparation of Cell Lysates

For detection of processed SREBP protein, cells were treated with 25 µg/ml N-acetyl-leucyl-leucyl-norleucinal (ALLN) for 2 hours before lysis.

Solutions:
TNET: 1% Triton X100, 1 mM sodium orthovanadate, 1 mM DTT, 50 mM Tris pH 7.5, 300 mM NaCl, 1 mM EGTA and Protease-Inhibitor-Cocktail (Roche) or Triton/sodium deochycholate lysis buffer: 1% Triton X100, 0.2% sodium deoxycholate, 140 mM NaCl, 10% glycerol, 50 mM Tris pH 8, Protease-Inhibitor-Cocktail and 25µM ALLN
4× SDS-Buffer: 320 mM Tris/HCl ph 6.8, 8% SDS, 300 mM DTT, 40% glycerol, 0.1% bromphenol-blue

2.6.1.1 Total cell lysates

Adherent cells:

In order to harvest any potentially detached apoptotic cells, the growth medium was transferred into a 15 ml centrifuge tube and centrifuged for 5 mins at 2000 rpm at 4°C. The supernatant was discarded. The cell monolayers were washed with cold PBS, which was used to resuspend the pellet. After a second centrifugation for 3 mins at 2000 rpm at 4°C the supernatant was discarded and the pellet was dissolved in TNET lysis buffer. Lysis buffer containing the resuspended pellet was added to the monolayer and the cells were incubated for 20 mins on ice on a rocker, scraped from the plate and collected into a microcentrifuge tube. After centrifugation for 5 mins at 13,000 rpm at 4°C, the supernatant was transferred into a new tube, snap frozen on dry ice and stored at -80°C.

Suspension cells:

The medium was transferred into a 15 ml centrifuge tube and centrifuged for 5 mins at 2000 rpm at 4°C. The supernatant was discarded. The plates were washed with cold PBS, which was used to resuspend the cell pellet. After a second centrifugation for 3 mins at 2000 rpm at 4°C the supernatant was discarded, the pellet dissolved in TNET lysis buffer and incubated for 20 mins on ice. After centrifugation at 13,000 rpm for 5 mins at 4°C the supernatant was transferred into a new tube, snap frozen on dry ice and stored at -80°C.

2.6.1.2 SDS-lysis

The medium was removed and cells were washed in cold PBS. Cells were then incubated in SDS-lysis buffer, scraped off the plate and transferred into a new tube. After incubation at 95°C for 5 mins, the lysate was vortexed and pipetted up and down several times to shear genomic DNA. The lysate was centrifuged for 10 mins at 13,000 rpm at 4°C and the supernatant was transferred into a new tube.

2.6.2 Cell Fractionation

Protein concentration of all fractions was determined using the Bradford method, described in 2.6.5.

2.6.2.1 Pierce protocol

Cell harvesting was prepared as described in section 2.6.1.1 with the modification that the cell pellet was left as dry as possible and estimated or weighed. Nuclear extraction was performed, using the NE-PERTM Nuclear and Cytoplasmic Extraction Reagents (Pierce), according to the manufacturer's instruction. The cytoplasmic and nuclear fractions were stored at -80°C and protein determined by Bradford assay for Western blot analysis.

2.6.2.2 Goldstein/Brown adapted protocol

Solution:
Buffer 1: 10 mM Hepes-KOH, 10 mM KCL, 1.5 mM MgCl2, 0.5 mM EDTA, 0.5 mM EGTA, 25µg/ml ALLN, + Protease-Inhibitor-Cocktail;
Buffer 2: 10 mM Hepes-KOH, 0.42 M NaCl, 1.5 mM MgCl2, 0.5 mM EDTA. 0.5 mM EGTA, 2.5% glycerol, Protease-Inhibitor-Cocktail

The standard method for fractionation of cells and purification of nuclei is based on a method of Dignam et al. (Dignam et al., 1983). Cells were harvested as described above, collected by centrifugation at 3000 rpm for 5 mins at 4°C and the nuclear fraction was prepared as described by Wang et al. (1994) with modification (Wang et al., 1994). The pellet was resuspended in 3 volumes of buffer 1 and incubated for 10 mins on ice. Passing them 15 times through a 23 gauge-needle disrupted cells and the lysate was centrifuged at 3200 rpm (1000 g) for 5 mins at 4°C. The pelleted nuclei were resuspended in 1.5 times pellet volume of buffer 2, incubated on a rotator for 30 mins at 4°C and centrifuged for 15 mins at 13,000rpm. The supernatant was designated as the nuclear fraction. The supernatant from the 1000 g centrifugation was centrifuged at 100,000 × g for 30 mins at 4°C to obtain the membrane fraction (pellet). The membrane fraction was dissolved in 100 µl SDS-lysis buffer. All fractions were snap frozen and stored at -80° before protein determination and Western blot analysis.

2.6.3 Transient transfection of cells

2.6.3.1 DNA transfection

The FAS promoter constructs and SYN promoter constructs were described before (Bennett et al., 1995; Swinnen et al., 2000). U2OS or U2OS myrAkt-ER cells were transfected using the Effectene® Transfection Reagent from Qiagen. The day before transfection, $1x10^5$ cells were plated in a well of a 6 well plate and cultured in medium containing 10% FCS. Transfections were carried out with 0.1-1.5 µg of plasmid DNA in 100 µl DNA-condensation buffer and Enhancer solution in a ratio of 1:8 (mass DNA [µg]: volume Enhancer [µl]). The mixture was then briefly vortexed, incubated at RT for 2-5 mins and briefly centrifuged. After adding 10 µl Effectene Transfection Reagent the mixture was mixed by pipetting up and down five times and incubated for 10 mins at RT to allow transfection complex formation. Meanwhile, the growth media were aspirated from the plate; cells were washed once with PBS and 1.5 ml fresh culture medium was added to the cells. 600 µl medium was added to the tube containing the transfection complexes, mixed by pipetting up and down twice and the mixture was added drop-wise to the cells. To ensure uniform distribution the dishes were gently swirled. The medium was exchanged for 1% FCS medium after 1 day and cells were treated with different drugs and inhibitors for 1-24 hours. Cells were harvested 2 days after transfection.

U2OS cells were transfected using the FuGENE6 Transfection Reagent from Roche. The day before transfection $1x10^5$ cells were plated in a well of a 6 well plate and cultured in 10% FCS. 0.4-1.5 µg DNA was mixed with Fugene6 reagent by gently tapping the tube at a ratio of 1:3 (volume FuGENE [µl]: mass DNA [µg]) in 200 µl growth medium. After incubation for a minimum of 15 mins at room temperature to allow transfection complex formation, the mixture was vortexed briefly, collected in the bottom of the tube by centrifugation and added drop-wise to the cells. The medium was exchanged after 1 day. Cells were harvested 2 days after transfection.

2.6.3.2 siRNA transfection

Dharmafect

Delivery of siRNA into U20S-AktER was performed using Dharmafect2 according to the manufacturer's guidelines (Dharmacon). Optimisation was performed with the Dharmacon siGlo GAPDH oligo and transfection efficiency was determined using FACS. Following optimisation, cells were transfected with either Non-Targeting siRNA SmartPool, GAPDH siRNA SmartPool or siRNA SmartPool against human target genes (all from Dharmacon) at a

final concentration of 70 nM. 24 hours following transfection the medium was replaced with fresh medium. 72 hours after transfection, the cells were harvested and assayed.

TransMessenger

U2OS-myrAkt-ER cells were seeded into a 24 well plate in medium containg10% FCS. After 24 hours, 0.8 µg of siRNA oligonucleotides specific for SREBP1 or SREBP2 or an unspecific control oligonucleotide were transfected using TransMessenger Transfection reagent kit (Qiagen) in serum free medium. For analysis of protein expression, medium was replaced with medium containing 0.5% FCS 3 hours post-transfection, cells were treated with 4-OHT or solvent for 48 hours and whole cell lysates were prepared. For analysis of FAS promoter activity, 24 hours after siRNA transfection, cells were transfected with pGL2-FAS. 24 hours post-transfection, medium was replaced with medium containing 0.5% FCS and cells were treated with 4-OHT or solvent for 24 hours. Cells were lysed and FAS promoter activity was analysed as described in section 2.12.

2.6.4 Harvesting of transiently transfected cells for reporter assay

Passive Lysis Buffer

The growth medium was removed and cells were washed with 4ml PBS. After complete removal of the PBS, 250 µl Passive Lysis Buffer (PLB) (Promega) was applied to the cells, which were immediately scraped off the dish and transferred to a new tube. After two freeze/thaw cycles to achieve complete lysis, the mixture was centrifuged for 30 seconds at 13,000 rpm at 4°C, the supernatant was transferred into a fresh tube and used for reporter enzyme analysis (2.12).

Reporter Lysis Buffer

The growth medium was removed and cells were washed with 4 ml PBS. After complete removal of the PBS, 250 µl Reporter Lysis Buffer (RLB) (Promega) was applied to the cells and plates were frozen at –80°C. Then cells were thawed on ice on a rocker, harvested with a cell scraper and transferred to a fresh tube. The tubes were vortexed for 10 seconds, centrifuged for 5 mins at 13,000 rpm at 4°C; the supernatant was transferred into a fresh tube and used for reporter enzyme analysis (2.12).

2.6.5 Protein determination by Bradford assay

Protein concentrations were determined with the Bio-Rad protein assay. Serial dilutions of a BSA protein standard (BioRad) and samples were made up in water and mixed with 250 µl dye

solution and incubated for 5-30 mins at RT. Absorption was measured at 595 nm using an ELISA plate reader. Protein concentration was calculated from the BSA standard curve.

2.7 SDS-PAGE and Transfer

2.7.1 SDS polyacrylamide gel electrophoresis (SDS-PAGE)

Solutions:
1M Tris/Cl ph 8.8 separating buffer: 1.5 M Tris-HCl pH 8.8, 0.4 % (w/v) SDS;
1M Tris/Cl ph 6.8 stacking buffer: 1.0 M Tris-HCl pH 6.8; 0.4 % (w/v) SDS; AA/Bis: 40 % (w/v) acrylamide, 0.8 % (w/v) bisacrylamide (Amresco); TEMED; 10 % (w/v) Ammonium persulphate (APS);
Running buffer: 190 mM glycine, 25 mM Tris-HCl, 1% (w/v) SDS, pH 8.8;
4x SDS-Buffer

SDS-PAGE was performed using 1.0 or 1.5 mm thick Bio-Rad minigels (Mini-Protean II electrophoresis cell). The separating gel was overlaid with water-saturated isobutanol. After complete polymerisation, the water/isobutanol was removed and the top of the gel washed with water before the stacking gel solution was added and a comb was put in. Samples were mixed with 4x SDS-Buffer and incubated at 95°C for 5 mins, centrifuged briefly to collect material at the bottom of the tube and loaded onto the gel using a Hamilton syringe. Gels were run for 30 mA until the dye front reached the end of the gel.

2.7.2 Transfer of proteins onto PVDF membrane (Immobilon)

Solutions:
Transfer buffer: 20 mM Tris, 150 mM glycine, 20 % (v/v) methanol, pH 8.3;
Ponceau S 2 % (w/v) in 3 % (w/v) TCA;
Blocking buffer: 3% BSA in PBS.

For the transfer of proteins a piece of Immobilon PVDF membrane (Millipore) was cut to the dimensions of the gel, hydrated for 1min in ethanol and equilibrated for 5min in transfer buffer. 4 pieces of Whatman 3MM paper and 2 sponge pads were also soaked in transfer buffer. After electrophoresis, the gel was briefly washed in transfer buffer and a gel sandwich was prepared as follows: The gel cassette was placed in a dish containing transfer buffer, a sponge pad was placed onto the cassette, two pieces of wet Whatman 3MM paper, the membrane, the gel, followed by 2 pieces of wet Whatman 3MM paper and another sponge pad. Air bubbles were

removed using a rubber roller. The cassette was closed and placed into a BioRad Mini Trans-Blot transfer cell that contained an ice-cooling unit, the membrane facing the anode. Transfer was performed for 1 hour at 200 mA at room temperature. After transfer the membrane was stained in Ponceau S and destained in dH2O to check for efficient transfer. Prior to incubation with antibodies, membranes were incubated in blocking buffer for 1 hour.

2.8 Immunological methods

2.8.1 Western blotting

Solutions:
Blocking buffer; PBS-T or TBS-T: 0.1% Tween20 in PBS or TBS;
PBS/milk or TBS/milk: PBS-T or TBS-T + 5% skimmed milk powder (Marvel);
ECL-reagent, ECL-plus (Amersham);
Anti-mouse-HRP: peroxidase-conjugated anti-mouse IgG antibody (Amersham) 1:2000 in PBS/milk;
Anti-rabbit-HRP: peroxidase-conjugated anti-rabbit IgG antibody (Amersham) 1:2000 in PBS/milk;
Anti-goat-HRP: peroxidase-conjugated rabbit anti-goat IgG (DAKO) 1:2000 in PBS/milk

After blocking, the PVDF membrane was incubated with the first antibody diluted in blocking buffer for 1 hour at room temperature or at 4°C overnight with gentle rocking. After 5 washes with PBS/milk for 5mins each, the membrane was incubated with the HRP-conjugated secondary antibody for 1h at room temperature with gentle rocking. After 4 washes for 5 mins with PBS-T and one wash with PBS for 5 mins, HRP-activity was detected by incubating the membrane with ECL-reagent for 1 min and exposure of the membrane to Hyperfilm-ECL.

To reprobe membranes, the antibodies were removed by incubating for 15 mins in 0.1 M Glycine pH 2.5 (stripping buffer). The membranes were washed 3 times in PBS before incubation with blocking buffer.

2.8.2 Cell Death ELISA

RPE myrAkt-ER cells were detached by incubation with trypsin/versene, washed and plated at a density of $1.5x10^5$ cells per well of a 6 well plate in 1.5 ml medium containing 1% FCS onto normal or polyHEMA coated plates and treated with 100 nM 4-OHT or solvent control (EtOH), or drugs as indicated. After 24 hours, suspension cells were harvested by centrifugation, washed

with ice-cold PBS and lysed in 500 µl incubation buffer (Cell Death Detection ELISA, Roche) for 30 mins on ice.

To prepare lysates from adherent cells, culture medium was removed and the cells were washed once in ice-cold PBS and lysed in 400 µl incubation buffer. In order to harvest any floating potentially apoptotic cells, the culture medium was centrifuged for 5 mins at 2000 rpm. The pellet was lysed in 100 µl incubation buffer and added to the adherent cell lysate. All lysates were centrifuged for 10 mins at 13,000 rpm at 4°C, 200 µl of each supernatant was carefully transferred into a fresh tube without disturbing the pellet and stored at –20°C. DNA fragmentation was quantified using the Cell Death Detection ELISA kit (Roche) according the to the manufacturer's instructions.

2.9 Visualization of GFP transfected cells

Images of EGFP (enhanced green fluorescence protein) co-transfected cells were taken under UV using a Zeiss Axiovert 25 microscope.

2.10 DNA techniques and molecular cloning

2.10.1 Quantitation of DNA

Solution:
TE-buffer: 10 mM Tris, ph 8.0, 1 mM EDTA

DNA dissolved in water or TE was placed in a quartz cuvette with a path length of 1 cm and the absorbance at wavelengths 260 nm and 280 nm was determined using a spectrophotometer. An OD260 of 1 corresponds to 50 µg/ml double stranded DNA and 33 µg/ml single stranded DNA. The ratio OD260/280 provides an estimate of the purity of DNA solutions and was usually between 1.7 and 2.0 for DNA preparations.

2.10.2 Preparation of plasmid DNA

Overnight cultures of bacterial clones transformed with the respective plasmid were harvested by centrifugation at 3000 rpm for 20 mins at 4°C. Small-scale preparations were performed using the QIAprep Spin Miniprep Kit (Qiagen). Large-scale purifications were performed using the Qiagen Plasmid Maxi Kit. DNA was resuspended in TE and stored at 4°C.

2.10.3 DNA agarose gel electrophoresis

Solutions:
TAE buffer: 40 mM Tris, 20 ml acetic acid, pH 8, 1 mM EDTA;
6× DNA loading buffer: 0.25 % bromphenol-blue (w/v), 0.25% xylencyanol FF (w/v) in TAE, 15% ficoll 400

Agarose gels were prepared by dissolving 0.8-1.2% agarose in TAE buffer by boiling. Ethidium bromide was added to a final concentration of 0.5 µg/ml. DNA samples were mixed with 6× DNA loading buffer and loaded. Electrophoresis was performed at 5-20 V/cm in TAE buffer and DNA was visualised and photographed on a UV transilluminator.

2.10.4 DNA digestion

For digestion, 0.2–0.5 µg DNA was incubated in the appropriate buffer with 10 U/µg restriction endonuclease in 20 µl reaction volume for 1 hour.

2.10.5 Bacterial transformation

Competent bacteria (2.2.1) were transformed by heat shock. Transformation of XL1-blue cells: 50 µl of competent bacteria were mixed with 50 ng of plasmid DNA and incubated for 30 mins on ice. Afterwards bacteria were heat-shocked for 1 mins at 42°C and immediately placed on ice. 100 µl of LB medium was added and 10-20% of the suspension was plated onto LB-Agar plates containing 50 µg/ml ampicillin. Transformation of XL10-gold cells: 1-10 µl of a mutagenesis reaction were mixed with 100µl competent cells containing 4 µl ß-ME and incubated on ice for 30 mins. Then, bacteria were heat-shocked for 30 seconds at 42°C and placed on ice for 2 mins. After adding 900 µl of preheated LB-medium, transformed cells were incubated at 37°C for 1 hour with slow shaking. 10% and 90% of the reaction were plated on LB-Agar plates containing 50 µg/ml ampicillin and incubated overnight at 37°C.

2.10.6 Site-directed mutagenesis

Site-directed mutagenesis was carried out according to the Stratagene QuikChange® II protocol. A pair of complementary primers was designed, 34-44 nucleotides long that represent the sequence of the target gene with the mismatch approximately in the middle of the primer. Primers (2.3.2.1) were designed with a minimum content of GC nucleotides of 40%, and with an annealing temperature (Tm) equal to or greater than 78°C, estimated by the following formula:

$Tm = 81.5 + 0.41\ (\%GC) - 675/N - \%\ \text{mismatch}$

%GC: content of guanosine or cytosine nucleotides in %

N: length of primer in number of nucleotides

The following PCR reactions were carried out to introduce the desired mutations: 10 or 30 ng of template DNA in the presence or absence of 5% DMSO were titrated in four different reactions with 125 ng of each primer, 2.5 mM dNTPs (Pharmacia), in a final reaction of 50 µl with 2.5 U PfuUltraTM HF DNA-Polymerase (Stratagene) in reaction buffer. The following PCR conditions were used in an MJ Research PTC-220 thermocycler.

Segment 1:	1 cycle	denaturation:	95°C, 30 seconds
Segment 2:	12-18 cycles	denaturation:	95°C, 30 seconds
		annealing:	55°C, 1 minutes
		extension:	68°C, 6.5 minutes

The duration of the extension step was adjusted according to the size of the plasmid used (1 min/kb). The size of the construct used was 6.4 kb. The number of cycles in segment 2 was dependent on the type of mutation that was introduced: 12 cycles were used for single base pair mismatches, 16 cycles for single amino acid changes (2-3 base pair mismatches), and 18 cycles for multiple amino acid changes.

10 µl of the PCR reactions were analysed on 1% agarose gels, and the reaction with the highest yield was digested with 10 U of Dpn I (Stratagene) for 1 hour at 37°C. 1-5 µl of the reaction was then used to transform E.coli XL10-Gold® Ultracompetent cells (Stratagene). Up to 4 clones per mutagenesis were analysed by nucleotide sequencing for the desired mutation and for the N-terminus to confirm the correct isoforms' sequence.

2.11 RNA techniques

2.11.1 Isolation of RNA

Total RNA from cells was isolated using the RNeasy kit (Qiagen) according to the manufacturer's instructions. Briefly, 350 µl RLT buffer was added per well of a 6 well plate, cells were then scraped and homogenised using a QIAshredder (Qiagen) to sheer the DNA. RNA was isolated by using the RNeasy spin columns, DNA was digested using the RNase-free DNase set (Qiagen) and eluted in 30 µl RNase-free water. The concentration and purity of RNA was assessed using a NanoDrop spectrophotometer by measuring optical density at 260 nm (OD260nm) and 280 nM (OD280nm). An OD260 nm of 1 corresponds to 40 µg/ml RNA. The ratio OD260/280nm provides an estimate of the purity of the RNA solutions and should be ~2.0 for RNA preparations. RNA was stored at -80°C.

2.11.2 RNA gel electrophoresis

The quality of total RNA was analysed on a 1.2% formaldehyde agarose gel in FA gel buffer (20 mM Mops, 2 mM sodium acetate, 1 mM EDTA, pH 7). Ethidium bromide was added to a final concentration of 0.5 µl/ml. 1 µg of RNA was mixed with loading buffer (5x buffer containing 0.25% bromophenol-blue, 4 mM EDTA, 7.2% (v/v) of 37% (12.3 M) formaldehyde, 20% (v/v) glycerol, 40% (v/v) FA gel buffer, 30.84% (v/v) formamide), incubated at 65°C for 5 min and electrophoresed at 5 V/cm in FA running buffer (20 mM Mops, 5 mM sodium acetate, 1 mM EDTA, 2% (v/v) of 37% (12.3 M) formamide). Alternatively, the RNA was run on a

Agilent Bioanalyser. The 28S ribosomal RNA band should be present at approximately twice the amounts of the 18S rRNA.

2.11.3 Complementary (cDNA) synthesis

cDNA was synthesised from total RNA with the Superscript II enzyme (Invitrogen) according to the manufacturer's protocol using oligo dT20 or gene specific primers (2.3.2.2).

2.11.4 Quantitative real-time PCR

cDNA was used as a template for semiquantitative PCR (q-rtPCR) analysis monitoring the real-time increase in fluorescence of SYBR Green (Applied Biosystems) on a Chromo4 detector system (Bio-Rad, formerly MJ Research). Gene-specific primers were designed using PrimerExpress software (Applied Biosystems). Relative transcript levels of target genes are normalised to GAPDH or ß-actin RNA levels. Primer sequences are listed in 2.3.2.3. Usually, 50 ng of cDNA and 300 nM of each primer were used in a final reaction volume of 25 µl. Thermocycling conditions were: first denaturation at 95°C for 10 mins, then denaturation at 95°C for 15 seconds, annealing and extension at 60°C for 1 mins (40 cycles), and a dissociation curve profile was performed at the end of each run: denaturation at 95°C for 15 seconds, annealing and extension at 60°C for 20 seconds, and then slowly increasing the temperature to 95°C and taking measurements every 1°C increase. Thereby a dissociation curve can be plotted for each primer pair, a single peak should be visible representing the generation of only one product. The comparative CT method (ΔΔCT) was employed to measure relative transcript levels (Livak and Schmittgen, 2001). For this calculation to be valid, the efficiency of the target amplification (eg. SREBP, FAS) and the efficiency of the reference amplification (eg. Actin γ, GAPDH) must be approximately equal. Therefore, a standard curve with dilution of the template was performed and the ΔCT (which is CT target – CT reference) values were plotted against each template concentration. If the efficiencies of the two amplicons are approximately equal, the plot of log input (template) versus ΔCT has a slope of approximately zero.

2.11.5 Nucleotide sequencing

Fluorescent cycle sequencing was performed using gene specific primers (2.3.2.1) and the BigDye Terminator v3.1 Kit (Applied Biosystems). Reactions were carried out in a volume of 20 µl containing 250 ng dsDNA, 5pmol primer and 8µl Terminator Ready Reaction mix. PCR conditions were as follows:

25 cycles	denaturation	at 96°C for 10 seconds
	annealing	at 55°C or 61°C for 5 seconds
	extension	at 60°C for 4 minutes

The annealing temperature was 3°C lower than the Tm of the used primers. To remove unincorporated dye, samples were purified using the DyeEx 2.0 Spin Kit (Qiagen) according to the instructions. Samples were processed for electrophoresis, separated by electrophoresis and visualized by staff of the Equipment Park, LRI, Cancer Research UK. Sequence analysis and alignments were performed using DNA Strider™1.3f6 (CEA).

2.12 Reporter Assays

2.12.1 Dual-Luciferase® Reporter Assay

For the Dual-Luciferase reporter Assay, which sequentially measures firefly and Renilla luciferase in one reaction tube, cells were lysed using the passive lysis protocol. 20 µl of cell lysate were transferred into an opaque 96 well plate and 100 µl Luciferase Assay Reagent (LARII) was added. The reaction mixture was mixed by 5 times pipetting up and down. The plate was then placed into the luminometer (Bioluminat LB, Berhold) and readings were taken. Firefly luciferase catalyzed photon emission was detected and analysed using the Revelation software. After recording the firefly luciferase activity measurement, the plate was removed from the luminometer, 100 µl of Stop & Glo® Reagent was added and the reaction was mixed by pipetting up and down 5 times. The plate was again placed into the luminometer and another reading was taken. Renilla luciferase activity was recorded and used to normalize firefly luciferase activity.

2.12.2 Luciferase Assay

To determine firefly luciferase activity in the same lysate as ß-Galactosidase activity, cells were lysed using Reporter Lysis Buffer (RLB). 20 µl of cell lysate was transferred into a 96 well plate and 100 µl Luciferase Assay Reagent was added. The reaction mixture was mixed by pipetting 5 times up and down. The plate was then placed into the luminometer (Bioluminat LB, Berhold) and the reading was taken. Firefly luciferase catalyzed photon emission was detected and analysed using the Revelation program.

2.12.3 ß-Galactosidase Assay

Solutions:
CPRG reagent buffer: PBS, 1 mM MgSO4, 4.25vol% ß-mercaptoethanol,
0.4 mg/ml CPRG (Chlorophenolred-ß-D-galactopyranoside)

20 µl cell lysate was transferred into a 96 well plate and 200 µl CPRG reagent buffer was added. After incubation at 37°C for 15 mins to 2 hours, the reaction was quantified by measuring absorption at 595 nm using a spectrophotometer and readings were normalized to a blank containing CPRG reagent buffer and 20 µl Reporter Lysis Buffer (RLB).

2.13 Lipid measurement

RPE cells were plated in medium containing 1% lipoprotein deficient serum (LPDS) and treated with 100 nM 4-OHT for 48 hours. Cellular lipids were extracted using a dual-phase-extraction method. Cells were washed twice with ice-cold PBS, dissolved in methanol, scraped off and transferred into centrifuge tubes. An equal volume of ice-cold chloroform was added and tubes were mixed for 30 seconds. The same volume of ice-cold de-ionised water was added and tubes were mixed for 30 seconds. Phase separation was achieved by centrifugation at 10,000 rpm for 20 mins at 4°C. The chloroform phase, containing cellular lipids, was transferred into a glass tube and air-dried. Lipid extracts were reconstituted in 600 µl deuterated choloform (which was used as an internal standard for spectral normalization) and freshly prepared 0.008% v/v tetramethylsilane was used as a chemical shift reference (0ppm). Proton NMR spectra of the lipid extracts were acquired using a Bruker 600-MHz (Bruker Avance; Bruker GmbH, Germany) NMR system. Spectra were obtained using a 300 pulse, spectral width of 9 KHz, repetition time of 6 s and 32 k data points. Peaks were assigned according to Sze and Jardetzky (Sze and Jardetzky, 1990). The relative lipid levels were then standardized to the number of cells. Metabolite analysis by NMR were carried out by Y.-L. Chung (CRUK Magnetic Resonance Group, St. Georges Hospital, London).

2.14 Culture of Drosophila *cell lines and flies*

2.14.1 Cell culture

Kc167 cells were cultured at 23°C in Schneider's medium (Gibco) supplemented with 10% foetal bovine serum (FBS), 50 U/ml penicillin and 50 mg/ml streptomycin (Invitrogen). The cells were split using a 1:5 ration of culture to fresh medium every 3-4 days. For experiments,

cells were seeded at a concentration of $1x10^6$ cells/ml in 75 cm^2 flasks (30 ml per flask) or in six-well plates (3 ml per well).

2.14.2 Fly culture

Flies were raised in tubes and bottles containing fly food (26 litres contains 0.8% [w/v] agar, 326 g dry yeast, 1800 g maize meal, 108 g soya flour, 1800 g malt, 900 ml molasses, 180 ml proprionic acid) at 18°C or 25°C depending on the experimental requirements.

2.15 dsRNA Production

Individual DNA fragments approximately 700 bp in length, containing coding sequences for the proteins to be silenced were amplified by PCR. Each primer (2.3.2.4) used in the PCR contained a 5' T7 RNA polymerase binding site (GAATTAATACGACTCACTATAGGGAGA) followed by sequences specific for the targeted genes. The PCR products were purified by using the High Pure PCR Purification Kit (Roche Molecular Biochemicals). The purified PCR products were used as templates for the MEGASCRIPT T7 transcription kit (Ambion, Austin, USA) to produce dsRNA. The dsRNA products were ethanol-precipitated and resuspended in water. The dsRNAs were annealed by incubation at 65°C for 30 mins followed by slow cooling to RT. Six micrograms of dsRNA were analyzed by 1% agarose gel electrophoresis to ensure that the majority of the dsRNA existed as a single band of approximately 700 bp. The dsRNA was stored at -20°C.

2.16 dsRNA treatment of Kc167 cells

Kc167 cells were plated into 6 well plates using *Drosophila* serum-free expression medium (DES, Invitrogen) at $1x10^6$ per well. 15-30 μg of dsRNA was added immediately, and the plates were gently agitated to mix the RNA and cells before incubating at 23°C for 60 mins. 2 ml of Schneider's *Drosophila* medium with 10% (v/v) heat-inactivated foetal calf serum was then added and the plates were incubated for an additional 4 days to allow for turnover of the target mRNAs before harvesting. These treatments were carried out by Megan Cully (STL, CRUK-LRI).

2.17 Isolation of RNA from Kc167 cells

Total RNA from Kc167 cells was isolated using the RNeasy kit (Qiagen) according to the manufacturer's instructions. Briefly, cells were harvested by titration and pelleted by centrifugation at 1000 × g. Cell pellets were transferred into a microcentrifuge tube and washed twice with ice-cold PBS, following resuspension in 350 µl RLT buffer, and homogenisation using a QIAshredder (Qiagen) to sheer the DNA. RNA was isolated by using the RNeasy spin columns, DNA was digested using the RNase-free DNase set (Qiagen) and eluted in 30 µl RNase-free water.

The concentration and purity of RNA was assessed using a NanoDrop spectrophotometer by measuring optical density at 260nm (OD260nm) and 280nM (OD280nm). An OD260nm of 1 corresponds to 40 µg/ml RNA. The ratio OD260/280nm provides an estimate of the purity of the RNA solutions and should be ~2.0 for RNA preparations. RNA was stored at -80°C.

2.18 Kc167 cell size analysis

Kc167 cells were cultured as described in 2.14.1 in 6 well plates and triplicate wells were used for each time point. A total of 300 µl from each well was resuspended in culture media and analysed for cell volume and cell count using a Z2 Coulter Counter (Multisizer II, Beckman–Coulter). The remaining cells were collected by centrifugation, fixed by vortexing and incubated in cold 70% ethanol at 4°C for at least 30 mins, then washed twice in PBSA and resuspended in 500 µl of 20 µg/ml RNaseA (Sigma-Aldrich) and 40 µg/ml propidium iodide in PBSA (Sigma-Aldrich). Propidium iodide-stained cells were analysed for cell cycle profile on a FACScalibur flow cytometer using CellQuest (Becton Dickinson). These analyses were carried out by Megan Cully (STL, CRUK-LRI).

2.19 Isolation of larval RNA

Total RNA from second instar larvae was isolated using the RNeasy kit (Qiagen) according to the manufacturer's instructions. Briefly, second instar larvae were hand picked from culture samples into a microcentrifuge tube, washed twice with PBS and briefly spun down. The larval pellet was immediately frozen in liquid N_2 and squelched with a pestle. The homogeneous pellet was resuspended in an adequate amount of RLT buffer, and homogenised using a QIAshredder (Qiagen) to sheer the DNA. RNA was isolated by using the RNeasy spin columns, DNA was digested using the RNase-free DNase set (Qiagen) and eluted in 30 µl RNase-free water. The concentration and purity of RNA was assessed as in 2.17.

2.20 Fly Genetics

2.20.1 Making transgenic flies

2.20.1.1 Preparation of UAS-dSREBP^{RNAi} construct

A sequence comprising 700 bp of the 5' end of the *dSREBP* was amplified by PCR from genomic DNA. The purified and digested inverted repeats were then separated by gel electrophoresis, purified and cloned into the pWIZ-UAST vector. XL1-blue bacteria were transformed and plasmid DNA extracted using QIAprep (Qiagen). The presence of the inverted repeats was confirmed by digestion and gel electrophoresis. A positive clone with the inserts of the predicted size was prepared for embryo injections by mixing with the helper plasmid pTURBO, which contains the transposase. The pWIZ-UAST-dSREBP-dsRNA construct generated was used for injection.

2.20.1.2 Germline transformation

UAS-dSREBP^{RNAi} transgenic flies were generated by P element-mediated germline transformation (Rubin and Spradling, 1982). DNA was injected into the posterior end of *yw* embryos. This was carried out by Terence Gilbank (CRUK-LRI).

After injection, the embryos were incubated at 18°C until they hatched. Hatched larvae were placed in standard fly food and allowed to develop to adulthood. The resulting adult males (G_0s) were crossed individually to groups of two or three balancer female flies and their progeny (F_1s) scored for red eyes (w+), which indicated germline integration of the transgene. Flies carrying the transgene were mapped by further crosses to flies with balancer chromosomes. Single transgenic males were crossed to SM6a/Cyo ; Tm3/Tm6b virgins twice to determine which chromosome the insertions are on. Balanced adult flies were mated *inter se* to establish a stock. Homozygous virgins and males were selected in subsequent generations to eliminate balancer chromosomes.

2.20.2 Fly lines

The *yw* line originating from Ernst Hafen's laboratory was used as wild type control and the background for the UAS-dSREBP^{RNAi} transgenic lines.

Generation of the yw; P(UAS-dSREBP^{RNAi}/UAS-dSREBP^{RNAi}) and yw; P(UAS-dSREBP^{RNAi}/UAS-dSREBP^{RNAi}); P(UAS-dSREBP^{RNAi}/UAS-dSREBP^{RNAi}) fly lines was described in section 2.20.1.2.

Daughterless-GAL4, engrailed-GAL4 UAS-GFP/Cyo, MS1096-GAL4, wgSp1/Cyo; P(w+ Dpp-GAL4)/TM6b, yw; P(w+, UAS-Dp110WT), yw; P(w+, UAS-Dp110[KD]), w; UAS-gfp, UAS-Dp110[KD]/SM6a-TM6b; dpp-GAL4]/SM6a-TM6b, en-GAL4 UAS-GFP UAS-Dp110[KD]/SM6a fly lines were obtained from S. Leevers (CRUK-LRI). MS1096-GAL4 UAS-Dp110WT was a gift from Hugo Stocker (ETH-Zuerich, Switzerland).

The UAS-dSREBP fly lines obtained from the Bloomington Stock Center (BSC) have the following genotypes: stock 8236: yw; P(UAS-HLH106.Exel)3, stock 8237: P(UAS-HLH106.Exel)1; yw, stock 8238: P(UAS-HLH106.Ndel)1; yw, stock 8239: yw; P(UAS-HLH106.Ndel)2, stock 8240: yw; P(UAS-HLH106.Ndel)3, stock 8241: yw; P(UAS-HLH106.NTdel)3, stock 8242: P(UAS-HLH106.NTdel)1; yw, stock 8243: P(UAS-HLH106.Cdel)1; yw, stock 8244: yw; P(UAS-HLH106.Cdel)2.

2.21 Phenotypic analysis of flies

For analysis of ubiquitous, wing, lethal and development phenotypes flies were scored 3-4 days after eclosure. For body weight measurement, 3 day old male flies were used (n = 30).

2.21.1 Mounting wings

Wings were dehydrated in ethanol, mounted in euparal (Agar Scientific) and allowed to harden at 60°C overnight.

2.21.2 Fly and wing imaging

The Leica Firecam software using either a Leica MZ FLIII or a Zeiss Axioplan2 imaging microscope connected with a Leica DFC420C camera was used to generate wing and fly images. Wing area and circumference were measured using Adobe Photoshop software.

2.21.3 Cell number analysis

Cell numbers were assessed by counting the number of wing hairs in a 10,000 μm^2 rectangle at the junction between the wing margin and L2 for the anterior compartment and below the

intersection between the posterior cross-vein and L5 for the posterior compartment. The area measured in the anterior compartment was that between the anterior margin and L3 and in the posterior compartment that between L4 and the posterior margin.

2.22 Statistical analysis

Data are represented as mean values. Error bars represent the range of determinations, standard deviation (SD) or standard error of the mean (SEM) (Cumming et al., 2007). Statistical significance was calculated using a two-tailed student's t-test assuming equal variances, if not otherwise stated.

3 Chapter 3: Activation of expression of lipid biogenesis genes by Akt/PKB requires SREBP

3.1 Introduction

The serine threonine kinase Akt is a downstream effector of phosphatidylinositol 3 kinase (PI3K) and has been found to be involved in regulation of several cellular processes by promoting cell survival, proliferation and metabolism (Manning and Cantley, 2007). Akt is an important mediator of the metabolic effects of insulin in several important physiological target tissues (Manning and Cantley, 2007). Among the first Akt targets identified were glycogen synthase kinsae-3α (GSK3α) and -3β (GSK3β) (Cross et al., 1995). Phosphorylation by Akt causes inhibition of GSK3α/β and activates glycogen synthesis in myocytes (Cross et al., 1995). It has recently been published that Akt regulates hepatic fatty acid oxidation via direct phosphorylation and inhibition of the transcription factor PGC-1α (Li et al., 2007). Akt has been implicated in promoting cell cycle progression by regulating cyclin D1 stability (Diehl et al., 1998) and modulating expression and subcellular localisation of the cdk inhibitors $p27^{Kip1}$ (Kops et al., 2002; Shin et al., 2002) and $p21C^{Cip2/WAF1}$ (Zhou et al., 2001a). Akt regulates the activity of a number of transcription factors, most notably the FoxO family of transcriptional regulators (Burgering and Kops, 2002), which are directly phosphorylated by Akt resulting in inactivation of the transcription factors by cytoplasmic retention (Takaishi et al., 1999, Kops, 1999 #1012, del Peso, 1999 #1078). Although some of the substrates of Akt, such as Bad, are directly involved in the regulation of apoptosis it has been recognised that regulation of transcription by inactivation of ASK1 and FoxO proteins may contribute to Akt pro-survival function (Brunet et al., 2001a; Downward, 2004).

Sterol regulatory element binding proteins (SREBP) consist of three closely related members, SREBP1a, SREBP1c and SREBP2 (Eberle et al., 2004). They have been identified as mediators of the effect of sterols on expression of enzymes involved in lipid and cholesterol homoeostasis (Yokoyama et al., 1993). SREBPs belong to the family of basic helix-loop-helix-leucine zipper (bHLH-Zip) transcription factors and consist of an N-terminal transactivation domain, the bHLH-Zip DNA-binding domain and two hydrophobic transmembrane domains (Yokoyama et al., 1993). They are synthesised as inactive precursors bound to the endoplasmic reticulum (ER) (Brown and Goldstein, 1999; Sato et al., 1994). In order to be transcriptionally active, the N-terminal part of the SREBP protein has to be cleaved by a mechanism termed regulated intramembrane processing (RIP) (Rawson, 2003; Wang et al., 1994). In the nucleus, SREBPs bind as dimers to sterol regulatory element (SRE) and E-Box DNA sequences found in the promoter regions of a number of genes involved in cholesterol and fatty acid biosynthesis. Studies in knockout and transgenic mice have shown that SREBP1c preferentially regulates genes involved in fatty acid biosynthesis while SREBP2 mainly regulates genes of the cholesterol pathway (Horton et al., 2003). SREBP target gene promoter analysis showed that SREBP1a can bind to SREs in the HMG-CoA reductase and fatty acid synthase promoter (Bennett et al., 2004).

A number of studies have addressed the regulation of SREBP gene expression *in vivo* and *in vitro*. SREBP1a is expressed at low constitutive levels *in vivo* but appears to be the predominant form in cultured cells (Shimomura et al., 1997a). Expression of SREBP1c and SREBP2 seems to be subject to distinct regulation *in vivo*. Both genes contain SREs in their promoter region (Amemiya-Kudo et al., 2000; Sato et al., 1996) and regulation through a feed-forward loop has been described (Horton et al., 2003). Transcription from the SREBP1c promoter is modulated by insulin and glucagon (Fleischmann and Iynedjian, 2000; Shimomura et al., 1999). In addition, sterols have been shown to activate SREBP1c expression by inducing binding of liver X-activated receptor (LXR) to LXR elements on its promoter (Bobard et al., 2005; Deng et al., 2002; Repa et al., 2000).

LXR is a ligand-activated transcription factor that senses cholesterol homeostasis and regulates hepatic cholesterol lipid metabolism. The transcriptional activity of LXR is stimulated by sterol intermediates, glucose or the synthetic agonist T0901317 and inhibited by the antagonists PUFA such as arachidonic acid (Chen et al., 2004; Mitro et al., 2007; Yang et al., 2006a).

This chapter describes the regulation of transcription of genes encoding enzymes involved in lipid biosynthesis by the Akt kinase. SREBP activity is studied by examining the expression of the two rate-limiting enzymes for the fatty acid and cholesterol biosynthetic pathways, fatty acid

synthase and HMG-CoA synthase, and the involvement of Akt in the regulation of transcription of SREBP is tested. This study shows that Akt-induced transcription of lipid biosynthesis genes requires SREBP activity.

3.2 Akt induced changes in gene expression

This thesis was based on data obtained from a microarray experiment performed by Dr. Almut Schulze (GEA, CRUK-LRI), which will be described in chapter 3.2.3 briefly. The aim of the microarray experiment was to identify new pathways downstream of Akt.

3.2.1 The myrAkt-ER construct

In order to identify changes in gene expression that are the result of activation of Akt, an inducible version of the kinase in which a constitutively active form of Akt1 (myrAkt) fused to the hormone-binding domain of the estrogen receptor (myrAkt-ER) was used (Kohn et al., 1998). Instead of the PH-domain this form of Akt contains an N-terminal src myristoylation sequence, which leads to constitutive localisation to the plasma membrane independent of PI3K activity. The C-terminal part of the protein is fused to a mutated form of the murine estrogen receptor (ER^{TM}), which has been engineered to bind selectively to the estrogen antagonist 4-hydroxytamoxifen (4-OHT) instead of its natural ligand 17ß-estradiol (Figure 3-1) (Littlewood et al., 1995). It has been demonstrated that 4-OHT activates the kinase activity of the Akt-ER fusion protein (Kohn et al., 1998). The myrAkt-ER fusion protein was stably expressed in human retinal pigment epithelial cells (RPE) using retroviral gene transfer. The hTERT-RPE1 (RPE) cell line is a telomerase-immortalized cell line expressing exogenous hTERT (the human telomerase reverse transcriptase subunit). These cells have an indefinite life span, a normal phenotype and can be used to study biochemical and physiological aspects of cell growth (Bodnar et al., 1998). Most of the solid tumours derive from epithelial cells, making RPE cells a good model system to study cancer development.

3.2.2 Activation of myrAkt-ER protects RPE cells from detachment-induced apoptosis

Akt requires two essential phosphorylations to become fully active. PDK1 phosphorylates the activation loop of the Akt kinase domain on threonine 308 (T308) (Alessi et al., 1997) and mTOR complex 2 (mTORC2) phosphorylates Akt on the hydrophobic motif at serine 473 (S473) (Hresko and Mueckler, 2005; Sarbassov et al., 2005). Akt phosphorylates GSK3α on

serine 21 and GSK3β on serine 9, which leads to inactivation of both proteins (Cross et al., 1995).

To determine whether the Akt fusion protein is active and phosphorylates endogenous Akt substrates, RPE myrAkt-ER cells were plated on normal (adherent) or polyHEMA coated plates (suspension) and treated with 100 nM 4-OHT or solvent (EtOH) in minimal medium for 24 hours. Cells were lysed and equal protein amounts of the total cell lysates were subjected to SDS-PAGE and western blot analysis using phosphospecific antibodies. 4-OHT stimulation resulted in an activation of the fusion protein detected by the phosphorylation on S473 as well as phosphorylation of the Akt substrates GSK3α/β (Figure 3-2). The mobility of the fusion protein in SDS-PAGE indicates a size of approximately 90 kDa (compared to 60 kDa for endogenous Akt protein), which corresponds to the estimated size.

During tumour development activation of Akt can prevent detached cells from undergoing apoptosis (Frisch and Screaton, 2001). Normal epithelial cells have to bind to components of the extracellular matrix for survival and loss of this interaction leads to detachment induced apoptosis (also termed anoikis). Attachment of cells to components of the extracellular matrix induces endogenous Akt activation and Akt has been shown to protect epithelial cells from detachment-induced apoptosis (Khwaja et al., 1997).

Figure 3-2 A shows activation of myrAkt-ER in adherent (A) and suspension (S) cells resulting in phosphorylation of Akt substrates under both conditions. Activation of myrAkt-ER also led to protection from detachment-induced apoptosis in these cells (Figure 3-2 B). Untreated RPE myrAkt-ER cells cultured in suspension showed a five to six fold increase in apoptosis compared to adherent cells. Activation of Akt by 4-OHT treatment for 24 hours, resulted in a reduction in apoptosis in suspension cells to the level of adherent cells. Although the effect of active Akt on suspension cells after 48 hours 4-OHT treatment was less protective than after 24 hours, a significant reduction in apoptosis was still measured.

Taken together, this shows that the stably expressed myrAkt-ER fusion protein is functional in RPE cells. The protein is active only in the presence of 4-OHT, and the active myrAkt-ER construct phosphorylates Akt kinase substrates and protects cells from detachment-induced apoptosis.

3.2.3 Analysis of gene expression profiles in response to Akt activation

Changes in gene expression in response to activation of the myrAkt-ER fusion protein in RPE cells were analyzed by performing comparative hybridisation of RNA prepared from 4-OHT treated cells and ethanol treated controls to cDNA microarrays. Since detachment from the matrix leads to repression of the activity of endogenous Akt protein (data not shown), the myrAkt-ER construct was activated in these cells under adherent and suspension conditions. To eliminate 4-OHT induced effects, the same experiment was performed with parental cells (data not shown). Among the 10,000 cDNA clones represented on the array 160 were found that showed reproducible regulation in response to 4-OHT treatment in myrAkt-ER, but not in parental cells in either adherent or suspension cells in four replicate experiments. Functional classification of genes found to be up- or down-regulated in response to Akt activation revealed that a large number of up-regulated genes (24 cDNA clones) code for enzymes that are involved in sterol or fatty acid biosynthesis (Figure 3-3 A). Expression profiles of these 24 clones (mapping to 15 distinct genes) are represented in the panel in Figure 3-3 B. A number of these genes (marked by asterisks) have been previously reported to be regulated by the SREBP family of transcription factors (Horton et al., 2003). Although many of these probes are also regulated by Akt activation in adherent cells, the magnitude of modulation is more pronounced in suspension cells indicating that repression of endogenous Akt activity by loss of matrix attachment results in inhibition of expression of those genes.

3.3 Akt induces expression of genes involved in sterol and fatty acid biosynthesis

Experiments presented in this subchapter verify the microarray results by independent methods.

3.3.1 Akt induces expression of fatty acid synthase at the mRNA and protein level

In order to investigate whether the observed changes in gene expression in response to Akt activation can be reproduced by an independent method, mRNA and protein expression of selected genes were analysed. By semiquantitative PCR (q-rtPCR) analysis, Akt activation induced accumulation of transcripts of the fatty acid synthase (FAS), HMG-CoA reductase (HMGR) and HMG-CoA synthase (HMGS) genes (Figure 3-4 A).

In a parallel experiment, whole cell lysates were analysed for FAS protein (Figure 3-4 B). After 24 or 48 hours of Akt activation the FAS protein level is increased in adherent and suspension cells. The fold induction of FAS expression in response to Akt activation is higher in suspension cells compared to adherent cells. Furthermore, the basal protein as well as the mRNA level of FAS is lower in suspension cells. This indicates that matrix attachment may contribute to basal FAS expression.

3.3.2 Stimulation of fatty acid synthase and HMG-CoA synthase promoter by Akt activation

To determine whether regulation of expression of cholesterol and fatty acid biosynthesis genes by Akt involves activation of SREBP transcription factors, reporter gene assays using the rat fatty acid synthase and the human HMG-CoA synthase promoters were performed. Transfection experiments were done in human osteosarcoma cells (U2OS). U2OS cells are epithelial-like cells, which can be transfected with high efficiency. U2OS cells stably expressing myrAkt-ER (U2OS myrAkt-ER) have been developed.

The FAS gene is regulated by SREBP transcription factors through SRE sequences in its promoter. A sterol responsive element at position -54 to -71 consisting of two direct repeat SREs and one palindromic E-Box in the rat FAS promoter mediate SREBP-induced transcription in cultured cells (Magana and Osborne, 1996). In addition, a single SRE located at position -150 to -141 is thought to be involved in nutritional regulation of FAS expression *in vivo* (Latasa et al., 2003; Latasa et al., 2000) (Figure 3-5 A). The HMGS promoter is also regulated by SREBP through two well-defined SREs (SRE-1 and SRE-2) flanked by adjacent NF-Y and Sp1 binding sites (Swinnen et al., 2000) (Figure 3-5 B).

The 150 bp fragment of the rat FAS promoter, comprising both SREBP regulated elements, was transfected into U2OS myrAkt-ER cells and relative luciferase activity measured after treatment with 100 nM 4-OHT for 24 hours. Figure 3-5 C shows that ectopic activation of Akt results in a 4-fold induction of transcription of the FAS reporter construct. In contrast, the FAS construct lacking the SREBP binding-sites (-150/-73) showed no regulation by Akt. Activation of Akt also induced HMGS promoter activity although to a lesser extent, but activation was abolished when the SRE-1 site was mutated (Figure 3-5 D). This suggests that Akt can stimulate expression of FAS at the transcriptional level, which is mediated by cis-acting elements present in the proximal FAS promoter (-73/-43). 4-OHT treatment had no effect on FAS-promoter activity in parental U2OS cells (data not shown).

3.3.3 Induction of fatty acid synthase and HMG-CoA synthase expression by Akt is dependent on *de novo* protein synthesis

Having shown that activation of Akt results in enhanced expression of FAS and HMGS, the question arose whether Akt activates transcription of these genes directly. In order to investigate this, cells were pre-treated with the translation inhibitor cycloheximide (CHX) and after 24 hours of Akt activation, mRNA levels were analysed by q-rtPCR. Akt-dependent induction of FAS and HMGS expression is completely blocked by CHX treatment (Figure 3-6). Furthermore, CHX treatment alone dramatically reduces the basal transcript level of both genes, indicating that transcription of the FAS and HMGS genes requires *de novo* protein synthesis of a factor involved in their transcription. Importantly, these data suggest that Akt-mediated activation of FAS and HMGS is dependent on *de novo* protein synthesis, possibly of one or more transcription factors, which could be SREBPs.

3.4 Induction of fatty acid synthase, HMG-CoA synthase and HMG-CoA reductase by Akt requires SREBP-1

In order to investigate whether activation of SREBP transcription factors are required for Akt dependent activation of FAS and HMGS expression, dominant-negative SREBPs were generated and an RNAi approach targeting SREBPs was employed.

3.4.1 Construction of dominant-negative forms of mature SREBP1a, SREBP1c and SREBP2

SREBP transcription factors belong to the family of bHLH transcription factors that contain a conserved E-R/K-X-R sequence (X representing any amino acid) in their DNA binding domain. However, SREBP proteins have an atypical tyrosine residue (E-K-R-Y) in the DNA binding domain instead of the arginine found in other bHLH transcription factors such as c-Myc. This substitution determines the DNA binding specificity of SREBP proteins towards SRE, SRE-like and E-Box motifs (Kim et al., 1995). It has been shown that substitution of the tyrosine residue with alanine leads to loss of DNA binding activity, but still allows dimerisation resulting in decreased availability of wild type SREBP and preventing the expression of SREBP target genes (Foretz et al., 1999b; Kim and Spiegelman, 1996). The amino-terminal fragment of SREBP1c (amino acids 1-403) containing a point mutation, which replaces tyrosine (aa 321) with alanine has been shown to act as a dominant negative form *in vivo* (Swinnen et al., 2000).

Dominant negative (DN) forms of mSREBP1a, 1c and 2 were designed. The conserved tyrosine residue in the bHLH region of mSREBP1a (at amino acid 335), mSREBP1c (at amino acids 321) and mSREBP2 (at amino acid 342) was substituted with alanine. For the tyrosine to alanine substitutions, the codon TAG was converted into GCC (Figure 3-7 A/B). For subsequent experiments the following constructs were used: mature SREBP1a[Y335A] (m1a[YA]), mature SREBP1c[Y321A] (m1c[YA]) and mature SREBP2[Y342A] (m2[YA]).

In order to test the specificity and the dominant negative effect of the three constructs, the wild-type FAS promoter together with mature SREBPs and DN-SREBPs were expressed in different combinations in U2OS cells. Expression of the mSREBP isoforms alone induces FAS reporter transcription. Simultaneously, expression of DN-SREBP blocks the induction of FAS promoter expression by mSREBP (Figure 3-8 A). Every DN-SREBP isoform is able to act in a dominant negative fashion to inhibit transactivation of all co-expressed mSREBP isoforms, indicating that the three DN-SREBP proteins form homo and heterodimers with the wild-type mSREBP isoforms. This is consistent with published data showing that a DN-SREBP1 construct inhibits the transactivation of co-transfected SREBP1 and SREBP2 (Rishi et al., 2004). In addition, the DN-SREBP constructs showed no effect on apoptosis (data not shown).

Taken together, this shows that the three mSREBP[YA] constructs are effective and that each isoform can inhibit the transactivation of mSREBP1a, 1c and 2 in co-transfection assays.

3.4.2 Effect of dominant-negative SREBP on induction of FAS and HMGS promoters' expression by Akt

To determine the role of SREBP in Akt mediated activation of FAS and HMGS, U2OS myrAkt-ER cells were co-transfected with dominant-negative SREBPs and either FAS or HMGS promoters. Co-transfection of dominant negative m1a[YA], m1c[YA] or m2[YA] abolishes activation of the FAS reporter construct in response to Akt activation (Figure 3-8 B). Although each individual DN-SREBP blocks FAS expression by Akt, a slight residual activation of FAS by Akt is observed. However triple transfection of all DN-SREBP isoforms completely blocks the Akt effect. Furthermore, all three mSREBP[YA] isoforms reduce the basal expression level of the FAS reporter by 40% to 80%.

Induction of the HMGS promoters (SYN-wt) by Akt is less pronounced than the induction of the FAS promoter (Figure 3-8 C). Expression of the dominant negative forms of SREBP1c and 2 prevents the effect of active Akt on SYN-wt. Although m1a[YA] protein reduces the basal

expression level of the SYN-wt construct to the level of co-transfected m1c[YA] and m2[YA], SYN-wt is still residually induced in response to Akt activation (Figure 3-8 C).

3.4.3 Silencing of SREBP blocks induction of FAS, HMGS and HMGR by Akt

The same question was addressed using specific silencing of SREBP1 and SREBP2 expression by RNA interference (RNAi) in U2OS myrAkt-ER cells. Transfection of siRNA oligonucleotides directed against SREBP1 or SREBP2 resulted in selective reduction in expression of the respective proteins as shown in Figure 3-9 A.

Accumulation of FAS and HMGS mRNAs in response to Akt was completely abolished after transfection of siRNA oligonucleotides targeting both SREBP1 and SREBP2 expression simultaneously (Figure 3-9 B/C). Transfection of SREBP1 siRNA alone was sufficient to block activation of FAS and HMGS transcripts in response to Akt. Although silencing of SREBP2 significantly reduces the basal expression level of FAS and HMGS, it did not block the fold induction of FAS and HMGS expression by Akt (Figure 3-9 B/C).

In a parallel experiment, Akt dependent induction of FAS protein expression in U2OS myrAkt-ER cells after 48 hours of 4-OHT treatment was analysed (Figure 3-9 A). Transfection of unspecific siRNA oligonucleotides did not alter induction of FAS by Akt (unspecific, lanes 3 and 4). Transfection of siRNA oligonucleotides directed against either SREBP1 (lanes 5 and 6) or SREBP2 (lanes 7 and 8) only partially blocked Akt induced FAS expression. Silencing of both SREBP1 and SREBP2 was required to completely block Akt induced FAS expression (lanes 9 and 10).

In an additional approach using reporter constructs the effect of ablation of SREBP expression on the activation of FAS (-150/-43) and HMGS (SYN-wt) promoters by Akt was determined. Transfection of either SREBP1 or SREBP2 siRNA oligonucleotides was sufficient to significantly reduce Akt induced FAS promoter activation. However, presence of both siRNA oligonucleotides was required to completely block activation of the FAS promoter in response to Akt (Figure 3-9 B). Transfection of SREBP1 siRNA alone or both siRNA oligonucleotides completely block activation of the SYN-wt promoter construct in response to Akt. Although silencing of SREBP2 significantly reduces the basal expression level of SYN-wt, it did not block the fold induction of SYN-wt expression by Akt (Figure 3-9 C).

Taken together these results indicate that SREBP1, and maybe to a much lesser extent SREBP2, are required for activation of expression of genes involved in sterol and fatty acid biosynthesis by Akt.

3.5 Akt induces expression of SREBP1 and SREBP2

In order to investigate whether SREBPs gene expression increase in response to Akt activation, mRNA and protein expression of all SREBP isoforms were analysed in RPE myrAkt-ER cells. q-rtPCR analysis using isoform specific primers shows an increase in SREBP1a and SREBP1c transcripts after 24 hours Akt activation in adherent and suspension cells, while transcripts for SREBP2 are only marginally modulated (Figure 3-10 A).

In a parallel experiment, whole cell lysates were analysed for full length SREBP1 and SREBP2 proteins (Figure 3-10 B). It should be noted that the antibody against SREBP1 detects both isoforms (SREBP1a and SREBP1c). After 24 or 48 hours of Akt activation SREBP1 and SREBP2 protein levels are increased in adherent and suspension cells.

3.6 Inhibition of PI3-kinase blocks activation of SREBP-1 by insulin

The next question was whether endogenous Akt is able to activate SREBPs expression. The PI3K and MAPK pathways have been shown to be involved in the activation of SREBPs target genes (Eberle et al., 2004).

3.6.1 Insulin stimulates FAS and HMGS promoter expression

Figure 3-11 A) shows a time course of EGF and insulin treatment in U2OS cells. While activation of Akt in response to EGF is only transient, insulin leads to strong activation that can still be detected by phosphorylation on S473 8 hours after the treatment.

In U2OS cells insulin stimulates transcription from the co-transfected FAS promoter (FAS -150/-43) (Figure 3-11 B). This activation is reduced in the presence of the PI3K inhibitor LY294002, however a residual induction by insulin on FAS promoter expression is observed. In the presence of a specific inhibitor of MAPK, UO126, insulin still induces FAS promoter activity although to a somewhat lesser extent. Furthermore, whole cell lysates were analysed for FAS protein expression. FAS protein is increased in response to 24 hours insulin stimulus,

however treatment with LY294002 completely blocked the accumulation of endogenous FAS protein by insulin (Figure 3-11 C).

Transcription from the HMGS promoter (SYN-wt) was only slightly altered by insulin treatment (Figure 3-11 D). However, treatment with LY294002 not only fully blocked the effect of insulin, it also significantly decreased SYN-wt expression. In contrast, the MAPK inhibitor UO123 did not affect the transcription level of the SYN-wt promoter construct.

These data indicate that the PI3K pathway is required for induction, but is also necessary for maintenance of the basal transcription level of the two rate-limiting genes involved in lipid biogenesis. These data are also consistent with published findings showing that the PI3K inhibitors LY294002 and wortmannin block the insulin-stimulated accumulation of the FAS transcript. In contrast, inhibition of MAPK has little influence on FAS expression (Wang and Sul, 1998).

3.6.2 Insulin stimulates SREBP1 expression

In order to investigate whether endogenous activation of the PI3K/Akt pathway also induces expression of SREBPs, RPE cells were treated with insulin in the absence or presence of the PI3K inhibitor LY294022, and protein and mRNA levels were analysed. Both EGF and insulin stimulus for 24 hours lead to an increase of SREBP1 protein while SREBP2 expression is only marginally changed. Induction of SREBP1 by EGF or insulin can be blocked by treatment with LY294002 (Figure 3-12 A). In a parallel experiment, mRNA levels were analysed by q-rtPCR and Figure 3-12 B) shows that inhibition of PI3K by LY294002 abolishes the insulin-dependent increase in SREBP1a and SREBP1c transcripts. The inhibitor of MAPK, UO126, has no effect on the induction of either SREBP1 transcript in response to insulin treatment. However, both inhibitors UO126 and to a greater extent LY294002, reduce the baseline transcription level of the SREBP1 isoforms (Figure 3-12 B). Consistent with Figure 3-12 A) showing that SREBP2 protein expression is only marginally changed in response to insulin or EGF, and the SREBP2 mRNA level is not modulated by insulin. However, inhibition of PI3K and MAPK leads to a reduction in basal transcription level (Figure 3-12 C).

These experiments indicate that activation of PI3K downstream of the EGF and insulin receptor is required for induction of SREBP1. In addition, the PI3K and MAPK pathways may also be necessary for maintenance of the basal transcription of all three SREBP transcription factors.

3.7 Transcriptional regulation of SREBP

Having shown that Akt activates transcription of SREBP, it was of interest to determine, whether this is a direct or indirect regulation.

3.7.1 Induction of SREBP expression by Akt is dependent on *de novo* protein synthesis

Inhibition of *de novo* translation by CHX allows the distinction between direct activation of SREBP transcription and indirect activation via induction of a mediator factor by Akt.

Akt-dependent induction of SREBPs expression is dependent on *de novo* protein synthesis as it is completely blocked by CHX treatment (Figure 3-13). Active Akt is required to induce expression of SREBP1a, while activation of Akt is also necessary for basal level expression of SREBP1c and SREBP2 mRNA (Figure 3-13). Transcription of SREBP1c and SREBP2 depends on *de novo* translation, presumably of their own transcripts leading to mature SREBPs, which are required for full activation of transcription of SREBP1c and SREBP2. This is consistent with the described feed-forward loop through which SREBP1c and SREBP2 are transcriptionally regulated (Horton et al., 2003). The dramatic reduction in SREBP1c and SREBP2 basal expression levels indicates that transcription of these genes requires the presence of mSREBPs.

These data suggest that translation of an intermediate factor activated by Akt is required for SREBPs transcription.

3.7.2 Activation of LXR stimulates FAS and SREBP1 expression

It has been reported that the liver X-activated receptor (LXR) is important for insulin-mediated activation of SREBP1c transcription and stimulation of fatty acid synthase expression (Chen et al., 2004). Having shown that endogenous activation of Akt by insulin causes induction in expression of SREBPs and FAS it was of interest to investigate whether LXR is an intermediate factor responsible for Akt-dependent lipogenic gene expression.

In order to investigate whether SREBP, FAS and HMG-CoA synthase are transcriptionally regulated in response to the LXR agonist T0901317 or the LXR antagonist arachidonic acid (AA), RPE cells were treated with the respective drugs for 24 hours. q-rtPCR analysis using isoform specific primers showed an increase in SREBP1a, SREBP1c and FAS transcripts after

LXR activation by T0901317, while transcripts for SREBP2 and HMGS are not modulated. The LXR antagonist, arachidonic acid did not alter the level of expression of SREBP, FAS or HMGS (Figure 3-14 A). In a parallel experiment, whole cell lysates were analysed for expression of SREBP1 and FAS protein. 24 hours of T0901317 treatment leads to accumulation of full length SREBP1 as well as FAS protein, while the LXR antagonist arachidonic acid has no effect under the conditions used here (Figure 3-14 B). The addition of sterols (cholesterol and 25-hydroxycholesterol) to the growth medium led to an increase in SREBP1a and SREBP1c expression, while expression of the SREBP2 gene was not affected (Figure 3-14 C). The mechanism of SREBP mRNA accumulation may be via sterol-induced LXR activity (Repa et al., 2002).

These experiments show that SREBP1 and FAS, but not SREBP2 and HMGS are positively regulated in response to activation of LXR. These findings are consistent with published data (DeBose-Boyd et al., 2001; Schultz et al., 2000). In addition, the effect of LXR-mediated FAS expression has been shown to be direct since the FAS promoter contains LXREs, and also indirect due to induction of SREBP1c expression (Joseph et al., 2002).

3.7.3 Modulation of LXR activity does not affect Akt-induced FAS and ACL expression

The next question was whether LXR is required for SREBP-dependent induction of expression of lipid biosynthesis genes in response to Akt activation. Whole cell lysates were analysed for FAS and ATP-citrate lyase (ACL) protein, after 24 hours activation of the myrAkt-ER fusion protein by 4-OHT treatment. Activation of Akt led to an accumulation of FAS and ACL protein, which was not affected by the presence of the LXR antagonist arachidonic acid under the conditions used here. Although T0901317 treatment resulted in a higher basal expression level of FAS and ACL, it does not block the accumulation of FAS and ACL in response to Akt activation. However, a slight reduction in fold change of FAS protein by Akt activation in the presence of T0901317 is observed (Figure 3-14 D). In addition, it should be noted that arachidonic acid does not alter accumulation of FAS and ACL in response to LXR activation by T0901317.

Taken together, these results show that Akt activates FAS and ACL expression on top of LXR agonist stimulus, which indicates that LXR is only partly responsible for induction of transcription of SREBP1 or other lipogenic genes in response to Akt activation.

3.8 Discussion

The Akt kinase is a crucial component of signal transduction pathways that regulate cell growth, proliferation and survival in response to growth factors. It is activated in cells that have lost the tumour suppressor PTEN and is required for the oncogenic action of Ras proteins. Akt is also a major mediator of the metabolic functions of insulin in liver, muscle and adipose tissue and involved in reducing the levels of circulating glucose in the blood stream. SREBPs are transcription factors that control lipid and cholesterol biosynthesis by regulating expression of key regulatory enzymes of this pathway, such as fatty acid synthase (FAS). This chapter describes the analysis of changes to the transcriptional profile induced by Akt activation in a human epithelial cell line (RPE). The results indicate that Akt induces gene expression of enzymes involved in the regulation of lipid biosynthesis, mediated via activation of SREBP.

Out of 10.000 cDNA clones present on the DNA microarrays used here, 146 clones were identified that showed reproducible up- or down regulation in response to Akt activation in either adherent cells or cells cultured in suspension (Figure 3-3). As previous results in other epithelial cell lines suggested (Khwaja et al., 1997), Akt activation induced protection from detachment-induced apoptosis (anoikis) in RPE cells (Figure 3-2). However, no obvious changes in gene expression that could contribute to the survival function of Akt could be observed. Although it might be possible that genes involved in Akt dependent survival are not represented on the microarray used here, this result indicates that protection from anoikis in RPE cells may involve direct phosphorylation of apoptotic modulators like Bad (Datta et al., 1997; del Peso et al., 1997). A large proportion of genes up-regulated by Akt activation code for enzymes that are involved in lipid metabolism. Among them are three enzymes that catalyse the rate limiting steps of cholesterol and fatty acid biosynthesis, HMG-CoA synthase, HMG-CoA reductase and fatty acid synthase, respectively. Since it had been shown previously that the SREBP family of transcription factors regulates the majority of these genes, it was investigated whether Akt can activate SREBP-dependent transcription. Activation of Akt was sufficient to induce transcription from the FAS and HMGS promoters and this was dependent on the presence of an intact SRE (Figure 3-5).

The data presented strongly suggest that activation of transcription of genes involved in lipogenesis by Akt is likely to be mediated by SREBP. Dominant negative forms of all three SREBP isoforms, in which a highly conserved tyrosine residue in the DNA binding domain was exchanged for alanine were used (Figure 3-7). This mutation has previously been shown to abolish DNA binding of SREBP proteins while still allowing dimerisation resulting in dominant negative function (Kim et al., 1995). These results indicate that expression of dominant negative SREBP1a, SREBP1c or SREBP2 was sufficient to repress Akt-dependent activation of the FAS

and HMGS promoters (Figure 3-8). In addition, specific gene silencing by siRNA was used to selectively down-regulate SREBP1 or SREBP2 expression. Analysis of activity of the FAS and HMG-CoA synthase promoters as well as expression of FAS and HMGS showed that ablation of SREBP1 almost completely blocked Akt dependent regulation of these genes (Figure 3-9). In contrast, Akt dependent regulation could still be observed, albeit to a lesser extent, after ablation of SREBP2 expression. The discrepancy between the results obtained with RNAi and dominant negative mutants is most likely due to formation of heterodimers between dominant negative proteins and endogenous SREBP (Rishi et al., 2004). It has been shown that the SREBP1a/2 heterodimer activates target gene expression to a similar extent to the respective homodimers (Datta and Osborne, 2005). The ability to form heterodimers explains the observation that DN-SREBP1a interferes with the transcriptional activity of all three SREBP family members SREBP1a, 1c and SREBP2 and vice versa. In contrast, small interfering RNAs inhibit only the family member they are homologous to.

There are significant differences in the regulatory mechanisms between the three isoforms. SREBP1c is mainly transcriptionally regulated, whereas SREBP1a and SREBP2 may be principally regulated at the post-transcriptional level (Eberle et al., 2004). There is evidence that insulin-mediated regulation of SREBP is tissue-specific (Kim et al., 2004; Nadeau et al., 2004). Activation of SREBP1 expression in response to growth factor treatment (EGF or insulin) and induction of transcription from the FAS promoter were sensitive to inhibition of PI3K (Figure 3-12). This is in keeping with a role for the PI3K/Akt pathway in mediating insulin-induced activation of SREBP1c in liver and primary hepatocytes (Fleischmann and Iynedjian, 2000; Sul et al., 2000) and underlines the critical involvement of Akt in the nutritional regulation of lipogenic gene expression by insulin. Although the ERK/MAP-kinase pathway has been implicated in regulating the transcriptional activity of SREBP (Kotzka et al., 2000; Roth et al., 2000) the MEK inhibitor UO126 had only a minor effect on FAS promoter activity in the cells used here (Figure 3-11).

Induction of FAS, HMGS, SREBP1a and SREBP1c in response to Akt activation was blocked in the presence of cycloheximide (Figure 3-6 and Figure 3-13). These results imply that activation of SREBP dependent gene expression by Akt involves an indirect mechanism that requires *de novo* protein synthesis. It is possible that Akt induces an intermediate transcription factor that then regulates SREBP dependent gene expression.

It has been demonstrated that the SREBP1c promoter contains two important insulin-response elements, an SRE complex (SRE, E-box, NF-Y, and SP1-binding sites) and two liver X receptor (LXR)-response elements (LXREs) (Cagen et al., 2005; Deng et al., 2002). LXRα and LXRβ are nuclear hormone receptors that coordinate hepatic lipid metabolism, and are required for full

induction of SREBP1c by insulin (Chen et al., 2004). It has been demonstrated that T0901317 (LXR agonist) and oxysterol treatment is associated with up-regulation of SREBP1c and its target genes (Repa et al., 2000; Schultz et al., 2000). In contrast, polyunsaturated fatty acids (e.g. arachidonic acid) function as LXR antagonists and inhibit SREBP1 expression (Hannah et al., 2001; Ou et al., 2001; Yoshikawa et al., 2002). Interestingly, beside the observed regulation of FAS and SREBP1c expression by LXR, T0901317 treatment also led to an increase in the SREBP1a transcript (Figure 3-14). Promoter analysis revealed one LXR site approximately 3500bp upstream of the TSS, which could be involved in activation of SREBP1a expression by LXR. It has recently been published that LXRα/ß also sense glucose (Mitro et al., 2007). D-glucose and D-glucose-6-phosphate bind directly to LXR and induce expression of LXR target genes, e.g. SREBP1c and FAS (Mitro et al., 2007). One of the most important physiological functions of Akt is to stimulate glucose uptake in response to insulin (Eguez et al., 2005; Kohn et al., 1996). This would suggest an indirect role for Akt on SREBP-mediated induction of lipogenesis gene expression via activation of LXR, by stimulating glucose uptake. The possibility was tested and the results showed that arachidonic acid treatment did not block Akt-induced activation of FAS and ACL. Furthermore, activation of Akt was sufficient to further increase ACL and FAS protein levels in the presence of T0901317 (Figure 3-14). These findings are an indication that Akt may activate SREBP processing, which would lead to enhanced FAS and ACL expression levels as well as SREBP transcription. This hypothesis would be consistent with the report that the LXR mediates insulin dependent transcription of SREBP1c, while an acute insulin stimulus leads to rapid accumulation of the mature, transcriptionally active form in a PI3K-dependent manner (Hegarty et al., 2005).

In summary, the results presented in this chapter provide evidence that activation of transcription of genes encoding for fatty acid and cholesterol synthesis by Akt requires SREBP activity and that SREBPs may be essential mediators of the regulation of lipid biosynthesis by the Ras/PI3K/Akt pathway.

Figure 3-1 Schematic presentation of the wild-type Akt and myrAkt-ER fusion protein

(A) shows the domain structure of wild-type Akt protein. **(B)** The myrAkt-ER fusion protein, which has been deleted in the PH-domain, contains a Src myristoylation sequence (myr) and the hormone binding domain of a mutant murine estrogen receptor (ER) that selectively binds 4-hydroxytamoxifen (4-OHT) instead of its natural ligand 17-ß-estradiol. **(C)** Conditional activation of myrAkt-ER: after being directed to the membrane by the myristoylated residue, Akt becomes independent of PIP3 levels. In the presence of 4-hydroxytamoxifen (4-OHT) the hormone binding domain of the estrogen receptor changes conformation, heatshock proteins dissociate and the two phosphorylation sites (S473 and T308) become accessible for phosphorylation by PDK1 and TORC2. This leads to activation of the Akt kinase. PH-domain: pleckstrem homology domain, ER: estrogen receptor, T/Thr: threonine, S/Ser: serine, HA: hemagglutinin-tag

Figure 3-1

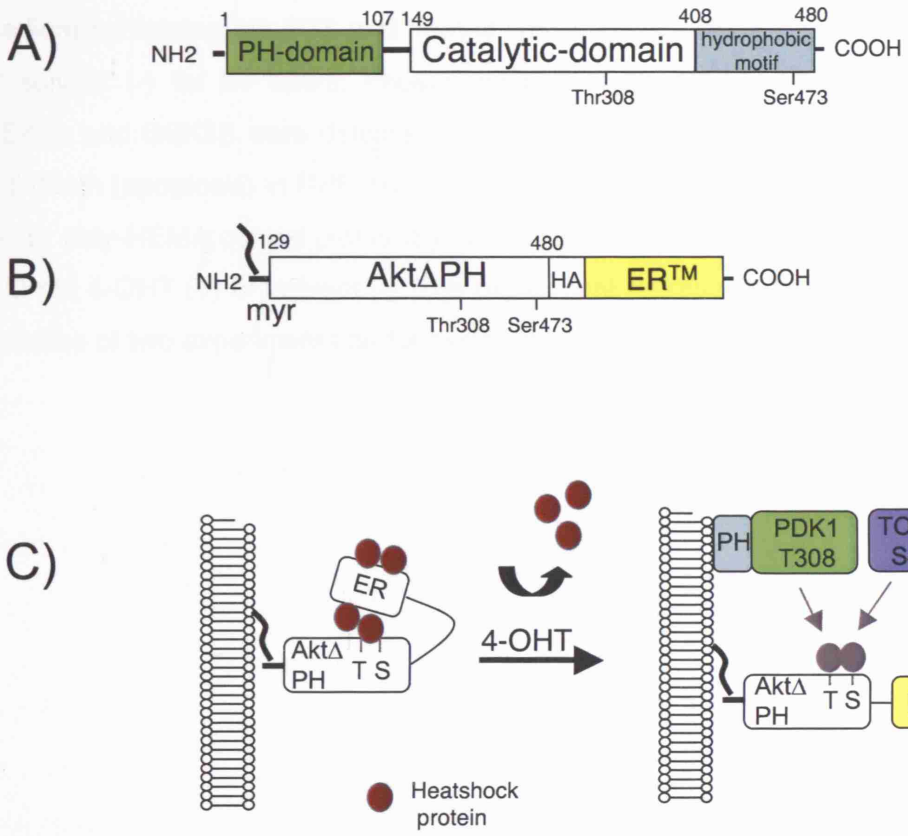
A)
1
107
149
408
480
NH2
PH-domain
Catalytic-domain
hydrophobic motif
COOH
Thr308
Ser473
B)
129
480
NH2
AktΔPH
HA
ER™
COOH
myr
Thr308
Ser473
C)
ER
Akt Δ PH
T S
4-OHT
PH
PDK1 T308
TORC2 S473
Akt Δ PH
T S
ER
Heatshock protein

Figure 3-2 Activation of myrAkt-ER protects RPE cells from detachment-induced apoptosis

(A) RPE myrAkt-ER cells were plated on normal (A) or poly-HEMA coated dishes (S) in medium containing 1% FCS and treated with 100 nM 4-hydroxytamoxifen (4-OHT) (+) or solvent (-) for 24 hours. Phosphorylation of myrAkt-ER and the Akt substrates GSK3α and GSK3β were detected using phosphospecific antibodies. **(B)** Detection of cell death (apoptosis) in RPE myrAkt-ER cells after 24 and 48 hours culture on normal (A) or poly-HEMA coated plates (S) in medium containing 3% FCS in the presence of 100 nM 4-OHT (+) or solvent (-). The experiment represents the means and standard variation of two experiments performed in duplicates.

Figure 3-2

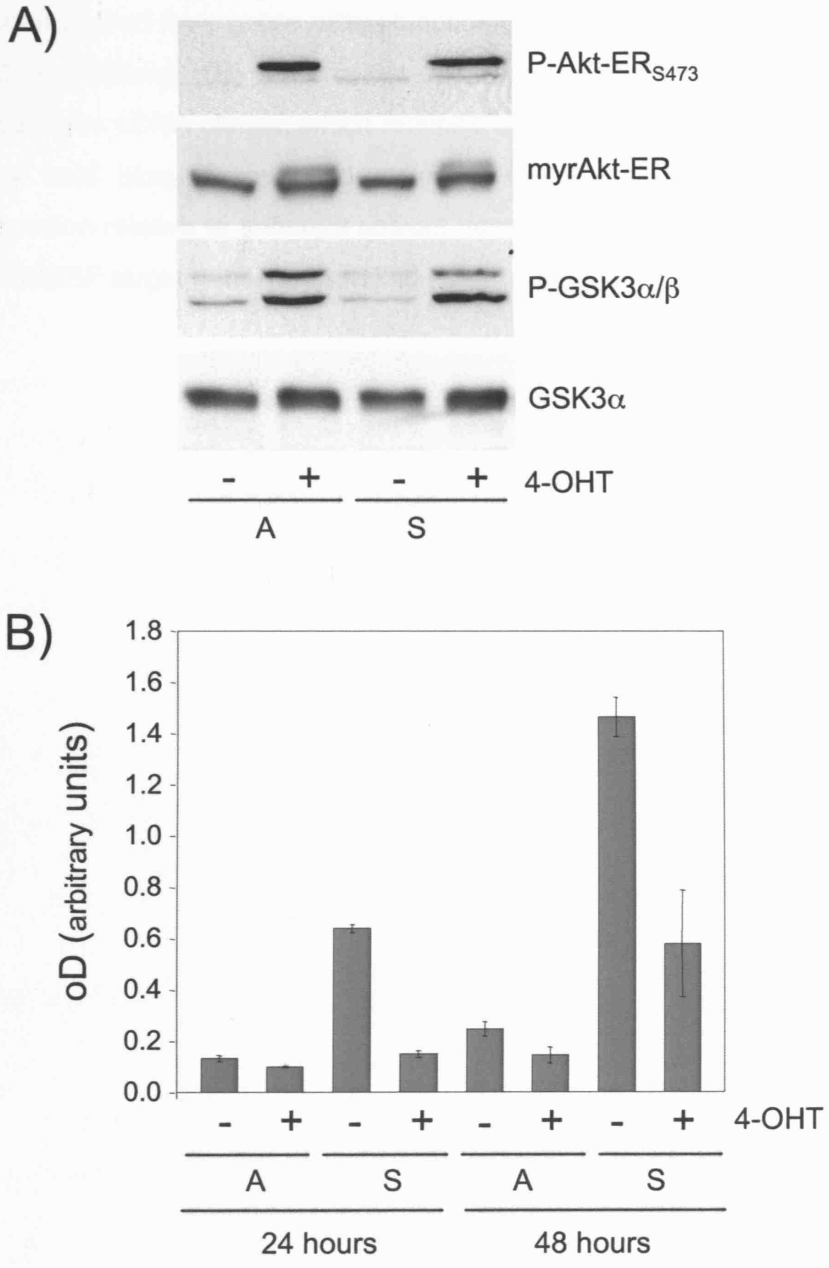
A)
P-Akt-ER$_{S473}$
myrAkt-ER
P-GSK3α/β
GSK3α
- + - + 4-OHT
A S
B)
oD (arbitrary units)
1.8
1.6
1.4
1.2
1.0
0.8
0.6
0.4
0.2
0.0
- + - + - + - + 4-OHT
A S A S
24 hours 48 hours

Figure 3-3 A large proportion of Akt induced genes are involved in cholesterol and fatty acid biosynthesis

(A) Functional classification of genes, which are found to be up- or down-regulated in response to Akt activation in RPE cells. Pie charts represent the fraction of cDNA clones derived from genes within functional categories as classified by their associated GO annotations. **(B)** Two colour representation of expression profiles of 24 Akt responsive cDNA clones, which mapped to genes that are involved in cholesterol and fatty acid biosynthesis. Red indicates up-regulation and green indicates down-regulation relative to adherent solvent treated control cells. Genes previously identified as SREBP target genes are marked (*).

Figure 3-3

A)

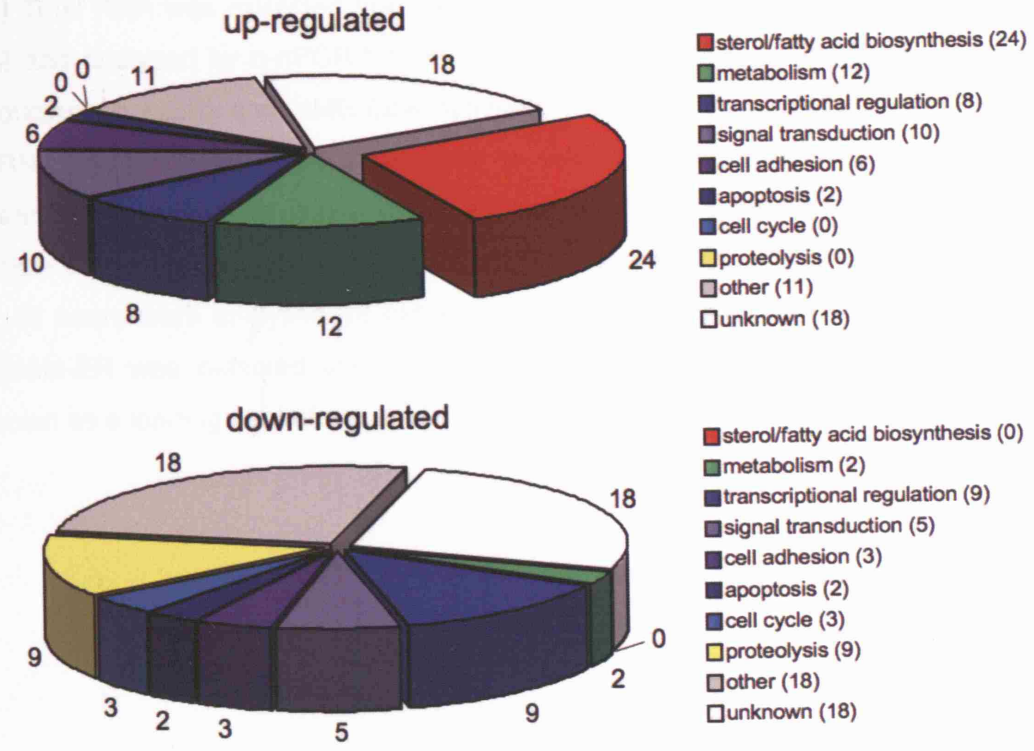
up-regulated
0
0
11
18
2
6
10
8
12
24
sterol/fatty acid biosynthesis (24)
metabolism (12)
transcriptional regulation (8)
signal transduction (10)
cell adhesion (6)
apoptosis (2)
cell cycle (0)
proteolysis (0)
other (11)
unknown (18)
down-regulated
18
18
9
3
2
3
5
9
0
2
sterol/fatty acid biosynthesis (0)
metabolism (2)
transcriptional regulation (9)
signal transduction (5)
cell adhesion (3)
apoptosis (2)
cell cycle (3)
proteolysis (9)
other (18)
unknown (18)

B)

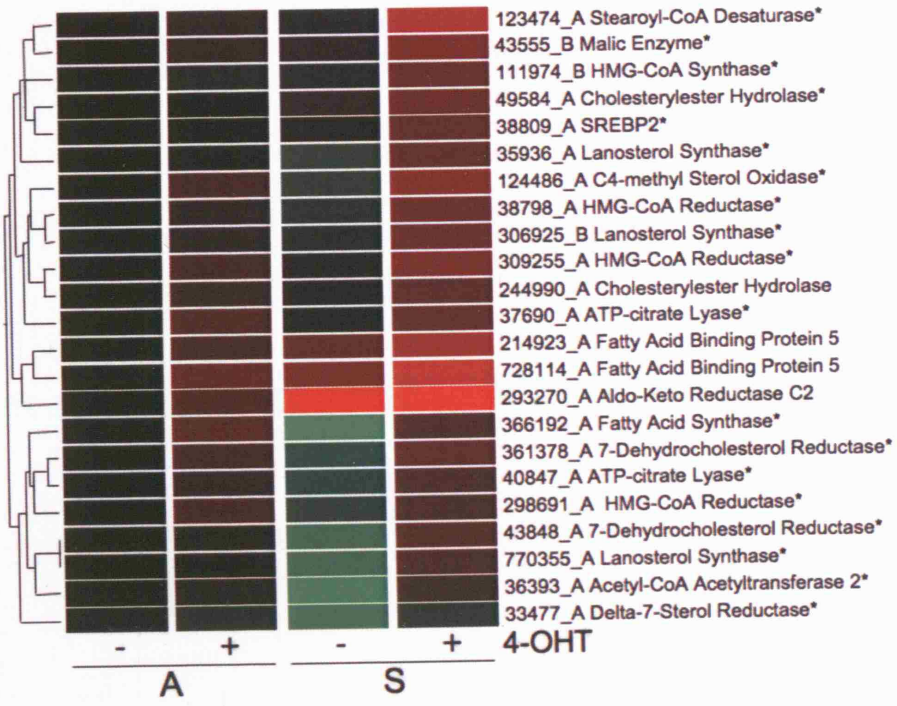
123474_A Stearoyl-CoA Desaturase*
43555_B Malic Enzyme*
111974_B HMG-CoA Synthase*
49584_A Cholesterylester Hydrolase*
38809_A SREBP2*
35936_A Lanosterol Synthase*
124486_A C4-methyl Sterol Oxidase*
38798_A HMG-CoA Reductase*
306925_B Lanosterol Synthase*
309255_A HMG-CoA Reductase*
244990_A Cholesterylester Hydrolase
37690_A ATP-citrate Lyase*
214923_A Fatty Acid Binding Protein 5
728114_A Fatty Acid Binding Protein 5
293270_A Aldo-Keto Reductase C2
366192_A Fatty Acid Synthase*
361378_A 7-Dehydrocholesterol Reductase*
40847_A ATP-citrate Lyase*
298691_A HMG-CoA Reductase*
43848_A 7-Dehydrocholesterol Reductase*
770355_A Lanosterol Synthase*
36393_A Acetyl-CoA Acetyltransferase 2*
33477_A Delta-7-Sterol Reductase*
- + - +
4-OHT
A
S

Figure 3-4 Differential expression of Akt target genes involved in cholesterol and fatty acid biosynthesis

(A) Total RNA was extracted from cells treated as in the experiment shown in Figure 3-2 and analysed by q-rtPCR for expression of fatty acid synthase (FAS), HMG-CoA reductase (HMGR) and HMG-CoA synthase (HMGS). The values represent relative mRNA abundance and are normalised to GAPDH. The experiment represents the means and standard deviation (± SD) of three experiments performed in duplicates. **(B)** Whole cell lysates of adherent and suspension cells treated with 100 nM 4-OHT for 24 or 48 hours were analysed for expression of fatty acid synthase (FAS). Activation of myrAkt-ER was detected using a phosphospecific antibody against S473. Actin is shown as a loading control.

Figure 3-4

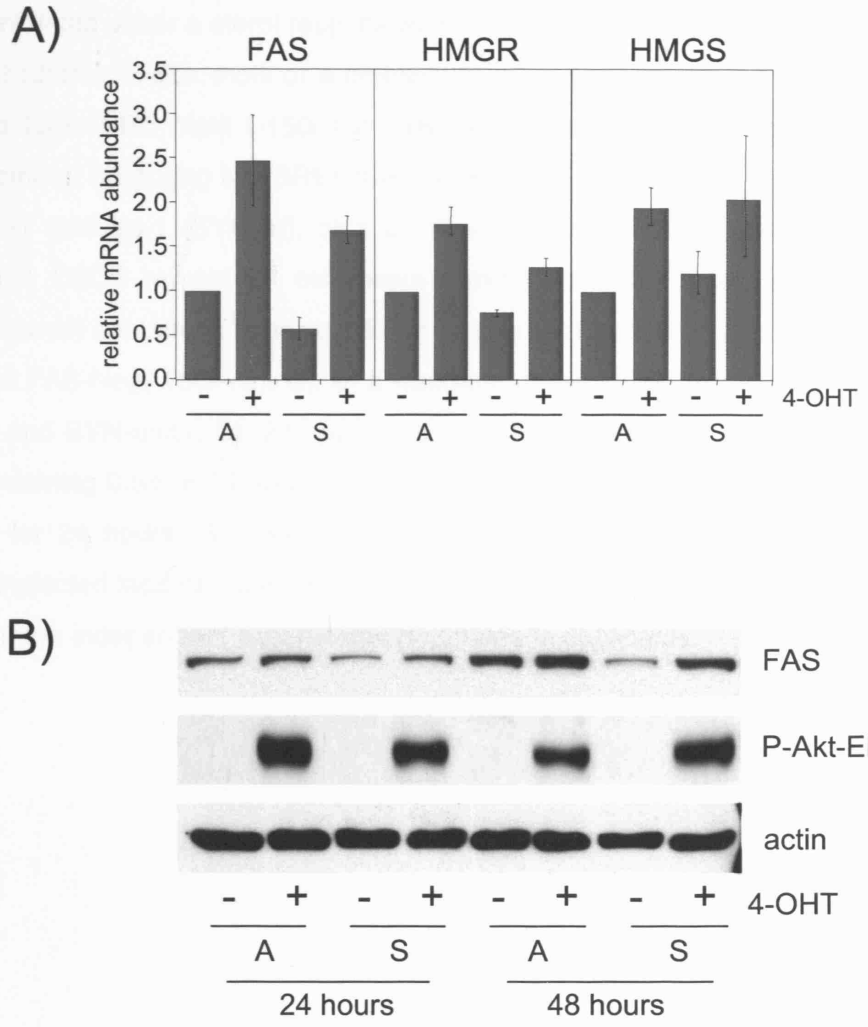
A)
FAS
HMGR
HMGS
relative mRNA abundance
3.5
3.0
2.5
2.0
1.5
1.0
0.5
0.0
- + - + - + - + - + - +
4-OHT
A S A S A S
B)
FAS
P-Akt-ER$_{S473}$
actin
- + - + - + - +
4-OHT
A S A S
24 hours
48 hours

Figure 3-5 Akt induces expression of the fatty acid synthase and HMG-CoA synthase promoters

Luciferase reporter constructs: **(A)** A fragment of the rat fatty acid synthase promoter containing either a sterol responsive element (-150/-43) consisting of two SRE and one palindromic E-Box motif or a deletion mutant (-150/-73) containing only a nutritionally-regulated SRE motif (-150/-131). **(B)** A fragment of the human HMG-CoA synthase promoter harboring two SREs (SRE-1 and SRE-2) flanked by auxiliary binding sites for NF-Y and Sp-1 (SYN-wt), or a construct in which SRE-1 was mutated (SYN-mut1). **(C/D)** U2OS myrAkt-ER cells were transfected with 0.1 μg of a luciferase reporter construct containing either a 150 bp fragment of the rat FAS promoter (FAS(-150/-43) and FAS-Neg(-150/-73), C), or a fragment of the HMG-CoA synthase promoter (SYN-wt and SYN-mut1, D). 24 hours post-transfection, medium was replaced with medium containing 0.5% FCS and cells were treated with 100 nM 4-OHT (+) or solvent control (-) for 24 hours. Relative luciferase activity was normalised to the activity of a co-transfected lacZ expression plasmid. The data represent mean and standard deviation of three independent experiments performed in duplicates.

Figure 3-5

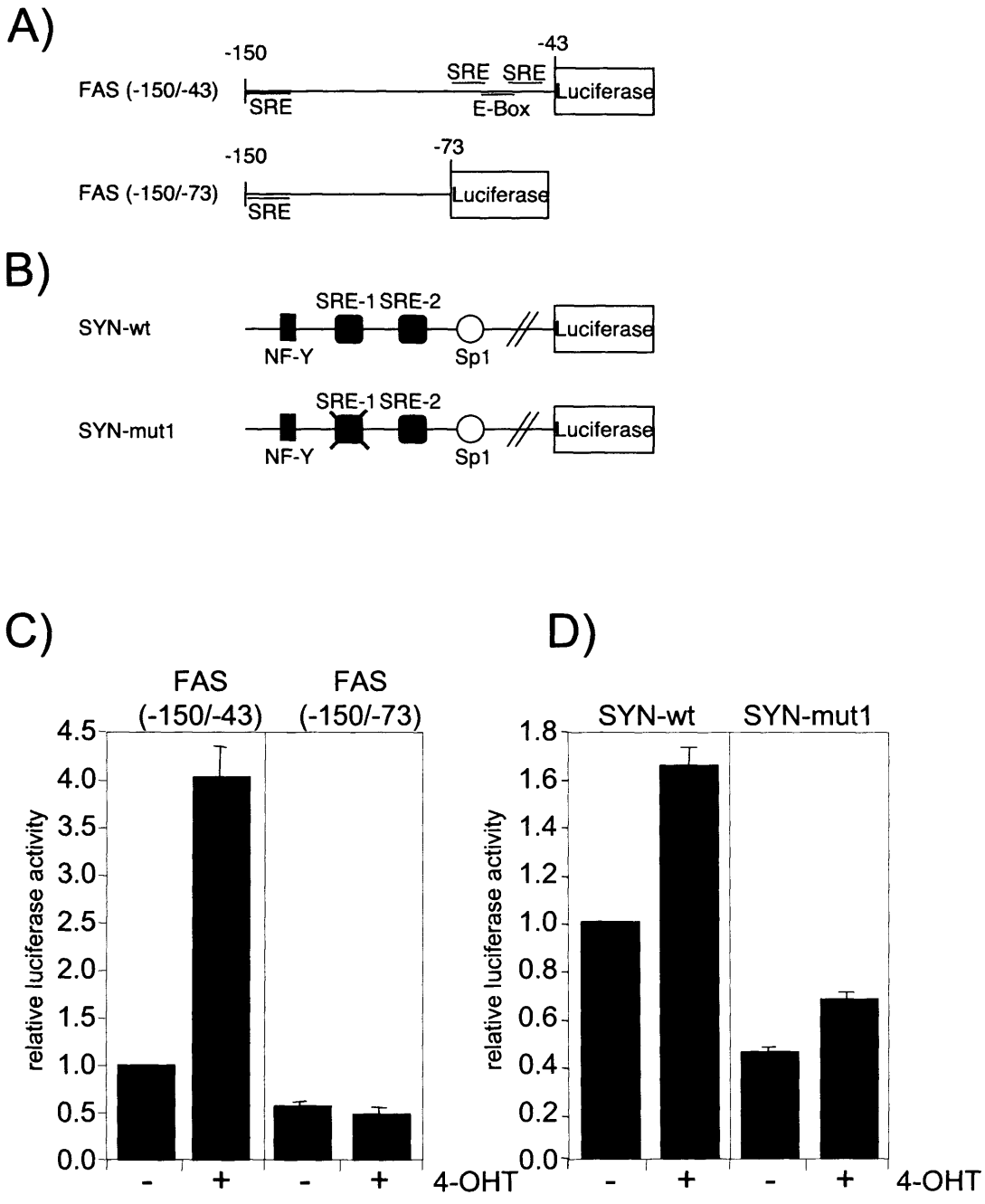
A)
-150
-43
SRE SRE
FAS (-150/-43)
SRE
E-Box
Luciferase
-150
-73
FAS (-150/-73)
SRE
Luciferase
B)
SRE-1 SRE-2
SYN-wt
NF-Y
Sp1
Luciferase
SRE-1 SRE-2
SYN-mut1
NF-Y
Sp1
Luciferase
C)
FAS (-150/-43)
FAS (-150/-73)
relative luciferase activity
4.5
4.0
3.5
3.0
2.5
2.0
1.5
1.0
0.5
0.0
- + - +
4-OHT
D)
SYN-wt
SYN-mut1
relative luciferase activity
1.8
1.6
1.4
1.2
1.0
0.8
0.6
0.4
0.2
0.0
- + - +
4-OHT

Figure 3-6 Activation of fatty acid synthase and HMG-CoA synthase by Akt requires *de novo* protein synthesis

RPE myrAkt-ER cells were plated in medium containing 1% FCS and treated with 100 nM 4-hydroxytamoxifen (4-OHT) (+) or solvent (-) in the presence or absence of 2 μg/ml cycloheximide (CHX) for 24 hours. Total RNA was analysed for expression of fatty acid synthase (FAS, left panel) or HMG-CoA synthase (HMGS, right panel) by q-rtPCR. Values represent relative mRNA abundance and are normalised to GAPDH. The experiment represents the means and standard deviation of three experiments performed in duplicates.

Figure 3-6

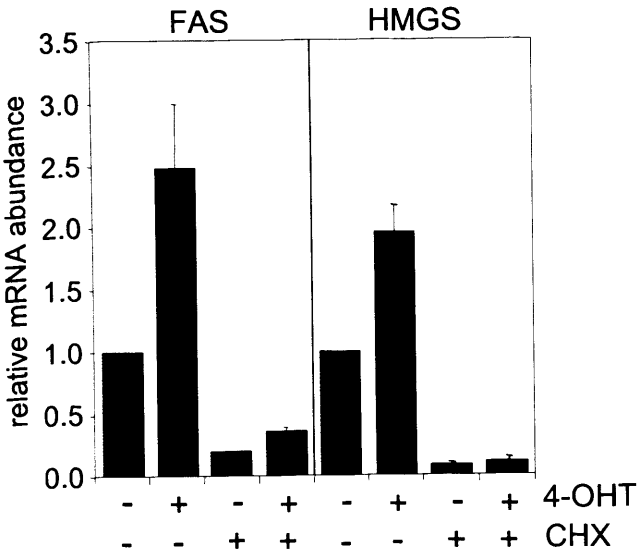
FAS
HMGS
relative mRNA abundance
3.5
3.0
2.5
2.0
1.5
1.0
0.5
0.0
- + - + - + - + 4-OHT
- - + + - - + + CHX

Figure 3-7

A) SREBP1a[Y335A] and SREBP1c[Y321A]

335/321

```
gcc cac aac gcc att gag aag cgc tac cgc tcc tcc atc aat gac aaa atc att
 A   H   N   A   I   E   K   R   Y   R   S   S   I   N   D   K   I   I

gcc cac aac gcc att gag aag cgc gcc cgc tcc tcc atc aat gac aaa atc att
 A   H   N   A   I   E   K   R   A   R   S   S   I   N   D   K   I   I
```

B) SREBP2[Y342A]

342

```
agg cgg aca acc cat aat atc att gag aaa cga tat cgc tcc tcc atc aat gac
 R   R   T   T   H   N   I   I   E   K   R   Y   R   S   S   I   N   D
agg cgg aca acc cat aat atc att gag aaa cga gct cgc tcc tcc atc aat gac
 R   R   T   T   H   N   I   I   E   K   R   A   R   S   S   I   N   D
```

Figure 3-7 Sequences of the DNA binding domains of SREBP1a, SREBP1c and SREBP2

Bases marked red are substituted and the amino acids marked in yellow represent the conserved and mutated sequences in the basic-HLH DNA binding region. **(A/B)** Tyrosine mutagenesis with a single amino acid exchange, the tyrosine residue (SREBP1a: aa 335, SREBP1c: aa 321 (A), SREBP2: aa 342 (B)) was replaced by alanine. The dominant-negative mature SREBP constructs have the following nomenclature: m1a[YA], m1c[YA] and m2[YA].

Figure 3-8 Activation of fatty acid synthase and HMG-CoA synthase promoter expression by Akt requires SREBP function

(A) U2OS myrAkt-ER cells were transfected with 0.1 μg FAS reporter construct (FAS(-150/-43) together with 1 ng of expression plasmids coding for mature SREBP1a (m1a), mature SREBP1c (m1c) and mature SREBP2 (m2), and 0.1 μg of plasmid coding for dominant negative mutants of mature SREBP1a (m1a[YA]), SREBP1c (m1c[YA]), SREBP2 (m2[YA]) or empty vector, as indicated. 24 hours post-transfection, medium was changed to 0.5% FSC for an additional 24 hours before harvest. Relative luciferase activity was normalised to the activity of a co-transfected lacZ expression plasmid and data show one experiment. **(B/C)** U2OS myrAkt-ER cells were transfected with 0.1 μg FAS reporter construct (FAS(-150/-43), B) or 0.1 μg HMG-CoA synthase reporter construct (SYN-wt, C) together with 0.1 μg of expression plasmids for dominant negative mutants of SREBP or empty vector, as indicated. 24 hours post-transfection, cells were treated with 100 nM 4-OHT (+) or solvent (-) in medium containing 0.5% FCS for an additional 24 hours. Relative luciferase activity was normalised to the activity of a co-transfected lacZ expression plasmid. Data represent mean $\pm$ SD of three independent experiments performed in duplicates.

Figure 3-8

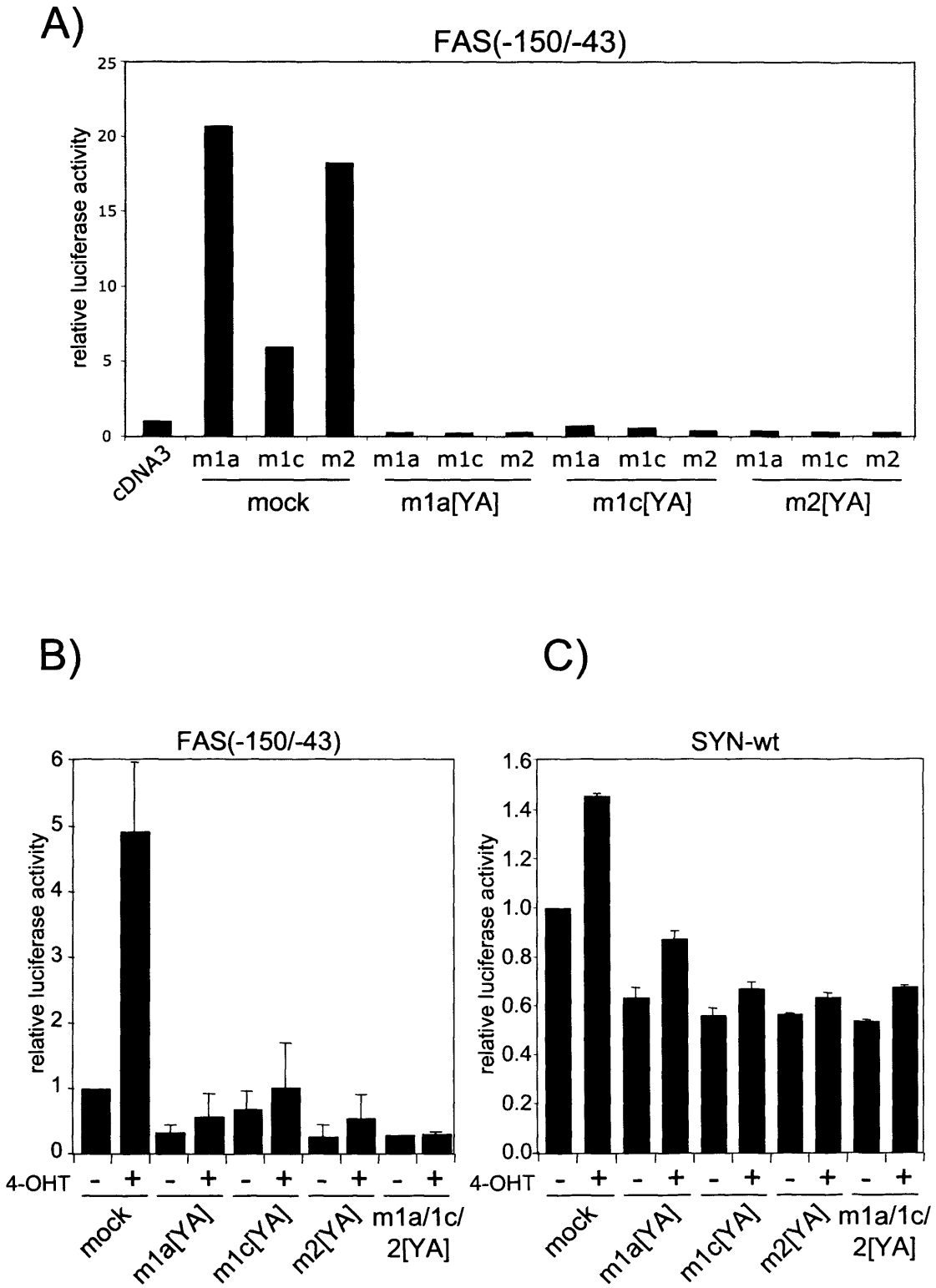
A)
FAS(-150/-43)
relative luciferase activity
25
20
15
10
5
0
cDNA3
m1a m1c m2 m1a m1c m2 m1a m1c m2 m1a m1c m2
mock
m1a[YA]
m1c[YA]
m2[YA]
B)
FAS(-150/-43)
relative luciferase activity
6
5
4
3
2
1
0
4-OHT - + - + - + - + - +
mock
m1a[YA]
m1c[YA]
m2[YA]
m1a/1c/2[YA]
C)
SYN-wt
relative luciferase activity
1.6
1.4
1.2
1.0
0.8
0.6
0.4
0.2
0.0
4-OHT - + - + - + - + - +
mock
m1a[YA]
m1c[YA]
m2[YA]
m1a/1c/2[YA]

Figure 3-9 Silencing of SREBP blocks fatty acid synthase, HMG-CoA synthase and HMG-CoA reductase expression by Akt

(A) U2OS myrAkt-ER cells were transfected with 0.8 μg siRNA oligonucleotides specific for SREBP1 or SREBP2 or an unspecific control oligonucleotide as indicated. 3 hours post-transfection, medium was replaced with medium containing 0.5% FCS and cells were treated with 100 nM 4-OHT (+) or solvent (-) for 48 hours. Whole cell lysates were analysed for expression of fatty acid synthase (FAS), full length SREBP1 and SREBP2. Activation of the myrAkt-ER fusion protein was determined using a phosphospecific antibody. Actin is shown as a loading control. **(B/C)** U2OS myrAkt-ER cells were treated as in A) and subsequently transfected with 0.1 μg FAS reporter construct (FAS(-150/-43), B) or 0.1 μg HMG-CoA synthase reporter construct (SYN-wt, C). 24 hours post-transfection, medium was replaced with medium containing 0.5% FCS and cells were treated with 100 nM 4-OHT (+) or solvent (-) for 24 hours. Relative luciferase activity was normalised to the activity of a co-transfected lacZ expression plasmid. Data represent mean of two independent experiments performed in duplicate. **(D/E)** U2OS myrAkt-ER cells were treated as in A). Total RNA was analysed for expression of fatty acid synthase (FAS, D) and HMG-CoA synthase (HMGS, E) by q-rtPCR. Transcription levels are normalised to gapdh mRNA levels and are shown relative to vehicle treated control. Error bars represent $\pm$ the range of two experiments performed in duplicate.

Figure 3-9

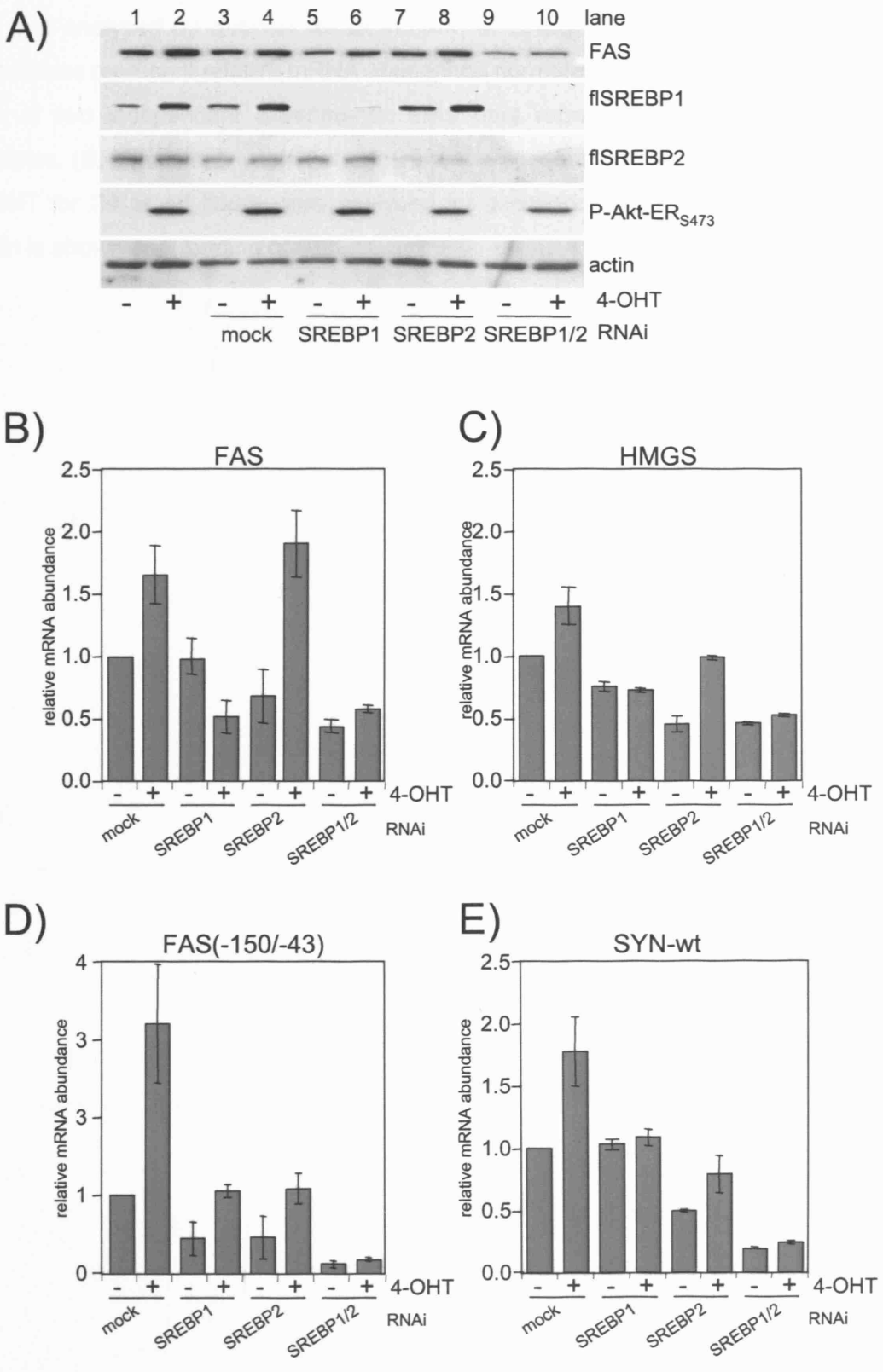
A)
1 2 3 4 5 6 7 8 9 10 lane
FAS
flSREBP1
flSREBP2
P-Akt-ER$_{S473}$
actin
- + - + - + - + - + 4-OHT
mock SREBP1 SREBP2 SREBP1/2 RNAi
B)
FAS
relative mRNA abundance
2.5
2.0
1.5
1.0
0.5
0.0
- + - + - + - + 4-OHT
mock SREBP1 SREBP2 SREBP1/2 RNAi
C)
HMGS
relative mRNA abundance
2.5
2.0
1.5
1.0
0.5
0.0
- + - + - + - + 4-OHT
mock SREBP1 SREBP2 SREBP1/2 RNAi
D)
FAS(-150/-43)
relative mRNA abundance
4
3
3
1
0
- + - + - + - + 4-OHT
mock SREBP1 SREBP2 SREBP1/2 RNAi
E)
SYN-wt
relative mRNA abundance
2.5
2.0
1.5
1.0
0.5
0.0
- + - + - + - + 4-OHT
mock SREBP1 SREBP2 SREBP1/2 RNAi

Figure 3-10 Differential expression of SREBP1 and SREBP2 by Akt

(A) Total RNA was extracted from cells treated as in the experiment shown in Figure 3-2 and analysed by q-rtPCR for expression of SREBP1a, SREBP1c and SREBP2. The values represent relative mRNA abundance normalised to GAPDH. Data represent one of two independent experiments; error bars represent the range of duplicate samples. **(B)** Whole cell lysates of adherent and suspension cells treated with 100 nM 4-OHT for 24 or 48 hours were analysed for expression of SREBP1 and SREBP2. Actin is shown as a loading control.

Figure 3-10

A)

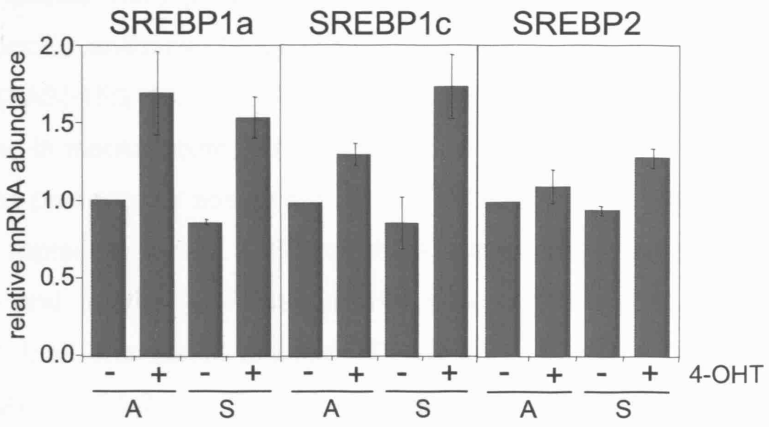

B)

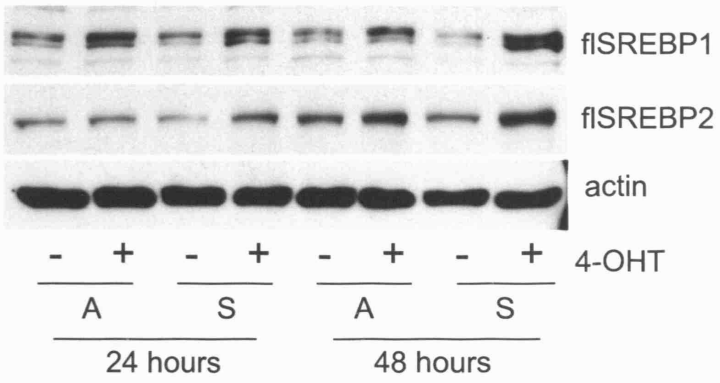

Figure 3-11 Activation of endogenous Akt by EGF or insulin induces HMG-CoA synthase and fatty acid synthase promoter expression

(A) U2OS cells were treated with 10 ng/ml EGF or 10 μg/ml insulin for 2, 4 and 8 hours. Total cell lysates were prepared and analysed for phosphorylation of Akt using a phosphospecific antibody. **(B/C)** U2OS cells transfected with 0.1 μg FAS reporter construct (FAS(-150/-43), B) or HMG-CoA synthase promoter construct (SYN-wt, C) were placed in medium containing 0.5% FCS and induced with 10 μg/ml insulin for 24 hours in the presence or absence of 50 μM LY294002 or 30 μM UO126, respectively. The data represent mean ± SD of three independent experiments performed in duplicates and relative luciferase activity was normalised to the activity of a co-transfected lacZ expression plasmid. **(D)** Whole cell lysates of cells treated with 10 μg/ml insulin for 24 hours in the presence of 50 μM LY294002 were analysed for expression of fatty acid synthase (FAS). GAPDH is shown as a loading control.

Figure 3-11

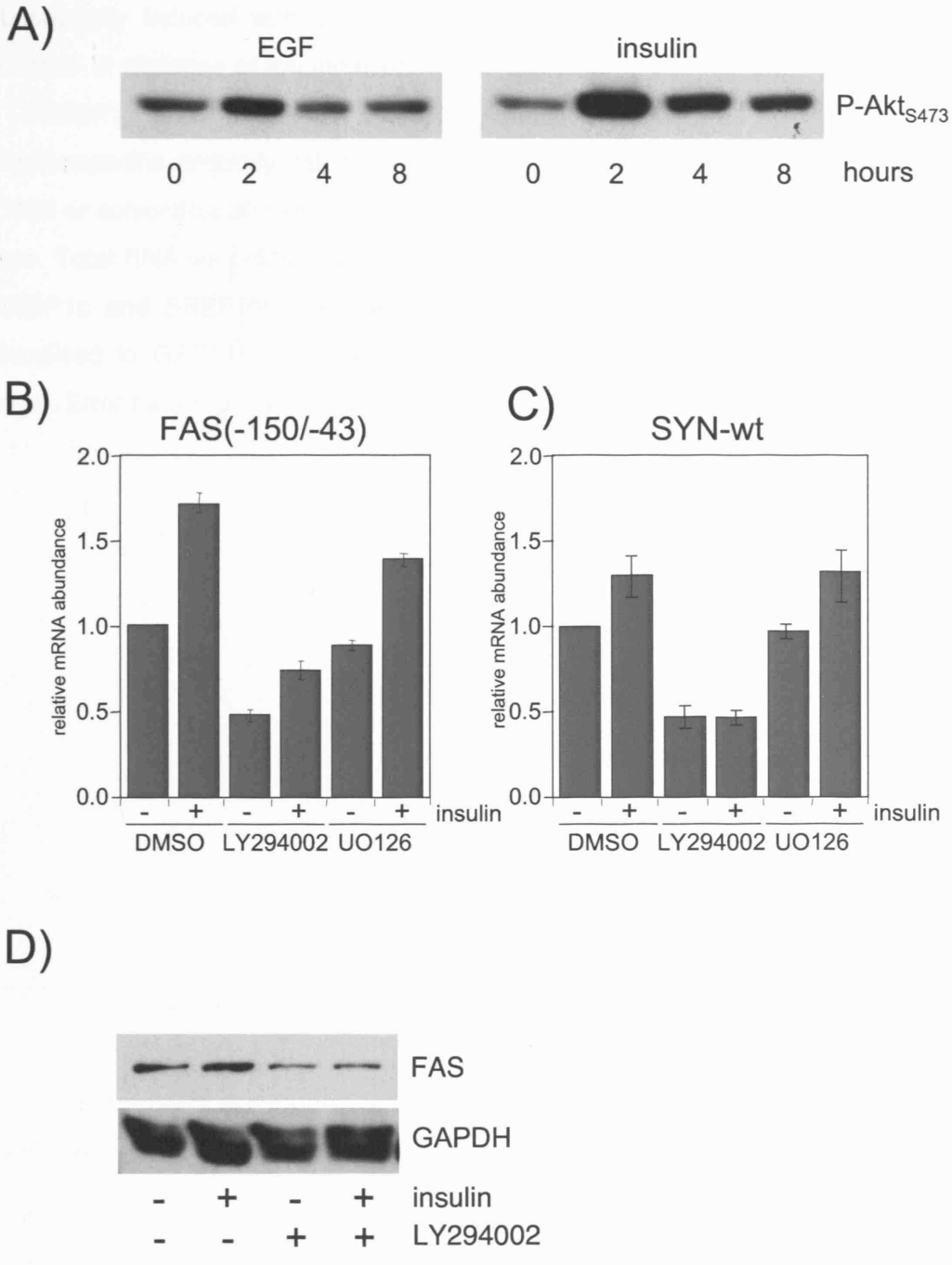
A)
EGF
insulin
P-Akt$_{S473}$
0 2 4 8
0 2 4 8
hours
B)
FAS(-150/-43)
relative mRNA abundance
2.0
1.5
1.0
0.5
0.0
- + - + - +
insulin
DMSO LY294002 UO126
C)
SYN-wt
relative mRNA abundance
2.0
1.5
1.0
0.5
0.0
- + - + - +
insulin
DMSO LY294002 UO126
D)
FAS
GAPDH
- + - + insulin
- - + + LY294002

Figure 3-12 Activation of endogenous Akt by EGF or insulin induces SREBP1 accumulation

(A) RPE cells were treated with 50 μM LY294002 or solvent for 30 minutes and subsequently induced with 10 ng/ml EGF or 10 μg/ml insulin for 24 hours in the presence or absence of the inhibitor. Whole cell lysates were analysed for expression of SREBP1 and SREBP2. Phosphorylation of Akt was detected using a phosphospecific antibody. **(B)** RPE cells were treated with 50 μM LY294002, 30 μM UO126 or solvent for 30 minutes and subsequently induced with 10 μg/ml insulin for 24 hours. Total RNA was extracted and analysed by q-rtPCR for expression of SREBP1a, SREBP1c and SREBP2. The values represent relative mRNA abundance and are normalised to GAPDH. A representative result of three independent experiments is shown. Error bars represent $\pm$ the range of duplicate samples.

Figure 3-12

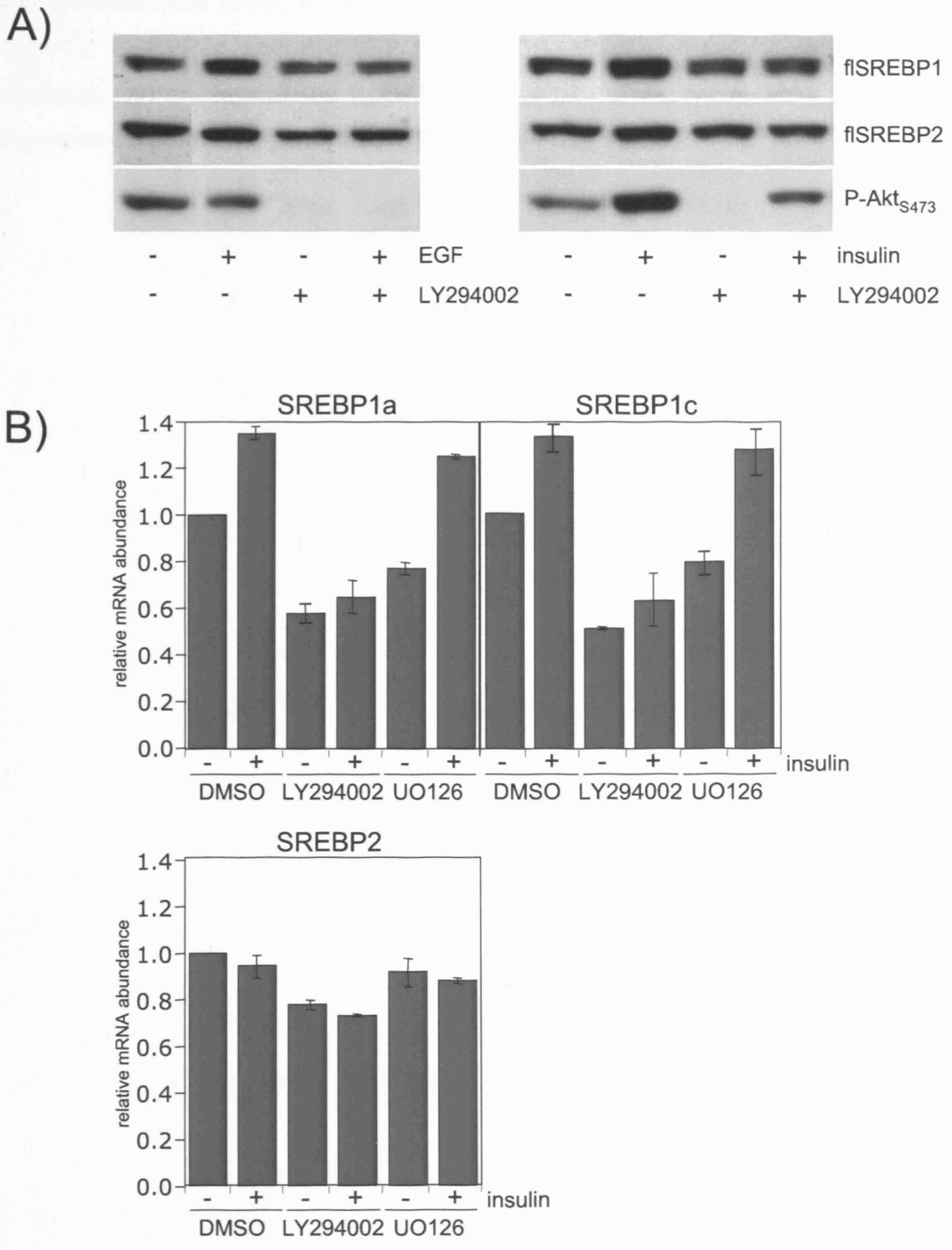
A)
flSREBP1
flSREBP2
P-Akt$_{S473}$
- + - + EGF - + - + insulin
- - + + LY294002 - - + + LY294002
B)
SREBP1a
SREBP1c
relative mRNA abundance
1.4
1.2
1.0
0.8
0.6
0.4
0.2
0.0
- + - + - + - + - + - + insulin
DMSO LY294002 UO126 DMSO LY294002 UO126
SREBP2
relative mRNA abundance
1.4
1.2
1.0
0.8
0.6
0.4
0.2
0.0
- + - + - + insulin
DMSO LY294002 UO126

Figure 3-13 Activation of SREBP1 by Akt requires *de novo* protein synthesis

RPE myrAkt-ER cells were plated in medium containing 1% FCS and treated with 100 nM 4-hydroxytamoxifen (4-OHT) (+) or solvent (-) in the presence or absence of 2 μg/ml cycloheximide (CHX) for 24 hours. Total RNA was analysed for expression of SREBP1a, SREBP1c and SREBP2 by q-rtPCR. Values represent relative mRNA abundance and are normalised to GAPDH. The data represent mean ± SD of three independent experiments performed in duplicate.

Figure 3-13

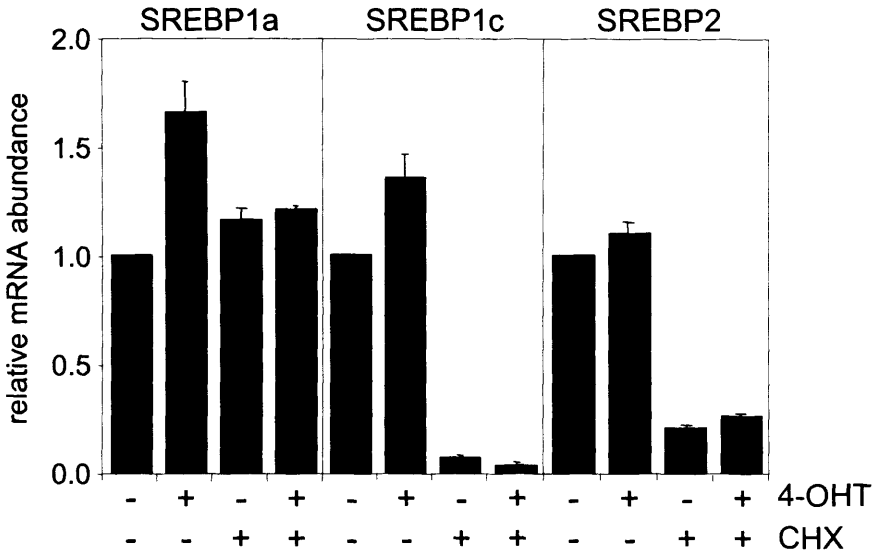
SREBP1a
SREBP1c
SREBP2
relative mRNA abundance
2.0
1.5
1.0
0.5
0.0
- + - + - + - + - + - +
4-OHT
- - + + - - + + - - + +
CHX

Figure 3-14 SREBP dependent activation of ACL and FAS expression by Akt does not require LXR activity

(A) RPE cells were plated in medium containing 10% FCS, starved for 24 hours in 1% lipoprotein deficient serum (LPDS) and subsequently treated with 1 μM T090117 (T090), 100 μM arachidonic acid (AA) or solvent (DMSO) for 24 hours. Total RNA was extracted and analysed by q-rtPCR for expression of SREBP1a, SREBP1c, SREBP2, fatty acid synthase (FAS) and HMG-CoA synthase (HMGS). The values represent relative mRNA abundance and are normalised to GAPDH. **(B)** Whole cell lysates from cells treated as in (A) were analysed for expression of FAS and SREBP1. Actin is shown as a loading control. **(C)** RPE cells were plated in medium containing 10% FCS, starved for 24 hours in 1% LPDS and subsequently treated with mixture of 10 μg/ml cholesterol and 1 μg/ml 25-hydroxycholesterol (sterols) or solvent (DMSO) for 24 hours. Total RNA was extracted and analysed by q-rtPCR for expression of SREBP1a, SREBP1c and SREBP2. The values represent relative mRNA abundance and are normalised to GAPDH. **(D)** RPE myrAkt-ER cells were treated with 1 μM T090117 (T090), 100 μM arachidonic acid (AA) or solvent (DMSO) for 30 mins and subsequently stimulated with 100 nM 4-OHT for 24 hours. Whole cell lysates were analysed for expression of FAS and ATP-citrate pro-S-lyase (ACL), respectively. Activation of myrAkt-ER was detected using a phosphospecific antibody against S473. Actin is shown as a loading control. All q-rtPCR data represent mean $\pm$ SD of three independent experiments performed in duplicate.

Figure 3-14

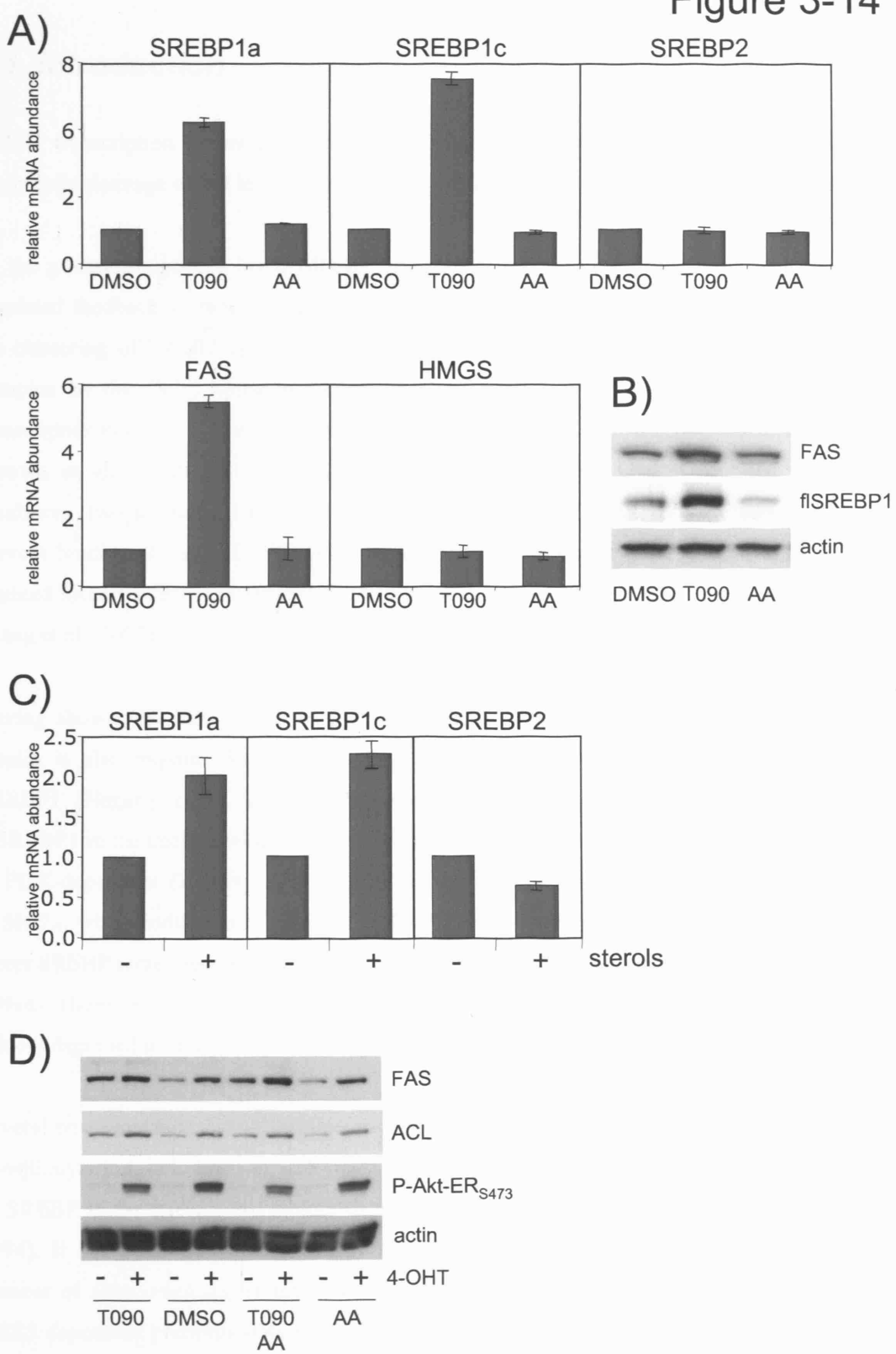
A)
SREBP1a
SREBP1c
SREBP2
relative mRNA abundance
8
6
2
0
DMSO
T090
AA
FAS
HMGS
4
B)
FAS
flSREBP1
actin
C)
2.5
2.0
1.5
1.0
0.5
0.0
sterols
D)
ACL
P-Akt-ER$_{S473}$
4-OHT
T090
DMSO
T090
AA
AA

4 Chapter 4: Regulation of SREBP activity by Akt

4.1 Introduction

SREBP transcription factors are regulated at several levels, including transcription, processing, proteolytic cleavage of full length SREBP and posttranslational modification of mature SREBP.

At the posttranscriptional level, SREBP processing is controlled by cholesterol in a tightly regulated feedback system. When intracellular sterol concentrations are low, SCAP mediates the clustering of SREBP into COPII-coated vesicles. These vesicles carry the SCAP/SREBP complex to the Golgi apparatus where two proteolytic steps are required to release the transcriptionally active N-terminal part of the protein, which then translocates to the nucleus (Brown et al., 2002; Sun et al., 2007; Yang et al., 2002a). Under saturated cholesterol conditions, two additional ER-located proteins, termed INSIG1 and INSIG2, bind to SCAP and prevent binding of the SREBP/SCAP complex to COPII proteins (Sun et al., 2005). The ER-retained SREBPs cannot be processed, resulting in inhibition of SREBP dependent transcription (Yang et al., 2002a).

Having shown that insulin induces SREBP1 mRNA (Figure 3-12), it has been reported that insulin is also required for processing of the mature and transcriptionally active form of SREBP1 (Hegarty et al., 2005). Acute insulin exposure leads to rapid accumulation of mSREBP1 in the nucleus within 1 hour (Yellaturu et al., 2005). This rapid cleavage of SREBP1 is PI3K-dependent (Hegarty et al., 2005). In the liver, insulin downregulates expression of INSIG2a, which induces processing of SREBP1c (Yabe et al., 2003). In contrast INSIG1 is a direct SREBP target gene and insulin stimulates expression of INSIG1 via induction of SREBP activity (Bengoechea-Alonso and Ericsson, 2007). INSIG2 protein is stable and INSIG1 is rapidly degraded in sterol-depleted cells (Gong et al., 2006).

Several posttranslational modifications regulate nuclear SREBP stability and activity, including phosphorylation, ubiqitination, acetylation and sumoylation. The transcriptionally active form of SREBP in the nucleus are rapidly degraded in a ubiquitin-dependent manner (Wang et al., 1994). It has been shown that GSK3ß regulates mSREBP1 stability by phosphorylating a number of sites, resulting in inhibition of expression of its target genes (Kim et al., 2004). GSK3 dependent phosphorylation promotes mSREBP binding to the E3 ubiquitin ligase Fbw7 and thus leads to mSREBPs ubiquitination and degradation by the proteasome pathway (Sundqvist et al., 2005).

Two mTOR complexes regulate the mTOR-signalling network. mTORC1 is rapamycin sensitive and responds to growth factors (EGF/insulin), nutrient availability and energy status of the cells. mTORC2 is rapamycin insensitive and phosphorylates Akt on serine 473. Akt phosphorylation of TSC2 causes inhibition of the function of the TSC1/TSC2 complex, and allows Rheb dependent activation of mTORC1. In contrast, low cellular energy level activates AMPK, which phosphorylates TSC2 leading to activation of the TSC1/TSC2 complex. This results in inhibition of mTORC1 activity. mTORC1 activity can be monitored by the phosphorylation status of its targets S6-kinase1/2 and 4E-BP, which are involved in the regulation of protein translation (Wullschleger et al., 2006). In the system used here, phosphorylation of the S6K target ribosomal protein S6 (S6rb) was determined to indicate mTORC1 activity.

The previous chapter showed that Akt-dependent induction of lipogenic genes requires SREBP activity. In this chapter, the mechanism of activation of SREBP1 by Akt is studied. Mature SREBP1 accumulates very rapidly in the nucleus in response to Akt activation. Several inhibitors are used to dissect stability, processing and translational regulation, to determine how Akt could control transcriptional activity of SREBP1. Activation of SREBP by Akt was not affected by inhibition of GSK3. However, Akt induced SREBP maturation and target gene expression requires mTORC1 activity.

4.2 Posttranslational regulation of SREBP by Akt

The nuclear form of SREBPs is regulated by several modifications, which alter its stability by targeting mature SREBP for degradation, or enhances its transcriptional activity, as measured by the expression levels of FAS and HMG-CoA synthase. In addition sterols control the processing of SREBPs. Lipoproteins consist of protein and lipids (e.g. cholesterol) and are ingredients in FCS. Cells cultured in lipoprotein deficient serum (LPDS) show an elevated level of mSREBP in the nucleus compared with those cultured in FCS (data not shown). Therefore, to enhance to sensitivity of detection of mSREBP and also SREBPs transcriptional activity, some experiments were performed in LPDS.

4.2.1 Akt induces accumulation of mature SREBP1 in the nucleus

In order to investigate the mechanism of activation of SREBP by Akt, it is relevant to know whether activation of Akt results in accumulation of mSREBP. To dissect a possible difference in the kinetics of accumulation of full length and mature SREBP in response to Akt activity, a time course experiment on whole cell lysates and nuclear extracts was performed in parallel.

Activation of Akt led to accumulation of flSREBP1 detectable after 6 and 8 hours of 4-OHT treatment (Figure 4-1 A). In contrast, an increased level of the 65 kDa N-terminal fragment of mSREBP1 was already detected in nuclear extracts after 1 hour of 4-OHT treatment (Figure 4-1 B). This indicates that appearance of mature SREBP in the nucleus precedes the increase in full length SREBP in response to Akt activation.

Having shown that Akt activation increases the level of SREBP1 transcript (Figure 3-10), it was of interest to determine whether accumulation of mSREBP depends on *de novo* transcription in response to Akt activation. Therefore cells were treated for a short time with the transcription inhibitor actinomycin D prior to activation of Akt. Figure 4-1 C) shows that accumulation of mSREBP1 in response to Akt activation is independent of transcription.

Taken together, these data show that Akt–induced accumulation of mature SREBP1 precedes accumulation of full length SREBP1 independently of *de novo* transcription.

Next, to evaluate whether activation of endogenous Akt in response to insulin leads to induction of mSREBP1 and 2, whole cell lysates of RPE cells were analysed for accumulation of processed SREBPs (Figure 4-1 D). It should be noted that the band labelled C-termSREBP2 represents the C-terminal portion of the protein. While mSREBP1 protein level increases in response to 2 hours of insulin stimulation, processed SREBP2 protein level remains unchanged. Furthermore, the induction of mSREBP1 by insulin can be blocked by treatment with the specific PI3K-inhibitor LY294002. LY294002 also strongly attenuated C-termSREBP2 protein (Figure 4-1 D). This indicates that activation of the PI3K/Akt pathway downstream of the insulin receptor is required for induction of processing of SREBP1 and maintenance of the level of mSREBP2. This result is consistent with published data showing an accumulation of mSREBP1 within 1 hour of insulin stimulation (Yellaturu et al., 2005).

4.3 Sterol-regulated processing of SREBP

SREBPs are synthesised as inactive precursors bound to the endoplasmic reticulum (ER) (Brown and Goldstein, 1999; Sato et al., 1994). When intracellular sterol concentrations are low, SREBPs are processed and activate expression of their target genes (Brown et al., 2002; Yang et al., 2002a). In contrast, high sterol concentrations inhibit SREBP processing and expression of SREBPs target genes declines (Yang et al., 2002a).

4.3.1 Akt-induced nuclear accumulation of mature SREBP1 is sterol sensitive

To determine whether Akt stimulates SREBPs maturation via modulating the function of components of the sterol-sensitive processing machinery, cells were cultured in the presence or absence of sterols, and negative and positive regulators of SREBP processing were co-transfected before Akt was subsequently activated.

Activation of myrAkt-ER by 4-OHT treatment for 24 hours led to increased levels of mSREBP1, but did not induce SREBP2 cleavage (Figure 4-2 A). The addition of sterols (cholesterol and 25-hydroxycholesterol) to the growth medium led to a marked reduction in processing of both SREBP1 and SREBP2. Activation of Akt was not sufficient to induce accumulation of nuclear SREBP1 in the presence of sterols (Figure 4-2 A). The same effect could be seen on mSREBP1 after short-time activation of Akt. Sterols completely block nuclear accumulation of mSREBP1 in response to 2 hours of Akt activation (Figure 4-2 B). Long-term activation of Akt induces an increase in full length SREBP1 and FAS protein levels. Furthermore, sterols block the induction of FAS expression by Akt. At the same time, expression of full length SREBP1 was increased by sterol treatment. Interestingly, activation of Akt does not further increase flSREBP1 protein level in the presence of sterols (Figure 4-1 C). This accumulation is most likely due to activation of LXR by sterols. The newly synthesised SREBP1 precursor protein cannot be processed in the presence of sterols and therefore accumulates in the ER.

In addition, U2OS myrAkt-ER cells were transiently transfected with the reporter constructs containing fragments of the FAS promoter (FAS(-150/-43)) or the HMG-CoA synthase promoter (SYN-wt). Akt-dependent activation of these promoter fragments was completely blocked in the presence of sterols (Figure 4-2 D). This indicates that activation of SREBP-dependent transcription of both promoters by Akt is sterol sensitive.

Furthermore, the FAS reporter construct was co-transfected into U2OS myrAkt-ER cells together with expression plasmids coding for INSIG2 and SCAP, respectively. Overexpression of INSIG2 significantly reduced induction of expression of the FAS reporter in response to Akt, while overexpression of SCAP led to an increase in FAS expression, which was further enhanced by activation of Akt (Figure 4-2 E). Exogenous expression of INSIG might not be sufficient to sequester all SREBP-SCAP complexes in the ER. This could explain the residual increase in FAS promoter expression in response to Akt activation.

It has been shown that insulin activates processing of SREBP1c through downregulation of INSIG2a in liver (Yabe et al., 2003). Expression of INSIG1 and INSIG2 after Akt activation was analysed by q-rtPCR. No significant changes in INSIG expression that could be responsible for induction of SREBP processing in response to Akt activation could be observed (Figure 4-2 F). INSIG2a and INSIG2b differ in their tissue distribution with INSIG2a being specifically expressed in liver. Primers used to detect INSIG were derived from sequences common to INSIG2a and 2b. However, since INSIG2a expression is restricted to the liver it is likely that the data in Figure 4-2 E (right panel) represent INSIG2b expression.

Taken together, these data show that Akt-dependent activation of SREBP is sterol sensitive, and activation of Akt is not sufficient to bypass the sterol-dependent SREBP processing to activate lipogenic gene expression.

4.3.2 Activation of SREBP1 by Akt requires ER to Golgi transport

In order to investigate whether Akt-dependent activation of SREBPs requires proteolysis in the Golgi, nuclear extraction was performed in the presence and absence of brefeldin A. Brefeldin A is a very selective inhibitor of the anterograde ER to Golgi transport, which leads to protein accumulation in the ER and rapid Golgi disassembly (Klausner et al., 1992; Nebenfuhr et al., 2002). Nuclear extracts were analysed for mSREBP1 after 2 hours of Akt activation. Activation of Akt was not sufficient to induce accumulation of mSREBP1 in the nucleus in the presence of brefeldin A (Figure 4-3 A). In addition, analysis of whole cell lysates shows that inhibition of ER/Golgi translocation with brefeldin A treatment completely blocks induction of SREBP1 and FAS protein in response to 24 hours of Akt activation (Figure 4-3 B). This indicates that the proteolytic steps taking place in the Golgi, including the RIP, are essential for SREBPs maturation by Akt, to release the transcriptionally active N-terminal fragment required for induction of SREBPs target genes. Taken together, activation of SREBP1 in response to Akt requires translocation of the SREBP-SCAP complex from the ER to the Golgi. Thus, it is likely that Akt acts upstream of SREBPs processing in the Golgi.

4.4 Regulation of stability of nuclear SREBP

Mature SREBPs are very unstable and catabolised rapidly (Wang et al., 1994). It has been reported that nuclear SREBP1 is ubiquitinated by the ubiquitin ligase Fbw7 in response to GSK3 phosphorylation, resulting in rapid degradation by the proteasome pathway (Sundqvist et al., 2005). Akt-mediated phosphorylation and inhibition of GSK3 prevents GSK3 from phoshporylating and inhibiting its substrates (Cross et al., 1995). These data suggest a

mechanistic model for regulation of SREBP by Akt. Inhibition of GSK3 by Akt could result in a stabilisation of mature SREBP and enhanced target gene expression.

4.4.1 Inhibition of proteasome-dependent protein degradation or silencing of Fbw7 does not block activation of SREBP1 by Akt

In order to test this model, firstly, RPE myrAkt-ER cells were treated with MG-132, an inhibitor of the 26S proteasome, and nuclear proteins were extracted. Figure 4-4 A) shows that inhibition of the proteasome stabilized mature SREBP. However, accumulation of mature SREBP was still observed after 2 hours of Akt activation.

Next, the Fbw7-containing SCF E3 ubiquitin ligase complex was targeted using an RNAi approach. U2OS myrAkt-ER were transiently transfected with a plasmid coding for shRNAs targeting Fbw7 isoforms (Nateri et al., 2004). Fbw7 silencing led to stabilization of mSREBP1, however accumulation of mSREBP1 was further enhanced in response to Akt activation. In contrast, overexpression of Fbw7 (Flag-Fbw7) completely attenuated mature SREBP protein (Figure 4-4 B). Furthermore, co-transfection of Flag-Fbw7 blocked induction of FAS promoter activity by Akt (Figure 4-4 C).

These data show that inhibition of the proteasome or silencing of E3 ubiquitin ligase stabilise the mature form of SREBP1. However, both treatments do not block Akt-dependent accumulation of mSREBP1.

4.4.2 Activation of SREBP1 by Akt is independent of GSK3 activity

To test the role of GSK3 in Akt-dependent regulation of SREBP, the specific GSK3 inhibitor SB216763 was used. Figure 4-5 A) shows that treatment with the GSK3 inhibitor SB216763 stabilised the phosphorylated form of ß-catenin, indicating that the inhibitor is working. Furthermore, inhibition of GSK3 did not block accumulation of full length SREBP1 or induction of FAS expression in response to Akt activation. It is worthwhile to note that in SB296763 treated cells, full length SREBP1 accumulates compared to untreated cells. GSK3 inhibition seems to affect stability of the full length SREBP1 in a similar way as has been described for the mature form.

To investigate the implication of GSK3 inhibition on mature SREBP1, nuclear extraction was performed after cells were treated for 2h with 4-OHT either in the absence or presence of SB296763. GSK3 inhibition did not block the Akt dependent accumulation of mSREBP1 in the

nucleus (Figure 4-5 B). In addition, a reporter construct containing a fragment of the FAS promoter (FAS(-150/-43) was transfected into U2OS myrAkt-ER. Although, inhibition of GSK3 slightly increased the basal transcription level of the FAS reporter, Akt-dependent activation of this promoter was not blocked in the presence of SB296763 (Figure 4-5 C). This indicates that activation of SREBP-dependent transcription of FAS by Akt is not GSK3 sensitive.

Taken together, these data show that treatment with the proteasome inhibitor MG-132 or silencing of Fbw7 does not abolish nuclear accumulation of SREBP1 or activation of fatty acid synthase expression in response to Akt activation. Furthermore, Akt-dependent accumulation of mature SREBP1 in the nucleus does not involve GSK3, and expression of the SREBP1 target gene FAS by Akt was not affected by inhibition of GSK3. Therefore, Akt activation of SREBP1 is GSK3 independent and stabilization is not the primary mechanism of SREBP activation in the system used here.

4.5 mTOR dependent regulation of SREBP

mTORC1 is a key regulator of cell growth and metabolism and senses cellular energy status via the AMPK-TSC pathway, availability of nutrients (in particular amino acids) and growth factors stimuli via the PI3K-Akt pathway. mTORC1 activates S6K and inhibits 4EBP, leading to protein synthesis and promoting cell growth. mTORC1 is rapamycin sensitive, while the second mTOR complex, mTORC2, is rapamycin insensitive and is one of the kinases shown to phosphorylate Akt on serine 473 (Wullschleger et al., 2006). mTORC1 activity was monitored by detecting the phosphorylation of the S6K target S6rb in the system used here.

4.5.1 Inhibition of mTORC1 blocks Akt dependent activation of SREBP1

To test whether Akt dependent activation of SREBP requires mTOR activity, cells were treated with the mTORC1 (mTOR/Raptor) inhibitor rapamycin.

q-rtPCR data showed that increased expression of SREBP1a, SREBP1c and FAS transcripts in response to 48 hours of Akt activation was blocked by treatment with rapamycin (Figure 4-6 A). In a parallel experiment, whole cell lysates were analysed for FAS and SREBP1 protein levels. While induction of FAS protein by Akt was fully blocked in the presence of rapamycin, the Akt-dependent increase in SREBP expression was only reduced (Figure 4-6 B). To investigate

whether mTOR is involved in processing of SREBP, nuclear extracts were analysed to detect mSREBP1 accumulation in the nucleus. Short and long-time rapamycin treatment totally inhibited Akt dependent accumulation of mSREBP1 (Figure 4-6 C). This indicates that activation of mTORC1 is required for Akt-induced accumulation of mature SREBP1 and activation of FAS expression.

4.5.2 Silencing of mTOR blocks activation of SREBP1 by Akt and overexpression of mTOR activates SREBP1 in the absence of Akt activity

To further investigate whether the observed role of mTORC1 in the activation of SREBP in response to Akt can be reproduced by independent methods, U2OS myrAkt-ER cells were transfected either with siRNA oligonuclotides targeting mTOR or with an expression construct coding for the mTOR protein.

Transfection of siRNA oligonucleotides directed against FRAP1 (mTOR) resulted in reduction of expression of the respective protein. Silencing of mTOR did not interfere with the activation of the myrAkt-ER protein detected by phosphorylation on serine 473 and threonine 308 as well as phosphorylation of the Akt substrates GSK3α/ß (Figure 4-7 A). However, transfections of mTOR siRNA oligonucleotides were sufficient to block Akt-induced accumulation of full length and mature SREBP1. This is associated with a block of increased FAS and ACL expression stimulated by Akt (Figure 4-7 B).

Furthermore, overexpression of mTOR led to induction of full length and mature SREBP1 as well as FAS protein. These accumulations were not further increased by activation of Akt (Figure 4-7 C). These data indicate that mTOR is a crucial target for Akt dependent activation of SREBP.

4.5.3 Activation of fatty acid synthase in response to insulin requires mTORC1 activity

It has been shown in a cell type-dependent manner that prolonged rapamycin treatment reduces the levels of mTORC2 below those needed to maintain Akt signalling (Sarbassov dos et al., 2006). mTORC2 activates Akt by direct phosphorylation of the serine 473 residue (Hresko and Mueckler, 2005; Sarbassov et al., 2005). In addition, active mTORC1 attenuates insulin

signalling through the negative feedback loop mediated by S6K, which phosphorylates and inhibits insulin receptor substrate 1 (Harrington et al., 2005; Radimerski et al., 2002a).

In order to investigate the effects of long term rapamycin treatment on endogenous Akt activity as well as on SREBP and FAS expression in the cell system used, parental RPE cells were treated with the mTORC1 inhibitor rapamycin for 48 hours. This resulted in activation of Akt detected by increased phosphorylation on serine 473 and threonine 308 by simultaneous disappearance of the phosphophorylation signal of S6rb (Figure 4-8 A). This result suggests that in the experimental system used, endogenous Akt activity is elevated by inhibition of mTORC1, presumably due to inhibition of the negative feedback loop mediated by S6K. This is consistent with published data showing that mTROC1 inhibition with rapamycin increases Akt phosphorylation and activity through feedback loops (O'Reilly et al., 2006). However, the basal expression level of FAS and full length SREBP1 was significantly reduced in response to rapamycin treatment (Figure 4-8 A).

In addition, 24 hours insulin stimulus resulted in induction of FAS expression. q-rtPCR data showed that the insulin-induced increase in FAS transcript is blocked in the presence of rapamycin (Figure 4-8 B). In a parallel experiment, whole-cell lystaes were analysed for FAS protein. Although 24 hours rapamycin treatment resulted in increased Akt phosphorylation, insulin-dependent activation of FAS expression was completely blocked by rapamycin (Figure 4-8 C).

Taken together, these observations suggest that activity of mTORC1 is required for Akt-induced accumulation of mature SREBP1 in the nucleus and expression of SREBP target genes. Therefore, mTORC1 may act downstream of Akt on induction of SREBP1 activity and FAS expression.

4.5.4 Activation of SREBP by Akt requires glycolysis and can be inhibited by AMPK

It has been suggested that Akt also activates TORC1 signalling by preserving a high cellular energy level (Hahn-Windgassen et al., 2005), at least partly, via maintenance of nutrient uptake and activation of glycolysis (Edinger and Thompson, 2002; Manning and Cantley, 2007). Membrane translocation of glucose transporters that promote glucose uptake as well as induction of glycolysis by Akt provides the cells with metabolites and energy. mTORC1 senses the energy status of a cell through AMP-activated kinase (AMPK). Interfering with the ATP production by blocking glycolysis or by glucose depletion increases the AMP/ADP level and

leads to AMPK activation, resulting in direct phosphorylation and activation of TSC2 and inhibition of mTORC1 signalling. The AMP analogue AICAR activates AMPK and inhibits mTORC1 dependent phosphorylation of S6K and 4E-BP1 (Plas and Thompson, 2005). So far it is not known whether depletion of metabolites of the glycolytic pathway are sensed directly by the TOR pathway.

First, the influence of AMPK activation on mTORC1 dependent SREBP processing was tested. Whole cell lystaes were analysed after 24 hours of Akt activation in the presence and absence of AICAR treatment. While myrAkt-ER activation was unaffected, Akt-induced FAS, ACL and full length SREBP expression was completely inhibited by AICAR (Figure 4-9 A). After short time Akt activation, nuclear extracts were analysed for mSREBP1 protein. AICAR treatment partially blocked accumulation of mSREBP1 in the nucleus in response to Akt activation (Figure 4-9 B).

In order to investigate whether activation of SREBP-dependent transcription by Akt requires glucose or an active glycolytic pathway, RPE myrAkt-ER cells were either glucose starved or glycolysis was inhibited by the addition of glucose analogue 2-deoxyglucose (2DG). 2DG is transported into the cells via glucose transporters where it is phosphorylated by hexokinases but cannot be further metabolised. By competing with glucose for hexokinases, 2DG inhibits glycolysis, leading to cellular energy starvation (Chi et al., 1987).

Glucose starvation or 2DG treatment for 24 hours resulted in a full block of Akt-dependent induction of FAS expression and full length SREBP1 protein level (Figure 4-10 A). Analysis of nuclear extracts showed that nuclear accumulation of mSREBP1 in response to Akt was already inhibited after 3 hours of glucose starvation or 2DG treatment (Figure 4-10 B). This indicates that glucose and glucose catabolism are required for activation of SREBP1 by Akt. This is consistent with data showing that acute glucose stimulation results in nuclear translocation of SREBP1c and expression of its target genes within 3 hours (Guillet-Deniau et al., 2004).

Taken together, theses data show that activation of AMPK and inhibition of glycolysis as well as rapamycin treatment result in abolished mTORC1 signalling. These treatments also result in a block of Akt-mediated accumulation of mature and full length SREBP1 as well as SREBP-dependent target gene expression, indicating that mTORC1 is involved in the regulation of SREBP by Akt.

4.6 Translational regulation of SREBP

mTORC1 regulates translation via 4E-BP and S6K1. mTORC1 together with PDK1 phosphorylates and activates S6K1, whereby phosphorylation of 4E-BP by mTOR leads to release of the translation initiation factor eIF4E (Hay and Sonenberg, 2004; Tee and Blenis, 2005).

Having shown that Akt-induced activation of SREBP1 depends on mTORC1 activity, the question arose whether mTORC1-mediated *de novo* protein synthesis might be a mechanism of activation of SREBP by Akt. mSREBPs stimulate transcription of their own genes, which would interfere with the detection of *de novo* SREBP synthesised protein. Therefore the positive feedback loop that leads to transcription of the SREBP genes has to be inhibited. Brefeldin A blocks SREBP processing via inhibiting the ER-Golgi transport and thus depletes cells of mSREBPs.

At time point zero, an equal number of recently transcribed mRNA copies of SREBP1 exist in the DMSO and brefeldin A treated cells. If Akt activates translation, it would be presumed that short time activation of Akt should result in accumulation of full length SREBP1 even in the presence of brefeldin A treatment. To test this hypothesis, Akt was activated and full length SREBP1 protein was detected at several time points. Activation of Akt led to a time-dependent accumulation of full length SREBP1 in DMSO treated cells, while brefeldin A treated samples showed a decrease in SREBP1 protein levels over time, independent of Akt activation (Figure 4-11 A). This suggests that *de novo* transcription of SREBP1 requires mSREBP1, and that the availability of mature SREBP1 is necessary for Akt-induced accumulation of full length SREBP1.

In a second approach (Figure 4-11 B), accumulation of newly synthesised SREBP1 was analysed following release from inhibition of protein synthesis by cycloheximide (CHX). Cells were pretreated with CHX, which blocks translational elongation and *de novo* protein synthesis by interfering with the 60S ribosome subunit. After 3 hours, cells were washed with PBS and treated with 4-OHT for 1, 2 or 4 hours in the presence or absence of the proteasome inhibitor ALLN. One hour after CHX was removed, the level of full length SREBP1 protein had recovered to basal level. After two hours, ALLN treatment led to accumulation of full length SREBP1 compared to non-ALLN treated cells. At all three timepoints, activation of Akt was not sufficient to induce accumulation of full length SREBP1 in the presence or absence of ALLN (Figure 4-11 B).

In a third approach (Figure 4-11 C), translation and degradation of SREBP were blocked simultaneously. CHX and MG-132 together provide a defined tool for analysis of full length and mature SREBP1, in which synthesis of full length SREBP1 protein is blocked by CHX and proteasomal degradation of the mature form is inhibited by MG-132. RPE myrAkt-ER cells were treated with 4-OHT for 2 hours in the presence or absence of CHX and the proteasome inhibitor MG-132 alone or in combination. Whole cell lysates and nuclear extraction were performed in parallel experiments. Consistent with Figure 4-4 A proteasome inhibition did not block the Akt-dependent accumulation of mSREBP1. However, activation of Akt was not sufficient to induce accumulation of mSREBP1 in the presence of CHX, independent of proteasome inhibition. CHX alone led to total disappearance of full length and mature SREBP1, while the presence of MG-132 partially stabilized both SREBP1 forms (Figure 4-11 C). This is consistent with data showing that SREBPs are very unstable proteins and ALLN prevents degradation of mSREBPs (Wang et al., 1994). Additional experiments are necessary to determine the role of Akt in regulation of SREBP translation.

The observation that activation of Akt did not result in accumulation of mSREBP1 under the described conditions, argues that protein synthesis is required for Akt-induced activation of SREBP1. However, the previous findings suggested *de novo* translation of full length SREBP1 is not affected by Akt. This indicates that either translation of an unstable intermediate factor required for SREBP processing or ER to Golgi translocation could be possible mechanisms of Akt dependent activation of SREBP1.

4.7 Discussion

SREBPs are a family of transcription factors that regulate fatty acid and cholesterol homeostasis within a cell. Unbalanced lipid biosynthesis is reported to have an impact on various diseases such as diabetes, obesity and cancer. Therefore, regulation of SREBP transcription factors is very tight and occurs on several levels; integrating availability of nutrients and metabolic substrates, cellular energy status and mitogenic stimuli (Eberle et al., 2004).

Time course experiments, comparing the appearance of full length and mature SREBP1, reveal that accumulation of mature SREBP1 precedes accumulation of full length SREBP in response to Akt activation. Induction of mSREBP in the nucleus could already be detected after 1 hour of Akt activation (Figure 4-1). This is consistent with published data reporting that acute insulin exposure leads to rapid cleavage of SREBP1 in a PI3K dependent mechanism in hepatocytes (Hegarty et al., 2005).

In response to low intracellular sterol concentrations, SREBPs are activated by proteolytic cleavage in the Golgi and the N-terminal cleavage product translocates to the nucleus (Brown and Goldstein, 1997). In the presence of sterols, INSIG binds to SCAP and inhibits translocation of SREBP to the Golgi (Yang et al., 2002a). SREBP processing requires ER to Golgi translocation, as inhibition with brefeldin A blocked nuclear accumulation of mSREBP1 in response to Akt activation (Figure 4-3). Furthermore, Akt-induced nuclear mSREBP1 was also sensitive to inhibition by sterols indicating that Akt does not abolish the sterol sensing SREBP processing machinery. Sterols completely blocked activation of transcription from the SRE containing FAS and HMGS promoter reporter constructs. In contrast, SREBP2 processing was not affected by Akt activation (Figure 4-2). Furthermore, since ablation of SREBP2 expression by RNAi was less efficient in blocking Akt dependent activation of SREBP target genes, it can be concluded that Akt preferentially regulates SREBP1 processing. However, it seems unlikely that Akt activates processing through direct phosphorylation of flSREBPs or a protein involved in SREBP processing. No high stringency Akt phosphorylation sites could be identified in SREBP proteins, SCAP, INSIG or site 1 and site 2 proteases. Only SCAP contains a conserved medium stringency Akt site, which faces the ER lumen. Expression of SCAP enhanced the basal level of FAS promoter activity, which could be further increased by Akt (Figure 4-2). It has been reported that insulin induces processing of SREBP1c in the liver by down-regulating expression of INSIG2a (Yabe et al., 2003). No significant changes in the expression of INSIG1 and INSIG2 in response to Akt activation were observed (Figure 4-2), indicating that regulation of INSIG2a by insulin may be restricted to hepatocytes.

SREBP1c can be phosphorylated by GSK3 resulting in inhibition of its transcriptional activity (Kim et al., 2004). The mechanism proposed by Sunquist et al. involves the Fbw7 ubiquitin ligase. Upon GSK3 phsophorylation, Fbw7 binds to nuclear SREBP1, which results in ubiquitination and rapid proteasomal degradation of mSREBPs (Sundqvist et al., 2005). While these findings provide a mechanistic model for Akt regulation of SREBP activity, the data described here do not support the involvement of GSK3 in Akt-dependent regulation of SREBP. GSK3 inhibition did not block Akt-induced accumulation of mature and full length SREBP1. In addition, expression of FAS and activation of the FAS promoter was not affected by GSK3 inhibition (Figure 4-5). This is supported by the finding that neither proteasome inhibitors nor silencing of Fbw7 abolished activation of SREBP and FAS by Akt (Figure 4-4). In addition, recent data imply that Akt does not affect the stability of exogenous mature SREBP (C. Santos, unpublished result). These data indicate that activation of SREBP by Akt does not involve stabilization of the mature protein and is independent of GSK3. Interestingly, several GSK3 targets like ß-catenin are not regulated by Akt. The existence of two different GSK3 pools in the cells has been discussed (Pearl and Barford, 2002). It is possible that Akt-regulated GSK3 does

not target SREBP in the system used here. Therefore it would be of interest to investigate whether activation of Akt inhibits GSK3 dependent phosphorylation of SREBP.

Activation of SREBP by Akt involves mTORC1 activity. Both inhibition of mTORC1 with rapamycin (Figure 4-6) and silencing of mTOR by RNAi (Figure 4-7) inhibited expression of FAS and ACL, as well as mSREBP accumulation in the nucleus in response to Akt activation. A possible role for the mTOR pathway in lipid homeostasis has been discussed (Wullschleger et al., 2006), which makes mTORC1 a potential downstream mediator of insulin/Akt mediated metabolism. One of the kinases regulating Akt activity by phosphorylating serine 473 is mTORC2 (Hresko and Mueckler, 2005; Sarbassov et al., 2005). Together with the phosphorylation of threonine 308 by PDK1, S473 phosphorylation is necessary for full Akt activation (Alessi et al., 1996). In the cell system used here, 48 hours of rapamycin treatment resulted in activation of endogenous Akt. Although Akt was fully active, rapamycin blocked the induction of FAS by insulin (Figure 4-8). These results suggest that activation of SREBP1 and induction of expression of SREBP1 target genes depends on activity of mTORC1.

mTORC1 also senses cellular energy status via AMP-activated protein kinase (AMPK). In response to low cellular energy levels (high AMP/ATP ratio), AMPK is activated and phosphorylates TSC2 leading to inhibition of mTORC1 (Inoki et al., 2003a). Long-term energy depletion induced by 2-deoxyglucose treatment or glucose withdrawal causes a rise in intracellular AMP concentration, which triggers activation of AMPK by LKB1 (Woods et al., 2003) but also stimulates phosphorylation of IRS-1 by AMPK, which inhibits the PI3K/Akt pathway (Tzatsos and Tsichlis, 2007).

Inhibition of glycolysis by glucose deprivation or addition of 2-deoxyglucose (2-DG) abolishes the induction of FAS and full length SREBP1 as well as nuclear accumulation of mSREBP in response to Akt activation (Figure 4-10). This is consistent with published data showing that activation of SREBP1c in rat myocytes monitored by nuclear translocation and lipogenic gene expression requires glucose (Guillet-Deniau et al., 2004). In addition, activation of AMPK with AICAR blocked Akt dependent activation of SREBP1 and expression of SREBP target genes (Figure 4-9). Inhibition of glycolysis or activation of AMPK also blocked mTORC1-dependent signalling. These data are in agreement with publications showing that both 2-DG and AICAR treatments result in inhibition of TORC1 activity assayed by phosphorylation of S6K and 4E-BP (Dennis et al., 2001; Xiang et al., 2004). The importance of AMPK as a major regulator of lipid biogenesis has been already reported. Zhou et al. (2001) showed that metformin or AICAR mediated activation of AMPK blocks insulin-induced SREBP1c mRNA and protein as well as expression of FAS (Zhou et al., 2001c).

The best-studied targets of TORC1 in mammalian cells are the translational regulators S6K and 4E-BP1 (Hay and Sonenberg, 2004; Tee et al., 2004). The PI3K/Akt pathway is involved in translational regulation of mRNAs containing 5'-TOP elements. Computational sequence analysis of the 5'UTR of frog, mouse and human SREBP1a did not reveal a well-conserved 5'-TOP element (A. Schulze, personal communication). Additional experiments are required to fully rule out the possibility that Akt affects translation of SREBP1.

It seems possible that Akt activates SREBP1 by stimulating ER-Golgi transport of the SREBP/SCAP complex. It has been published that dominant-negative Akt prevents translocation of co-transfected SCAP-GFP from the ER to the Golgi (Du et al., 2006). ER/Golgi localization is also essential for mTOR activity. Deletion of an ER localization sequence (ELS) or brefeldin A treatment inhibits mTOR-dependent S6K phosphorylation (Buerger et al., 2006; Liu and Zheng, 2007). Therefore, the brefeldin A-induced block of mSREBP accumulation by Akt could also be an effect of impaired mTORC1 signalling (Figure 4-3). A conserved TOR signalling (TOS) motif in S6K is required for binding and phosphorylation by mTORC1 (Nojima et al., 2003). Computational alignment of several SREBP1 homologue sequences revealed a conserved element similar to the TOS motif (A. Schulze, personal communication). Therefore, a proposed model for the mechanism of regulation of SREBP by Akt would be that in response to activation of Akt, mTORC1 associates with SREBP1 via the TOS-like motif in SREBP1, and might phosphorylate components of the SREBP/SCAP complex. This could cause a conformational change of SCAP allowing SCAP to bind the COPII protein sec24, resulting in ER to Golgi translocation and rapid processing of SREBP1. However, it is also possible that regulation of SREBP activity by Akt occurs on several levels. Akt could activate SREBP processing through mTORC1. In addition, Akt could also contribute to transcription of SREBP genes via direct and indirect activation of additional transcription factors, such as LXR and Sp1.

4.8 Critique of chapters 3 and 4

General criticisms of chapter 3 and 4 are the low number of replicates and the absence of statistical analysis. In both chapters, q-rtPCR and luciferase reporter experiments were performed in duplicate and repeated independently at least twice. Most experiments were repeated three times. Only the data shown in Figure 3-8 A) represent a single experiment without duplicates.

Statistical analysis emphasises the biological significance of data and is therefore required to supports the concept. If the measured effects are pronounced (e.g. Figure 3-5 C) a significant p-value will be obtained from a low number of replicates. If the results show only small differences in response to treatment (e.g. Figure 3-10 A or 3-11 B and C), a larger number of measurements is required. This allows the comparisons of two groups of measurements using a student's t-test. P-values of 0.05 or lower indicate significance and validate the hypothesis. Chapter 3 and 4 could be improved by designing the experiments more carefully regarding number of replicate measurements, which would allow statistical analysis.

The interpretation of some data presented in chapter 3 and 4 was not always fully backed up by the experimental data. In some cases, data were interpreted as significant without statistical analysis. The interpretations of the following Figures are now revised:

Figure 3-2 B) Although the effect of active Akt on suspension cells after 48 hours 4-OHT treatment was less protective than after 24 hours, a reduction in apoptosis was still measured.

Figure 3-9 B and C) Although silencing of SREBP2 strongly reduces the basal expression level of FAS and HMGS, it did not block the fold induction of FAS and HMGS expression by Akt. Transfection of either SREBP1 or SREBP2 siRNA oligonucleotides was sufficient to robustly reduce Akt-induced FAS promoter activation (Figure 3-9 B). Although silencing of SREBP2 substantially reduces the basal expression level of SYN-wt, it did not block the fold induction of SYN-wt expression by Akt (Figure 3-9 C).

Figure 3-11 D) Transcription from the HMGS promoter (SYN-wt) was only slightly altered by insulin treatment. However, treatment with LY294002 not only fully blocked the effect of insulin, it also drastically decreased SYN-wt expression (Figure 3-11 D).

Figure 4-2 E) Overexpression of INSIG2 reduced induction of expression of the FAS reporter in response to Akt, while overexpression of SCAP led to an increase in FAS expression, which was further enhanced by activation of Akt (Figure 4-2 E).

Figure 4-2 F) Expression of INSIG1 and INSIG2 after Akt activation was analysed by q-rtPCR. No changes in INSIG expression that could be responsible for induction of SREBP processing in response to Akt activation could be observed (Figure 4-2 F).

Figure 4-8 A) The basal expression level of FAS and full length SREBP1 was reduced in response to rapamycin treatment (Figure 4-8 A).

The interpretation of data presented in Figure 3-14 D) states that Akt-induced FAS and ACL expression does not depend on LXR activity. This statement was based on the assumption that the LXR inhibitor arachidonic acid had been effective. However, the analysis of this experiment lacked the positive control of the arachidonic acid treatment, showing that arachidonic acid treatment affects LXR target gene expression. Since the inhibitory effect of arachidonic acid on LXR activity is not shown, no inference can be made as to whether modulation of LXR affects Akt dependent SREBP target gene expression. In order to clarify this point, the expression of LXR target genes should be monitored in the presence or absence of arachidonic acid by western blotting or q-rtPCR.

In the experiment shown in Figure 4-3, Brefeldin A was used to inhibit anterograde ER to Golgi transport. Analysis of whole cell lysates shows that inhibition of ER/Golgi translocation with Brefeldin A treatment completely blocks induction of flSREBP1 and FAS protein in response to 24 hours of Akt activation (Figure 4-3 B). This indicates that the proteolytic steps taking place in the Golgi, including the RIP, are essential for SREBPs maturation, and to release the transcriptionally active N-terminal fragment required for induction of SREBPs target genes in response to Akt activation. Since Brefeldin A prevents ER to Golgi translocation of SREBP1 in either the presence or absence of Akt activation and therefore by its nature stops SREBP processing, the design of the experiment does not infer the mechanism of SREBP activation in response to Akt. Further experiments are required to dissect whether Akt activates SREBP post or pre trafficking.

It should be noted that experimental design is very important, since it affects the quality of the data that can be obtained from the experiment. This is crucial for the interpretation of the experiment and determines whether significant conclusions can be drawn. Therefore, experimental variables such as time points, controls and number of independent replicates have to be considered in advance. Good experimental design allows the application of statistical data analysis, which is crucial to support any hypothesis.

Figure 4-1 Activation of Akt induces rapid accumulation of mature SREBP1 in the nucleus

(A) RPE myrAkt-ER cells were cultured in 1% LPDS and treated with 100 nM 4-hydroxytamoxifen (4-OHT) for the times indicated. Whole cell lysates were analysed for expression of fatty acid synthase (FAS) and full length SREBP1. Activation of myrAkt-ER was analysed using a phosphospecific antibody. **(B)** Cells were treated as in (A) and nuclear extracts were prepared and analysed for the presence of the 65 kDa mature form of SREBP1. **(C)** RPE myrAkt-ER cells were cultured in 1% LPDS and treated with 1 μg/ml actinomycin D or solvent (DMSO) for 30 mins and subsequently stimulated with 100 nM 4-OHT for 2 hours. Nuclear extracts were prepared and analysed for the presence of mature SREBP1. **(D)** RPE cells were starved overnight in 1% LPDS and subsequently treated with 50 μM LY294002 or solvent for 30 mins, then induced with 1 μg/ml insulin for 2 hours. Whole cell lysates were analysed for expression of mature SREBP1 and cleaved SREBP2. Phosphorylation of Akt was detected using a phosphospecific antibody. GAPDH is shown as a loading control for whole cell lysates. Lamin is shown as a loading control for nuclear extracts.

Figure 4-1

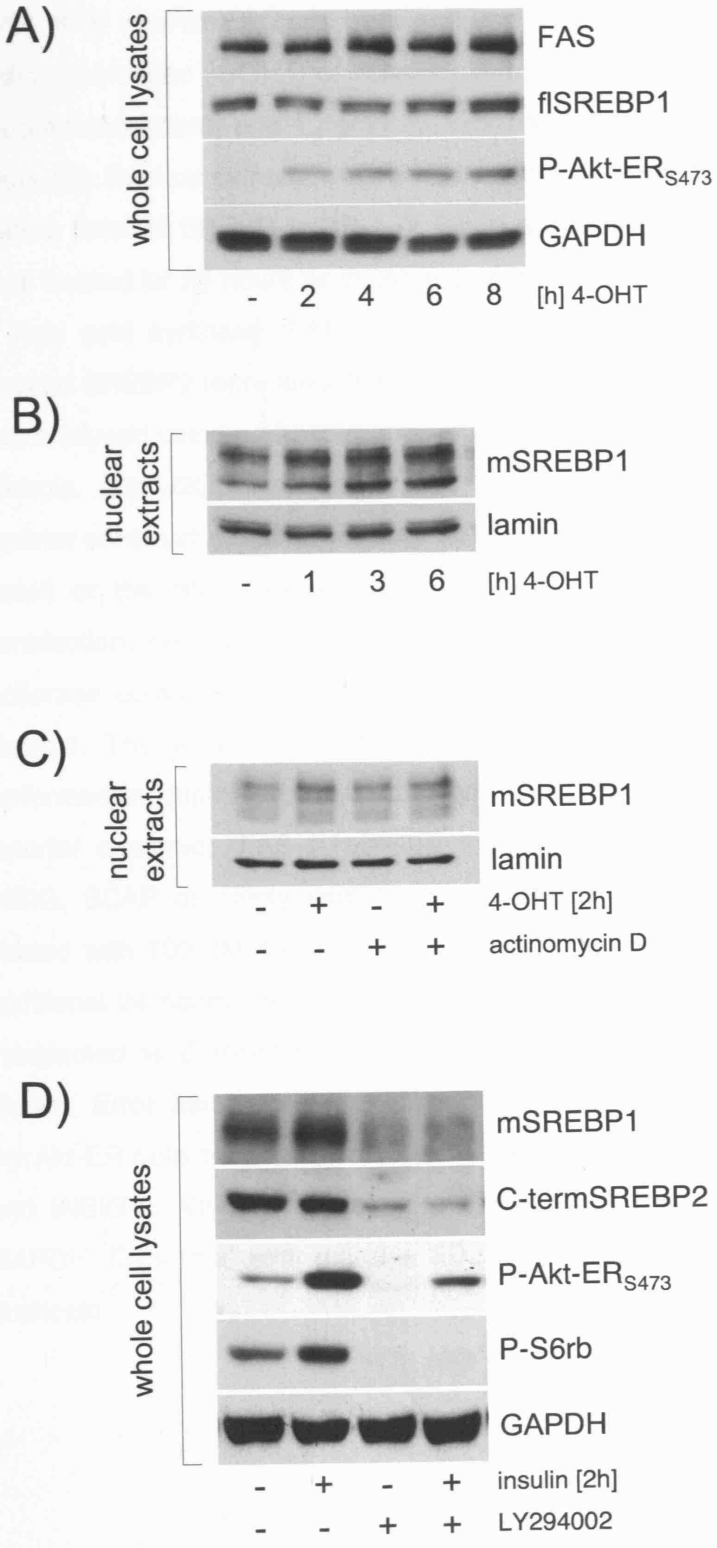
A)
whole cell lysates
FAS
flSREBP1
P-Akt-ER$_{S473}$
GAPDH
- 2 4 6 8 [h] 4-OHT
B)
nuclear extracts
mSREBP1
lamin
- 1 3 6 [h] 4-OHT
C)
nuclear extracts
mSREBP1
lamin
- + - + 4-OHT [2h]
- - + + actinomycin D
D)
whole cell lysates
mSREBP1
C-termSREBP2
P-Akt-ER$_{S473}$
P-S6rb
GAPDH
- + - + insulin [2h]
- - + + LY294002

Figure 4-2 Akt-induced nuclear accumulation of mature SREBP1 is sterol sensitive

(A/B) RPE myrAkt-ER cells were cultured in 1% LPDS and treated with 100 nM 4-hydroxytamoxifen (4-OHT) or solvent either in the presence or absence of a mixture of 10μg/ml cholesterol and 1 μg/ml 25-hydroxycholesterol (sterols) for 24 hours (A) or 2 hours (B). Nuclear extracts were prepared and analysed for the presence of the 65 kDa mature form of SREBP-1. DP-1 or lamin are shown as loading controls. **(A/C)** Cells were treated for 24 hours as in (A) and whole cell lysates were analysed for expression of fatty acid synthase (FAS), full length SREBP1 and cleaved SREBP2. Note that cleaved SREBP2 represents the C-terminal part of the protein. Activation of myrAkt-ER was analysed using a phosphospecific antibody. GAPDH or actin are shown as loading controls. **(D)** U2OS myrAkt-ER cells were transfected with 0.1 μg of a luciferase reporter construct containing a fragment of either the FAS promoter (FAS(-150/-43), left panel) or the HMG-CoA synthase promoter (SYN-wt, right panel). 24 hours post-transfection, cells were treated with 100 nM 4-OHT and sterols as in (B). Relative luciferase activity was normalised to the activity of a co-transfected lacZ expression plasmid. The error bars represent $\pm$ the range of two independent experiments performed in duplicate. **(E)** U2OS myrAkt-ER cells were transfected with 0.1μg FAS reporter construct (FAS (-150/-43)) together with 0.1μg of expression plasmids for INSIG, SCAP or empty vector, as indicated. 24 hours post-transfection, cells were treated with 100 nM 4-OHT (+) or solvent (-) in medium containing 0.5% FCS for an additional 24 hours. Relative luciferase activity was normalised to the activity of a co-transfected lacZ expression plasmid and data of one representative experiment is shown. Error bars represent $\pm$ the range of duplicates. **(F)** Total RNA from RPE myrAkt-ER cells treated as in (B) was analysed by q-rtPCR for expression of INSIG-1 and INSIG-2. Values represent relative mRNA abundance and are normalised to GAPDH. Data represent mean $\pm$ SD of three independent experiments performed in duplicate.

Figure 4-2

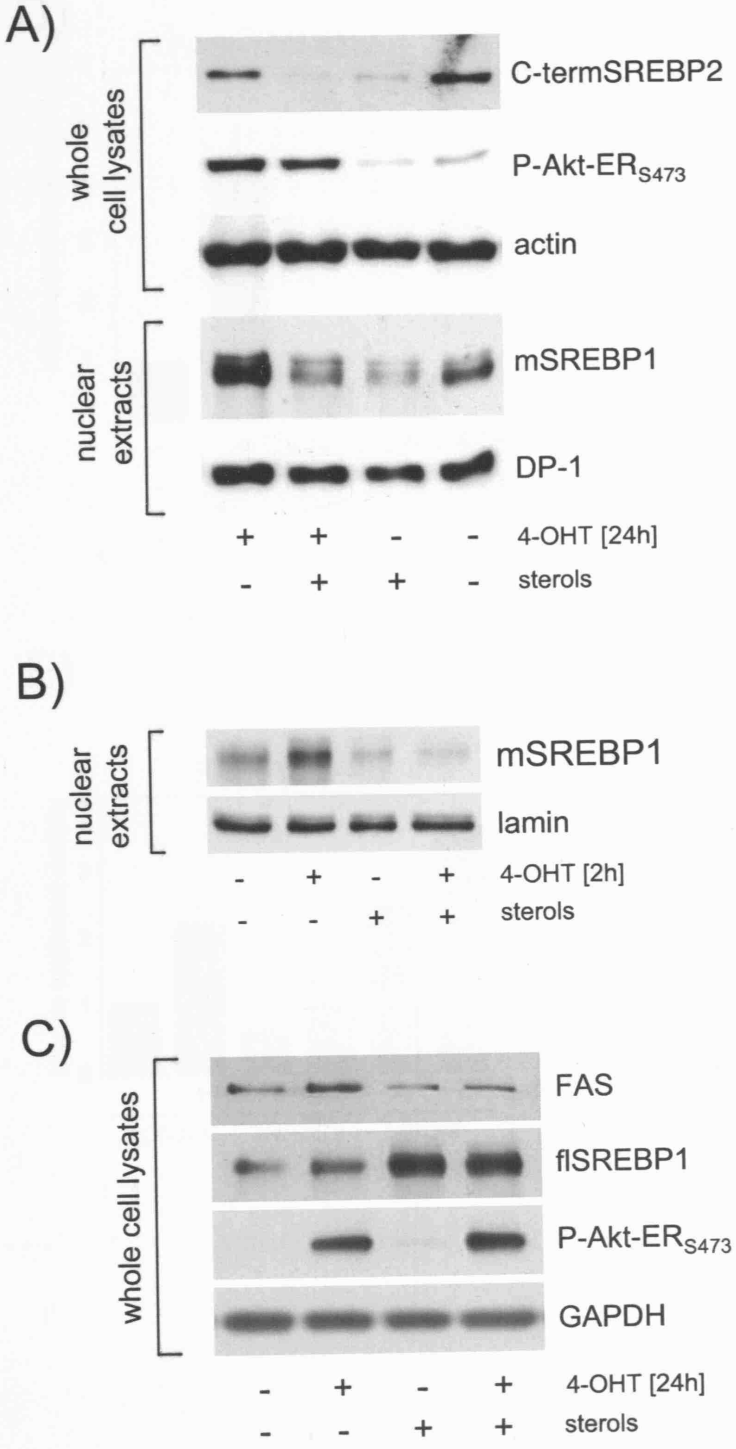
A)
whole cell lysates
C-termSREBP2
P-Akt-ER$_{S473}$
actin
nuclear extracts
mSREBP1
DP-1
+ + - - 4-OHT [24h]
- + + - sterols
B)
nuclear extracts
mSREBP1
lamin
- + - + 4-OHT [2h]
- - + + sterols
C)
whole cell lysates
FAS
flSREBP1
P-Akt-ER$_{S473}$
GAPDH
- + - + 4-OHT [24h]
- - + + sterols

Figure 4-2

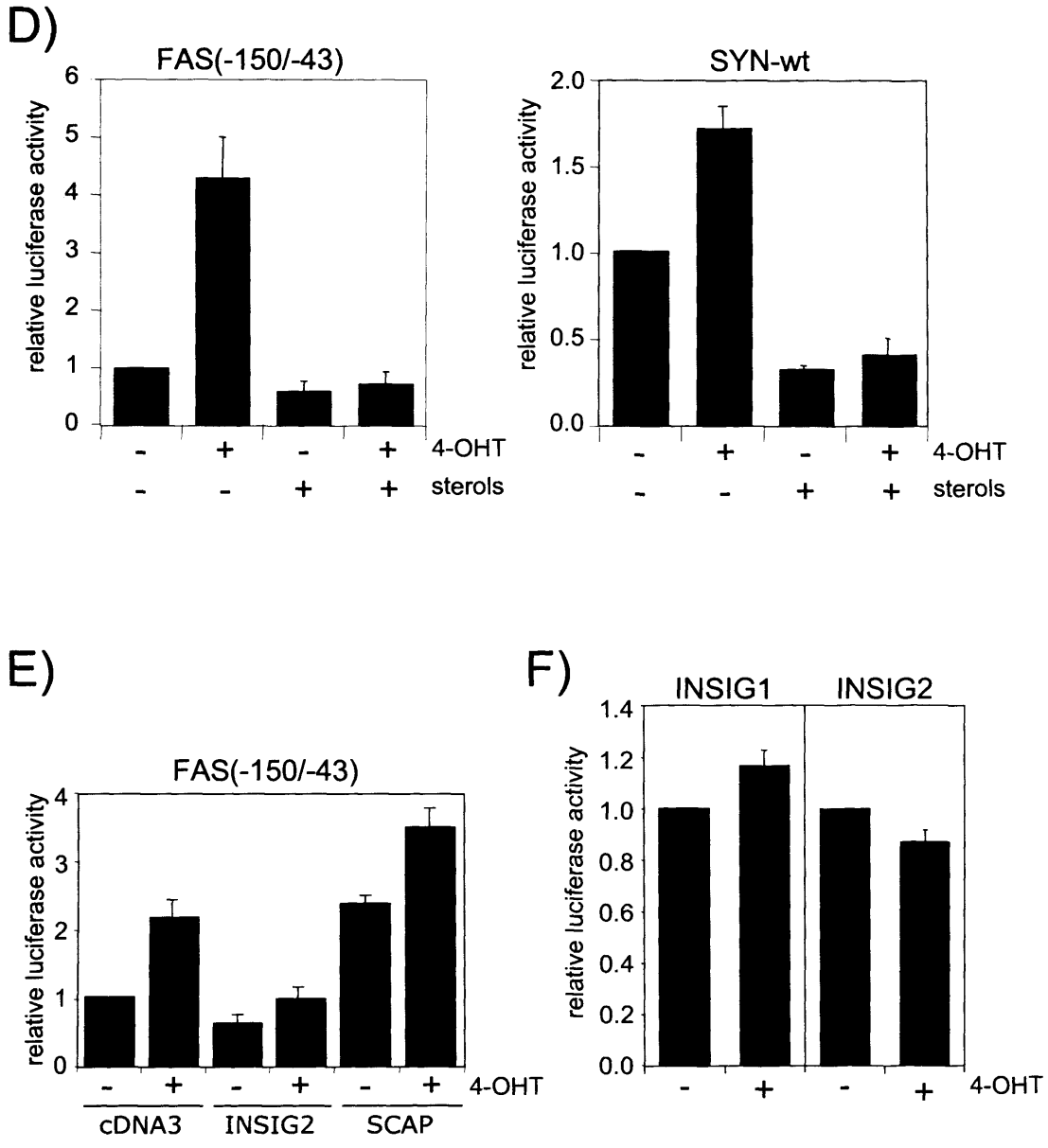
D)
FAS(-150/-43)
relative luciferase activity
6
5
4
3
2
1
0
- + - + 4-OHT
- - + + sterols
SYN-wt
relative luciferase activity
2.0
1.5
1.0
0.5
0.0
- + - + 4-OHT
- - + + sterols
E)
FAS(-150/-43)
relative luciferase activity
4
3
2
1
0
- + - + - + 4-OHT
cDNA3
INSIG2
SCAP
F)
INSIG1
INSIG2
relative luciferase activity
1.4
1.2
1.0
0.8
0.6
0.4
0.2
0.0
- + - + 4-OHT

Figure 4-3 Activation of SREBP1 by Akt requires ER to Golgi transport

(A) RPE myrAkt-ER cells were cultured in 1% LPDS and then treated with 20 ng/ml brefeldin A for 30 mins and subsequently stimulated with 100 nM 4-hydroxytamoxifen (4-OHT) or solvent for 2 hours. Nuclear extracts were prepared and analysed for the presence of mature SREBP-1. Lamin, a nuclear protein, is shown as a loading. **(B)** Cells were treated for 24 hours as in (A) and whole cell lysates were analysed for expression of fatty acid synthase (FAS) and full length SREBP1. Activation of myrAkt-ER was analysed using a phosphospecific antibody. GAPDH is shown as a loading control.

Figure 4-3

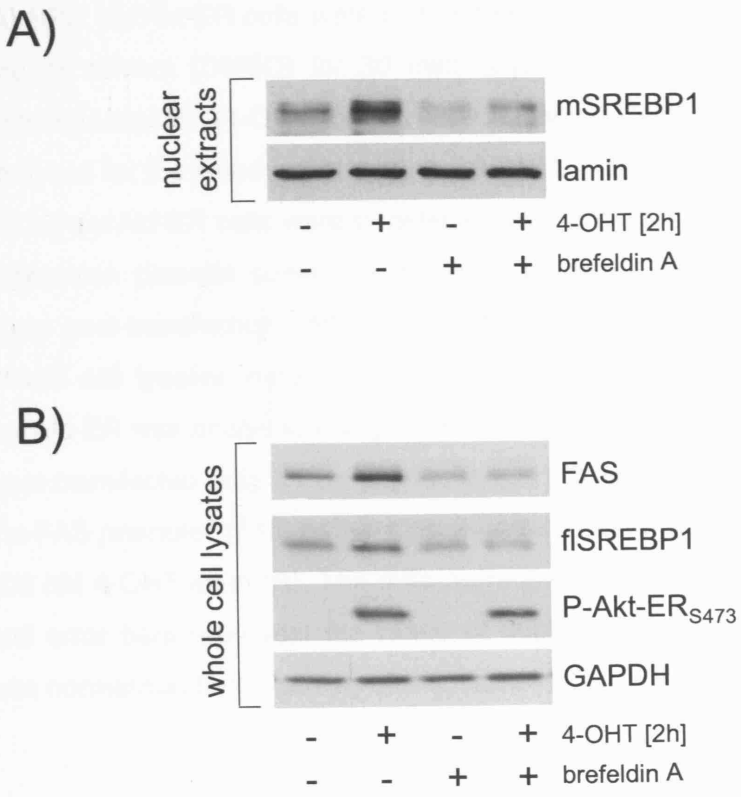
A)
nuclear extracts
mSREBP1
lamin
- + - + 4-OHT [2h]
- - + + brefeldin A
B)
whole cell lysates
FAS
flSREBP1
P-Akt-ER$_{S473}$
GAPDH
- + - + 4-OHT [2h]
- - + + brefeldin A

Figure 4-4 Activation of SREBP1 by Akt is independent of the proteasomal degradation machinery

(A) RPE myrAkt-ER cells were cultured in 1% LPDS and then treated with 50 μM MG-132 or solvent (DMSO) for 30 mins and subsequently stimulated with 100 nM 4-hydroxytamoxifen (4-OHT) or solvent for 2 hours. Nuclear extracts were prepared and analysed for the presence of mature SREBP1. Lamin is shown as a loading control. **(B)** U2OS myrAkt-ER cells were transfected with 0.1 μg of a pSuper empty vector, pSuper expression plasmid coding for shRNAs targeting Fbw7 isoforms or Flag-Fbw7. 24 hours post-transfection, cells were treated with 100 nM 4-OHT or solvent for 24 hours. Whole cell lysates were analysed for expression of mature SREBP1. Activation of myrAkt-ER was analysed using a phosphospecific antibody. **(C)** U2OS myrAkt-ER cells were transfected with 0.1 μg of a luciferase reporter construct containing a fragment of the FAS promoter (FAS (-150/-43)). 24 hours post-transfection, cells were treated with 100 nM 4-OHT as in (B). The data represent one out of two independent experiments and error bars represent the range of duplicate samples. Relative luciferase activity was normalised to the activity of a co-transfected lacZ expression plasmid.

Figure 4-4

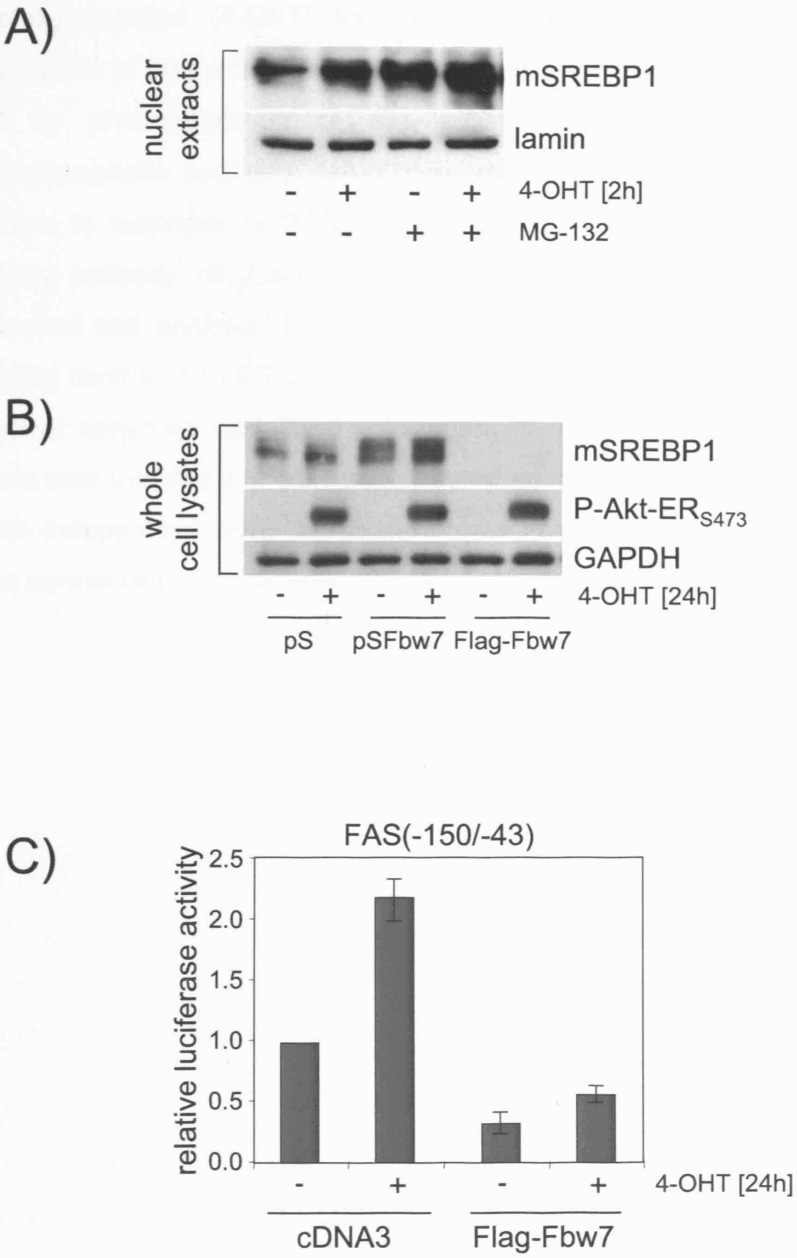
A)
nuclear extracts
mSREBP1
lamin
- + - + 4-OHT [2h]
- - + + MG-132
B)
whole cell lysates
mSREBP1
P-Akt-ER$_{S473}$
GAPDH
- + - + - + 4-OHT [24h]
pS
pSFbw7
Flag-Fbw7
C)
FAS(-150/-43)
relative luciferase activity
2.5
2.0
1.5
1.0
0.5
0.0
- + - + 4-OHT [24h]
cDNA3
Flag-Fbw7

Figure 4-5 Activation of SREBP1 by Akt is independent of GSK3 activity

(A) RPE myrAkt-ER cells were cultured in 1% LPDS and treated with 5 μM SB216763 or solvent (DMSO) for 30 mins and subsequently stimulated with 100 nM 4-hydroxytamoxifen (4-OHT) for 24 hours. Whole cell lysates were analysed for expression of fatty acid synthase (FAS) and full length SREBP1. Activation of myrAkt-ER by phosphorylation of Akt substrates GSK3α/β was detected using a phosphospecific antibody. GAPDH is shown as loading control. Stabilisation of ß-catenin in response to GSK3 inhibition was monitored using a phosphospecific ß-catenin antibody. **(B)** Cells were treated for 2 hours as in (A). Nuclear extracts were prepared and analysed for the presence of mature SREBP1. Lamin is shown as a loading control. **(C)** U2OS myrAkt-ER cells were transfected with 0.1 μg of a luciferase reporter construct containing a fragment of the FAS promoter (FAS (-150/-43)). 24 hours post-transfection, cells were treated as in (A). The data represent mean $\pm$ SD of three independent experiments performed in duplicate and relative luciferase activity was normalised to the activity of a co-transfected lacZ expression plasmid.

Figure 4-5

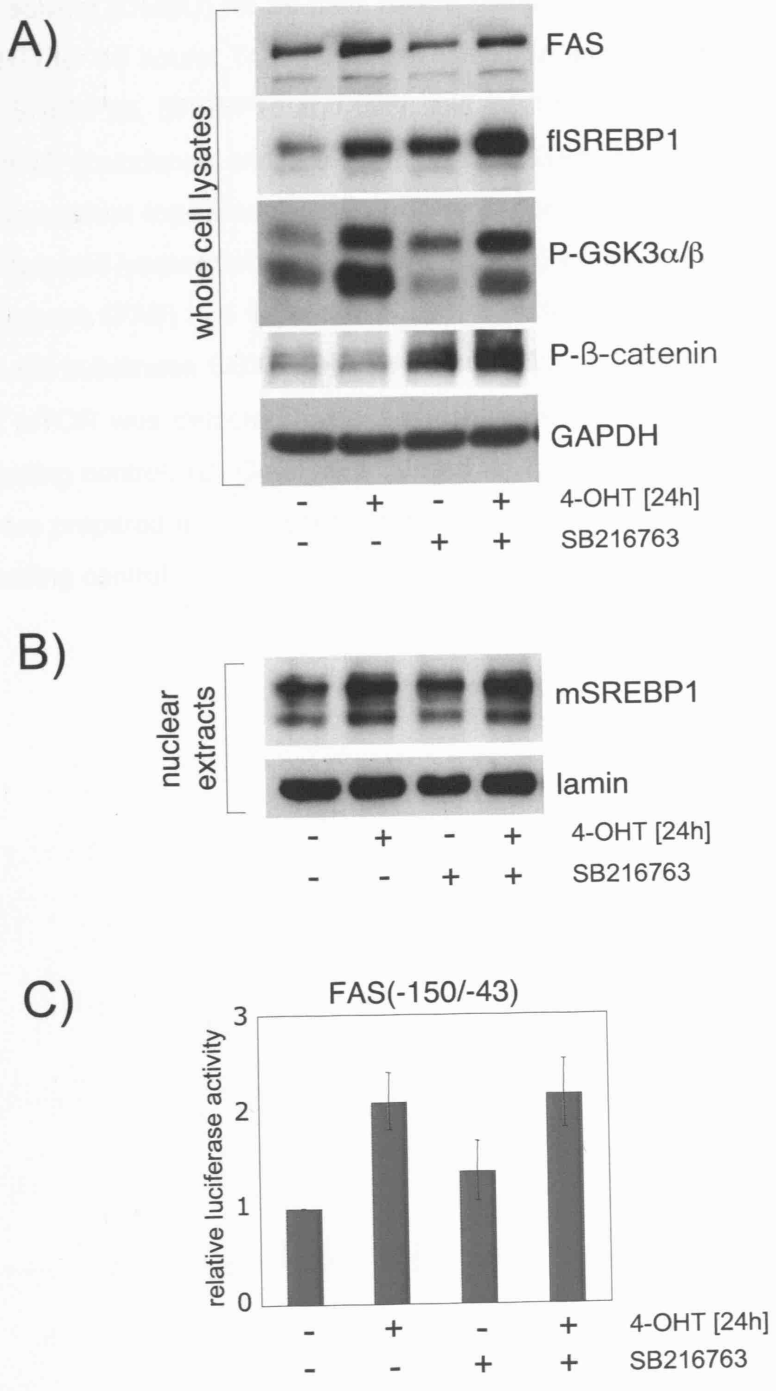
A)
whole cell lysates
FAS
flSREBP1
P-GSK3α/β
P-β-catenin
GAPDH
- + - +
- - + +
4-OHT [24h]
SB216763
B)
nuclear extracts
mSREBP1
lamin
- + - +
- - + +
4-OHT [24h]
SB216763
C)
FAS(-150/-43)
relative luciferase activity
0
1
2
3
- + - +
- - + +
4-OHT [24h]
SB216763

Figure 4-6 Inhibition of mTORC1 blocks activation of SREBP1 by Akt

(A) RPE myrAkt-ER cells were cultured in 1% LPDS and treated with 50 nM rapamycin or solvent (DMSO) for 30 mins before stimulation with 100 nM 4-hydroxytamoxifen (4-OHT) for 48 hours. Total RNA was extracted and analysed by q-rtPCR for expression of SREBP1a, SREBP1c and fatty acid synthase (FAS). The values represent relative mRNA abundance and are normalised to GAPDH. The data represent one of three independent experiments and error bars represent the range of duplicate samples. **(B)** Whole cell lysates from cells treated as in (A) were analysed for expression of fatty acid synthase (FAS) and full length SREBP1. Activation of myrAkt-ER and phosphorylation of Akt substrates GSK3α/β were detected using phosphospecific antibodies. Inhibition of mTOR was detected using a phosphospecific S6rb antibody. GAPDH is shown as loading control. **(C)** Cells were treated for 2 or 48 hours as in (B) and nuclear extracts were prepared and analysed for the presence of mature SREBP1. Lamin is shown as a loading control.

Figure 4-6

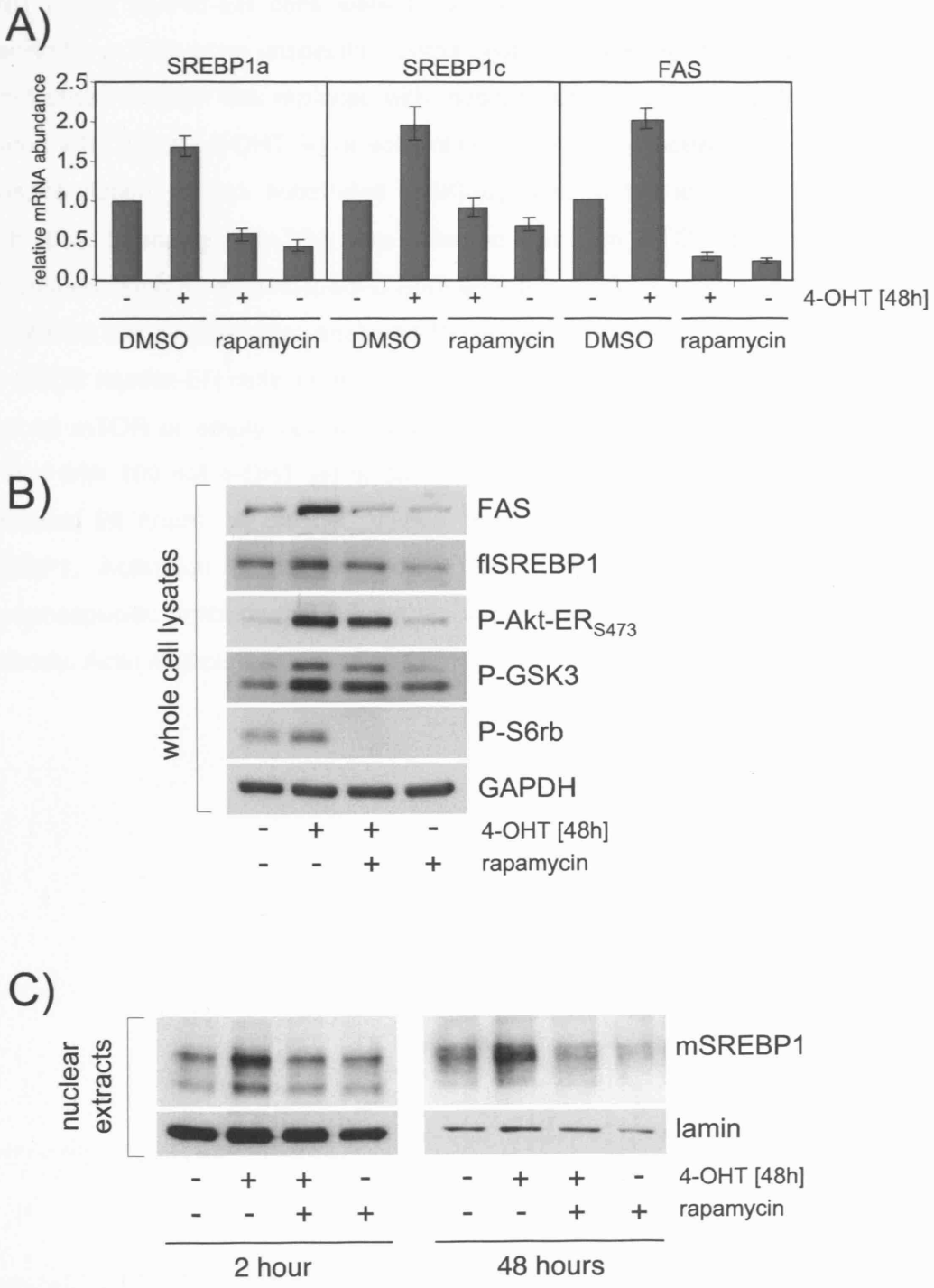
A)
SREBP1a
SREBP1c
FAS
relative mRNA abundance
2.5
2.0
1.5
1.0
0.5
0.0
- + + - - + + - - + + -
4-OHT [48h]
DMSO
rapamycin
DMSO
rapamycin
DMSO
rapamycin
B)
whole cell lysates
FAS
flSREBP1
P-Akt-ER$_{S473}$
P-GSK3
P-S6rb
GAPDH
- + + - 4-OHT [48h]
- - + + rapamycin
C)
nuclear extracts
mSREBP1
lamin
- + + - - + + - 4-OHT [48h]
- - + + - - + + rapamycin
2 hour
48 hours

Figure 4-7 Silencing of mTOR blocks activation of SREBP1 by Akt and overexpression of mTOR activates SREBP in the absence of Akt activity

(A/B) U2OS myrAkt-ER cells were transfected with 70 nM siRNA oligonucleotides specific for mTOR or an unspecific control oligonucleotide as indicated. 24 hours post-transfection, medium was replaced with medium containing 0.5% LPDS and cells were treated with 100 nM 4-OHT (+) or solvent (-) for 48 hours. Activation of myrAkt-ER and phosphorylation of Akt substrates GSK3α/β was detected using phosphospecific antibodies. Silencing of mTOR was detected using an mTOR antibody, activity was determined using a phosphospecific S6rb antibody. Actin is shown as a loading control (A). Whole cell lysates were analysed for expression of FAS, ACL and SREBP1 (B). **(C)** U2OS myrAkt-ER cells were transfected with 0.4 μg expression construct for wild-type rat mTOR or empty vector, as indicated. 24 hours post-transfection, cells were treated with 100 nM 4-OHT (+) or solvent (-) in medium containing 0.5% FCS for an additional 24 hours. Whole cell lysates were analysed for expression of FAS and SREBP1. Activation of the myrAkt-ER fusion protein was determinsed using a phosphospecific antibody. mTOR activity was detected using a phosphospecific S6rb antibody. Actin is shown as a loading control.

Figure 4-7

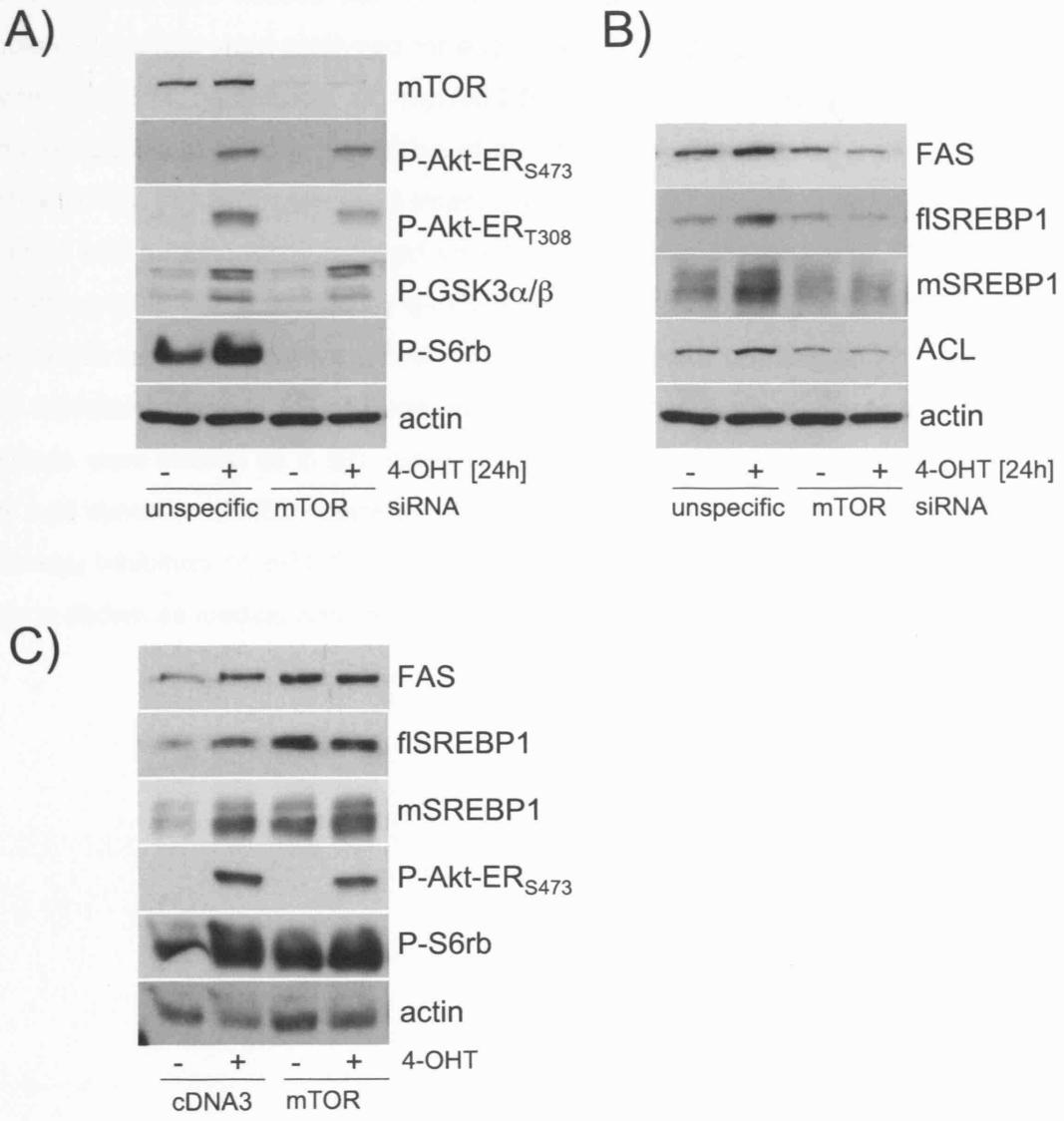
A)
mTOR
P-Akt-ER$_{S473}$
P-Akt-ER$_{T308}$
P-GSK3α/β
P-S6rb
actin
- + - + 4-OHT [24h]
unspecific mTOR siRNA
B)
FAS
flSREBP1
mSREBP1
ACL
actin
- + - + 4-OHT [24h]
unspecific mTOR siRNA
C)
FAS
flSREBP1
mSREBP1
P-Akt-ER$_{S473}$
P-S6rb
actin
- + - + 4-OHT
cDNA3 mTOR

Figure 4-8 Activation of fatty acid synthase in response to insulin requires mTORC1 activity

(A) RPE cells were treated with 50 nM rapamycin or solvent (DMSO) for 48 hours. Whole cell lysates were analysed for expression of fatty acid synthase (FAS) and full length SREBP1. Activation of myrAkt-ER was detected using S473 and T308 phosphospecific antibodies. Inhibition of mTOR was detected using a phosphospecific S6rb antibody. **(B)** RPE cells were treated with 50 nM rapamycin or solvent (DMSO) for 30 mins and subsequently induced with 1 μg/ml Insulin for 24 hours. RNA prepared from these cells was analysed by q-rtPCR for expression of fatty acid synthase (FAS). The values represent relative mRNA abundance and are normalised to GAPDH. The data represent mean $\pm$ SD of three independent experiments performed in duplicate. **(C)** Cells were treated as in (B) and whole cell lysates were analysed for expression of fatty acid synthase (FAS). Activation of myrAkt-ER was detected using phosphospecific antibody. Inhibition of mTOR was detected using a phosphospecific S6rb antibody. Actin is shown as loading control.

Figure 4-8

A)

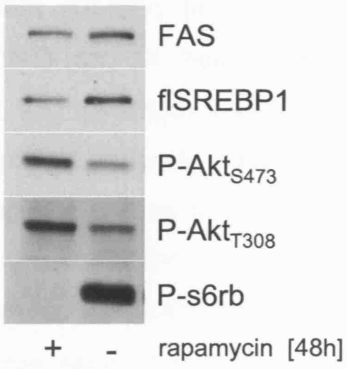

B)

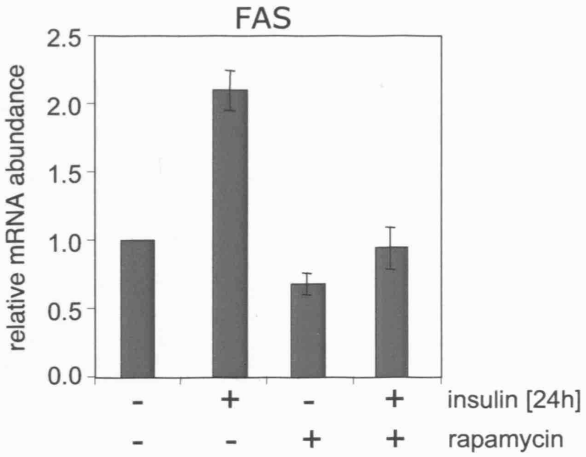

C)

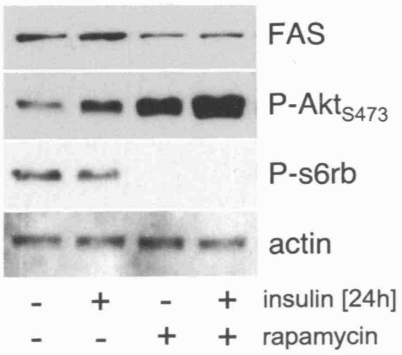

Figure 4-9 Activation of AMPK blocks Akt dependent activation of SREBP1

(A) RPE myrAkt-ER cells were cultured in 1% LPDS and treated with 50 nM rapamycin, 2 mM AICAR or solvent (DMSO) for 30 mins before induction with 100 nM 4-hydroxytamoxifen (4-OHT) for 24 hours. Whole cell lysates were analysed for expression of FAS, ACL and full length SREBP1. Activation of myrAkt-ER was detected using a phosphospecific antibody. mTOR activity was detected using a phosphospecific S6rb antibody. Actin is shown as loading control. **(B)** RPE myrAkt-ER cells were treated with 2 mM AICAR or solvent (DMSO) for 30 mins before induction with 100 nM 4-hydroxytamoxifen (4-OHT) for 2 hours. Nuclear extracts were prepared and analysed for the presence of mature SREBP1. Lamin is shown as a loading control.

Figure 4-9

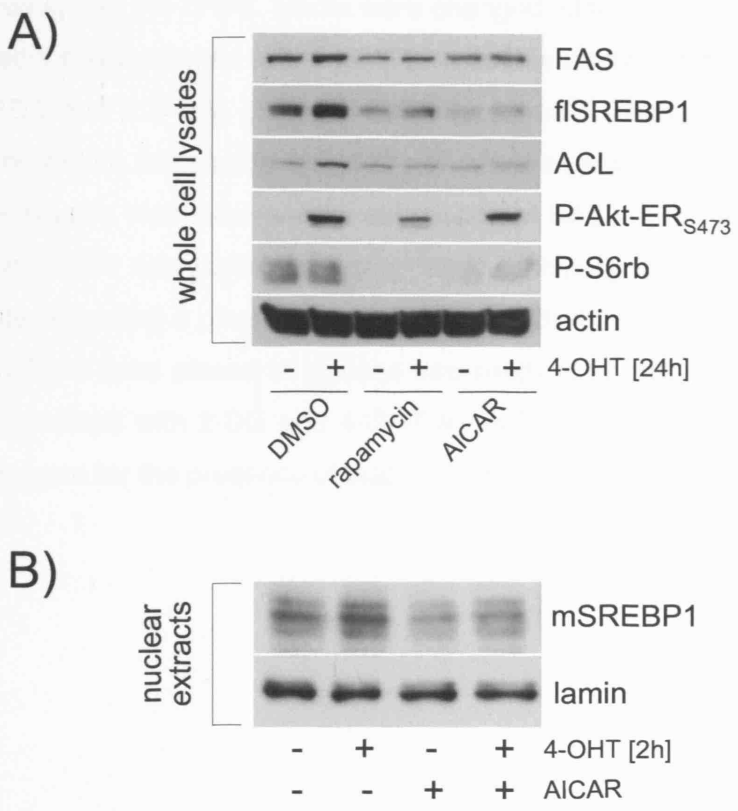
A)
whole cell lysates
FAS
flSREBP1
ACL
P-Akt-ER$_{S473}$
P-S6rb
actin
- + - + - + 4-OHT [24h]
DMSO
rapamycin
AICAR
B)
nuclear extracts
mSREBP1
lamin
- + - + 4-OHT [2h]
- - + + AICAR

Figure 4-10 Activation of SREBP1 by Akt requires glycolysis

(A) RPE myrAkt-ER cells were plated in medium containing 10% FCS and starved overnight in 1% LPDS. Media were changed either to 1% LPDS containing glucose free media supplemented with 1 mM Na^+ pyruvate/methylpyruvate or medium containing 1% LPDS and 2.5 mM glucose. Cells were treated with 2-deoxy-glucose (2-DG) for 30 mins before stimulation with 100 nM 4-hydroxytamoxifen (4-OHT) for 24 hours. Whole cell lysates were analysed for expression of FAS and full length SREBP1. Activation of myrAkt-ER was detected using a phosphospecific antibody. mTOR activity was detected using a phosphospecific S6rb antibody. GAPDH is shown as loading control. **(B)** Cells were placed in glucose-free medium or medium containing 2.5 mM glucose and treated with 2-DG and 4-OHT as indicated. Nuclear extracts were prepared and analysed for the presence of mature SREBP1. Lamin is shown as a loading control.

Figure 4-10

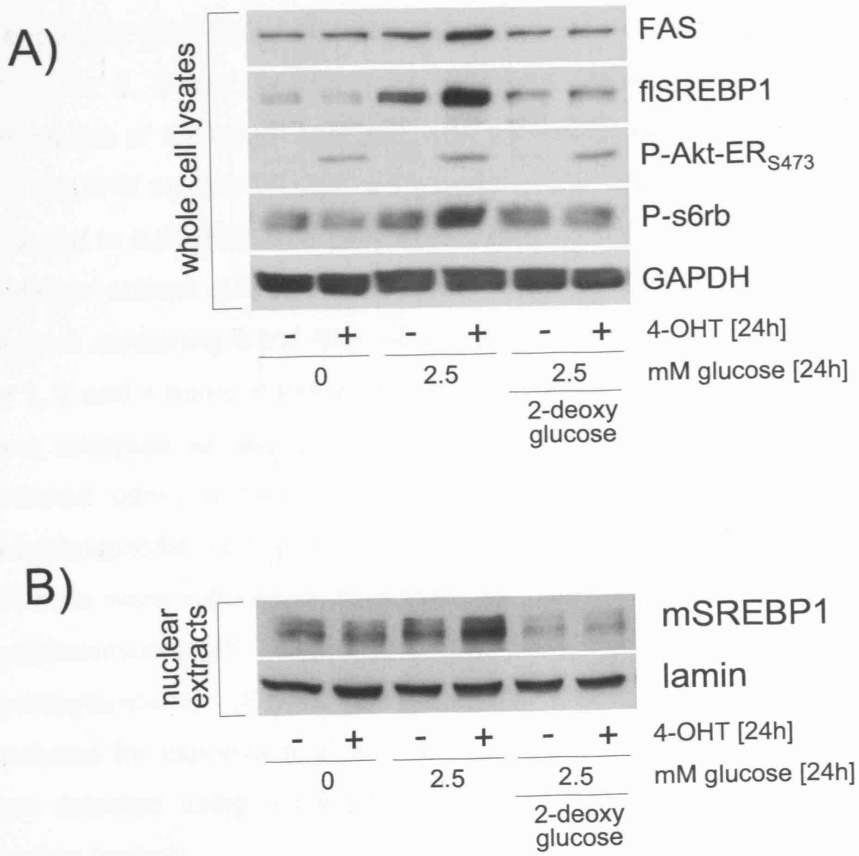
A)
whole cell lysates
FAS
flSREBP1
P-Akt-ER$_{S473}$
P-s6rb
GAPDH
- + - + - +
4-OHT [24h]
0
2.5
2.5
mM glucose [24h]
2-deoxy glucose
B)
nuclear extracts
mSREBP1
lamin
- + - + - +
4-OHT [24h]
0
2.5
2.5
mM glucose [24h]
2-deoxy glucose

Figure 4-11 Activation of SREBP1 by Akt is independent of *de novo* protein synthesis

(A) RPE myrAkt-ER cells were cultured in 1% LPDS and treated with 20 ng/ml brefeldin A or solvent (DMSO) for 30 mins before induction with 100 nM 4-hydroxytamoxifen (4-OHT) for 3, 8 and 24 hours as indicated. Whole cell lysates were analysed for expression of full length SREBP1. **(B)** Schematic representation of treatment used in (C). **(C)** RPE myrAkt-ER cells were plated in medium containing 10% FCS. Media were changed to 0.5% FCS and cells were subsequently treated with 2 μg/ml cycloheximide (CHX) or solvent (DMSO) for 3 hours. Cells were washed twice with PBS, placed in medium containing 0.5% BSA and induced with 100 nM 4-hydroxytamoxifen (4-OHT) for 1, 2 and 4 hours indicated in the presence or absence of ALLN. Whole cell lysates were analysed for expression of full length SREBP1. Activation of myrAkt-ER was detected using phosphospecific antibody. mTOR activity was detected using a phosphospecific S6rb antibody. GAPDH is shown as loading control. **(D)** RPE myrAkt-ER cells were cultured in 1% LPDS and treated with 50 μM MG-132 (MG), 2 μg/ml cycloheximide (CHX) or solvent (DMSO) for 30 mins before stimulation with 100 nM 4-hydroxytamoxifen (4-OHT) for 2 hours. Nuclear and cytoplasmic extracts were analysed for expression of full length and mature SREBP1. Activation of myrAkt-ER was detected using a phosphospecific antibody. GAPDH and lamin are shown as loading controls.

Figure 4-11

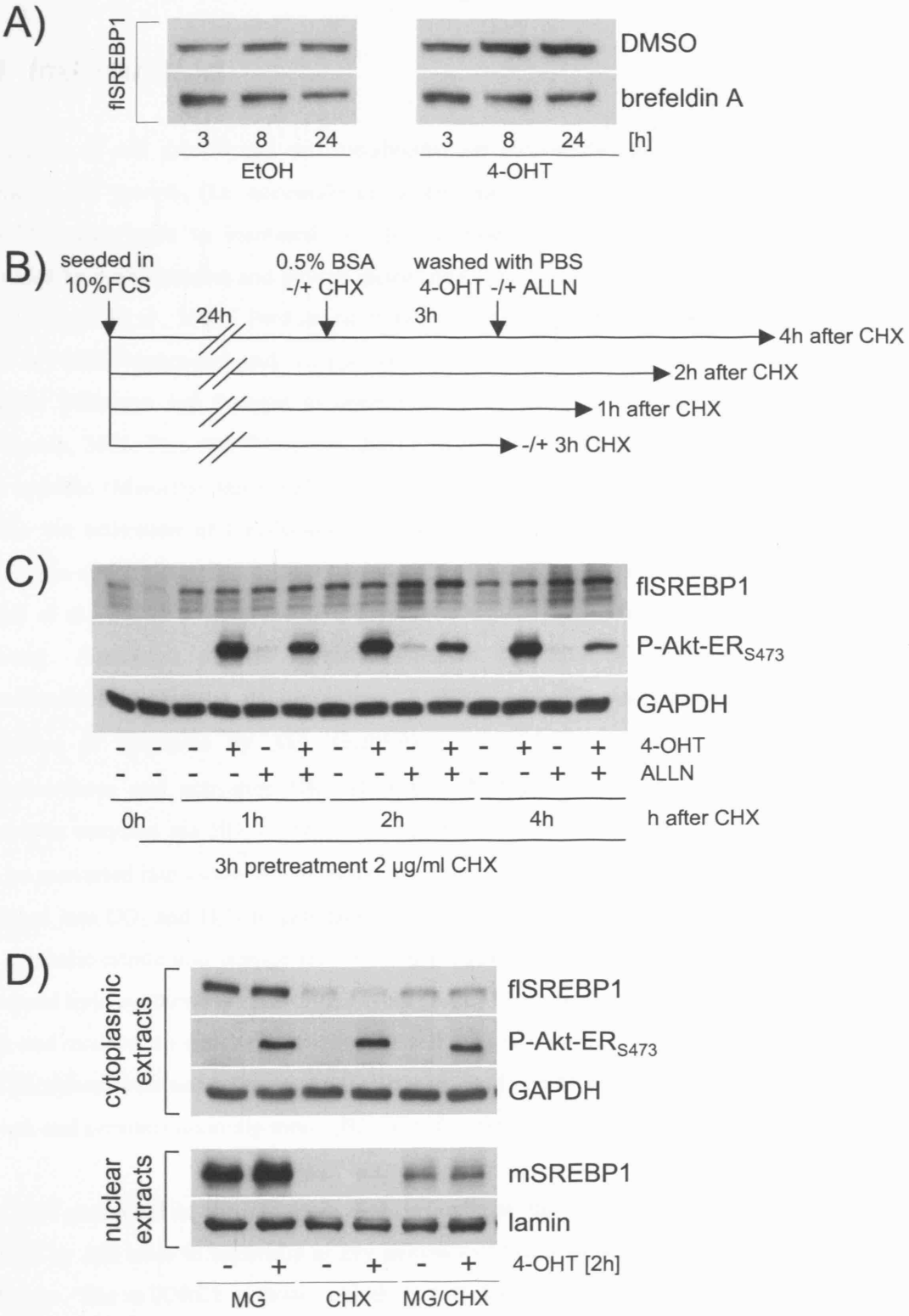
A)
flSREBP1
DMSO
brefeldin A
3 8 24
3 8 24 [h]
EtOH
4-OHT
B)
seeded in 10%FCS
0.5% BSA -/+ CHX
washed with PBS 4-OHT -/+ ALLN
24h
3h
4h after CHX
2h after CHX
1h after CHX
-/+ 3h CHX
C)
flSREBP1
P-Akt-ER$_{S473}$
GAPDH
4-OHT
ALLN
0h 1h 2h 4h
h after CHX
3h pretreatment 2 µg/ml CHX
D)
cytoplasmic extracts
flSREBP1
P-Akt-ER$_{S473}$
GAPDH
nuclear extracts
mSREBP1
lamin
4-OHT [2h]
MG CHX MG/CHX

5 Chapter 5: Regulation of cell metabolism and cellular growth control by Akt

5.1 Introduction

Regulation of cell growth and cell metabolism are inexorably linked (Jin et al., 2007). Akt promotes cell growth, (i.e. accumulation of cell mass), predominantly through activation of mTORC1 that leads to increased cell size (Edinger and Thompson, 2002). mTORC1 is regulated by both nutrients and growth factors and plays a conserved role in cell growth control (Wullschleger et al., 2006). Besides its ability to enhance protein synthesis through mTORC1, other mTORC1-dependent and -independent functions of Akt regulating nutrient uptake and anabolic pathways are thought to contribute to an increase in cell growth (Edinger and Thompson, 2002; Plas and Thompson, 2005). Akt-regulated anabolic metabolism is highly cell type specific (Manning and Cantley, 2007). Upon insulin stimulation, Akt enhances glucose uptake via activation of translocation of the glucose transporter 4 (GLUT4) to the plasma membrane and by increasing expression of GLUT1 (Calera et al., 1998; Kohn et al., 1996; Welsh et al., 2005). Within the cell, glucose is metabolised into pyruvate by the glycolytic pathway. Activation of Akt directly increases the rate of glycolysis by stimulating mitochondrial association of hexokinase 2 (HK), and this association is responsible for inhibition of apoptosis by Akt (Gottlob et al., 2001; Majewski et al., 2004). Akt phosphorylates and activaties HK2 (Robey and Hay, 2006) and increases expression of glycolytic enzymes via HIF-1α actiavtion (Lum et al., 2007; Semenza et al., 1996). Pyruvate can be converted into lactate or enters the tricarboxylic acid cycle (TCA cycle), where it is fully oxidised into CO_2 and H_2O to generate ATP. In liver and adipose tissue, glucose is converted via cytosolic citrate into storage fat. The key enzyme that converts glycolytic carbon flux into increased lipid synthesis is ATP-citrate lyase (ACL). ACL converts cytosolic citrate into acetyl-CoA and oxalacetate thereby supplying the cell with an essential metabolite for lipid synthesis. Akt phosphorylates and activates ACL (Berwick et al., 2002). Inhibition of ACL abolishes cell growth and prevents tumourigenesis (Bauer et al., 2005; Hatzivassiliou et al., 2005).

The data presented in the previous chapters indicate that mTORC1-dependent activation of SREBP by Akt leads to induction of key enzymes of the cholesterol and fatty acid biosynthesis pathways. The mTORC1 pathway senses growth factors and availability of nutrients for the regulation of macromolecule synthesis. This suggests an orchestrated regulation of protein and lipid synthesis by the Akt/TORC1 pathway. It seems obvious that an increase in cell size cannot be achieved without *de novo* membrane synthesis. Activation of lipid synthesis via activation of

SREBP could therefore be an important mechanism for the regulation of cell growth by the Akt/TORC1 pathway.

De-regulation of the PI3K/Akt/TORC1 pathway drives cell growth in a manner independent of intra- and extra-cellular signals (Shaw and Cantley, 2006). TSC tumours are termed hamartomas to indicate their overgrowth phenotype. These hamartomas develop cortical tubes containing giant cells (Kwiatkowski, 2003), implying that growth regulatory pathways are altered in these tumours.

Several studies show that SREBP activity is upregulated in different cancer types. It seems likely that this activation contributes to cell transformation and tumour development (Menendez and Lupu, 2006). Accumulation of fatty acids and cholesterol has been described for a number of solid tumours (Alo et al., 1996; Pizer et al., 1998; Rashid et al., 1997) and fatty acid synthase has been discussed as a metabolic oncogene in prostate cancer (Baron et al., 2004). Cholesterol is a component of membrane lipid rafts that are involved in signalling processes (Simons and Ikonen, 2000) and aberrant regulation of cholesterol synthesis may contribute to cancer development and progression (Hager et al., 2006). These data indicate a link between metabolism and cell growth regulation by the PI3K/Akt/TORC1 pathway in cancer.

This chapter describes several experiments in which intracellular metabolite concentrations as well as metabolite uptake and secretion are monitored by nuclear magnetic resonance (NMR) analysis. Activation of Akt results in induction of glucose and amino acid uptake, lactate production, as well as fatty acid and phosphoglyceride biosynthesis. Most changes in metabolite concentrations require mTORC1 activity. Furthermore, increase in cell size in response to Akt activation is blocked by rapamycin. Finally, activation of mSREBP is sufficient to induce an increased cell size in RPE cells.

5.2 Akt induces accumulation of metabolites

Cell growth is defined by accumulation of cell mass, which depends on enhanced protein synthesis. Akt has been suggested to promote amino acid uptake and protein synthesis via regulation of cell surface expression of amino acid transporters and activation of protein translation, in an mTORC1-dependent manner (Wullschleger et al., 2006).

Whole cell extracts from RPE myrAkt-ER cells after 48 hours of Akt activation were analyzed for total protein content. In parallel, cell numbers were determined. Total protein was divided by the total number of cells and compared to solvent treated control cells. As anticipated,

activation of Akt resulted in an accumulation of protein per cell (Figure 5-1). Treatment with the mTORC1 inhibitor rapamycin reduced the Akt dependent increase in protein concentration per cell.

All experiments in this chapter were performed in 1% LPDS. In order to assay *de novo* lipid synthesis, cells should be cultured in media containing fewer lipids. Cells cultured in FCS could derive the lipids they require from the media via uptake, instead of via intracellular *de novo* synthesis. Furthermore cells cultured in 1% LPDS are starved resulting in a less active PI3K/TORC1 pathway. This enhanced the relative signal of Akt activation by 4-OHT to untreated control.

In order to examine the changes in the metabolic profile that are associated with Akt activation, a high resolution NMR analysis on both lipid and water-soluble metabolites was performed. RPE myrAkt-ER cells were treated with 4-OHT or solvent. After 48 hours, cells were harvested and metabolites extracted using a dual-phase extraction method. To determine metabolite production and uptake, culture media from treated and untreated cells were collected and examined by NMR. Having shown that induction of SREBP by Akt requires mTORC1 activity, it was of interest to investigate whether inhibition of mTORC1 could specifically interfere with the changes induced by Akt in the metabolic profile. Therefore the experiments described above were repeated in the presence of the mTORC1 inhibitor rapamcyin. All experiments were performed in collaboration with Y.-L. Chung and J.R. Griffiths (CRUK Magnetic Resonance Group, St. Georges Hospital and Molecular Imaging, CRUK Cambridge Research Institute).

5.2.1 Akt induces accumulation of metabolites required for the synthesis of biological membranes

Having shown that Akt induces expression of enzymes involved in cholesterol and fatty acid biosynthesis, the following question concerned whether this would result in an accumulation of products of these pathways. Figure 5-2 shows various lipid metabolites in extracts from RPE myrAkt-ER cells after 48 hours of Akt activation compared to solvent treated control cells in the absence or presence of rapamycin. A highly significant increases in triacylglcyride (saturated fatty acids (139%) and unsaturated fatty acids (145%)) and phosphoglyceride (phosphatidylethanolamine (135%), phosphatidylcholine (137%) and phosphatidylglycerol (130%)) levels were found in response to Akt activation in these cells (Figure 5-2). The Akt-dependent induction could be significantly reduced for most of the lipids by treatment with the mTORC1 inhibitor rapamycin. In particular, accumulation of phosphatidylcholine by Akt is completely and significantly blocked by rapamycin. Rapamycin treatment on its own did not

significantly decrease lipid concentration (Figure 5-2). Cells are starved in 1% LPDS, therefore the activity of the PI3K/mTORC1 pathway is low and no major effect of rapamycin treatment is expected. However, the data indicate, at least in the experimental system used, that inhibition of mTORC1 does not activate ß-oxidation of FA, although mTORC1 activity is essential for Akt-induced lipid biosynthesis.

Saturated and unsaturated fatty acids are required for the synthesis of phosphoglycerides such as phosphatidylglycerol, phosphatidylethanolamine and phosphatidylcholine as well as sphingomyelin, which, together with cholesterol, form the building blocks for biological membranes and phosphatidylcholine represents the major component of membranes of all mammalian cells. This finding indicates that Akt is involved, presumably via mTORC1, in synthesis of biological membranes.

5.2.2 Akt induces an increase in intracellular concentrations of water-soluble metabolites

The measured water-soluble metabolites were categorized into amino acids, glucose derivates, free head groups for the synthesis of phosphoglycerides and energy (sum of ATP + ADP and sum of NADH + NAD). Head groups determine the biophysical properties of phosphoglycerides.

Figure 5-3 includes measured water-soluble metabolites of RPE myrAkt-ER cells. The concentration of almost all detected intracellular metabolites was significantly increased in response to Akt activation. Activation of Akt increased the sum concentration of ATP + ADP and NADH + NAD by approximately 50%. This indicates sufficient energy supply for anabolic processes such as protein and lipid biosynthesis. Akt-dependent induction of most water-soluble metabolites measured was significantly blocked by treatment with the mTORC1 inhibitor rapamycin (Figure 5-3). Glutamine, acetate, glycerolphosphocholine (GPC) and NADH/NAD were not statistically significantly decreased by rapamycin compared to 4-OHT treatment alone. It is remarkable that the changes in metabolite concentrations vary between 30% and 100%. In particular, the changes in amino acid concentrations are quite diverse. The variations observed could be due to the fact that water-soluble metabolites are rapidly processed with different kinetics, which could lead to accumulation of one metabolite by concurrent reduction of another.

5.2.3 Akt induces uptake of glucose and amino acids and production of lactate

Having shown that Akt enhances the level of water-soluble metabolites, the next step was to assess whether the increase in intracellular concentration was due to elevated uptake from the extracellular media or due to induction of the intracellular production of the respective metabolite. Therefore, media from 4-OHT and solvent treated cells were analysed for changes in metabolite concentrations.

Activation of Akt caused increased glucose and amino acid uptake, and production of lactate, alanine, acetate, glycine and formate (Figure 5-4). All changes in metabolite concentration were statistically significant. In addition, the Akt-induced increase in glucose uptake and lactate and alanine production was completly blocked by treatment with rapamycin, which were statistically significant (Figure 5-4).

These data demonstrate that the Akt-mediated induction of glucose uptake and lactate production requires mTORC1 activity.

5.3 Cell size analysis

It has been published that Akt promotes increased mammalian cell size. The major effector of Akt controlled cell size is mTORC1, as rapamycin treatment alone decreases cell size and also interferes with the positive cell size effect of Akt (Edinger and Thompson, 2002; Faridi et al., 2003).

In this study, cell size was assessed by two methods, either by measuring forward light scatter (FSC) via fluorescence-activated cell sorter (FACS) or by Coulter counter analysis. FACS analysis is not an accurate cell size method. FSC measures the scattering of a life cell, which is only an indication for cell size. An increase in light scatter infers an increase in cell size. Coulter counter analysis determines mean electronic cell volume.

5.3.1 Increase in cell size by Akt requires TORC1

In order to determine whether activation of myrAkt-ER modulates human retinal pigment epithelial cells (RPE) cell size and whether the Akt effect is rapamycin sensitive, cell size was measured by using Coulter counter and flow cytometry. These experiments were performed by Beatrice Griffiths (GEA, CRUK-LRI).

Cells were starved overnight in 1% LPDS and treated for 24 hours of the indicated stimuli. Cells for FACS analysis were stained with a cell-permeant dye and analysis was restricted to live cells (PI negative). As shown in Figure 5-5, activation of Akt resulted in larger cells than control cells, as seen by a shift to the right of the mean FSC-A histogram (Figure 5-5 A). Cells for Coulter counter were not stained. Activation of Akt resulted in increased cell volume compared to control cells, as seen by a shift to the right of the mean cell volume (Figure 5-5 C). However, rapamycin treatment prevents the Akt-dependent increase in size of these cells as seen by the overlaid cell size diagrams (Figure 5-5 B and D). Cells were starved; therefore a further reduction in cell size by rapamycin treatment was not expected here. Quantitative analysis revealed an approximately 16% increase in cell size measured by Coulter counter, and a 7% increase measured by flow cytometry. In both approaches inhibition of mTORC1 activity using rapamycin completely blocked the positive Akt effect on cell size (Figure 5-5 E and F). These results demonstrate that activation of myrAkt-ER increases the size of RPE cells. Consistent with published data, these data support the model that Akt-regulated cell size is dependent on mTORC1 activity.

5.3.2 Activation of SREBP results in increased cell size

The finding that activation of Akt results in SREBP-dependent synthesis of membrane components required for cell growth with concomitant cell size increase, suggests that activation of SREBP could contribute to mediation of the Akt cell size effect. In order to analyse the effect of activation of SREBP on cell growth, inducible versions of the SREBP isoforms were generated. The N-terminal domains of SREBP1a and SREBP2 were fused to the hormone-binding domain of the estrogen receptor (mSREBP-ER) (Figure 5-6 A).

The first experiment carried out with these cell lines verified the functionality of the SREBP fusion proteins. RPE cells expressing mSREBP-ER were treated with 4-OHT for 24 hours, resulting in accumulation of FAS and ACL protein compared to the empty vector control (Figure 5-6 B). Although SREBP2 preferentially activates genes encoding enzymes for cholesterol biosynthesis, Stimulation of the mSREBP2-ER construct also induces expression of genes for fatty acid synthesis. However, activation of mSREBP1a enhanced expression of FAS and ACL to a greater extent than mSREBP-2 (Figure 5-6 B).

Next, cell size was analyzed in response to activation of the mSREBP-ER fusion proteins in RPE cells by measuring cell volume using the Coulter counter and forward scatter by flow cytometry. These experiments were performed by Beatrice Griffiths. After 24 hours of 4-OHT

treatment, cells analysed by FACS were stained with a cell-permeant DNA dye and propidium iodide. As shown in Figure 5-6 C, activation of mSREBP1a resulted in larger cells than the control cells, as seen by the shift to the right of the mean FSC-A histogram. Coulter counter analysis revealed an increase in cell volume after activation of mSREBP1a (Figure 5-6 D). However, treatment of mSREBP2-ER expressing cells with 4-OHT only marginally increased the size of these cells compared to that of controls, as seen by the overlaid cell size diagrams (Figure 5-6 C and D). In addition, FACS analysis after activation of mSREBP-ER showed no shift on RPE cell cycle distribution (data not shown) and 4-OHT treated empty vector cells did not show any alteration in cell size measured by Coulter counter and FACS (data not shown).

Quantitative analysis revealed an approximately 12% increase in cell size measured by Coulter counter and a 18% increase measured by flow cytometry for mSREBP1a and an approximately 2% increase by Coulter counter and a 6% increase measured by flow cytometry for mSREBP2 (Figure 5-6 E and F). The smaller increase in cell size in response to activation of mSREBP2 compared to mSREBP1a correlates with the immunoblotting results, showing higher induction of FAS and ACL expression by mSREBP1a (Figure 5-6 B). This would indicate that activation of SREBP1a and thus upregulation of fatty acid synthesis genes could contribute to cell size control.

Taken together, these data show that ectopic activation of mSREBP1a and to a lesser extent mSREBP2 is sufficient to increase cell size, which correlates with induced expression of FAS and ACL. This indicates that activation of SREBP contributes to cell growth.

5.4 Discussion

The most important question that arises from the results described in this thesis concerns the effect of SREBP activation by Akt on cell phenotype. The data shown in this chapter indicate that activation of Akt leads to an increase in intracellular concentration of saturated and unsaturated fatty acids, membrane phospholipids, amino acids, lactate and adenosine-containing compounds (Figure 5-2, Figure 5-3). Akt activation caused increased uptake of glucose and amino acids as well as production of lactate (Figure 5-4). These metabolic changes indicate that Akt activation stimulates glucose transport, glycolysis, protein and membrane component synthesis. Treatment with the specific mTORC1 inhibitor rapamycin blocked the Akt induced increase in intracellular lipids and most of the changes in water-soluble metabolites (Figure 5-2, Figure 5-3). Rapamycin treatment also inhibited Akt-mediated induction of glucose uptake and lactate production (Figure 5-4).

Inhibition of mTORC1 by rapamycin treatment blocked the Akt-mediated increase in concentration of most amino acids in RPE cells (Figure 5-3). This is consistent with the observation that mTORC1 activity is required for Akt stimulated amino acid uptake (Edinger and Thompson, 2002) and that rapamycin treatment decreases the mRNA level of several amino acid transporters (Peng et al., 2002). Rapamycin blocked glucose uptake and lactate production as well as the intracellular amount of ATP/ADP in RPE cells (Figure 5-3, Figure 5-4). In contrast, Peng et al., (2002) observed a 15% increase in intracellular ATP levels, a slight but significant increase in lactate production and glucose consumption after 24 hours of rapamycin treatment in lymphocytes (Peng et al., 2002). This could be explained by cell type specific differences in the Akt-mediated metabolic outcome in response to rapamycin treatment (Manning and Cantley, 2007). These observations also underline the importance of considering cell type specific effects of drug treatment.

Rapamycin also abolished the Akt-induced accumulation of metabolites that are synthesised by enzymes, which are transcriptionally regulated by SREBP. This is consistent with findings described in chapter 4 showing that mTOR activity is required for activation of SREBP by Akt. Inhibition of Akt-induced lipid biosynthesis by rapamycin could thus be mediated by inhibition of mTORC1-mediated SREBP activation. Rapamycin also blocks Akt-induced glucose uptake. The resulting glucose deprivation would lead to a lack of the carbon source necessary for *de novo* lipid synthesis. This would be consistent with the observed inhibition of lipid biosynthesis by rapamycin.

The observed changes in lipid concentration in response to Akt activation could also be independent of SREBP. It has recently been shown that Akt inhibits the activity of the transcription factor PGC-1α (Li et al., 2007). PGC-1α activates expression of enzymes involved in ß-oxidation of fatty acids and in gluconeogenesis (Puigserver, 2005). Akt also suppresses expression of genes encoding ß-oxidation enzymes by phosphorylating and inhibiting the transcription factor Foxa2 (Wolfrum et al., 2004). Therefore it is not clear, whether the observed increase in intracellular lipid concentration in response to Akt activation is due to inhibition of fatty acid oxidation or activation of *de novo* fatty acid synthesis. Further experiments are required to answer these questions.

So far, the analysis of regulation of cell growth has mainly been focussed on the PI3K effectors Akt, mTORC1 and S6K. Mice with deletions of two Akt isoforms (Akt1 and Akt2) show dwarfism and skeletal muscle atrophy due to a decrease in myocyte size (Peng et al., 2003). Consistent with published data, activation of Akt induced increased cell volume in RPE cells and this increase required mTORC1 activity (Figure 5-5). Clearly, an increase in cell size cannot be achieved without *de novo* membrane synthesis. Induction of lipid synthesis via

activation of SREBP could therefore be an important mechanism for cell growth regulation. Interestingly, ectopic expression of mature SREBP1a and to a lesser extent mature SREBP2 was sufficient to induce increased cell size in RPE cells (Figure 5-6). These data suggest that lipid synthesis is actively involved in the regulation of cell growth. It would be relevant to investigate any regulatory feedback mechanism of activated SREBPs and its target genes toward the PI3K/Akt/mTOR pathway, as it has been shown that FAS activity positively regulates Akt activation (Wang et al., 2005). However, preliminary data show that activation of SREBP does not result in activation of Akt or mTORC1 in RPE cells (data not shown).

Akt controls cell growth and regulates cellular metabolism and it is an intriguing possibility that Akt exerts its role in the regulation of both processes via mTORC1. Akt acts as a transducer of many functions initiated by growth factors and other receptors that activate PI3K. Thus Akt is able to activate protein synthesis, glycolysis and lipid biogenesis and to induce SREBP dependent transcription. This provides all the essential resources for a cell to grow in size until it reaches the size required for its function.

Figure 5-1 Activation of Akt induces an increase in intracellular protein concentration

RPE myrAkt-ER cells were treated with 50 nM rapamycin for 30 mins before stimulation with 100 nM 4-OHT or solvent (ethanol) for 48 hours in 1% LPDS. Cellular proteins were extracted and measured using a Bradford assay. Cell numbers were counted in parallel samples using a Neubauer chamber. Protein concentrations were normalized to cell number. Data shows one out of two similar experiments and error bars represent $\pm$ the range of two replicates.

Figure 5-1

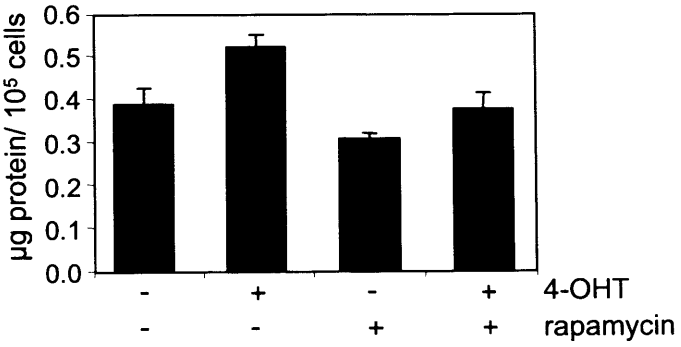

Figure 5-2 Activation of Akt induces an increase in intracellular concentrations of fatty acids and phosphoglycerides

RPE myrAkt-ER cells were treated as in Figure 5-1 for 48 hours in medium containing 1% LPDS. Cellular lipids were extracted and analysed by NMR spectroscopy. Metabolite data were normalised to cell number and are shown relative to vehicle treated control. The mean values ± Standard error of the mean (SEM) of five independent experiments are represented. P-values were calculated between 4-OHT treated and control cells (* $P < 0.01$) and 4-OHT plus rapamycin and 4-OHT samples (** $P < 0.05$). P-values were calculated using a two-tailed student's t-test assuming equal variances. Metabolite analysis by NMR were carried out by Y.-L. Chung (CRUK, Magnetic Resonance Group, St. Georges Hospital, London).

Figure 5-2

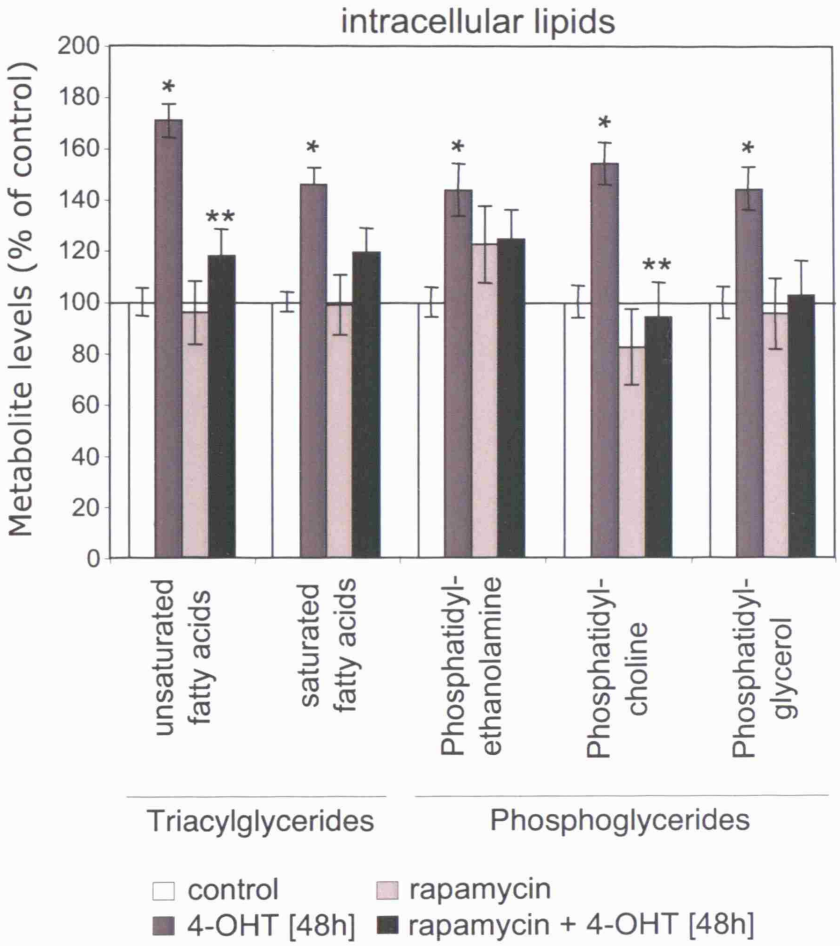
intracellular lipids
Metabolite levels (% of control)
200
180
160
140
120
100
80
60
40
20
0
*
**
unsaturated fatty acids
saturated fatty acids
Phosphatidyl-ethanolamine
Phosphatidyl-choline
Phosphatidyl-glycerol
Triacylglycerides
Phosphoglycerides
control
rapamycin
4-OHT [48h]
rapamycin + 4-OHT [48h]

Figure 5-3 Activation of Akt induces an increase in intracellular concentrations of water-soluble metabolites

RPE myrAkt-ER cells were treated as in Figure 5-1 for 48 hours in medium containing 1% LPDS. Water-soluble metabolites were extracted and analysed by NMR spectroscopy. Metabolite data were normalised to cell number and are shown relative to vehicle treated control. The mean values ± SEM of five independent experiments are represented. P-values were calculated between 4-OHT treated and control cells (* $P < 0.02$) and 4-OHT plus rapamycin and 4-OHT treated samples (** $P < 0.02$). P-values were calculated using a paired student's t-test assuming equal variances. Key: PC - phosphocholine, GPC - glycerophosphocholine, PE - phosphoethanolamine. Metabolite analysis by NMR were carried out by Y.-L. Chung (CRUK, Magnetic Resonance Group, St. Georges Hospital, London).

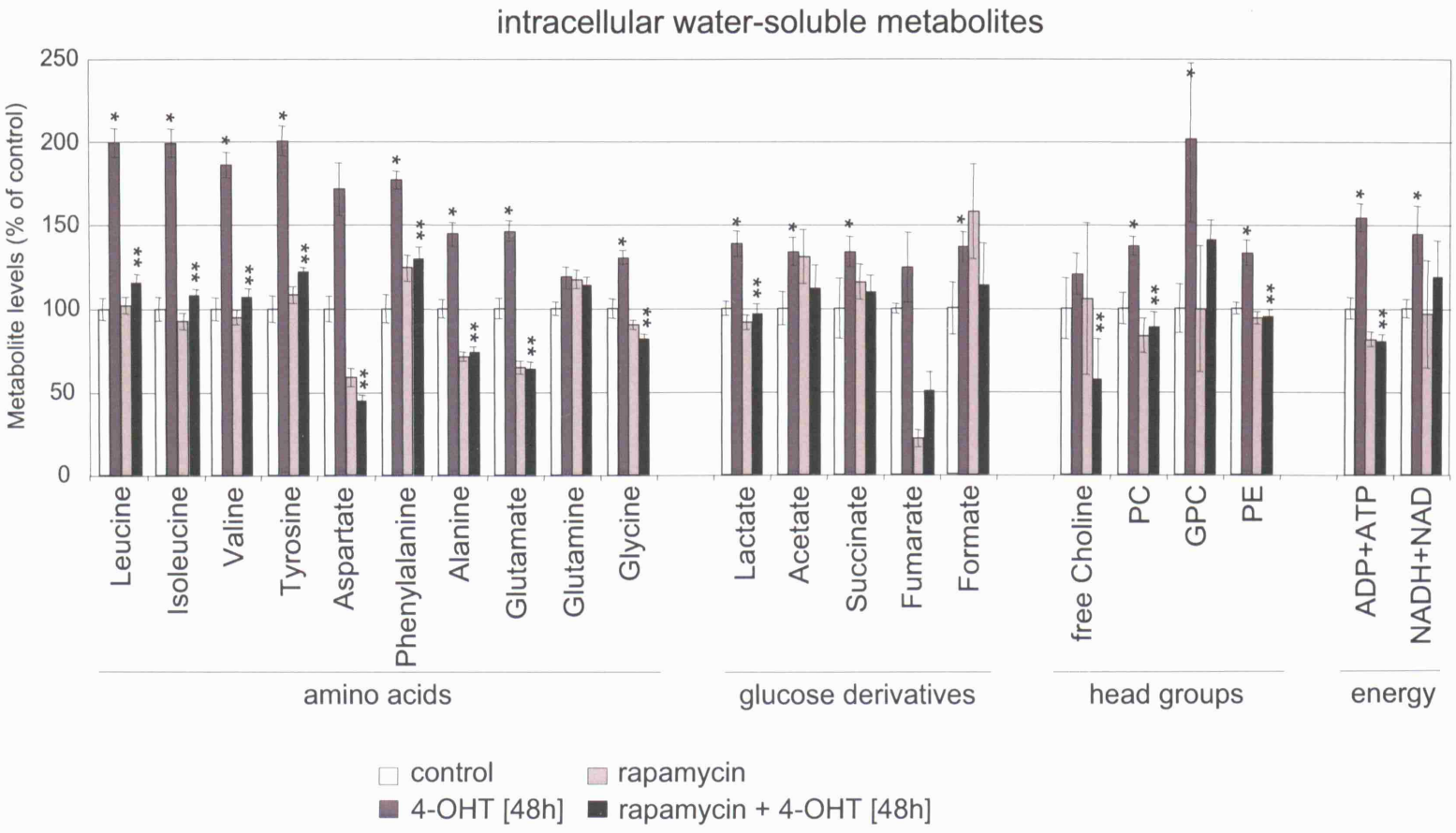
intracellular water-soluble metabolites
Metabolite levels (% of control)
250
200
150
100
50
0
Leucine
Isoleucine
Valine
Tyrosine
Aspartate
Phenylalanine
Alanine
Glutamate
Glutamine
Glycine
Lactate
Acetate
Succinate
Fumarate
Formate
free Choline
PC
GPC
PE
ADP+ATP
NADH+NAD
amino acids
glucose derivatives
head groups
energy
control
rapamycin
4-OHT [48h]
rapamycin + 4-OHT [48h]

Figure 5-3

Figure 5-4 Akt-mediated glucose uptake and lactate production is mTORC1 dependent

RPE myrAkt-ER cells were treated as in Figure 5-1 for 48 hours in medium containing 1% LPDS. Medium was collected and analysed by NMR spectroscopy. Metabolite data were normalised to cell number and are shown relative to vehicle treated control. The mean values ± SEM of four independent experiments are represented. P-values were calculated between 4-OHT treated and control cells (* $P < 0.05$) and 4-OHT plus rapamycin and 4-OHT treated samples (** $P < 0.05$). P-values were calculated using a paired student's test assuming equal variances. Metabolite analysis by NMR were carried out by Y.-L. Chung (CRUK, Magnetic Resonance Group, St. Georges Hospital, London).

Figure 5-4

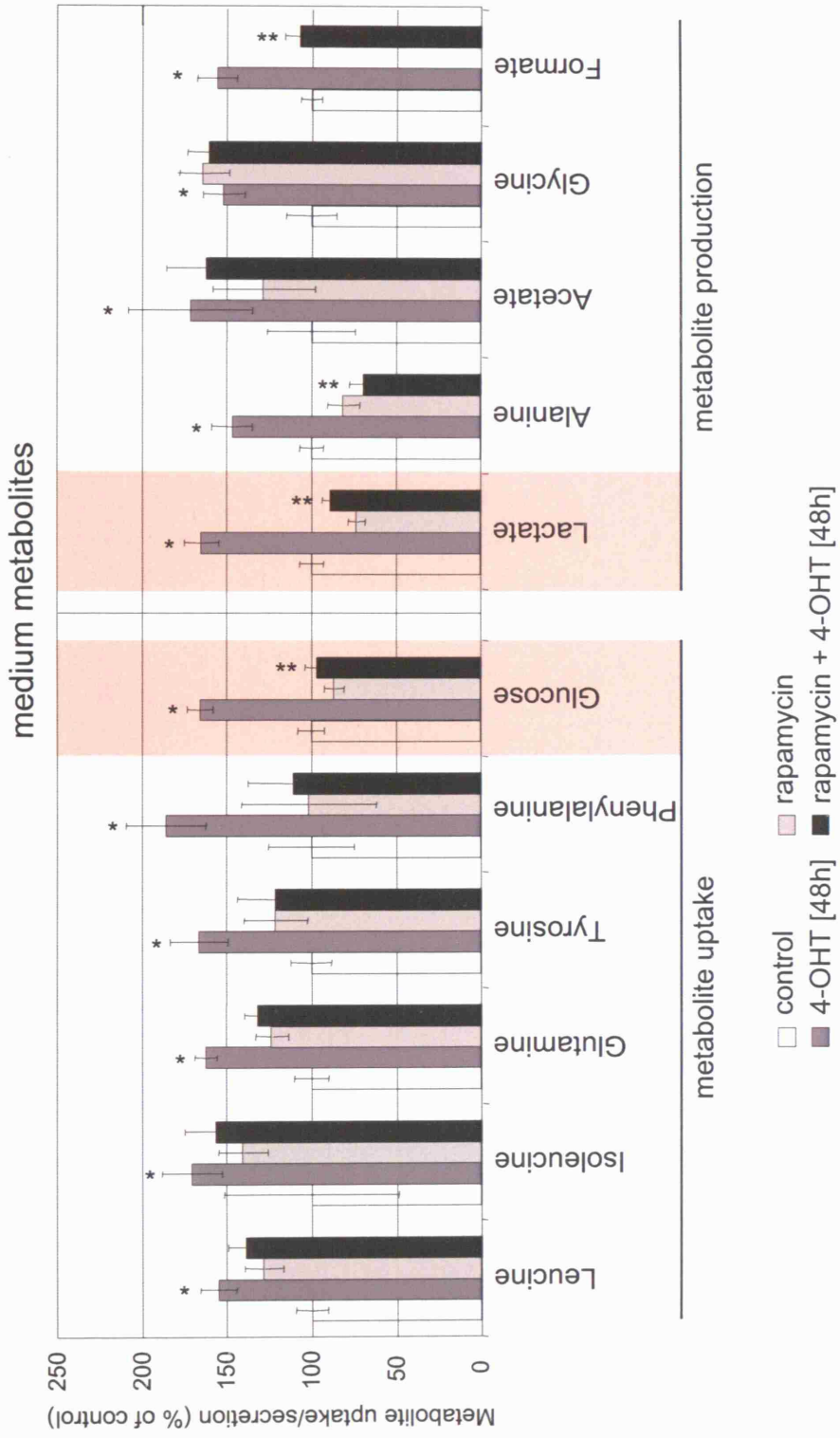
medium metabolites
Metabolite uptake/secretion (% of control)
250
200
150
100
50
0
Leucine
Isoleucine
Glutamine
Tyrosine
Phenylalanine
Glucose
Lactate
Alanine
Acetate
Glycine
Formate
metabolite uptake
metabolite production
control
rapamycin
4-OHT [48h]
rapamycin + 4-OHT [48h]

Figure 5-5 Akt-induced increase in cell size requires mTORC1 activity

RPE myrAkt-ER cells were stimulated with 100 nM 4-OHT (blue or black lines) or solvent (red or grey lines) in the presence or absence of 50 nM rapamycin as indicated for 24 hours in 1% LPDS. Cell size was assessed by measuring forward scatter (FSC) by FACS **(A/B/E)** or measuring electronic cell volume (Coulter Counter) **(C/D/F)**. Representative of three experiments is shown; error bars represent the range of duplicate samples. Experiments were performed by Beatrice Griffiths (GEA, CRUK-LRI).

Figure 5-5

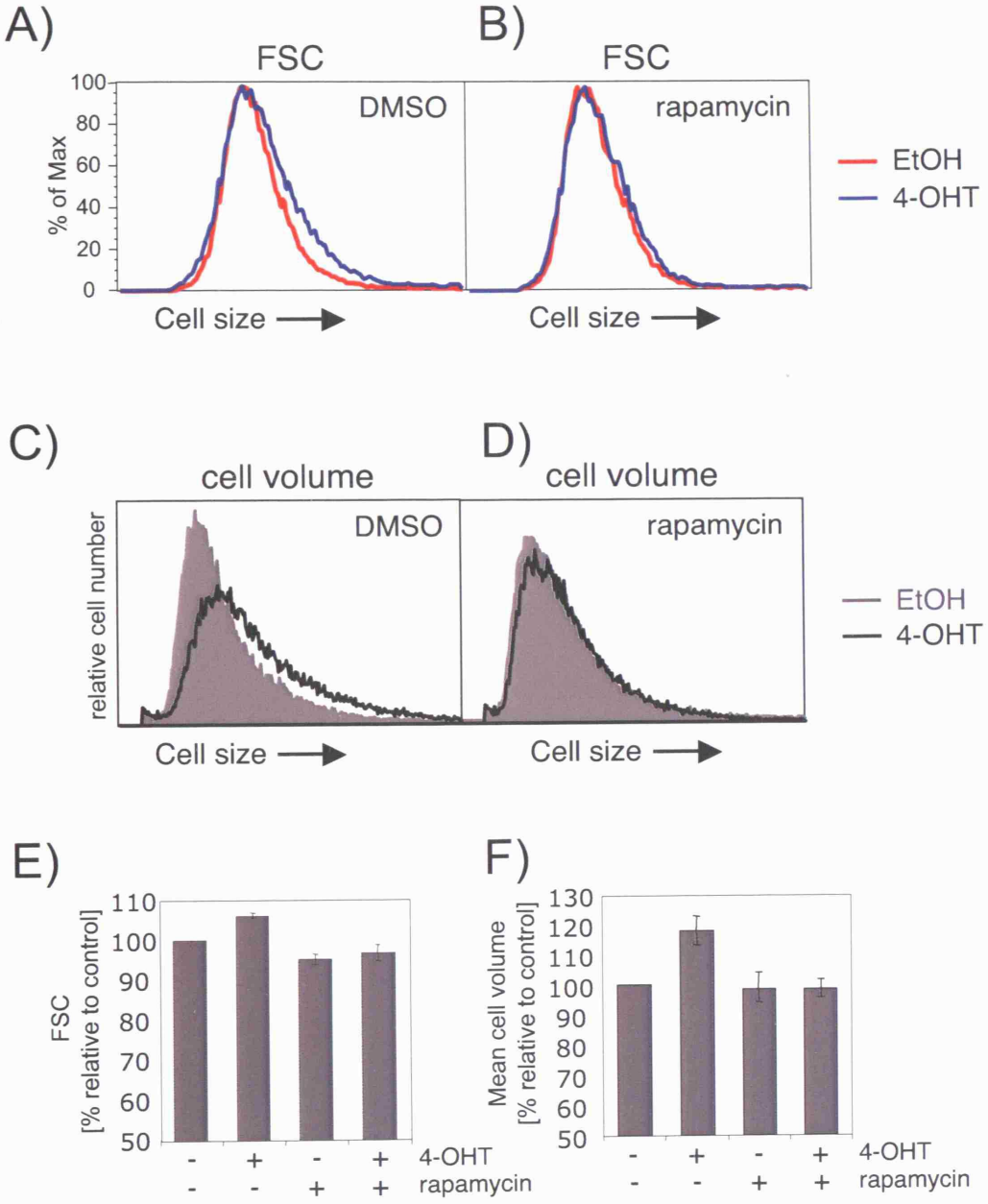
A)
FSC
DMSO
% of Max
100
80
60
40
20
0
Cell size
B)
FSC
rapamycin
Cell size
EtOH
4-OHT
C)
cell volume
DMSO
relative cell number
Cell size
D)
cell volume
rapamycin
Cell size
EtOH
4-OHT
E)
FSC
[% relative to control]
110
100
90
80
70
60
50
- + - +
4-OHT
- - + +
rapamycin
F)
Mean cell volume
[% relative to control]
130
120
110
100
90
80
70
60
50
- + - +
4-OHT
- - + +
rapamycin

Figure 5-6 Activation of mature SREBP1a induces increase in cell size

(A) The mature SREBP-ER fusion protein contains the N-terminal half of the protein (aa 1-490 for SREBP1a and aa 1-468 for SREBP2) fused to the hormone binding domain of a mutant estrogen receptor (ER) that selectively binds 4-hydroxytamoxifen (4-OHT). **(B)** RPE mSREBP-ER cells were stimulated with 100nM 4-OHT for 24 hours in 1% LPDS, total cell lysates were prepared and analysed for SREBP target gene expression (FAS and ACL). **(C-F)** RPE mSREBP-ER cells were stimulated with 100 nM 4-OHT (blue or black lines) or solvent (red or grey lines) in the presence or absence of 50 nM rapamycin as indicated for 24 hours in 1% LPDS. Cell size was assessed by measuring forward scatter (FSC) by FACS **(C)** or measuring electronic cell volume (Coulter Counter) **(D)**. One out of at least four similar experiments is shown. Represented FACS data are done in single samples **(E)**. Coulter data represent the mean cell volume (MCV) and error bars represent the range of duplicate samples **(F)**. Experiments were performed by Beatrice Griffiths (GEA, CRUK-LRI).

Figure 5-6

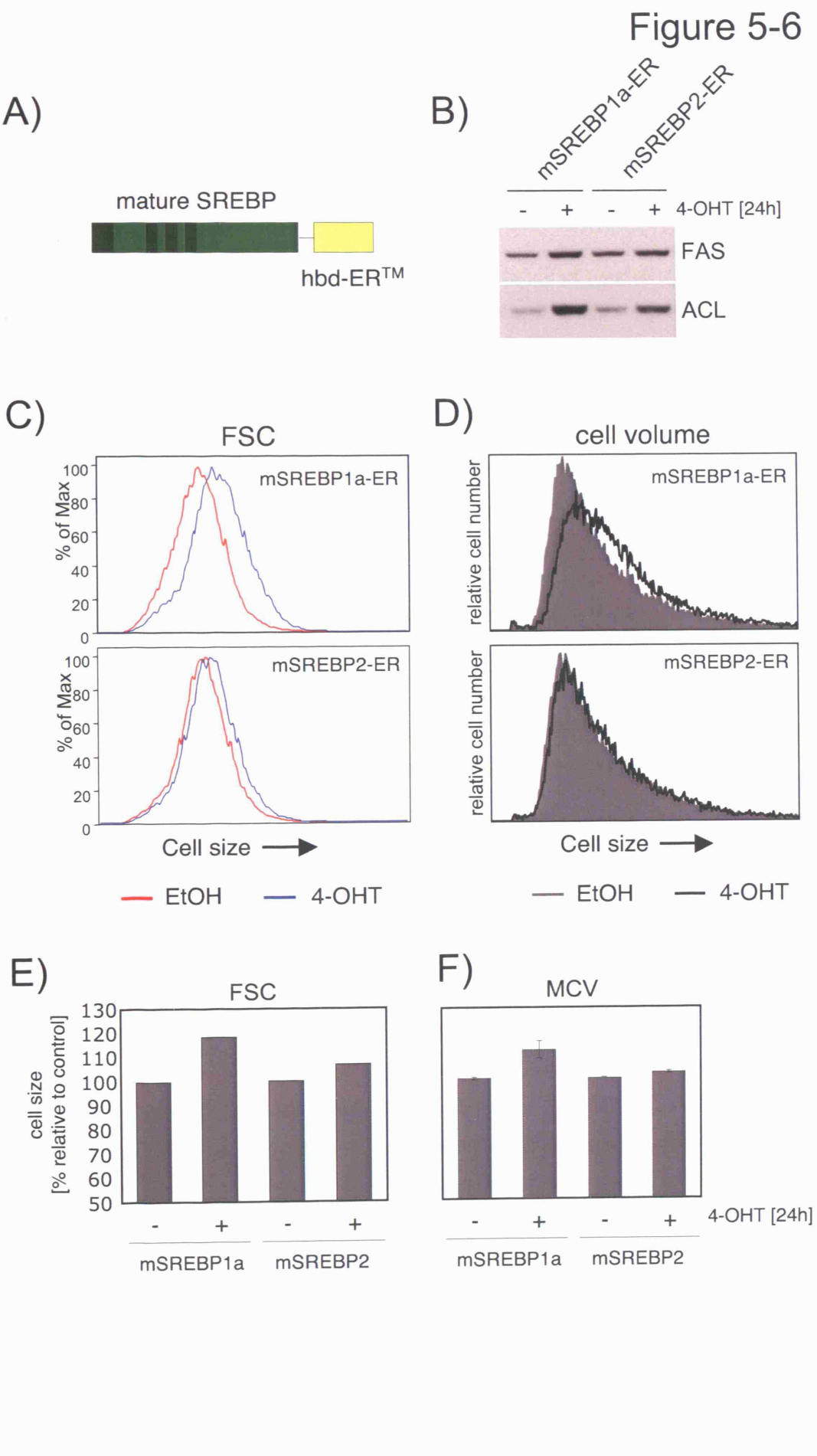
A)
mature SREBP
hbd-ER™
B)
mSREBP1a-ER
mSREBP2-ER
- + - + 4-OHT [24h]
FAS
ACL
C)
FSC
mSREBP1a-ER
mSREBP2-ER
% of Max
100
80
60
40
20
0
Cell size
EtOH
4-OHT
D)
cell volume
mSREBP1a-ER
mSREBP2-ER
relative cell number
Cell size
EtOH
4-OHT
E)
FSC
cell size
[% relative to control]
130
120
110
100
90
80
70
60
50
- + - +
mSREBP1a
mSREBP2
F)
MCV
- + - + 4-OHT [24h]
mSREBP1a
mSREBP2

6 Chapter 6: dSREBP involvement in regulation of organ and cell size control in *Drosophila melanogaster*

6.1 Introduction

The previous chapters of this thesis described the identification of regulation of SREBP by the PI3K/Akt/mTOR pathway and its contribution to cell growth in human cell lines. Activation of Akt resulted in an accumulation of saturated and unsaturated fatty acids and phosphoglycerides, which are involved in the biosynthesis of biological membranes and could contribute to an increase in cell size. The PI3K/Akt pathway has been implicated in cell growth in mammalian cells (Kozma and Thomas, 2002) and regulation of cell and organ size in *Drosophila melanogaster* (Leevers and McNeill, 2005). To investigate the contribution of SREBP in cell size regulation *in vivo*, the fruit fly *Drosophila melanogaster,* was used.

At the larval stages, growth occurs mainly within endoreplicating tissue, like the gut, fat body and salivary glands. These tissues provide energy and metabolites for metamorphosis. Other tissues contributing to growth include mitotic tissues of the larval imaginal discs. *Drosophila* imaginal discs are epithelial monolayer sacs that reorganise during metamorphosis to give rise to adult epidermal structures such as eyes, wings and legs (Cohen et al., 1993).

The contribution of insulin/insulin-like growth factor signalling (IIS) towards cell growth has been studied intensively in *Drosophila melanogaster*. Most components of the IIS signalling pathway are well conserved between *Drosophila* and vertebrates. For instance, the IIS controls glucose uptake and nutrient storage as well as cell and body size in both flies and mice (Edgar, 2006). It has also been shown that many IIS components are regulating cell and organ size in a cell autonomous manner. The *Drosophila* phosphoinositide 3-kinase, Dp110, promotes cell and organ growth (Leevers et al., 1996) and the *Drosophila* tumour suppressor PTEN antagonizes the Chico/PI3-kinase signalling dependent cell growth effect (Bohni et al., 1999; Goberdhan et al., 1999). The dTOR pathway is also an important growth regulator in flies (Oldham et al., 2000; Stocker et al., 2003; Zhang et al., 2000). dTOR can be activated by the IIS but more importantly responds to cellular levels of nutrients (amino acids) and energy that collectively determine the size of the cell (Oldham and Hafen, 2003; Wullschleger et al., 2006). Mutations in *TSC1* and *TSC2* result in strong overgrowth of the eye (Gao and Pan, 2001; Potter et al., 2001; Tapon et al., 2001) and Rheb contributes to enhanced growth by activating dTOR-dS6K signalling (Patel et al., 2003; Stocker et al., 2003). Although is has been shown that dAkt

phosphorylates dTSC2 (Potter et al., 2002), it is not clear whether this phosphorylation is essential for dTOR activity during fly development (Dong and Pan, 2004). In addition, insulin-mediated activation of dS6K *in vitro* occurs via dPI3K/dAkt (Lizcano et al., 2003). There is no *in vivo* genetic evidence for a linear pathway resulting in activation of dS6K downstream of dPI3K. However, dPDK1 is required for dS6K activity *in vivo* (Radimerski et al., 2002b).

The genome of *Drosophila melanogaster* encodes a single SREBP homolog, dSREBP (HLH106, or CG8522) (Theopold et al., 1996). This makes dSREBP a suitable target for RNAi mediated silencing and *in vivo* studies. The SREBP processing proteins dS1P, dS2P and dSCAP, but not the negative regulator INSIG, are functionally conserved in flies (Seegmiller et al., 2002). In contrast to mammals, the phospholipid phosphatidylethanolamine rather than cholesterol regulates dSREBP processing (Dobrosotskaya et al., 2002). Furthermore, mutant dSREBP flies are fatty acid auxotroph suggesting that the essential function of SREBP in flies is the maintenance of fatty acid homeostasis (Kunte et al., 2006).

In this chapter, the role of dSREBP in cell size control *in vivo* and *in vitro* will be investigated. Transient silencing of dSREBP in *Drosophila* Kc167 cells leads to reduced cell volume and affects the cell size increase caused by TSC2 silencing. To address dSREBP function *in vivo*, several transgenic fly lines carrying an RNAi construct targeting dSREBP expression were generated and crossed to GAL4 expressing driver lines. Silencing of dSREBP or expression of dominant negative mutants of dSREBP results in developmental delay, increased lethality as well as reduced cell and organ size in flies. Moreover, genetic interaction studies imply that activation of dSREBP by the insulin receptor/PI3K pathway could contribute to cell growth regulation in flies.

6.2 *Silencing of dSREBP reduces cell size in* Drosophila melanogaster Kc167 *cells*

In order to investigate the effect of dSREBP and dFAS on cell size *in vitro*, the haemocyte-derived *Drosophila* cell line Kc167 was transiently transfected with double-stranded RNA (dsRNA) targeting *dSREBP*, *dFAS* and *GFP* in the absence or presence of dTSC2 dsRNA. Cell volume and cell size was measured by Coulter Counter and FACS, respectively. This work was done in collaboration with M. Cully (STL, CRUK-LRI).

Transient silencing of dTSC2 in Kc167 cells results in a significant increase in cell volume (18%) compared to the negative control RNAi (GFP) (Figure 6-1 A). In contrast, treatment with increasing concentrations of dsRNA targeting dSREBP or dFAS caused a 17% or 25%

reduction in cell volume, respectively. Interestingly, knockdown of dTSC2 was not sufficient to rescue the decrease in cell size caused by dSREBP and dFAS dsRNAi (Figure 6-1 A).

In order to rule out the possibility that silencing of dTSC2, dFAS or dSREBP could alter the cell cycle distribution of Kc cells, which could contribute to changes in cell size, cell cycle specific size was determined in Kc cells after silencing of the respective genes. Consistent with data obtained by Coulter Counter, dTSC2 silencing resulted in a significant increase in cell size, while dSREBP and dFAS silencing resulted in an significant decrease in cell size, as determined by forward scatter of the entire population (Figure 6-1 B). Analysis of the cell cycle distribution revealed that dTSC2 silenced cells displayed a small increase in the population of cells in S phase at the expense of those in G1, which is consistent with published data (Figure 6-1 C) (Tapon et al., 2001). The proportion of cells in G2/M remained unchanged. In contrast, dSREBP and dFAS displayed a slight decrease in the population of cells in S phase and an increase in G2/M phase compared to GFP control (Figure 6-1 C). Although small differences in the cell cycle distribution were observed, all cells gated into G1, G2/M and S phase showed the same cell size effect (Figure 6-1 D,E,F). Silencing of dSREBP or dFAS resulted in a decrease in cell size and inhibited the increase in cell size caused by dTSC2 silencing that is detectable during all stages of the cell cycle by FSC (Figure 6-1 D,E,F).

These data indicate that the transient silencing of dSREBP and dFAS causes reduction in cell volume and inhibits cell size increase in response to silenced dTSC2. The observed changes in cell size are not caused by altered cell cycle distribution. These results suggest that dSREBP and dFAS are required for cell size control in *Drosophila* cell culture and also suggest the possibility that dSREBP acts downstream of dTSC2 on cell size control.

6.3 Silencing of dSREBP affects cell and organ size in vivo

Flies have only one SREBP isoform, which makes it an easy target for RNAi mediated knock down for in vivo studies. To address the role of dSREBP in the regulation of cell and organ size *in vivo* several fly lines were generated containing a UAS-RNAi construct targeting dSREBP. Expression of the hairpin RNA molecule was achieved by crossing the flies with GAL4 expression driver strains allowing silencing of dSREBP in specific compartments (GAL4/UAS system) (Lee and Carthew, 2003). The effects of global knockdown and tissue specific silencing of dSREBP on the control of organ and cell size will be discussed in the following subchapters.

6.3.1 Strategy for the generation of the pWIZ-UAST dSREBP RNAi strain

The GAL4/UAS ectopic expression system is a commonly used tool for tissue-specific overexpression *in vivo* (Brand and Perrimon, 1993). This system uses the yeast transcription factor GAL4 and its target sequence, the Upstream Activating Sequence (UAS) element, to which GAL4 binds in order to activate gene transcription. Many fly lines have been generated expressing GAL4 under the control of various *Drosophila melanogaster* promoter sequences. The expression of the transgene is controlled by the presence of the UAS element. Since UAS promoter sequences are not found in *Drosophila melanogaster*, the transgene is maintained in a transcriptionally silent state. To activate transcription, the *UAS-transgenic* flies (responder lines) are mated with *GAL4* fly lines (driver lines). The progeny flies express the responder *UAS-transgene* in the pattern of the driver-dependent tissue specific GAL4 expression (Duffy, 2002).

Lee and Carthew (2003) developed the transgene RNAi vector pWIZ. This vector is derived from pUAST, which contains 5 tandem copies of the UAS element (Brand and Perrimon, 1993). The transgene is cloned as inverted repeats, which are separated by a functional intron of the white gene. When the transgene is expressed, the corresponding inverted repeats will form a long double-stranded 'hairpin' RNA. This dsRNA will be further spliced and cleaved by the Dicer nuclease and results in conditional silencing of gene activity in *Drosophila* in a tissue-specific manner (Bao and Cagan, 2006).

A sequence comprising 700 bp of the 5' end of the *dSREBP* cDNA was inserted as an inverted repeat into the pWiz vector. The *pWIZ-UAST-dSREBP-dsRNA* construct was used to generate transgenic RNAi strains by germline transformation of a *yw* host (Rubin and Spradling, 1982; Ryder et al., 2004). The *UAS-RNAi* construct was microinjected into the posterior end of *yw* embryos. Several independent insertion lines were recovered by screening for red eye males. The red eye phenotype is determined by the presence of the white gene in the construct. In order to map the insertion of the transgene to a specific chromosome, progeny flies were crossed with balancer strains of the 2nd ([w$^-$;SM6a/Cyo]), 3rd ([w$^-$;TM3/TM6]) and X-chromosomes ([w$^-$,FM7/P]). The resulting stocks contain the RNAi cassette on either the 2nd, the 3rd or the X chromosome. Homozygous viable stocks were established, retaining the isogenic *yw* background throughout. By combining an insertion on the 3rd chromosomes with an insertion on the 2nd chromosomes, lines were generated with two independent viable insertions on different chromosomes. This was done with the aim of achieving a stronger RNAi expression. Because the transgene is inserted at random sites, the expression and efficiency of gene silencing

between different strains is subject to variability. Differences in expression levels of the dSREBP^{RNAi} strains correspond to different phenotype strengths.

The dSREBP^{RNAi} strains generated were crossed to the *daugtherless-GAL4* (*da-GAL4*) driver line to assess the strengths of phenotype elicited by each line. Daughterless is a transcription factor involved in many biological processes (referenced to FlyBase) and is expressed ubiquitously from the start of embryonic development onward. The progeny were screened for the appearance of larvae, pupae and flies and distinct defects in wing development. All of the strains containing one insertion (Table 6-1) did not show any lethality or morphological phenotypes. Combinations of insertions in strains 4/18, 7/43 and10/22 showed lethality and displayed defects in wing development. The phenotypes observed might be due to stronger RNAi expression when two transgenes are present. Strains 10/18 and 15/18 apparently gave the strongest phenotype and were embryonic lethal. Larvae could be observed but further development seemed to be impaired as no pupae or flies appeared (Table 6-1). Based on these results, three RNAi strains were selected for further experiments (strain 8 = dSREBP^{RNAi1}, strain 10/22 = dSREBP^{RNAi2} and strain 15/18 = dSREBP^{RNAi3}) because they represent three severities of phenotype observed in response to dSREBP silencing.

6.3.2 Induction of pWIZ-dSREBP^{RNAi} expression using the *da-GAL4* driver results in ablation of dSREBP and dFAS expression

To test the efficiency of *dSREBP* silencing, the three representative fly lines containing either one (dSREBP^{RNAi1}) or two insertions (dSREBP^{RNAi2} and dSREBP^{RNAi3}) were crossed with the ubiquitous *da-GAL4* driver. Total RNA was extracted from second-instar larvae derived from *da-GAL4/UAS-SREBP^{RNAi}* and *da-GAL4/yw* control crosses. The expression levels of *dSREBP* and *dFAS* of silenced and control larvae were measured by q-rtPCR, using primers specific for dSREBP and dFAS (Dobrosotskaya et al., 2002). RNA levels of both genes were profoundly reduced in response to silenced dSREBP compared to the corresponding controls (Figure 6-2). Maternal expression of dSREBP^{RNAi3} reduced levels of endogenous *dSREBP* by over 75% and *dFAS* by 65%. A weaker silencing of *dSREBP* by expression of dSREBP^{RNAi2} led to a reduction in the RNA level of *dSREBP* by 35% and *dFAS* by 45%. Maternal expression of a single insertion (dSREBP^{RNAi1}) reduced *dSREBP* transcript levels by 20% and *dFAS* transcript levels by 5% compared to controls (Figure 6-2). This indicates a dose-dependent silencing of *dSREBP in vivo*, which is also reflected by a reduction in transcript level of the dSREBP target gene dFAS.

6.3.3 Maternal silencing of dSREBP results in developmental delay, reduced body size and body weight

Kunte and colleagues published that deletion of the *dSREBP* gene is lethal and prevents development beyond the second instar larval stage (Kunte et al., 2006). Because lethality precludes further study in the adult fly, the use of RNAi-dependent depletion of dSREBP provides one possibility to investigate dose-dependent phenotypic defects.

In order to further characterize the dSREBP^{RNAi1} and dSREBP^{RNAi2} fly lines, both RNAi strains were crossed with the ubiquitous *da-GAL4* driver. The appearance of larvae, pupae and flies was monitored and counted. At the end all pupae were counted to distinguish between dead and hatched pupae. This experiment was not designed to compare total number of offspring (pupae or flies) between the crosses, since the numbers of eggs or larvae were not determined. Therefore only relative numbers are given and observed pupae/flies were normalised to total number of offspring (flies (+ dead pupae)) in each cross. Weak silencing of dSREBP resulted in a dose-dependent developmental delay compared to *yw* (Figure 6-3 A-C). A 12-hour delay in the appearance of pupae and flies was observed in the dSREBP^{RNAi1} cross (B), while offspring of the dSREBP^{RNAi2} cross displayed a 48-hour delay in pupal appearance and adult eclosion (C). In addition to the developmental delay, a partial lethality was observed at the pupae stage. Figure 6-3 D shows dead pupae and empty pupal cases. 10% of pupae in the dSREBP^{RNAi1} cross and 22% of pupae in the dSREBP^{RNAi2} cross died before eclosion compared to 0% in the *yw* control cross (Figure 6-3 A-C). Half of the dSREBP^{RNAi2} female progeny displayed a very severe wing phenotype (Figure 6-3 E). Furthermore, adults of the dSREBP^{RNAi2} cross showed a very pronounced reduction in body size (Figure 6-3 F). Interestingly, the average body weight was reduced for both RNAi lines crossed with *da-GAL4*, by 20% or 29% in dSREBP^{RNAi1} or dSREBP^{RNAi2}, respectively (Figure 6-3 G). However, body weight measurement was done only once and could comprise impreciseness and error bars can't be generated. In addition, analysis of wing size showed a statistically significant reduction in wing area, by 6% or 11% in dSREBP^{RNAi1} or dSREBP^{RNAi2}, respectively (Figure 6-3 H).

Taken together, these results indicate that dSREBP is required during fly development (Table 6-1, (Kunte et al., 2006)). Weak silencing of dSREBP results in a dose-dependent developmental delay, reduced body weight and body size as well as reduced wing size, suggesting that dSREBP is essential for normal growth during *Drosophila* development.

6.3.4 dSREBP regulates organ size and cell size in the wing

The adult wing consists of two layers of ectodermal cells (dorsal and ventral) divided into sections by 5 longitudinal veins (L1 to L5). During wing development, the wing imaginal disc is a monolayer of epithelium (also described as a sac), of which the central region (the pouch) will develop into the wing blade. The wing disc is divided by anterior/posterior (A/P) and dorsal/ventral (D/V) compartment boundaries. The cell population of the posterior compartment expresses the transcription factor *engrailed*. Immediately anterior to the A/P boundary of the wing disc expression of *Decapentaplegic* (*Dpp*) is induced (Crozatier et al., 2004). The *MS1096* driver is expressed at high levels near uniformly in the wing-pouch region, but more strongly in the dorsal compartment (Capdevila and Guerrero, 1994).

6.3.4.1 Silencing of dSREBP results in reduces organ size and reduced cell size in the wing

The effect of depleted dSREBP function on overall body and organ size could be due to a non-autonomous role of dSREBP in humoral growth regulation or to an autonomous role in a tissue and cell type specific manner. To test whether depletion of dSREBP affects the size of organs autonomously, several wing specific GAL4 driver lines were used to express the $SREBP^{RNAi}$ transcript.

Silencing of dSREBP in different regions of the wing imaginal disc resulted in significant size reduction of the corresponding regions of the adult wing blade. Expression of the $SREBP^{RNAi}$ under the control of the *GAL4* driver line *MS1096,* where *GAL4* is highly expressed in the dorsal surface of the wing blade, resulted in wings that were smaller than controls (Figure 6-4 A-D). In addition, a characteristic upward curvature could be observed. Analysis of wing size showed a statistically significant reduction of 7% for $dSREBP^{RNAi1}$ (B), 12% for $dSREBP^{RNAi2}$ and of 19% for $dSREBP^{RNAi3}$ (C) wings compared to *yw* (A) wings (Figure 6-4 E). This reflects a dose dependent effect of dSREBP silencing on wing size.

Similarly, when dSREBP RNAi expression was induced along, and immediately anterior to, the A/P boundary of the wing disc by using the driver line *Dpp-GAL4*, the corresponding region of the adult wing was contracted (visualized by measuring the distance between longitudinal veins III and VI, Figure 6-5 A). Analysis of the respective wing area showed a statistically significant reduction of 7% for $dSREBP^{RNAi3}$ and of 5% for $dSREBP^{RNAi2}$ in compartment size compared to *yw* control (Figure 6-5 B), however in the $dSREBP^{RNAi1}$ cross no size effect was observed. *Dpp* is a very weak driver; therefore silencing of dSREBP could be weaker and the effect on wing size less pronounced compared to the strong *MS1096* driver.

To further examine the effect of dSREBP silencing on wing growth, dSREBP^{RNAi} was expressed in the posterior half of the wing, using the driver line *engrailed-GAL4* (*en-GAL4*). Quantitative analysis revealed that silencing of *dSREBP* resulted in a profound reduction in size of the posterior region of the wing, whereas the anterior region of the adult wing blade was not affected (Figure 6-6 E). Strong silencing of dSREBP (dSREBP^{RNAi3} D) led to a decrease in size of the posterior part by 16% and intermediate silencing (dSREBP^{RNAi2} C) showed an 8% reduction in size compared to *yw* (A) control (Figure 6-6 A-D). The measured decrease in the posterior compartment of wings expressing dSREBP^{RNAi1} (B) was not statistically significant. Consistent with Figure 6-4, the observed reduction in wing size is dose-dependent. Taken together, these data indicate that dSREBP is involved in organ size control.

The observed differences in wing size could be due to alterations in either cell size or cell number. Each cell in the adult wing secretes a single hair and the number of cells can be inferred from the number of hairs. As shown in Figure 6-6, silencing of dSREBP in the posterior compartment of the wing reduced its size. The number of hairs in a small area of fixed size and location in the posterior compartment of the wing was counted and compared with a quadrant of identical size in the anterior compartment of the same wing. In addition, wing cell number in the posterior compartment of flies from a control cross (GFP) was analysed (Figure 6-7 A). The cell number in the posterior compartment of SREBP^{RNAi3} wings was 22% higher than in the respective compartment of GFP control wings (Figure 6-7 B). Table 6-2 shows that cell density in the posterior part is 14% higher than in control GFP wing. This indicates a 1.13-fold reduction in cell size with no change in cell number. The reduction in cell size reduced the total area of the posterior region by approximately 13% (Table 6-2). Therefore the reduction in compartment size was caused by a decrease in cell size rather than cell number. These data are an indication but not a proof for cell autonomous cell size control by dSREBP and that final cell size may depend on dSREBP function in each individual cell.

6.3.5 Ectopic expression of dSREBP constructs *in vivo* affects fly development and organ size

Ectopic expression results in the expression of a protein at different levels, in different tissues, as well as at different stages of development from the endogenous protein. In addition to using the wild-type protein, mutated or truncated forms of the protein that are either constitutively activated (dominant active) or interfere with the function of the endogenous protein (dominant negative) can be ectopically expressed to investigate the role of the endogenous protein.

6.3.5.1 *UAS-dSREBP* lines

In order to investigate whether the observed organ and cell size dependency on dSREBP function can be reproduced by an independent approach, several *UAS-dSREBP* lines available from the Bloomington Stock Center (BSC) were examined for their effect on wing size. The lines used will be described briefly.

Stocks 8236 and 8237 contain a full-length dSREBP (wt-dSREBP) construct either inserted on the 3rd or X-chromosome, respectively. Stocks 3238 – 8242 contain two different dominant-negative dSREBP constructs (DN-dSREBP). The DN-dSREBP sequences encode for a dominant negative protein variant where the highly acidic transcription activation domain is deleted (DN75: Δ amino acid 1-75). Stocks 8241 and 8242 lack the N-terminus and the transmembrane spanning domains (DN75T). dSREBP binds as a dimer onto their target promoters. Deletion of the transactivation domain ablates the transcriptional activation of SREBP target genes, but allows dimerisation, thus inducing a dominant negative effect (Sato et al., 1994). A mature dSREBP protein variant, truncated before the first transmembrane domain, was inserted on the X- or 2nd chromosome to generate stocks 8243 and 8244, respectively. It is reported by the BSC that this protein is constitutively localized to the nucleus and is constitutively transcriptionally active (CA-dSREBP).

6.3.5.2 Ectopic expression of dominant negative dSREBP reduces organ size

The DN-dSREBP constructs were expressed from the *UAS* transgenes under the control of the *GAL4* driver line *MS1096*. Flies expressing dominant negative dSREBP in the dorsal compartment display an upward bending of the wing due to a decrease in cell size in the dorsal layer. To illustrate the phenotype, pictures of representative male and female flies were taken from DN-dSREBP^{8240} and *yw* control (Figure 6-8 A/B). Quantification of female and male wing size revealed that expression of DN-SREBPs resulted in a 10-50% decrease in wing area. DN-SREBP^{8238} and DN-SREBP^{8242} are located on the x-chromosome, therefore only the female offspring express the transgene and the driver together (Figure 6-8 C/D).

Furthermore, when selective DN-SREBP constructs (stocks 8239, 8240, 8241) were expressed throughout the posterior compartment of the wing using an *en-GAL4* driver, all animals showed smaller wings compared to *yw*. Quantification of wing size revealed a relatively moderate 4-7% reduction in whole wing size, which is caused by 6-9% reduction in the posterior compartment in relation to *yw* controls (Figure 6-8 E). The size of the anterior compartments was not affected. DN-dSREBP^{8240} showed the strongest phenotype, with an 11% difference between the anterior and posterior compartments normalised to *yw*.

However, in comparison with the obtained MS1096 data (Figure 6-8), where expression of the dominant negative construct 8240 led to a 50% reduction in wing size, the measured changes in wing size of the *en-GAL4* crosses are much smaller. *En-GAL4* is weaker expressed than *MS1096-GAL4*, which results in reduced expression of the dominant negative dSREBP constructs in *En-GAL4* crosses. This indicates that repression of dSREBP transcriptional activity by dominant negative proteins is dose dependent. To fully block endogenous dSREBP activity a certain amount of dominant-negative protein has to be present. *MS1096*, a very strong driver, leads to a high concentration of DN-dSREBP, which could saturate endogenous dSRBP and block transcription of its target genes. Expression of DN-dSREBP driven by *engrailed* might not generate a sufficient concentration of exogenous DN-dSREBP to saturate all endogenous dSREBP, and therefore dSREBP target gene expression might be reduced but not blocked.

6.3.5.3 Ectopic expression of wild type and constitutively active dSREBP results in severely reduced wing area

The full-length and mature dSREBP constructs were expressed from the *UAS* transgenes under the control of the *GAL4* driver line *MS1096*. Expression of wt- and CA-SREBP inserted on the 3rd and 2nd chromosome caused no wing phenotype and size analysis did not show an altered size in wing area compared to *yw* (data not shown), while flies expressing wt- or CA-dSREBP inserted on the x-chromosome resulted in a severely reduced wing area (Figure 6-9 A/B). Therefore it was not possible to mount them for size analysis. However the wing phenotypes suggest that the constructs are expressed in a dose-activity dependent manner. Flies expressing full-length dSREBP developed very small concave shrivelled wings (A) and expression of mature dSREBP led to an even more severe wing phenotype (strongly misshapen, B). It has been reported that nuclear mSREBP1a could inhibit cell growth by activating expression of the cyclin-dependent kinase inhibitor p21$^{WAF1/CIP1}$ (Inoue et al., 2005). Therefore overexpression of full-length or constitutively active mature dSREBP could result in growth arrest in the wing. This indicates that correct dSREBP expression is important for organogenesis.

6.3.5.4 Ectopic expression of *UAS-dSREBP* affects fly development

In order to address the question whether an altered activity of the dSREBP pathway could affect fly development, selected UAS-dSREBP lines were crossed with *da-GAL4* flies. As the wt-dSREBP and CA-dSREBP constructs are inserted on the x-chromosome, only the female offspring will express the transgene. The female offspring of the wt-dSREBP cross exhibited

severely underdeveloped wings, although the phenotype varied between individuals (Figure 6-10 A). In addition, female flies of this cross eclosed approximately two days later than the male offspring. Male flies hatched at the normal time compared to *yw* control. The female/male ratio of the wt-dSREBP offspring was reduced by 2.5 fold. Furthermore, expression of the constitutively active mature dSREBP led to approximately the same number of male flies in the offspring compared to *yw*, however no female flies were present in the progeny (Figure 6-10 B).

The observed lethality in the female offspring is activity dependent; females expressing full-length dSREBP hatched, although delayed and in a greatly reduced number, and displayed a severe wing phenotype. Expression of mature dSREBP is 100% lethal. These results are consistent with data shown in Figure 6-9 A/B, which shows a dose-activity dependent wing phenotype. The observed lethality can be explained by the possibility that SREBP activates the cyclin/cdk inhibitor p21, leading inhibition of cell growth (Inoue et al., 2005). Consistent with the observation that flies lacking dSREBP die during larvae development ((Table 6-1) (Kunte et al., 2006)), expression of a dominant negative form of dSREBP (DN-SREBP^{8239}) led to a 5-fold reduction in the number of female and male offspring compared to *yw* (Figure 6-10 B). This implies that dSREBP is required for fly development.

These data confirm the results obtained with the SREBP^{RNAi} lines and underline the importance of dSREBP in organ size control and whole organism development. Both a reduction of dSREBP activity (dSREBP^{RNAi}) or deregulation of dSREBP (CA-dSREBP) is fatal. Cells might sense the abundance of nuclear SREBP and altered SREBP levels result in growth arrest or apoptosis, and subsequent lethality. This supports the notion that a tight regulation of the dSREBP pathway is important for cell growth during fly development.

6.4 Regulation of dSREBP by the PI3K pathway

Increased activity of insulin signalling has been shown to promote growth in *Drosophila* (Edgar, 2006; Leevers and Hafen, 2004). Manipulations that alter the activity of components of the insulin signalling pathway result in a dramatic change in cell size in an cell-autonomous manner (Goberdhan et al., 1999, Verdu, 1999 #801; Leevers et al., 1996). In order to investigate whether the dPI3K/dAkt pathway regulates dSREBP, two approaches were chosen. Firstly, the *Drosophila* cell line Kc167 was used to evaluate the signalling connection *in vitro*. Secondly *in vivo*, co-expression of dPI3K together with dSREBP transgenes in the wing was analysed for synergistic phenotype effects.

6.4.1 Modulation of the PI3K/Akt pathway by RNAi regulates expression of dSREBP and dFAS in Kc 167 cells

Figure 6-1 showed that silencing of dTSC2 was not sufficient to block the dSREBP and dFAS RNAi dependent decrease in cell size. This might already indicate that dSREBP act downstream of TSC2 in controlling cell size. To verify this observation on the signalling and expression level, components of the dPI3K/dAkt pathway were targeted by RNAi and expression levels of dSREBP and dFAS were examined by q-rtPCR (experiments were carried out in collaboration with M. Cully, STL, CRUK-LRI).

Kc167 cells were treated with dsRNA targeting Dp110, dAkt, dPTEN, dSREBP, dFAS or green flourscent protein (GFP, control) for 72 hours. Total mRNA was extracted and expression of dSREBP and dFAS was quantified. Figure 6-11 shows that depletion of dSREBP and dFAS resulted in selective reduction in expression of the respective transcript; ablation of dSREBP expression also led to decreased activation of its target gene dFAS. Silencing of Dp110, the catalytic subunit of dPI3K, or dAkt was sufficient to significantly reduce dSREBP and dFAS mRNA levels. In contrast, treatment with dPTEN dsRNA, the negative regulator of dAkt and dPDK1 activity, led to an increase in expression of dFAS and dSREBP mRNA (Figure 6-11). However, the dFAS transcript levels do not follow the dSREBP profile for every dsRNA treatment, presumably due the possibility that additional transcriptional effectors regulate expression of FAS independently of SREBP. Furthermore, silencing of Dp110 reduced dFAS expression to a greater extent than dAkt silencing. This indicates that activation of a pathway parallel to Akt by PI3K could contribute to SREBP activity (Taniguchi et al., 2006).

To summarize, these results show that inhibition of the dPI3K/dAkt pathway leads to a downregulation of dSREBP and dFAS expression. In contrast, activation of the dPI3K/dAkt pathway results in an increase of dSREBP and dFAS expression. This points towards the possibility that in *Drosophila* Kc167 cells, like in human cell lines, dSREBP activity is regulated via the PI3K/Akt pathway.

6.4.2 Ectopic expression of Dp110 increases dSREBP and dFAS expression *in vivo*

The data shown above imply that dPI3K is required to activate dSREBP. This finding could be unique to Kc167 cells. To assess this possibility, the capacity of the *Drosophila* PI3K to modify dSREBP activity was analysed *in vivo*.

Overexpression of the PI3K catalytic subunit (Dp110WT) under the control of the *MS1096-GAL4* driver resulted in a 20% increase in wing size, while overexpression of a kinase-dead Dp110 construct (Dp110[KD]) led to a dramatic decrease in wing size by more than 2 fold (Figure 6-12 A). These findings are consistent with published data (Leevers et al., 1996; Weinkove et al., 1999).

Expression of dSREBP and dFAS was monitored in second instar larvae overexpressing Dp110WT using the ubiquitous *da-GAL4* driver. Larvae were homogenised and mRNA was extracted. The resulting cDNAs were analysed for abundance of dSREBP and dFAS transcripts by q-rtPCR. Ectopic expression of the *Drosophila* Dp110WT results in a 2-fold induction of transcription of dSREBP and dFAS (Figure 6-12 B). Taken together, activation of the PI3K pathway induces expression of dSREBP and dFAS *in vitro* and *in vivo*.

6.4.3 Silencing of dSREBP in a Dp110[KD] background does not further increase the reduction in wing area

In the wing, *dpp-GAL4* driven $SREBP^{RNAi3}$ expression caused a statistically significant but very small decrease in compartment size (Figure 6-13 A/B and E). Constitutive expression of a dominant negative Dp110 construct (Dp110[KD]) led to a dramatic reduction in compartment size by more than 30% compared to *dpp-GAL4* (Figure 6-13 A/C and E). Co-expression of $dSREBP^{RNAi3}$ in a *Dp110[KD]* background caused no further decrease in wing area (Figure 6-13 C/D and E).

To validate these results in another system, the *UAS-*$dSREBP^{RNAi2}$ and *UAS-*$dSREBP^{RNAi3}$ flies were crossed to *en-GAL4* at 25°C or an *en-GAL4* line that constitutively expresses Dp110[KD] (*en-GALA4 UAS-Dp110[KD]*) at 18°C. Consistent with previous data, silencing of dSREBP led to a significant decrease in the size of the posterior compartment of the wing of approximately 7% in the $dSREBP^{RNAi2}$ cross and 12% in the $dSREBP^{RNAi3}$ cross compared to the en-GAL4/*yw* cross (Figure 6-14 A/B and E). Constitutive expression a Dp110[KD] in the posterior compartment of the wings led to considerably smaller compartment size compared to the posterior area of the *en-GAL4* control flies (Figure 6-14 A/C). Size analysis of the wing revealed an approximately 30% decrease in posterior compartment, whereas the anterior compartment was not affected (data not shown). Constitutive expression of *Dp110[KD]* in a dSREBP-silenced background (*dSREBP*^{RNAi2} or *dSREBP*^{RNAi3}) did not further increase the reduction in size of the posterior compartment (Figure 6-14 C/D and F).

These results show that silencing of dSREBP does not enhance the reduction in wing size caused by ectopic expression of *Dp110[KD]*. This supports the hypothesis that dSREBP acts downstream of dPI3K *in vivo*.

6.4.4 Genetic interaction between dSREBP and Dp110

The next question investigated was whether silencing of dSREBP could antagonize the increase in wing size caused by overexpression of wild-type *Dp110* (Dp110WT). Constitutive expression of *Dp110WT* under the control of the wing-specific *MS1096-GAL4* driver led to an increase in wing area by nearly 20% compared to *yw* (Figure 6-15). Expression of $dSREBP^{RNAi2}$ and $dSREBP^{RNAi3}$ alone showed a 10% and 15% reduction in wing area, respectively. The Dp110WT-induced 1.17-fold increase in wing size was significantly reduced to 1.08-fold in the $dSREBP^{RNAi2}$ crosses and to 1.10-fold in the $dSREBP^{RNAi3}$ crosses (Figure 6-15). However, expression of *Dp110WT* in a dSREBP-silenced background still leads to a 7-10% increase in wing size. This partial rescue of the large *PI3K* overexpressing wing by $dSREBP^{RNAi2}$ can be explained by the fact that the PI3K targets Akt and TOR regulate several proteins implicated in organ growth.

Taken together, silencing of dSREBP significantly reduces the increase in wing size in response to Dp110WT expression. These data indicate an essential role for dSREBP in the regulation of organ size by the PI3K pathway in flies.

To determine a genetic interaction, wing phenotypes of flies expressing *Dp110WT*, *wt-dSREBP* and *CA-dSREBP* alone or together were monitored (Figure 6-16). *MS1096-GAL4* driven *wt-dSREBP* expression at 25°C caused a very misshaped wing phenotype; therefore the offspring were reared at 18°C to weaken transgene expression. Constitutive expression of *Dp110WT* caused a slight downward bending of the wing. Ectopic expression of the *wt-dSREBP* construct led to a strong concave wing phenotype. Co-expression of *Dp110WT* together with *wt-dSREBP* strongly enhanced the wing phenotype achieved by expression of these constructs alone. Interestingly, expression of mature dSREBP (CA-dSREBP) in the wing results in the same phenotype as co-expression of full-length dSREBP (wt-dSREBP) together with PI3K (Dp110WT). Co-expression of *CA-dSREBP* together with *Dp110WT* resulted in lethality (Figure 6-16).

These data support the hypothesis that processing of dSREBP requires activity of the dPI3K pathway. Overexpression of *Dp110WT* causes enhanced dAkt and dTOR activity, both may be required to process full-length dSREBP into mature dSREBP.

6.5 Discussion

In order to investigate the contribution of SREBP to cell growth and cell proliferation in *D.melanogaster* an *in vivo* RNA interference strategy was used. Several dSREBP-RNAi strains were generated containing the RNAi cassette on the 2nd or the 3rd chromosomes including single or double insertions. These strains exhibit different levels of silencing resulting in phenotypes of varying strength (Table 6-1). Flies mutant for *dSREBP* are not viable (Kunte et al., 2006). The dSREBP-RNAi lines are suitable tools to investigate dose-dependent phenotypic effects. Maternal silencing of dSREBP in the whole fly resulted in a dose-dependent developmental delay, increased lethality, reduced body weight and body size (Figure 6-3). Silencing of dSREBP in the developing wing resulted in decreased wing size (Figure 6-4), and cells expressing $dSREBP^{RNAi}$ were smaller than wild type cells (Table 6-2).

To confirm these results and to exclude off-target effects associated with long dsRNA, a second dSREBP RNAi sequence could be used. The RNAi cassette generated targets the first 700 amino acids. RNAi evaluation using E-RNAi (DKFZ, Germany; (Kulkarni et al., 2006)) revealed a second gene that may be targeted for silencing, CG11505. The molecular function of CG11505 is not known (Flybase database). These experiments could be repeated using the dSREBP-RNAi strain targeting the C-terminus (ID4360; VDRC), which was generated by the Dickson laboratory (IMP, Austria) and is now being used by the Vienna Drosophila RNAi Center (VDRC, Austria).

To verify the results obtained with the RNAi strains by an independent method, transgenic fly strains expressing dominant-negative dSREBP constructs were used. These constructs are similar to a dominant negative construct of mammalian SREBP that has been shown to be functional in blocking SREBP target gene expression in tissue culture (Sato et al., 1994). Maternal expression of DN-dSREBPs resulted in severe developmental defects (Figure 6-10). *MS1096-GAL4* driven expression of *DN-dSREBP* showed the same effect on wing size observed with dSREBP RNAi strains (Figure 6-8). Whilst silencing of dSREBP resulted in an approximately 20% decrease in wing size, overexpression of $DN\text{-}SREBP^{\delta 240}$ caused up to 50% reduction. The difference between the results obtained with the RNAi and dominant-negative dSREBP strains is most likely to be due to formation of heterodimers between dominant-negative proteins and endogenous dSREBP.

Inhibition of dSREBP activity by silencing or expression of dominant negative mutants of dSREBP reduces cell and organ size. The anticipated opposite result was that flies expressing

either full-length or mature dSREBP would develop bigger wings. However, *MS1096-GAL4* driven expression of wt- or CA-dSREBP resulted in very severe wing phenotypes (Figure 6-9). The observed wing phenotypes can be explained by published findings showing that overexpression of mSREBP1a causes a growth arrest most likely via activation of the cyclin kinase inhibitor p21 (Inoue et al., 2005). Another possibility would be that expression of the wt- or CA-dSREBP construct causes a dramatic overgrowth. This shows that activity of dSREBP has to be tightly regulated to allow proper development of the wing structure.

To determine whether the link between the PI3K/Akt pathway and SREBP identified by the results shown in previous chapters is conserved in flies, several approaches were applied. Ubiquitous expression of a *Dp110WT* driven by the *da-GAL4* resulted in an up-regulation of dSREBP and dFAS expression (Figure 6-12). This is consistent with *in vitro* data. Silencing of Dp110 and dAkt in Kc167 cells resulted in down-regulation of dSREBP and dFAS expression. dPTEN depletion provides an independent means to elevate PIP3 levels and increase Akt activity, leading to increased dSREBP and dFAS expression levels (Figure 6-11). In addition, expression of kinase dead Dp110 caused a decrease in wing size that could not be further enhanced by co-expression of $dSREBP^{RNAi}$ (Figure 6-13). In contrast, the increase in wing size caused by overexpression of Dp110 was reduced when dSREBP was silenced (Figure 6-15). This could indicate dSREBP as a key effector of dPI3K-driven growth. Furthermore, co-expression of the full-length dSREBP and the dPI3K catalytic subunit Dp110 resulted in the same wing phenotype as that caused by overexpression of mature dSREBP (Figure 6-16). These data indicate that PI3K signalling could activate dSREBP.

Having shown that rapamycin treatment blocks the Akt-dependent accumulation of mature SREBP in the nucleus (Figure 4-6), it is of interest to analyse whether activation of SREBP might be regulated by the TOR pathway in *Drosophila*. In support of this hypothesis, d*TSC2* knockdown was not sufficient to overcome the decrease in cell size caused by silencing of dSREBP and dFAS. This suggests that dSREBP could act downstream of dTSC in Kc167 cells. This hypothesis could be directly tested *in vivo*. *GMR-GAL4* driven expression of Rheb causes overgrowth of the eye (Stocker et al., 2003). The eye consists of photoreceptor cells, which contain large stacks of membrane, making it an interesting organ to study dSREBP activity. Having shown that dSREBP depletion affects cell size rather than cell number (Table 6-2), it seems likely that the dAkt pathway involving dS6K regulates the contribution of dSREBP to organ size. This would exclude regulation of dSREBP by dFoxO, which controls cell number (Junger et al., 2003).

Taken together, data described in this chapter provide evidence that dSREBP plays a very important role in cell and organ growth control during fly development. *In vitro* and *in vivo* data suggest that dSREBP could be an effector of dPI3K/dAkt and dRheb/dTOR driven-growth.

Figure 6-1 Silencing of dSREBP and dFAS reduces cell size in *Drosophila* Kc167 cells

(A) Kc167 cells were treated with dsRNA corresponding to GFP (control), dSREBP or dFAS in the absence or presence of dTSC2 dsRNA for 5 days. The cells were analysed for cell volume using a Z2 Coulter Counter. **(B-F)** Kc167 cells were treated with dsRNA as described in (A). Cells were collected by centrifugation, fixed by vortexing and incubated in cold 70% ethanol at 4˚C for at least 30 mins, then washed twice in PBSA and resuspended in 500 μl of 20 μg/ml RNaseA and 40 μg/ml propidium iodide in PBSA. Propidium iodide-stained cells were analysed on a FACScalibur flow cytometer for cell size (FSC) and cell cycle distribution (C). Data are the mean of three experiments $\pm$ SEM. Experiments were performed in collaboration with Megan Cully (STL, CRUK-LRI).

Figure 6-1

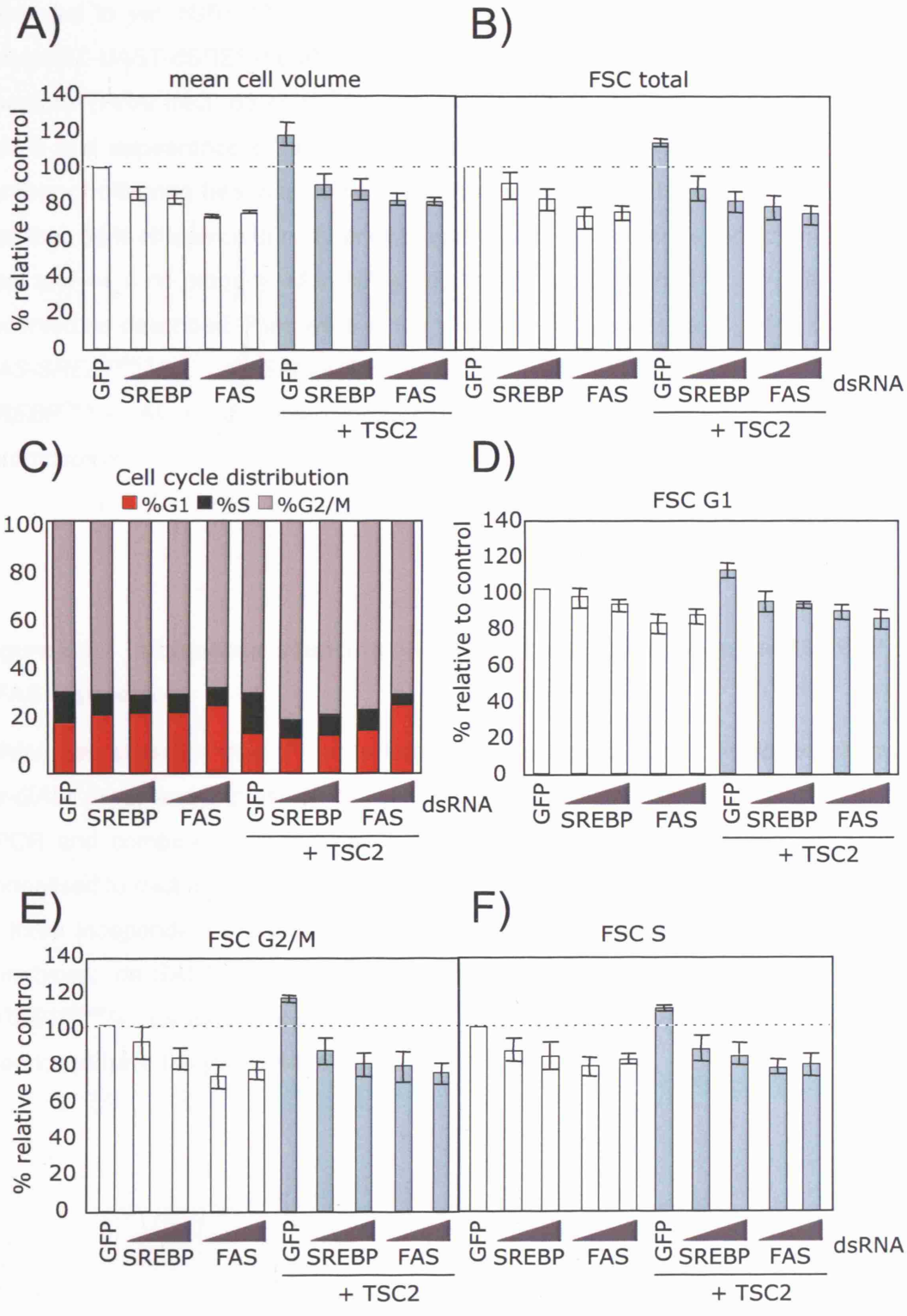
A)
mean cell volume
% relative to control
140
120
100
80
60
40
20
0
GFP
SREBP
FAS
GFP
SREBP
FAS
+ TSC2
B)
FSC total
GFP
SREBP
FAS
GFP
SREBP
FAS
+ TSC2
dsRNA
C)
Cell cycle distribution
%G1
%S
%G2/M
100
80
60
40
20
0
GFP
SREBP
FAS
GFP
SREBP
FAS
+ TSC2
dsRNA
D)
FSC G1
% relative to control
140
120
100
80
60
40
20
0
GFP
SREBP
FAS
GFP
SREBP
FAS
+ TSC2
E)
FSC G2/M
% relative to control
140
120
100
80
60
40
20
0
GFP
SREBP
FAS
GFP
SREBP
FAS
+ TSC2
F)
FSC S
GFP
SREBP
FAS
GFP
SREBP
FAS
+ TSC2
dsRNA

Table 6-1 Characterisation of UAS-dSREBP-dsRNAi fly strains

Table 6-1 shows dose-dependent lethality of constitutively expressed dSREBP-RNAi's compared to *yw*. dSREBP RNAi fly lines contain either one or two insertions of the P[w+pWIZ-UAST-dSREBP-dsRNAi] cassette represented by the number of RNAi insertions (RNAi ins.). dSREBP^{RNAi} strains were crossed with *daughterless-GAL4* (*da-GAL4*) and appearance of larvae, pupae and offspring flies was monitored. Relative number of offspring flies was compared to *yw* control and lethality was defined as - = less than 10% difference in number of progeny flies, + = 50 – 90% reduction in progeny flies, and ++ = no progeny. Morphology defects (morph. defects) in the offspring were observed as described. Flies were of the following genotypes: *da-GAL4/+, da-GAL4/+; UAS-SREBP^{RNAi}/+, da-GAL4/UAS-SREBP^{RNAi}, da-GAL4/UAS-SREBP^{RNAi}; UAS-SREBP^{RNAi}/+.* All of the genotypes mentioned have the yw markers on the X-chromosome.

Figure 6-2 Ubiquitous silencing of dSREBP reduces endogenous dSREBP and dFAS expression

mRNA was extracted from 2nd instar larvae expressing dSREBP^{RNAi} ubiquitously by the *da-GAL4* driver and expression of dSREBP and dFAS transcript was quantitated by q-rtPCR and compared to *yw* controls. Transcript levels of dSREBP and dFAS were normalised to dactin RNA levels and are presented as mean percentage changes ± SD of three independent experiments performed in duplicate. Flies were of the following genotypes: *da-GAL4/+, da-GAL4/UAS-SREBP^{RNAi1}, da-GAL4/UAS-SREBP^{RNAi2}; UAS-SREBP^{RNAi2}/+, da-GAL4/UAS-SREBP^{RNAi3}; UAS-SREBP^{RNAi3}/+.* All of the genotypes mentioned have the yw markers on the X-chromosome.

Tabel 6-1

strain	RNAi ins.	larvae	pupae	adults	lethality	morph. defects
8	1	+	+	+	-	-
10	1	+	+	+	-	-
15	1	+	+	+	-	-
18	1	+	+	+	-	-
22	1	+	+	+	-	-
43	1	+	+	+	-	-
04/18	2	+	+	+/-	+	misshapen wings
07/43	2	+	+	+/-	+	misshapen wings
10/22	2	+	+	+/-	+	misshapen wings
10/18	2	+	-	-	++	
15/18	2	+	-	-	++	

Table - 6-1 Characterisation of UAS-dSREBP-dsRNAi fly strains

Table 6-1 shows dose-dependent lethality of constitutively expressed dSREBP-RNAi's compared to *yw*. dSREBP RNAi fly lines contain either one or two insertions of the P[w+pWIZ-UAST-dSREBP-dsRNAi] cassette represented by the number of RNAi insertions (RNAi ins.). dSREBP^{RNAi} strains were crossed with *daughterless-GAL4* (*da-GAL4*) and appearance of larvae, pupae and offspring flies was monitored. Relative number of offspring flies was compared to *yw* control and lethality was defined as - = less than 10% difference in number of progeny flies, + = 50 – 90% reduction in progeny flies, and ++ = no progeny. Morphology defects (morph. defects) in the offspring were observed as described. Flies were of the following genotypes: *da-GAL4/+, da-GAL4/+; UAS-SREBP^{RNAi}/+, da-GAL4/UAS-SREBP^{RNAi}, da-GAL4/UAS-SREBP^{RNAi}; UAS-SREBP^{RNAi}/+*. All of the genotypes mentioned have the yw markers on the X-chromosome.

Figure 6-2

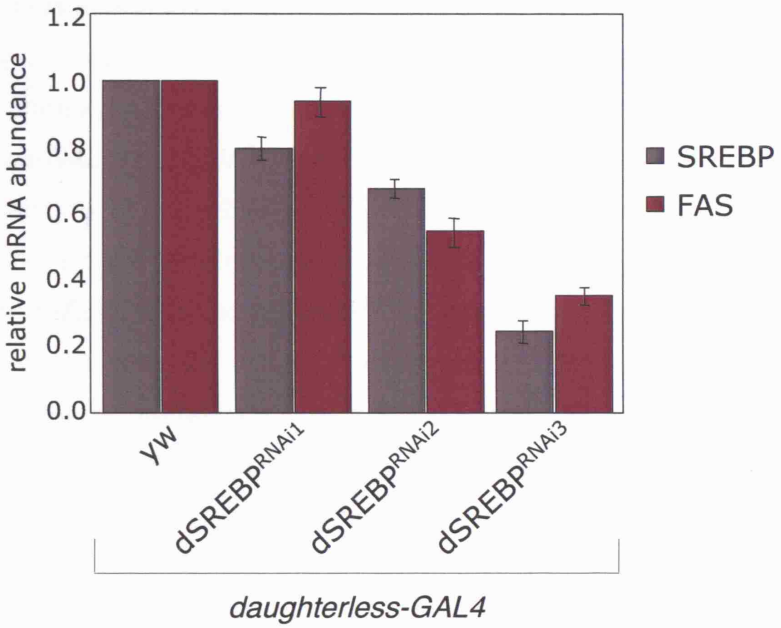
relative mRNA abundance
1.2
1.0
0.8
0.6
0.4
0.2
0.0
yw
dSREBP^RNAi1
dSREBP^RNAi2
dSREBP^RNAi3
daughterless-GAL4
SREBP
FAS

Figure 6-3 Characterization of the *dSREBP^{RNAi1}* and *dSREBP^{RNAi2}* fly lines

Yw (control), *dSREBP^{RNAi1}* and d*SREBP^{RNAi2}* flies were crossed with *da-GAL4* to analyse developmental stages, eclosion time, bodyweight and wing size. Pictures were taken to show observed phenotypes. **(A)** yw, **(B)** *dSREBP^{RNAi1}* and **(C)** d*SREBP^{RNAi2}* show number of pupae/flies normalised to total number of offspring (flies + dead pupae), (AEL = days after egg laying). Appearance of pupae and flies was recorded for 18 days. At day 18 total hatched and dead pupae (picture in **(D)**) were counted. **(E)** Representative phenotype of female and male offspring *da-GAL4/+*; d*SREBP^{RNAi2}*. **(F)** Comparison of *da-GAL4; dSREBP^{RNAi2}* and *da-GAL4/+* females 3 days after eclosion. **(G)** Adult body weights of *yw*, *dSREBP^{RNAi1}* and *dSREBP^{RNAi2}* males were measured 3 days after eclosion. Data represent cumulative weight of 30 flies, of each genotype. **(H)** Wing analysis of *dSREBP^{RNAi1}* and *dSREBP^{RNAi2}*. Data are shown as mean percentage changes $\pm$ SD, n = at least 20 wings. P-values were calculated using a two-tailed student's t-test assuming equal variance, (* $P < 1.0 \times 10^{-3}$). Flies were of the following genotypes: *da-GAL4/+, da-GAL4/UAS-SREBP^{RNAi1}, da-GAL4/UAS-SREBP^{RNAi2}; UAS-SREBP^{RNAi2}/+*. All of the genotypes mentioned have the yw markers on the X-chromosome.

Figure 6-3

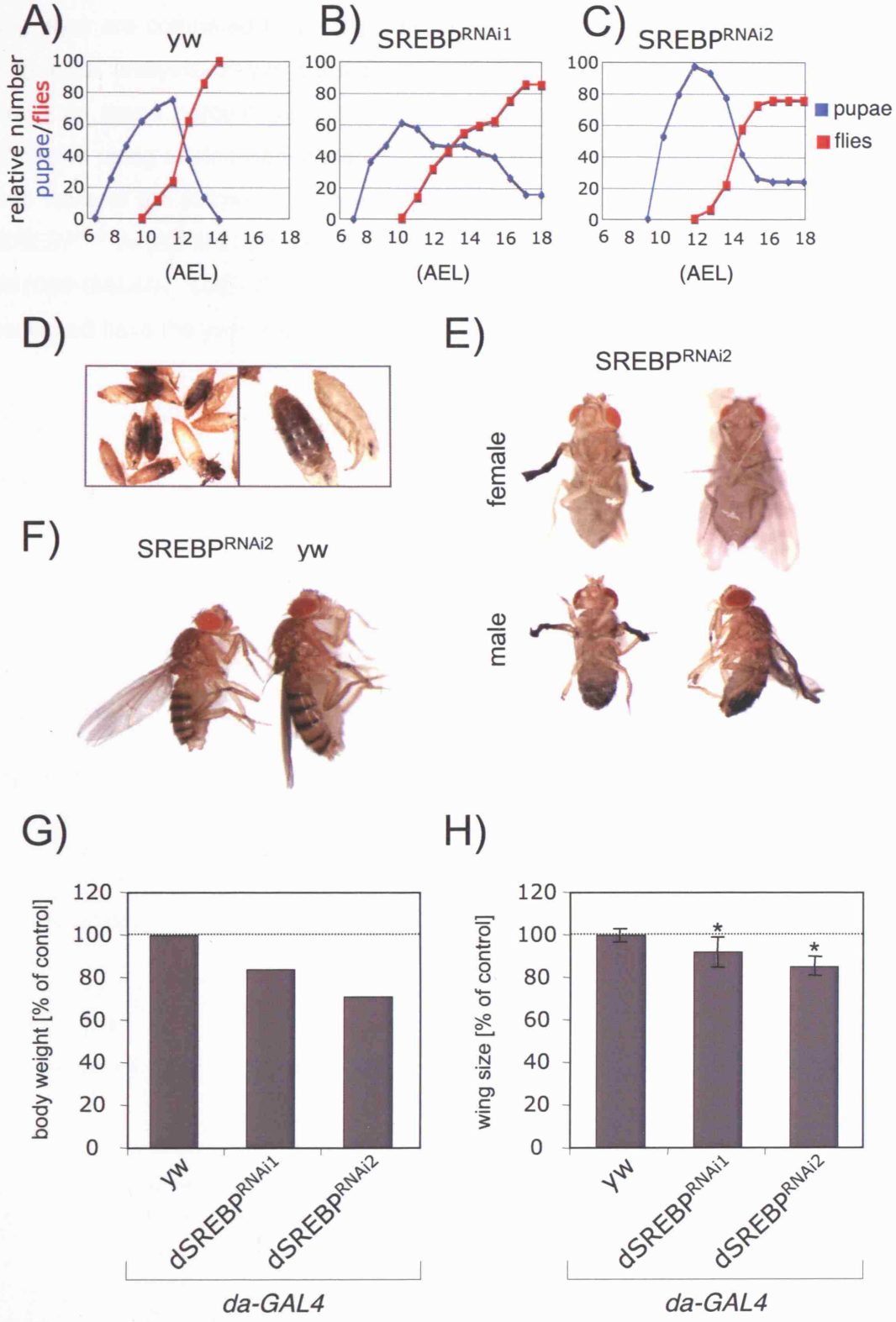
A)
yw
B)
SREBP^RNAi1
C)
SREBP^RNAi2
relative number
pupae/flies
100
80
60
40
20
0
6 8 10 12 14 16 18
(AEL)
pupae
flies
D)
E)
SREBP^RNAi2
female
male
F)
SREBP^RNAi2 yw
G)
body weight [% of control]
120
100
80
60
40
20
0
yw
dSREBP^RNAi1
dSREBP^RNAi2
da-GAL4
H)
wing size [% of control]
*
*

Figure 6-4 Silencing of dSREBP inhibits wing growth

Wings of flies expressing dSREBP^{RNAi1} **(B)** or dSREBP^{RNAi3} **(C)** and GAL4 in the dorsal wing layer are compared to yw **(A)**. **(D)** Overlay of images shown in (A) and (C). **(E)** Wing area analysis of yw, dSREBP^{RNAi1}, dSREBP^{RNAi2} and dSREBP^{RNAi3}. Data are shown as mean percentage changes ± SD, n = at least 20 wings. P-values were calculated using a two-tailed student's t-test assuming equal variance, (* $P < 1.0x10^{-5}$). Flies were of the following genotypes: *MS1096-GAL4/+* (A), *MS1096-GAL4/+; UAS-dSREBP^{RNAi1}/+* (B), *MS1096-GAL4/+; UAS-dSREBP^{RNAi3}/+; UAS-dSREBP^{RNAi3}/+* (C) and *MS1096-GAL4/+; UAS-dSREBP^{RNAi2}/+; UAS-dSREBP^{RNAi2}/+*. All of the genotypes mentioned have the yw markers on the X-chromosome.

Figure 6-4

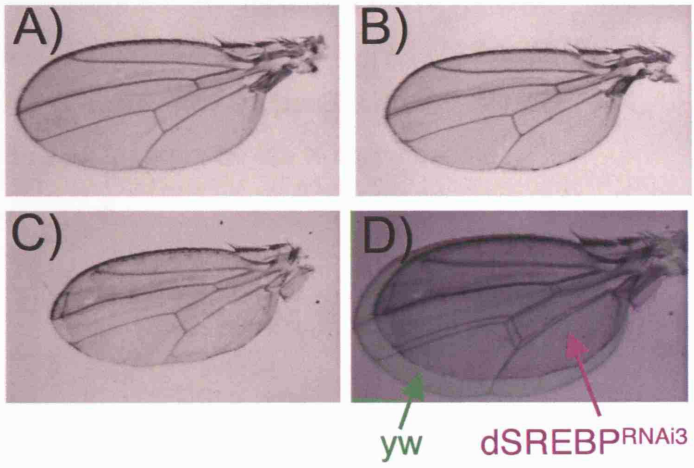
A)
B)
C)
D)
yw
dSREBP^RNAi3

E)

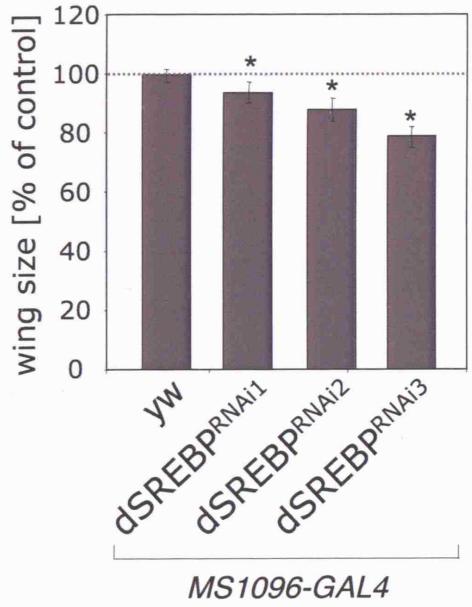
wing size [% of control]
120
100
80
60
40
20
0
*
*
*
yw
dSREBP^RNAi1
dSREBP^RNAi2
dSREBP^RNAi3
MS1096-GAL4

Figure 6-5 Silencing of dSREBP results in a smaller wing compartment

(A) Picture shows compartment of GAL4 expression using the *dpp* driver. **(B)** Wing area analysis of *yw*, d*SREBP*^{RNAi1}, d*SREBP*^{RNAi2} and d*SREBP*^{RNAi3} flies. Data are shown as mean percentage changes ± SD, n = at least 20 wings. P-values were calculated using a two-tailed student's t-test assuming equal variance. Flies were of the following genotypes: *UAS-dSREBP*^{RNAi1}*/+; dpp-GAL4/+*, *UAS-dSREBP*^{RNAi2}*/+; dpp-GAL4/UAS-dSREBP*^{RNAi2}, *UAS-dSREBP*^{RNAi3}*/+; dpp-GAL4/UAS-dSREBP*^{RNAi3}. All of the genotypes mentioned have the yw markers on the X-chromosome.

Figure 6-5

A)

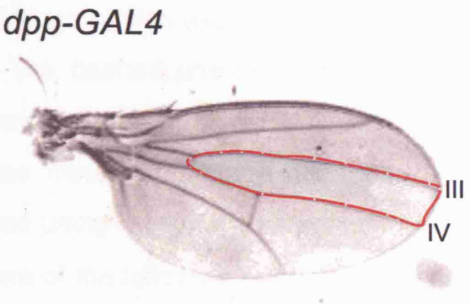
dpp-GAL4
III
IV

B)

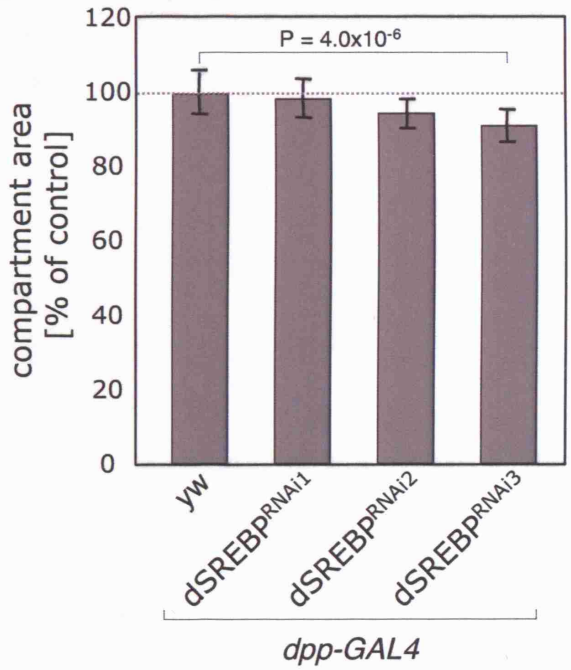
P = 4.0x10-6
compartment area
[% of control]
120
100
80
60
40
20
0
yw
dSREBPRNAi1
dSREBPRNAi2
dSREBPRNAi3
dpp-GAL4

Figure 6-6 Silencing of dSREBP results in a smaller posterior compartment of the wing

(A - D) Wings of flies expressing d*SREBP*^{RNAi} under the control of *engrailed-GAL4* (*en-GAL4*). The dashed line indicates the anterior/posterior compartment boundary. **(E)** Wing area analysis of *gfp*, d*SREBP*^{RNAi1}, d*SREBP*^{RNAi2} and d*SREBP*^{RNAi3} flies. Data are shown as mean percentage changes ± SD, n = at least 20 wings. P-values were calculated using a two-tailed student's t-test assuming equal variance, (* $P < 1.0x10^{-8}$). Flies were of the following genotypes: *en-GAL4 UAS-GFP/+* (A), *en-GAL4 UAS-GFP/+; UAS-dSREBP*^{RNAi1}*/+* (B), *en-GAL4 UAS-GFP/UAS-dSREBP*^{RNAi2}*; UAS-dSREBP*^{RNAi2}*/+* (C) and *en-GAL4 UAS-GFP/UAS-dSREBP*^{RNAi3}*; UAS-dSREBP*^{RNAi3}*/+* (D). The genotypes mentioned in (B-D) have the yw markers on the X-chromosome. The genotype mentioned in (A) has the w marker on the X-chromosome.

Figure 6-6

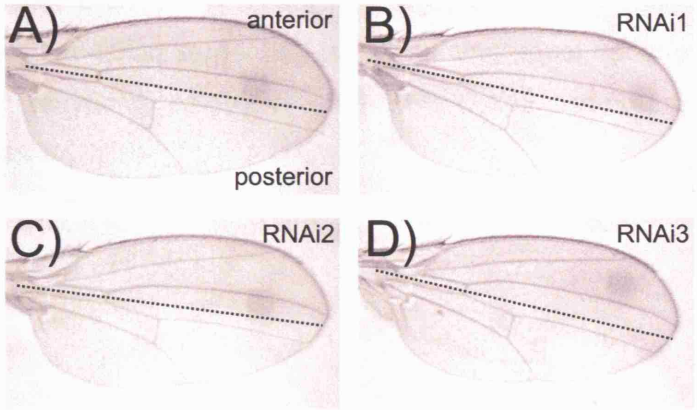
A)
anterior
posterior
B)
RNAi1
C)
RNAi2
D)
RNAi3

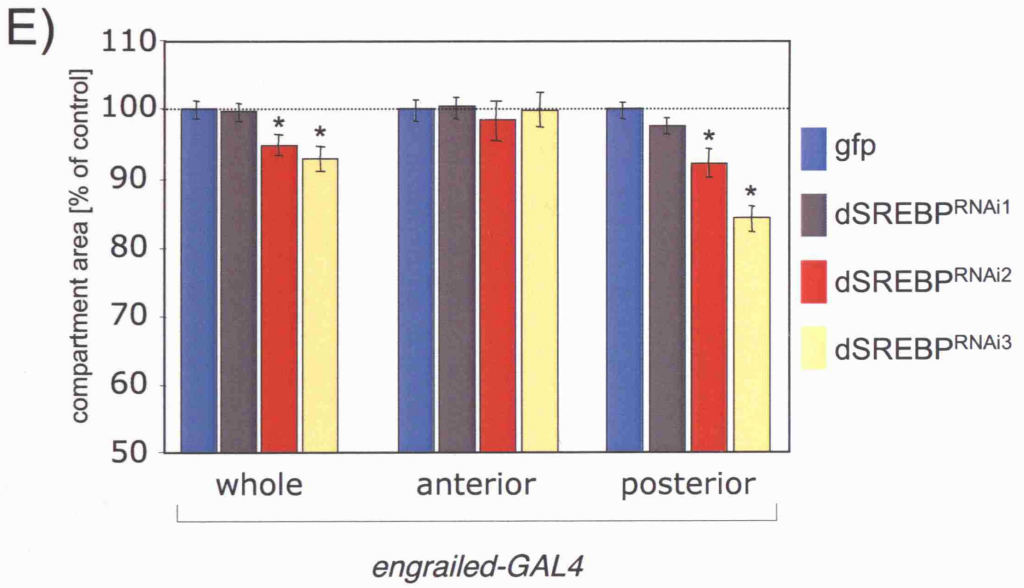
E)
compartment area [% of control]
110
100
90
80
70
60
50
*
*
*
*
whole
anterior
posterior
gfp
dSREBP^RNAi1
dSREBP^RNAi2
dSREBP^RNAi3
engrailed-GAL4

Figure 6-7 *In vivo* silencing of dSREBP affects cell size

(A) High magnification images of a region from the posterior and anterior compartments of wings shown in Figure 6-6 (A and D). **(B)** % cell number assessed by counting number of wing hairs on wing surface shown in (A) (n = at least 20). Data are shown as mean percentage changes ± SD, n = at least 20 wings. P-values were calculated using a two-tailed student's t-test assuming equal variances. Flies were of the following genotypes: *en-GAL4 UAS-GFP/+* and *en-GAL4 UAS-GFP/UAS-dSREBP^{RNAi3}; UAS-dSREBP^{RNAi3}/+*.

Figure 6-7

A)

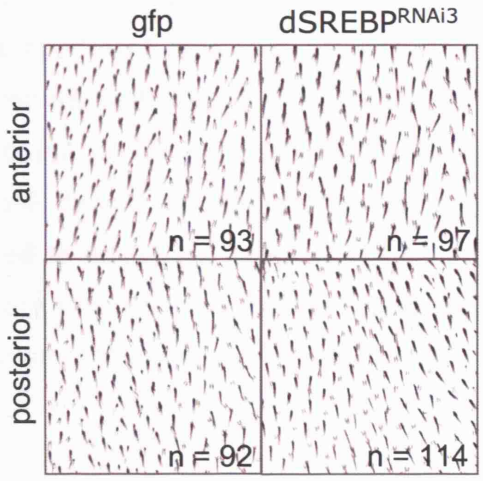
gfp
dSREBP^RNAi3
anterior
posterior
n = 93
n = 97
n = 92
n = 114

B)

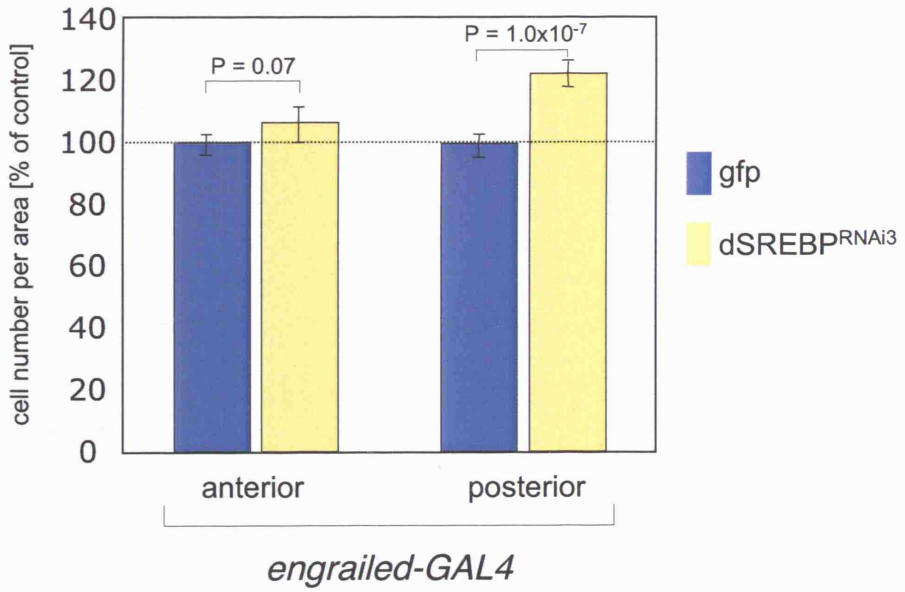
cell number per area [% of control]
140
120
100
80
60
40
20
0
P = 0.07
P = 1.0x10^-7
anterior
posterior
engrailed-GAL4
gfp
dSREBP^RNAi3

Table 6-2 Silencing of dSREBP reduces cell size but not cell number in *Drosophila*

UAS-dSREBP^{RNAi3} flies were crossed to en-GAL4 driver flies to silence dSREBP in the posterior compartment of the wing. At least 20 wings of each genotype were analysed. Cell density and compartment area was determined as described in Materials and Methods and is shown as mean values with standard deviations in brackets. Since cell density in the anterior part of flies expressing *UAS-SREBP^{RNAi3}* was higher compared to *UAS-gfp*, relative cell density of the anterior compartment in *UAS-gfp* and *UAS-SREBP^{RNAi3}* was used to adjust the numbers obtained in the posterior compartment. Adjusted numbers are indicated in columns marked with an asterisk. Flies had the following genotypes: *en-GAL4 UAS-GFP/+* and *en-GAL4 UAS-GFP/ UAS-dSREBP^{RNAi3}; UAS-dSREBP^{RNAi3}/+*.

	Cel densities (x 10^{-3} cells/µm²)		Area in compartement (x 10^4/µm²)		Cell density in posterior part (% of control)*	Area of posterior part (% of control)*	Cell number in posterior part (% of control)*
	Anterior	Posterior	Anterior	Posterior			
control	6.2 (0.2)	6.2 (0.3)	57.6 (1.5)	89.2 (2.3)	100	100	100
dSREBP^{RNAi3}	6.6 (0.2)	7.5 (0.6)	57.3 (1.8)	77.2 (2.5)	114	87	100

Table 6-2 Silencing of dSREBP reduces cell size but not cell number in *Drosophila*

UAS-dSREBP^{RNAi3} flies were crossed to en-GAL4 driver flies to silence dSREBP in the posterior compartment of the wing. At least 20 wings of each genotype were analysed. Cell density and compartment area was determined as described in Materials and Methods and is shown as mean values with standard deviations in brackets. Since cell density in the anterior part of flies expressing *UAS-SREBP^{RNAi3}* was higher compared to *UAS-gfp*, relative cell density of the anterior compartment in *UAS-gfp* and *UAS-SREBP^{RNAi3}* was used to adjust the numbers obtained in the posterior compartment. Adjusted numbers are indicated in columns marked with an asterisk. Flies had the following genotypes: *en-GAL4 UAS-GFP/+* and *en-GAL4 UAS-GFP/ UAS-dSREBP^{RNAi3}; UAS-dSREBP^{RNAi3}/+*.

Figure 6-8 Ectopic expression of dominant negative dSREBP constructs inhibit wing growth

Wing phenotype: pictures of whole fies expressing UAS-HLH106 transgenes and GAL4 in the dorsal wing layer. Flies were of the following genotypes: *MS1096-GAL4/+* **(A)** and *MS1096-GAL4/+; UAS-dSREBP^{8240}/+* **(B)**; dSREBP^{8240}: dominant negative dSREBP (DN-dSREBP) construct inserted on the 3rd chromosome. Pictures were taken at different magnifications. Wings of male **(C)** or female **(D)** flies were analysed for area size and compared to *yw* controls. Flies were of the following genotypes: *MS1096-GAL4/+*, *MS1096-GAL4/+; UAS-DN-dSREBP*, dSREBP^{8238}: dominant negative dSREBP (DN-dSREBP) construct inserted on the X-chromosome, dSREBP^{8239}: DN-dSREBP construct inserted on the 2nd chromosome, dSREBP^{8240}: DN-dSREBP construct inserted on the 3rd chromosome, dSREBP^{8241}: DN-dSREBP construct inserted on the 3rd chromosome, dSREBP^{8242}: DN-dSREBP construct inserted on the X-chromosome. Data are shown as mean percentage changes $\pm$ SD, n = at least 20 wings. P-values were calculated using a two-tailed student's t-test assuming equal variances, (* $P < 1.0x10^{-19}$ and ** $P < 1.0x10^{-12}$). **(E)** Wings of flies expressing UAS-dSREBP constructs using the engrailed-GAL4 driver were analysed for area of anterior and posterior compartments as well as whole wing size and compared to *yw* controls. Flies were of the following genotypes: *en-GAL4/+*, *en-GAL4/+; UAS-DN-dSREBP/+*. dSREBP^{8239}: DN-dSREBP construct inserted on the 2nd chromosome, dSREBP^{8240}: DN-dSREBP construct inserted on the 3rd chromosome, dSREBP^{8241}: DN-dSREBP construct inserted on the 3rd chromosome. Data are shown as mean percentage changes $\pm$ SD, n = at least 20 wings. P-values were calculated using a two-tailed student's t-test assuming equal variances, (* $p < 0.003$). All of the genotypes mentioned have the yw markers on the X-chromosome.

Figure 6-8

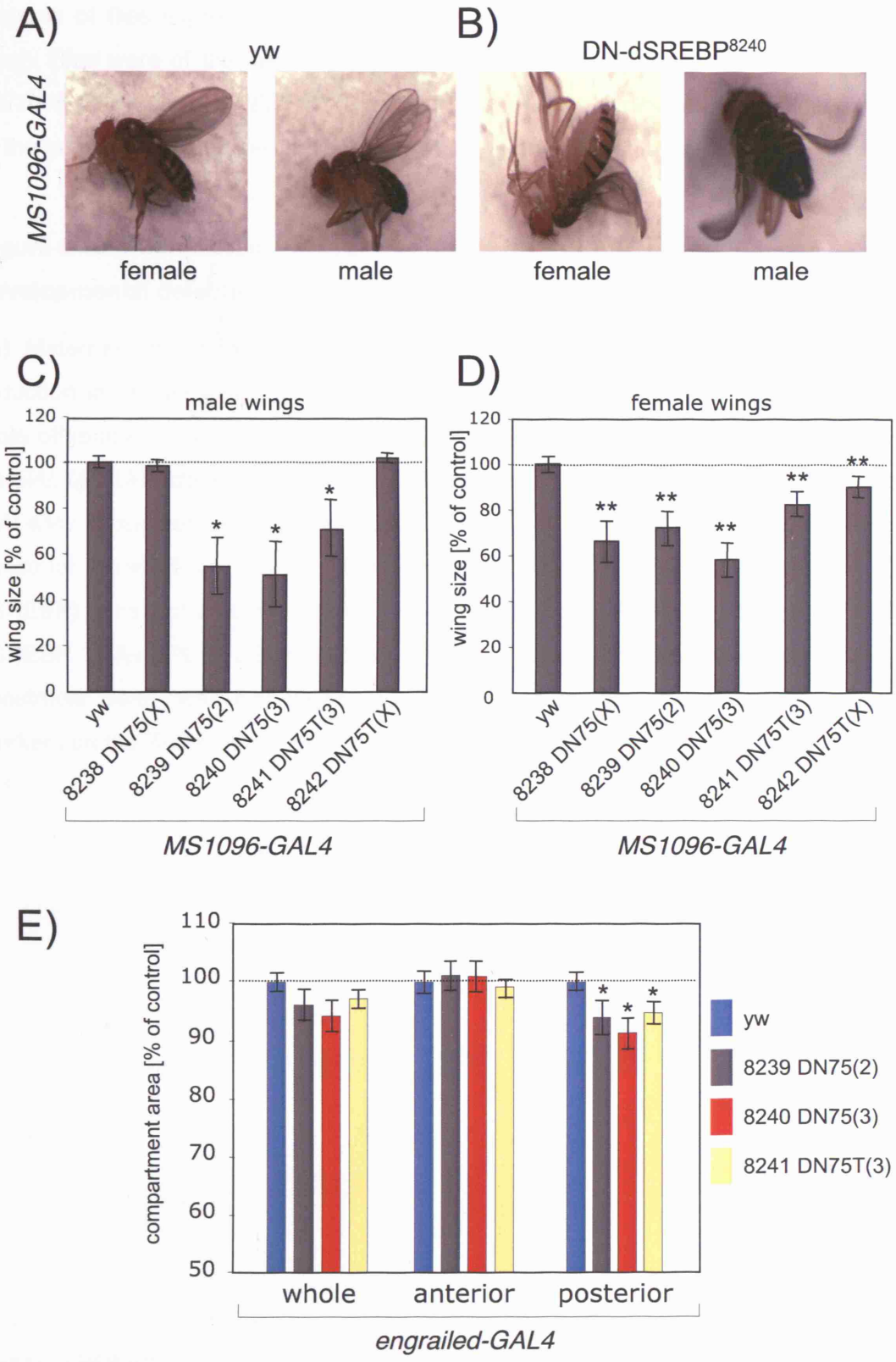
A)
yw
B)
DN-dSREBP8240
MS1096-GAL4
female
male
female
male
C)
male wings
wing size [% of control]
120
100
80
60
40
20
0
yw
8238 DN75(X)
8239 DN75(2)
8240 DN75(3)
8241 DN75T(3)
8242 DN75T(X)
MS1096-GAL4
D)
female wings
wing size [% of control]
MS1096-GAL4
E)
compartment area [% of control]
110
100
90
80
70
60
50
whole
anterior
posterior
engrailed-GAL4
yw
8239 DN75(2)
8240 DN75(3)
8241 DN75T(3)

Figure 6-9 Ectopic expression of full-length and mature dSREBP results in severely reduced wing area

Pictures of flies expressing *UAS-dSREBP* transgenes and *GAL4* in the dorsal wing layer. Flies were of the following genotypes: *MS1096-GAL4/UAS-dSREBP^{823}* **(A)** and *MS1096-GAL4/UAS-dSREBP^{8243}* **(B)**. Pictures are taken at different magnifications. All of the genotypes mentioned have the yw markers on the X-chromosome.

Figure 6-10 Ubiquitous expression of UAS-dSREBP transgenes cause developmental defects in *Drosophila*

(A) Maternal expression of wt-dSREBP driven by da-GAL4 results in a dramatic reduction in female offspring and causes a severe wing phenotype. **(B)** Female and male offspring of *da-GAL4/+; UAS-dSREBP^{8239}/+*, *da-GAL4/+; UAS-dSREBP^{8237}/+* and *da-GAL4/+; UAS-dSREBP^{8243}/+* were counted and compared to the offspring of a *da-GAL4/yw* cross set up using the same number of flies. dSREBP^{8239}: DN-dSREBP construct inserted on the 3rd chromosome, dSREBP^{8237}: wild type dSREBP (wt-dSREBP) construct inserted on the X- chromosome, dSREBP^{8243}: constitutively active dSREBP (CA-dSREBP) construct inserted on the X- chromosome. UAS-dSREBP constructs were maternally expressed. All of the genotypes mentioned have the yw markers on the X-chromosome.

Figure 6-9

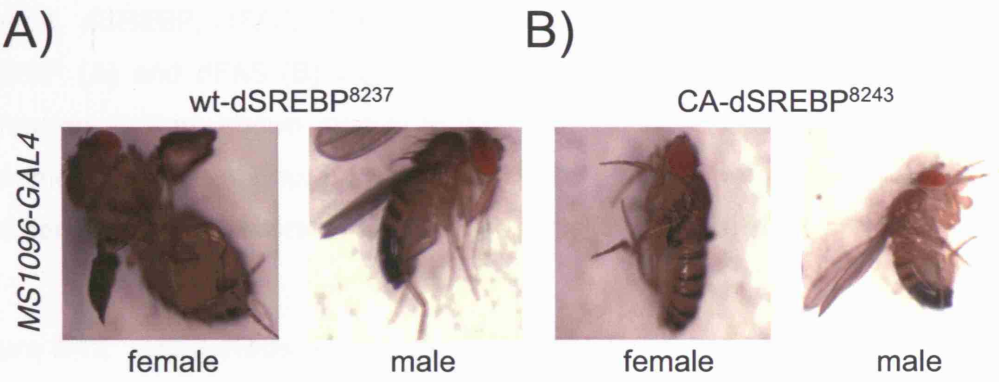

Figure 6-10

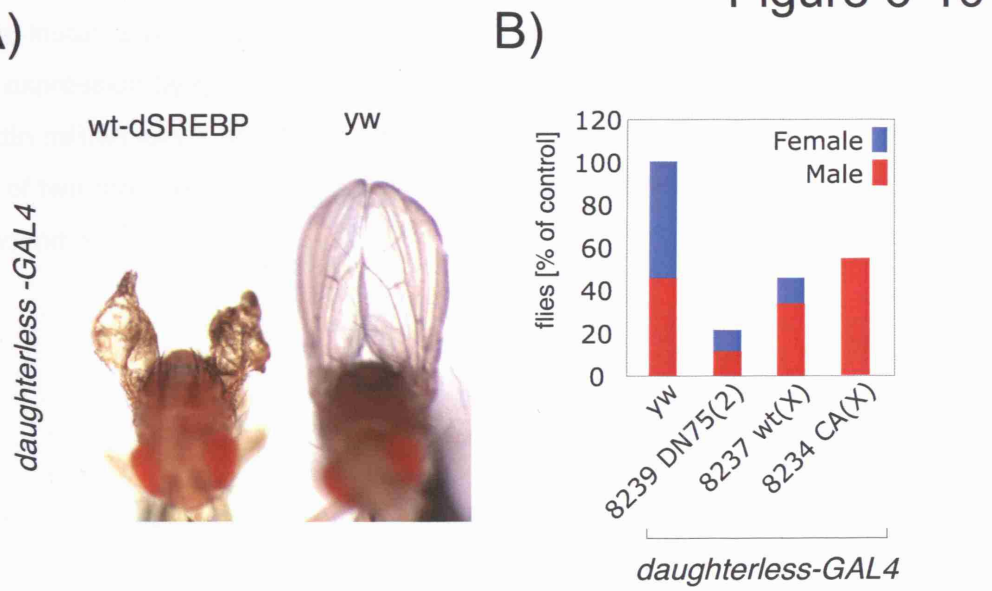

Figure 6-11 *In vitro* RNAi mediated silencing of components of the dPI3K pathway affects dSREBP and dFAS expression level

Cell lysates were prepared from Kc167 cells treated with dsRNA corresponding to GFP (control), dSREBP, dFAS, dPTEN, dAKT and dDp110 for 5 days. Expression of dSREBP **(A)** and dFAS **(B)** were determined by q-rtPCR and normalized to dactin expression and are shown relative to gfp treated control. One representative of two experiments is shown. Error bars represent ± the range of two replicates. Experiments were performed in collaboration with Megan Cully (STL, CRUK-LRI).

Figure 6-12 Ubiquitous expression of Dp110 increases dSREBP and dFAS expression

(A) Analysis of wings of flies expressing Dp110 and GAL4 in the dorsal wing layer. Data are shown as mean percentage changes ± SD, n = at least 20 wings. P-values were calculated using a two-tailed student's t-test assuming equal variances. Flies were of following genotypes: (A) *da-GAL/+*, *da-GAL4/ UAS-Dp110Wt* and (B) *MS1096-GAL4/+*, *MS1096-GAL4/+; UAS-Dp110Wt/+*, *MS1096-GAL4/+; UAS-Dp110[KD]/+*. **(B)** Second instar larvae expressing Dp110Wt ubiquitously were analysed for dSREBP and dFAS expression by q-rtPCR. Transcript levels of dFAS and dSREBP were normalized to dactin mRNA levels and are shown relative to yw control. Error bars represent ± the range of two replicates. All of the genotypes mentioned have the yw markers on the X-chromosome.

Figure 6-11

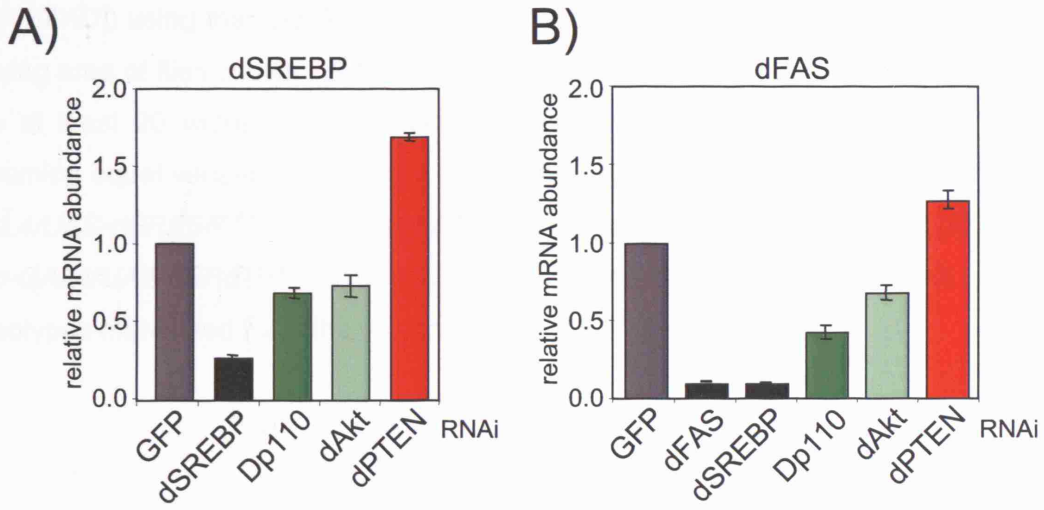

Figure 6-12

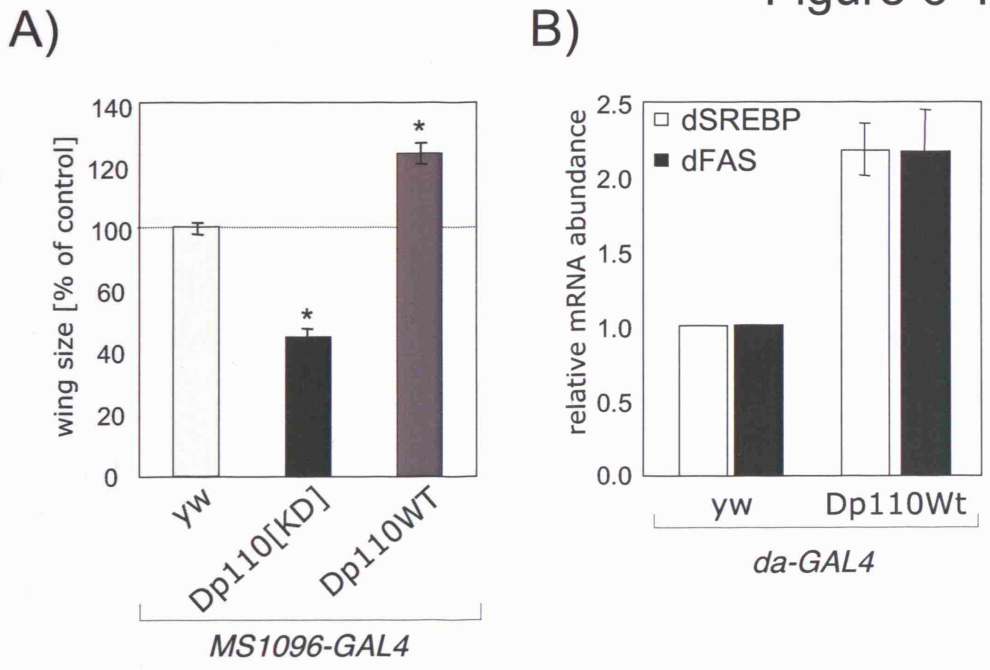

Figure 6-13 Silencing of dSREBP does not enhance the reduction in wing area caused by expression of kinase dead Dp110

(A-D) Pictures show wings of flies expressing *dSREBP^{RNAi3}* and kinase dead Dp110 (Dp110[KD]) using the *dpp-GAL4* driver (as described in Figure 6-5). **(E)** Quantification of wing area of flies shown in (A –D). Data shown are mean percentage changes ± SD, n = at least 20 wings. P-values were calculated using a two-tailed student's t-test assuming equal variance. Flies were of the following genotypes: *dpp-GAL4/+* (A), *dpp-GAL4/UAS-dSREBP^{RNAi3}; UAS-dSREBP^{RNAi3}/+* (B), *dpp-GAL4/+; UAS-Dp110[KD]/+* (C), *dpp-GAL4/UAS-dSREBP^{RNAi3}; UAS-Dp110[KD]/UAS-dSREBP^{RNAi3}* (D). All of the genotypes mentioned have the yw markers on the X-chromosome.

Figure 6-13

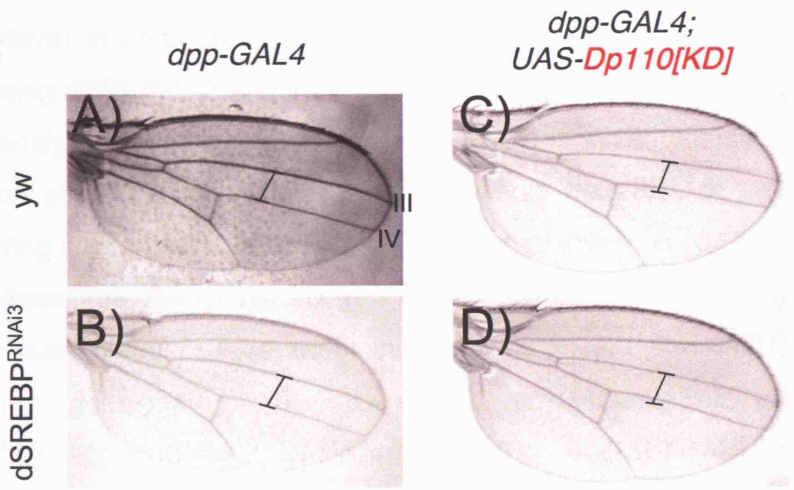
dpp-GAL4
dpp-GAL4;
UAS-Dp110[KD]
A)
C)
B)
D)
yw
dSREBP^RNAi3
III
IV

E)

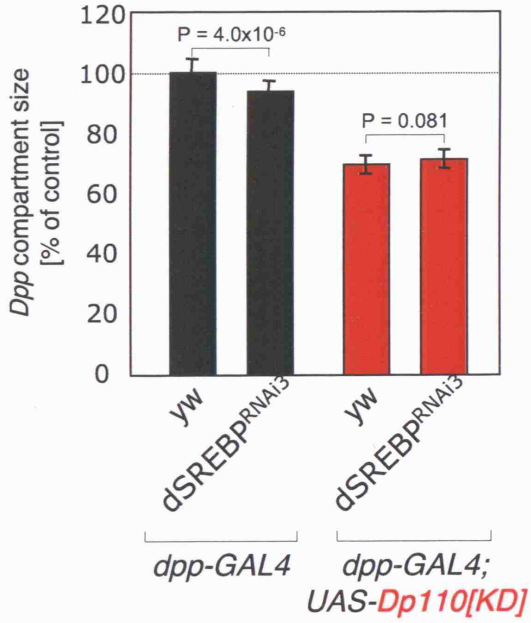
Dpp compartment size
[% of control]
120
100
80
60
40
20
0
P = 4.0x10^-6
P = 0.081
yw
dSREBP^RNAi3
yw
dSREBP^RNAi3
dpp-GAL4
dpp-GAL4;
UAS-Dp110[KD]

Figure 6-14 Silencing of dSREBP does not enhance the reduction in posterior compartment size caused by expression of kinase dead Dp110

(A/B) Pictures show wings of flies expressing *dSREBP^{RNAi3}* using the *engrailed-GAL4* (*en-GAL4*) driver at 25˚C (as described in Figure 6-6). **(C/D)** Pictures show wings of flies expressing d*SREBP^{RNAi3}* under the control of *en-GAL4 UAS-Dp110[KD]* at 18˚C **(E)** Wing area analysis of *yw*, d*SREBP^{RNAi2}* and d*SREBP^{RNAi3}* flies. Quantification of area of posterior and anterior compartment as well as whole wing size of wings is shown in (A/B). **(F)** Wing size analysis described in (E) of wings shown in (C/D). Data are shown as mean percentage changes ± SD, n = at least 20 wings. P-values were calculated using a two-tailed student's t-test assuming equal variance, (* $P < 0.001$). Flies were of the following genotypes: *en-GAL4/+* (A), *en-GAL4/UAS-dSREBP^{RNAi3}; UAS-dSREBP^{RNAi3}/+* (B), *en-GAL4 UAS-Dp110[KD]/+* (C), *en-GAL4 UAS-Dp110[KD]/UAS-dSREBP^{RNAi3}; UAS-dSREBP^{RNAi3}/+* (D). All of the genotypes mentioned have the yw markers on the X-chromosome.

Figure 6-14

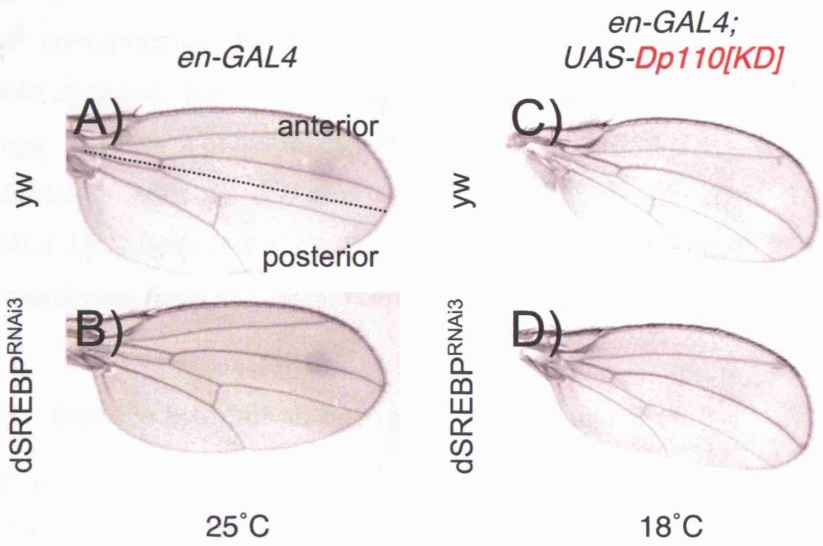
en-GAL4
en-GAL4;
UAS-Dp110[KD]
A)
anterior
posterior
yw
C)
yw
dSREBPRNAi3
B)
dSREBPRNAi3
D)
25˚C
18˚C

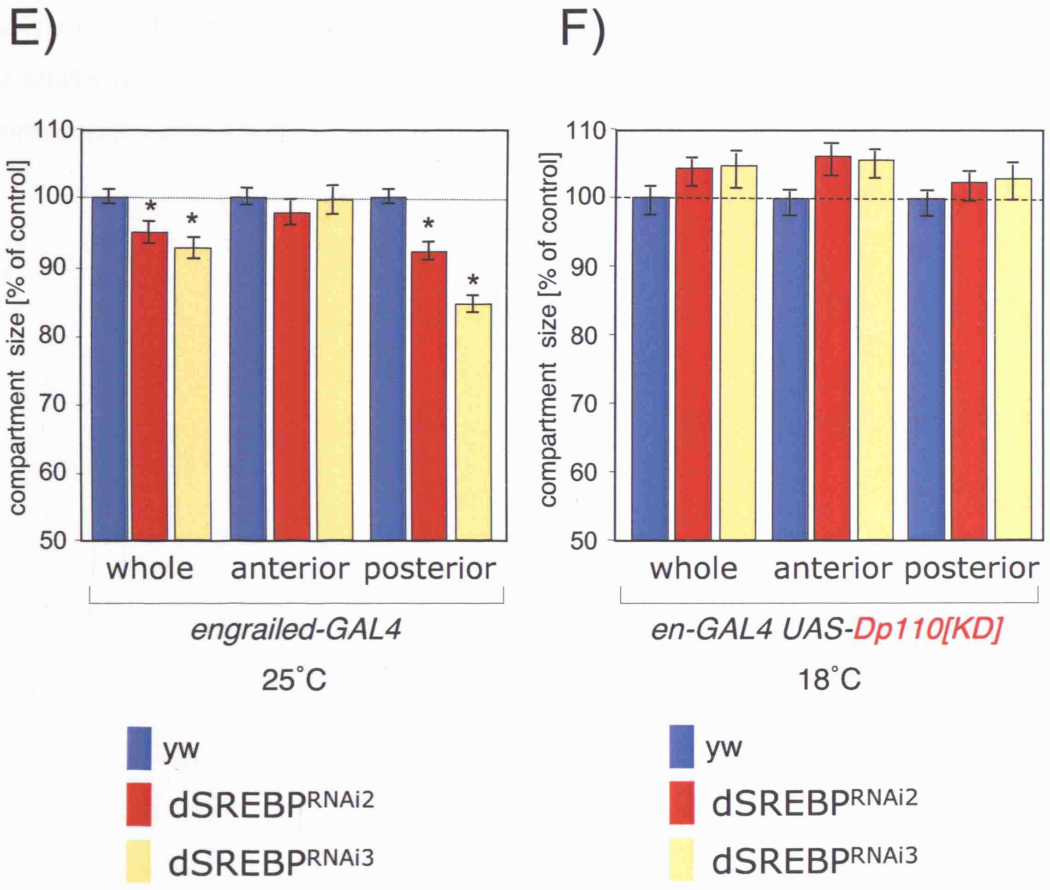
E)
F)
compartment size [% of control]
110
100
90
80
70
60
50
whole
anterior
posterior
engrailed-GAL4
25˚C
en-GAL4 UAS-Dp110[KD]
18˚C
yw
dSREBPRNAi2
dSREBPRNAi3

Figure 6-15 Silencing of dSREBP reduces the increase in wing size caused by overexpression of Dp110WT

Wing size analysis of flies expressing dSREBP^{RNAi2} or dSREBP^{RNAi3} in the presence or absence of co-expressed Dp110WT using the *MS1096-GAL4* driver. Numbers represent fold changes. Data are shown as mean percentage changes ± SD, n = at least 10 wings. Flies were of the following genotypes: *MS1096-GAL4/+*, *MS1096-GAL4 UAS-Dp110Wt/+*, *MS1096-GAL4/+; UAS-SREBP$^{RNAi2/3}$/+; UAS-SREBP$^{RNAi2/3}$/+*, *MS1096-GAL4 UAS-Dp110Wt/+; UAS-SREBP$^{RNAi2/3}$/+; UAS-SREBP$^{RNAi2/3}$/+*. All of the genotypes mentioned have the yw markers on the X-chromosome.

Figure 6-16 Genetic interaction between dSREBP and Dp110

Pictures of representative MS1096-GAL4/+ flies expressing the indicated UAS-trangenes. Crosses were performed at 18˚C and 25˚C as indicated. Flies were of the following genotypes: *MS1096-GAL4/+*, *MS1096-GAL4 UAS-Dp110Wt/+*, *MS1096-GAL4/UAS-SREBP^{8237}*, *MS1096-GAL4 UAS-Dp110Wt/UAS-SREBP^{8237}*, *MS1096-GAL4/UAS-SREBP^{8243}*. All of the genotypes mentioned have the yw markers on the X-chromosome. Arrows point to severely misshapen wings observed in two genotypes.

Figure 6-15

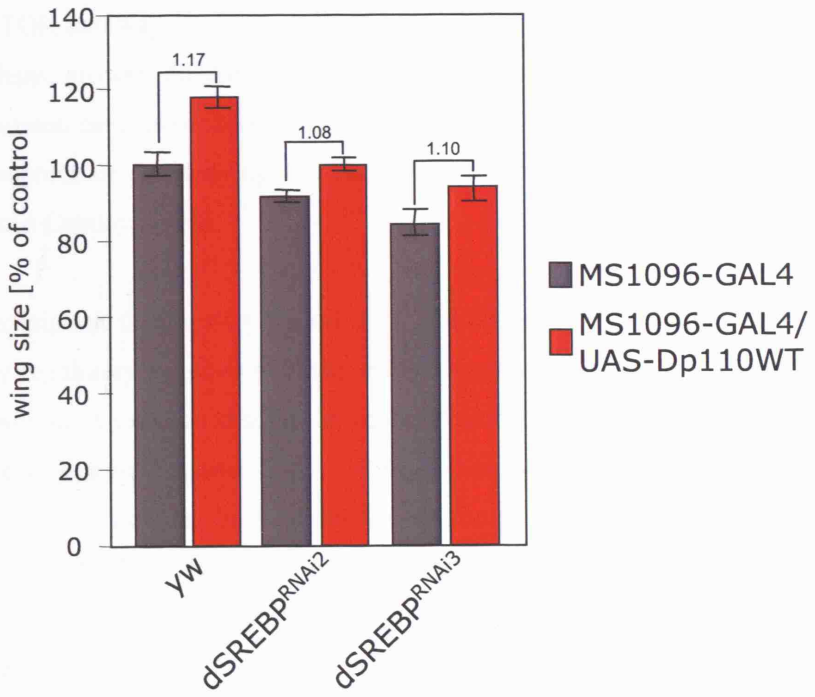

Figure 6-16

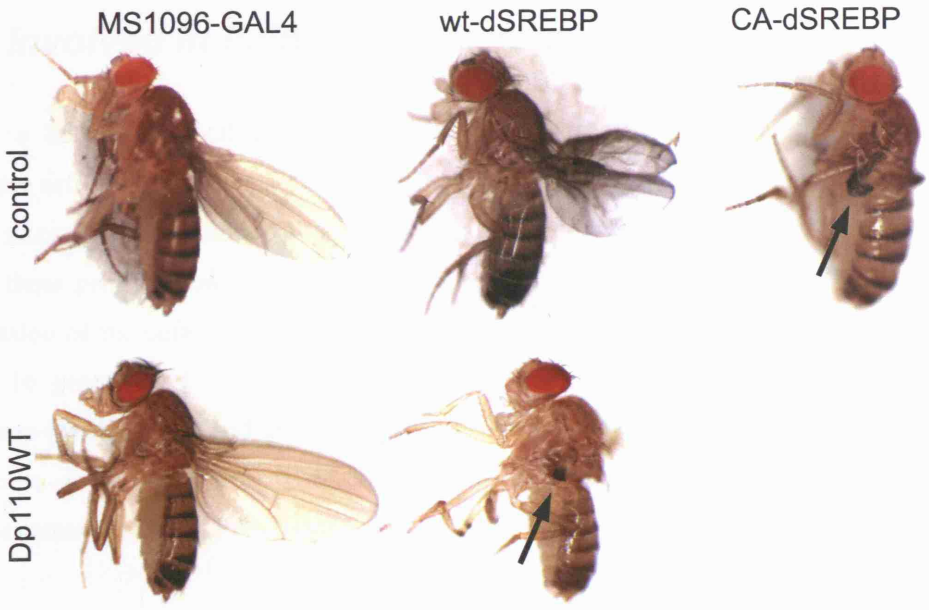

7 Chapter 7: Discussion

The PI3K/Akt/mTOR pathway is involved in many different cell biological processes such as survival, metabolism, growth, differentiation and cell proliferation. The observation that more than 30% of all human cancers contain a mutation in one or another PI3K pathway component, underlines the importance in studying the regulation of this pathway and its downstream effectors (Shaw and Cantley, 2006).

SREBPs are transcription factors that control lipid and cholesterol biosynthesis by regulating expression of key regulatory enzymes of these pathways such as fatty acid synthase. It has been reported that many solid tumours display an up-regulation of FAS expression and increased fatty acid synthesis (Menendez and Lupu, 2006). Likewise it is known that activation of SREBPs and FAS expression can be mediated by insulin or oncogenic Ras via the PI3K/Akt pathway (Yang et al., 2002b). The aim of the work described in this thesis was to analyse the regulation of lipid biosynthesis by the Akt/mTOR pathway and to understand its role in cell growth regulation.

7.1 Akt-dependent induction of transcription of genes involved in lipid biogenesis requires SREBPs

Using a hormone-inducible version of the Akt kinase (myrAkt-ER), the consequences of selective activation of one effector of the Ras/PI3K pathway was studied in epithelial cells. In a DNA microarray experiment, 145 genes were found upregulated in response to Akt activation. 16 of those genes encode enzymes involved in fatty acid synthesis, cholesterol biogenesis and generation of the cofactor NADPH, which is required for lipid synthesis (Figure 3-3). Among these 16 genes are FAS, HMG-CoA reductase and HMG-CoA synthase, the key limiting enzymes for fatty acid and cholesterol synthesis. The observed changes of mRNA abundance for these genes were reproduced by independent methods showing that activation of Akt induces transcription of FAS, HMGR and HMGS (Figure 3-4).

In order to investigate whether SREBP is required for Akt-induced expression of these genes, dominant-negative forms of mature SREBPs were co-transfected in the absence and presence of activated Akt. DN-SREBPs completely abolished Akt-induced activation of FAS and HMGS expression (Figure 3-8). In addition, silencing of SREBP1 and to a lesser extent of SREBP2 by RNAi blocked Akt-mediated transcription of FAS and HMGS (Figure 3-9). These data indicate

that activation of transcription of genes involved in fatty acid and cholesterol biosynthesis by Akt requires SREBP activity.

7.2 Regulation of SREBP activity by Akt

The subsequent question addresses the mechanism of regulation of SREBPs activity in response to Akt activation. SREBP activity is regulated at the transcriptional and translational level, by regulation of flSREBP processing as well as by posttranslational modifications of mature SREBP. Since the promoter sequences of all SREBP genes contain SRE elements ((Amemiya-Kudo et al., 2000; Sato et al., 1996) and unpublished observations), it is possible that induction of SREBP gene transcription is regulated by a feed-forward loop. Such a feed-forward mechanism has been reported for SREBP1c and SREBP2 (Bengoechea-Alonso and Ericsson, 2007). Akt-induced transcription of all SREBP isoforms is blocked by inhibition of *de novo* protein synthesis, indicating that Akt requires the activation of an intermediate factor for SREBP expression (Figure 3-13).

The rat SREBP1c promoter is induced by insulin through a 149bp fragment containing NF-Y, LXREs, SRE and SP1 sites, and mutation of the SRE completely abolishes the response of the SREBP1c promoter to insulin (Deng et al., 2002). It has recently been published that the Sp1 binding sites determine the basal and insulin induced expression of the rat SREBP1c promoter in hepatocytes (Deng et al., 2007). The promoter of the SREBP1a gene also contains several SP1 sites (Zhang et al., 2005); and SP1 has been reported to be involved in induction of VEGF expression by Akt (Pore et al., 2004). A mechanistic model suggests that insulin-induced SREBP1 gene expression is mediated via enhanced association of Sp1 with transcription factors (e.g. mSREBP1, LXRα, NF-Y), the distinct coactivator complex called ARC/Mediator (Yang et al., 2006b), and coactivators (e.g. SRC-1 and p300), which concomitantly increase the transactivator capacity of Sp1 (Deng et al., 2007). It is therefore possible that Akt modulates expression and/or activity of SP1 or other transcription factors that cooperate with mSREBPs. Although the two SP1 sites are conserved in mouse and human SREBP1a promoters (Zhang et al., 2005), these data have to be considered carefully with regard to the human homologue, since SREBP promoter sequences differ between mammalian species, which suggests that they may be regulated distinctly from each other (Tarling et al., 2004).

It has been speculated that insulin activates expression of the SREBP1c promoter by stimulating the production of an agonistic ligand required for LXR transactivation (Chen et al., 2004). Since Akt stimulates insulin-mediated glucose uptake (Kohn et al., 1996) and glucose directly binds and activates LXR, resulting in enhanced target gene expression (Mitro et al., 2007), it was of

interest to test whether LXR is the intermediate factor regulating SREBP expression in response to Akt activation. Activation of Akt further increased the expression levels of two SREBP target genes FAS and ACL in the presence of the LXR activator T0901317 (Figure 3-14).

SREBPs are synthesised as large precursor proteins in the ER membrane. To become transcriptionally active, SREBP requires proteolytic cleavage by two proteases in the Golgi, which releases the mature form. mSREBP translocates to the nucleus and induces expression of its target genes. Activation of Akt resulted in accumulation of mSREBP1 but not mSREBP2 in the nucleus within 1 hour, which preceded the appearance of flSREBP (Figure 4-1 and 4-2). These data imply that Akt regulates SREBP1 activity post-transcriptionally.

Since ablation of SREBP2 expression by RNAi was less efficient in blocking Akt-dependent activation of SREBP target genes and activation of Akt resulted in rapid accumulation of mSREBP1 but not mSREBP2, it seems likely that Akt activates only SREBP1 in the system used here. It should be noted that no SREBP1a or 1c isoform specific antibodies are available to date. This makes it impossible to distinguish differential regulation of the two SREBP1 isoforms by Akt. Although SREBP1a has not been described as an LXR target gene, both SREBP1 transcripts are upregulated in response to Akt and LXR activation (Figure 3-14). It would be of interest to know whether Akt stimulates the accumulation of the mature form of both isoforms with the same kinetics.

The observed rapid accumulation of mSREBP1 by Akt could either be due to enhanced SREBP processing or an increase in the stability of the mature form. When analysed using the Scansite software, SREBPs did not show any consensus phosphorylation sites for Akt. However, high stringency putative phosphorylation sites for GSK3 and Erk1/2 MAP kinases were found. Kotzka and colleagues demonstrate that Erk1/2 phosphorylates all mSREBPs *in vitro*. Mutation of Erk phosphorylation sites abolishes insulin or PDGF mediated phosphorylation and transcriptional activation of mSREBPs by Erk2 (Kotzka et al. 1998; Kotzka et al. 2000). In RPE cells, the MEK inhibitor UO126 had very little effect on SREBP-dependent transcription, whereby inhibition of PI3K using LY294002 abolished insulin-induced expression of FAS and SREBP1 (Figure 3-11 and 3-12). Although inhibition of GSK3 kinase activity enhanced stability of mature and full length SREBP1, it did not block Akt-induced accumulation of full length and mature SREBP1 nor the increase in FAS expression (Figure 4-5). GSK3 has been shown to phosphorylate mSREBP1, which is then recognized by the ubiquitin ligase Fbw7, resulting in ubiquitination and rapid proteasomal degradation of mSREBP1 (Sundqvist et al., 2005). However, in the system used here, neither silencing of Fbw7 nor inhibition of the proteasome blocked Akt-induced accumulation of mSREBP1 (Figure 4-4). Since the PI3K and the Wnt pathway control GSK3 activity, it has been speculated that GSK3 exists in two pools

(Pearl and Barford, 2002), which would explain why Akt does not regulate all GSK3 targets. Therefore GSK3-dependent regulation of SREBP1 could be independent of Akt activity. These data indicate that Akt does not regulate mSREBP1 stability and activation of SREBP1 does not require GSK3 in response to Akt activation.

Activation of SREBP requires COPII mediated budding of the SREBP/SCAP complex from the ER and translocation to the Golgi. SCAP interacts via its MELADL motif with the COPII protein sec 24 (Sun et al., 2005; Sun et al., 2007). Under sterol saturating conditions, INSIG binds to SCAP and induces a conformational change which prevents the recognition of the MELADL motif by sec 24 and blocks budding of the SREBP/SCAP complex (Radhakrishnan et al., 2007; Sun et al., 2007).

It is possible that Akt activates SREBPs by modulating the activity of components of the processing machinery. Activation of SCAP or inhibition of INSIG would lead to elevated SREBP processing and thus accumulations of mature SREBP. Changes in expression levels of both proteins in response to Akt activation were investigated as well as potential regulation by phosphorylation. SCAP protein levels and INSIG1/2 mRNA levels were not regulated in response to Akt activation (Figure 4-2). Scansite analysis reveals a medium stringency Akt phosphorylation site in SCAP. However, this site faces the lumen of the ER, making it very unlikely to be accessible for cytosolic Akt. In addition, Akt-induced processing of SREBP1 was sensitive to inhibition by sterols. Sterols also completely blocked activation of transcription of FAS and HMGS promoter reporter constructs (Figure 4-2). These data indicate that activation of Akt is not sufficient to overcome sterol-sensitive SREBP processing. Again, it would be of interest to dissect if the two SREBP1 isoforms are differently regulated in response to sterols.

Activation of SREBP by Akt requires ER to Golgi transport, since inhibition by brefeldin A completely blocked accumulation of mSREBP1 in the nucleus and inhibited target gene expression in response to Akt activation (Figure 4-3). Again, this indicates that Akt does not stabilise the nuclear mSREBP form, but may be required for processing. This is supported by findings showing that dominant-negative Akt prevents ER to Golgi translocation of SCAP-GFP (Du et al., 2006). It would be of interest to investigate whether activation of Akt enhances budding of the SCAP/SREBP complex by stimulating the interaction of SCAP with COPII proteins.

It has been reported that brefeldin A also interferes with mTOR signalling (Buerger et al., 2006) and Akt positively regulates mTORC1 activity via several ways (Manning and Cantley, 2007). Indeed, activation of SREBP by Akt requires mTORC1 activity. Inhibition of mTOR activity by

RNAi or using the specific inhibitor rapamycin blocked accumulation of mSREBP as well as induction of target genes in response to Akt activation (Figure 4-6 and 4-7).

mTORC1 also senses the cellular energy status via AMP-activated protein kinase (AMPK). In response to energy depletion (high AMP/ATP ratio), AMPK is activated and phosphorylates TSC2 leading to inhibition of mTORC1 (Inoki et al., 2003a). Under these conditions AMPK inhibits energy-consuming anabolic pathways and activates energy producing catabolic pathways (Hardie, 2005). AMPK dependent TORC1 inhibition would result in an activation of the PI3K/Akt pathway. However this activation is only transient, since long-term energy depletion induced by 2-deoxyglucose (2-DG) treatment or glucose starvation stimulates phosphorylation of IRS-1 by AMPK (Tzatsos and Tsichlis, 2007). Phosphorylation of IRS-1 at serine 794 inhibits the PI3K/Akt pathway and promotes apoptosis (Tzatsos and Tsichlis, 2007). Providing the cell with an adequate energy supply may also enhance mTORC1 activity. Akt activates mTORC1 not only by directly phosphorylating TSC2 and PRAS40, but also by maintaining a high ATP level in the cell via stimulating glucose uptake and glycolysis. A high ATP level leads to a concomitant decrease in the AMP/ATP ratio and inhibits AMPK-mediated phosphorylation and activation of TSC2 (Hahn-Windgassen et al., 2005). Simultaneous activation of AMPK and PI3K/Akt inhibits mTORC1 activation. This shows a dominant role for AMPK on TSC2, and implies that inhibition of AMPK is essential for mTORC1 signalling (Hahn-Windgassen et al., 2005).

Activation of AMPK by AICAR, or inhibition of glycolysis by glucose deprivation or addition of 2-DG abolished accumulation of FAS and flSREBP, as well as mSREBP in response to Akt (Figure 4-9 and 4-10). All treatments resulted in a block of activation of mTORC1 signalling by Akt, detected by the phosphorylation levels of S6rb. This indicates that direct and indirect activation of AMPK inhibits mTORC1 signalling, which is required for SREBP1 activity and induction of expression of lipogenic genes.

While these results clearly indicate a role for mTORC1 in regulation of SREBP activity, the mechanism of this regulation remains unclear. TOR has been implicated in vesicle transport (Neufeld, 2007), and localisation of mTOR to the ER and the Golgi plays an essential role in its regulation and downstream signalling (Buerger et al., 2006; Drenan et al., 2004). Interestingly, Drenan and colleagues (2004) proposed a model by comparing mTOR with SREBP, stating both proteins sense metabolite availability. SREBPs sense sterols in the ER and require translocation to the Golgi, whereas mTOR senses amino acids and requires ER/Golgi localisation (Drenan et al., 2004). Since computational analysis reveals a conserved TOS-like motif in the cytosolic loop of the C-terminus of SREBP1, mTOR could physically interact with

SREBP1 in the ER, which would allow phosphorylation of SREBP or SCAP, possibly promoting COPII protein interaction and budding.

The results presented in this thesis and recent literature suggest that the effect of Akt on lipogenic gene expression is complex because of cross-talk between multiple signal transduction pathways. The Ras/Erk, PI3K/Akt, Wnt/GSK3 and mTOR pathways could all affect SREBP-regulated lipogenic gene expression. Therefore regulation of SREBP activity by Akt may occur on several levels. Akt-dependent SREBP processing requires mTORC1 activity (Figure 4-6). mTORC1 could mediate Akt-induced activation of SREBP, or SREBP could integrate mTORC1 and Akt activity, and could require positive signals from both to become activated. In addition, Akt could also contribute to transcription of SREBPs via activation of additional transcription factors, such as LXR, ChREBP and Sp1. This activation may be direct via phosphorylation, or indirect by increasing intracellular concentrations of ligands such as glucose, or by activating glycolysis. Finally, Akt-dependent regulation of SREBP is likely to be cell type specific and could involve different SREBP isoforms.

7.3 Regulation of Metabolism and cell size by Akt

The PI3K/Akt signal-transduction pathway has been implicated in the regulation of metabolism. It is noteworthy that in human adults, *de novo* synthesis of fatty acids occurs nearly exclusively in the liver, adipose tissue, lactating breast and in the cycling endometrium. All other tissues derive the lipids they require from the circulatory system. Therefore, expression of lipogenic enzymes is low in most adult tissues (Menendez and Lupu, 2006; Swinnen et al., 2006). In contrast, many cancers show enhanced *de novo* lipid synthesis together with upregulated FAS expression (Kuhajda et al., 2000; Menendez and Lupu, 2004).

Having shown that Akt regulates SREBP1 activity, it was of interest to investigate the biological consequences of induction of genes encoding for fatty acid and cholesterol biosynthesis with regard to the metabolic profile and its contribution to cell growth control. Changes in concentrations of intracellular lipid and water-soluble metabolites were analysed by NMR. Activation of Akt resulted in an increase in the concentration of intracellular unsaturated and saturated fatty acids, membrane phospholipids and their precursors and amino acids (Figure 5-2 and 5-3). Inhibition of mTOR blocked the Akt-induced increase in lipids and most of the changes in water-soluble metabolites. mTORC1 activity was also required for Akt-mediated glucose uptake and lactate production as well as increased levels in ATP + ADP (Figure 5-4). These data indicate a central role for mTORC1 in Akt-mediated induction of lipid biosynthesis.

Akt regulates fatty acid biosynthesis on several levels (Figure 7-1). The main carbon source for *de novo* lipid synthesis is glucose. It has been shown that Akt stimulates glucose uptake via Glut4 translocation to the plasma membrane and increased expression of Glut1 (Welsh et al., 2005). A high glycolytic rate leads to raised production of cellular energy in the form of ATP. Activation of Akt causes an increase in the ATP + ADP levels as well as the NADH + NAD levels. Akt also directly activates ATP-citrate lyase (ACL) by phosphorylation (Berwick et al., 2002). ACL is the key enzyme that controls the flow of glucose carbons to lipid synthesis by regulating the availability of cytoplasmic acetyl-CoA (Bauer et al., 2005), which is the substrate for acetyl-CoA carboxylase (ACC) and fatty acid synthase (FAS). Activation of SREBP by Akt induces the expression of a number of enzymes involved in lipid biosynthesis, including ACL, FAS and ACC (Porstmann et al., 2005). In addition, Akt has been implicated in mediating cellular amino acid, iron and LDL uptake via regulation of cell surface localisation of several carriers, ion channels and receptors (Boehmer et al., 2004; Boehmer et al., 2003; Palmada et al., 2005).

There is growing evidence that mTORC1 signalling is involved in cellular metabolism, regulating processes that include amino acid uptake and protein biosynthesis, glucose homeostasis and fat metabolism (Wullschleger et al., 2006). mTORC1 and S6K positively regulate translation and ribosome biogenesis leading to an increase in cell mass. However, in addition to protein biogenesis, cholesterol and fatty acids are required for *de novo* membrane synthesis during cell growth. It has been shown that inhibition of mTORC1 by rapamycin treatment induces a metabolic programme that promotes the catabolism of nutrients for energy production while inhibiting energy consuming production of macromolecules (Peng et al., 2002). For example, mTORC1 activity is important for lipid accumulation during adipogenesis via regulation of PPARγ (Kim and Chen, 2004), and S6K1 mutant mice have reduced lipid levels due to increased fatty acid ß-oxidation in adipocytes (Um et al., 2004).

This raises the question whether the observed accumulation of lipid metabolites is due to inhibition of ß-oxidation of fatty acids or *de novo* lipid synthesis. Akt inhibits β-oxidation of fatty acids in the mitochondria by direct phosphorylation and inactivation of PGC1α (Li et al., 2007). PGC1α, in a complex with FoxO1, also stimulates the expression of genes involved in gluconeogenesis (Puigserver et al., 2003). Insulin mediated suppression of hepatic glucose production depends on the phosphorylation of FoxO by Akt, which disrupts the FoxO1/PGC1α complex and inhibits its transcriptional activity (Barthel and Schmoll, 2003). These data imply that the PI3K signalling pathway, through Akt and mTORC1, switches on anabolic pathways such as lipid and protein synthesis while at the same time shutting down catabolic functions like ß-oxidation that cells do not require when sufficient nutrients and energy are available.

The PI3K/Akt/mTOR pathway has been implicated in cell growth in mammalian cells (Kozma and Thomas, 2002). Akt1/Akt2 double-knockout mice exhibit severe growth deficiency (Peng et al., 2003). MEFs expressing a single allele of S6rb, in which all phosphorylatable serine residues are substituted by alanine, are significantly smaller than control MEFs (Ruvinsky et al., 2005). The results presented here show that activation of Akt causes an increase in cell volume in RPE cells (Figure 5-5). This increase is completely blocked in the presence of rapamycin, which is consistent with published data showing that the Akt-induced cell size increase is mTORC1 dependent (Edinger and Thompson, 2002). It seems obvious that an increase in cell size cannot be achieved without *de novo* membrane synthesis. Activation of lipid synthesis via activation of SREBPs could therefore be an important mechanism for the regulation of cell growth by Akt. Ectopic actiavtion of mSREBP1 is sufficient to induce an increase in cell size in RPE cells (Figure 5-6). These data suggests that activation of lipid biosynthesis contributes to cell growth and may even regulate cell growth independently of mitogenic signalling.

It has been demonstrated that induction of FAS expression and FA synthesis is mediated by PI3K/Akt signalling in H-Ras transformed MCF-10A cells (Yang et al., 2003). Swinnen et al. suggested that activation of SREBP leads to up-regulation of lipogenic genes in various types of cancer(Swinnen et al., 2002). This raises the question whether overexpression of FAS plays an active role during tumourigenesis or whether FA accumulation is simply the consequence of aberrant activation of regulatory pathways.

The metabolic differences between normal cells and cancer cells could provide a therapeutic window, which could be exploited for novel treatments. Many tumour cells have a constitutively active PI3K/Akt/mTOR pathway resulting in a high rate of glycolysis and lipid biosynthesis (Hatzivassiliou et al., 2005). Upon inhibition of metabolic pathways these tumour cells cannot adapt adequately to the induced metabolic stress, which can lead to apoptosis or necrosis in a process termed metabolic catastrophe (Jin et al., 2007).

Published data suggest the possibility of using inhibitors of cholesterol and fatty acid synthesis pathways as antitumour agents. Inhibition of FAS, which causes accumulation of malonyl-CoA, was found to induce cytotoxicity in human breast cancer (Pizer et al., 2000). Statins are drugs that lower cholesterol-levels by inhibiting HMG-CoA reductase and have been shown to have cytostatic effects and to prevent metastasis and tissue invasion (Brower, 2003).

7.4 Involvement of dSREBP in growth control in Drosophila melanogaster

In order to validate the results obtained with human cell culture *in vitro*, the involvement of SREBP in cell size regulation *in vivo* was investigated, using *Drosophila melanogaster* as a model organism.

The PI3K/Akt/mTOR pathway has been implicated in the regulation of cell and organ size in *Drosophila* (Leevers and Hafen, 2004). Activation of these pathways by insulin leads to increased protein biosynthesis and cell mass accumulation. Overexpression of dPI3K or dAkt results in increased cell and tissue growth (Verdu et al., 1999; Weinkove et al., 1999). In contrast, loss-of function mutations in the insulin receptor (inr) (Chen et al., 1996), the insulin receptor substrate (chico) (Bohni et al., 1999), dRheb (Stocker et al., 2003), dTOR (Zhang et al., 2000), and S6 kinase (dS6K) (Montagne et al., 1999) severely impair cellular growth and decrease organ size. Conversely, inactivating dPTEN or dTSC1/2 lead to an enhanced growth rate and increased cell size (Gao and Pan, 2001, Tapon, 2001 #76), which is similar to the phenotypes observed with increased dRas1 or dmyc activity (Johnston et al., 1999; Prober and Edgar, 2000). Another important downstream effector of insulin signalling is the dFoxO transcription factor. Insulin depletion promotes dFoxO-mediated reduction in cell number but not in cell size (Junger et al., 2003). dAkt seems to be the central player in controlling growth and body size in response to insulin. dAkt controls cell size by activating the dTOR/S6K pathway via phosphorylation of dTSC2 (Potter et al., 2002) and cell number by phosphorylation and inhibition of dFoxO (Junger et al., 2003). However, one report states that dTOR is not downstream of dAkt unless the PI3K pathway is highly activated (Dong and Pan, 2004). However, with the identification of Lobe, a potential homologue of PRAS40 in *Drosophila* (Sancak et al., 2007), there seem to be additional ways in which dAkt can activate dTOR.

Transient silencing of dSREBP caused a reduction in cell volume in *Drosophila* Kc162 cells and inhibited the size increase in response to TSC2 silencing (Figure 6-1). *In vivo*, silencing of dSREBP by expressing an RNAi construct targeting dSREBP resulted in a dose-dependent developmental delay, increased lethality as well as reduced body weight and size (Figure 6-3). This is consistent with recent findings showing that dSREBP is required for development beyond the third instar larval stage (Kunte et al., 2006). Silencing of dSREBP or expression of dominant negative mutants of dSREBP caused a reduction in organ size (Figure 6-4 and 6-8). This reduction in organ size is caused by a decrease in cell size rather than cell number (Table 6-2). Interestingly, expression of dominant negative or constitutive active mutants of dSREBP

also resulted in increased lethality, indicating that tight regulation of dSREBP activity is important for fly development (Figure 6-10).

Besides the well-defined role of the dPI3K/dAkt and dTSC/dTOR signal-transduction pathways in cell growth control, these pathways have also been implicated in the regulation of metabolism in *Drosophila melanogaster*. Disruption of insulin signalling in *Drosophila* results in altered glucose and lipid levels (Broughton et al., 2005; Rulifson et al., 2002). Loss of the IIS signalling antagonist dPTEN results in accumulation of active dAKT and causes the formation of highly enlarged lipid droplets in nurse cells in *Drosophila* ovaries (Vereshchagina and Wilson, 2006). *Melted* mutant flies produce 40% less fat than normal, due to lowered triglyceride production, which mimics the effect of nutrient deprivation. Melted protein can recruit dFoxO and the dTSC1/2 complex to the plasma membrane, leading to increased dTOR activity and inhibition of dFoxO function (Teleman et al., 2005). Reduction of dTOR function by the $dTOR^{7/p}$ mutant causes a decrease in lipid levels in the fat body, which could be explained by an increased utilization of lipids from pre-existing lipid stores and their conversion into ketone bodies (Luong et al., 2006). These data suggest the hypothesis that the regulation of dSREBP by the dPI3K/dAkt/dTOR pathway could be conserved in flies. Results in *Drosophila* KC162 cells, as well as in flies, indicate that activation of the dPI3K pathway leads to activation of dSREBP and expression of its target gene dFAS (Figure 6-11 and 6-12).

The physiological role of dSREBP in flies is the maintenance of fatty acid homeostasis. In *Drosophila* larvae, the main fat-accumulating tissues involved in *de novo* lipid synthesis are the fat body, oenocytes and the midgut. Oenocytes show functional similarity to human hepatocytes (Gutierrez et al., 2007). dSREBP expression is observed throughout larval development with substantial activity in these three tissues. *dSREBP* mutant larvae contain significantly less total fatty acid than wild type larvae and arrest at the end of the second larval instar (Kunte et al., 2006). From the beginning of the third instar, wild type larvae start to increase tremendously in mass (Church and Robertson, 1966). Rapidly growing larvae have a high demand for newly synthesized phospholipids for cell membrane synthesis. Therefore, the failure to provide lipids may partly explain the lethality of *dSREBP* mutant larvae prior to the transition into third instar (Kunte et al., 2006).

Humoral regulation of larval growth is controlled by the fat body (Britton et al., 2002). The dTOR pathway senses nutrients in the fat body and regulates growth of other tissues by modulating their PI3K pathway activity (Colombani et al., 2003). It would be of interest to investigate whether fat body specific silencing of dSREBP affects dTOR signalling and whether this has a cell autonomous growth effect. Oenocytes have been described to fulfil hepatocyte-like functions in the regulation of lipid metabolism (Gutierrez et al., 2007). Silencing of

dSREBP in these cells could affect lipid synthesis, storage or mobilisation as well as larval growth. Based on the proposed reciprocal signalling between oenocytes and fat body (Gutierrez et al., 2007), dSREBP activity in oenocytes could also be involved in growth control during larval development.

Our results provide evidence, both *in vitro* and at the organismal level, that dSREBP plays an essential function in dPI3K-regulated growth control during larval development and that regulation of dSREBP activity by the PI3K pathway could be conserved from fly to man.

7.5 Concluding remarks and outlook

Over the past 5 years, insight into the regulation and function of lipogenic pathways by the PI3K/Akt/mTOR pathway has been gained. The induction of expression of several enzymes involved in cholesterol and fatty acid biosynthesis by Akt requires SREBP (chapter 3). The data presented in this thesis indicate that Akt regulates SREBP activity through activation of SREBP processing. Activation of Akt results in rapid accumulation of mature SREBP1 in the nucleus and this process requires active mTORC1 (chapter 4). Furthermore, induction of glucose and amino acid uptake, lactate production as well as fatty acid and phosphoglyceride biosynthesis by Akt also requires mTORC1 activity (chapter 5). Silencing of dSREBP in *Drosophila* resulted in a significant developmental delay as well as a profound loss of viability (chapter 6). Tissue specific silencing of dSREBP in the wing resulted in a reduction in cell and organ size suggesting that activation of dSREBP by the PI3K/Akt pathway could be involved in cell growth control in flies. Therefore it can be postulated that induction of expression of lipogenic genes through activation of SREBP is part of an anabolic response to activation of the PI3K/Akt/TOR pathway and may be required for the induction of lipid biosynthesis during cell growth and proliferation (Figure 7-2).

In the future, it will be crucial to determine the mechanism of regulation of SREBP by Akt and mTORC1 and to further increase understanding of the activity of SREBP and its downstream effectors and their contribution to growth control and disease.

Rapid accumulation of mSREBP in the nucleus in response to Akt activation requires mTORC1 activity (Figure 4-6). The complexes between SREBP/SCAP and INSIG are large and it is therefore possible that their assembly and stoichiometry might influence the sorting of SREBP/SCAP into COPII vesicles. The identification of a conserved TOS motif in SREBP1 leads to the hypothesis that mTORC1 might interact with the SREBP/SCAP complex and could be involved in the ER to Golgi translocation. Therefore, it would be of interest to investigate

whether mTORC1 contributes to SREBP/SCAP complex assembly or ER/Golgi translocation. It is also possible that inhibition of mTORC1 activity results in a general block of COPII mediated ER-budding. In order to test the latter hypothesis, the localisation of SCAP-GFP and other known ER/Golgi proteins can be monitored in response to Akt activation in the absence or presence of the mTORC1 inhibitor rapamycin.

It has recently been reported that translation of the two SREBP target genes ACC and FAS is regulated by mTORC1 signalling in a PI3K/Akt-dependent manner in breast cancer cells (Yoon et al., 2007). Therefore, it is important to exclude the possibility that Akt affects SREBP translation through activation of mTORC1. mTORC1-mediated *de novo* protein synthesis is one of the most important biological consequences in response to growth factor activation and nutrient availability and it has a major contribution towards cell growth (Wullschleger et al., 2006).

Having shown that Akt induces expression of genes encoding enzymes involved in lipid biosynthesis via activation of SREBP, the question whether this also results in accumulation of products of these pathways was addressed (Figure 5-2). Although activation of Akt results in accumulation of saturated and unsaturated fatty acids as well as phosphoglycerides, it is not clear, whether this increase is due to inhibition of ß-oxidation or induction of *de novo* lipid biosynthesis, and whether the production of these metabolites requires activation of SREBP. Akt inhibits transcription factors involved in the expression of genes encoding ß-oxidation enzymes (Manning and Cantley, 2007). In order to answer these questions, the effect of SREBP silencing by RNAi on Akt-mediated lipid synthesis should be determined.

SREBP regulates expression of genes encoding enzymes for the production of lipids, which are important membrane components required for cell growth. Interestingly, activation of mSREBP1, and to a lesser extent mSREBP2, resulted in an increase in cell size, indicating that activation of SREBP itself can contribute to cell size increase (Figure 5-6). It would be relevant to investigate any regulatory feedback mechanism of activated SREBP and its target genes towards the PI3K/Akt/mTOR pathway. It has been shown that FAS activity positively regulates Akt activation in ovarian carcinoma cells (Wang et al., 2005). However, preliminary data indicate that activation of SREBP does not result in activation of Akt in RPE cells (data not shown).

Several SREBP target genes such as ACL and FAS are thought to play an important role in tumour formation and SREBPs are found up-regulated in several tumour types, including breast (Martel et al., 2006), glioblastoma (Ma et al., 2005a), prostate (Ettinger et al., 2004) and clear-cell renal carcinomas (ccRCC) (Brauweiler et al., 2007). Hypoxia, a common feature of many

cancers, has been shown to induce high levels of FAS expression (Menendez and Lupu, 2006). The yeast SREBP homologue Srel is activated in response to hypoxia and Srel responsive genes contribute to hypoxia adaptation and anaerobic growth (Hughes et al., 2005; Todd et al., 2006). In order to further increase our understanding of the contribution of lipid biosynthesis in tumour formation, it would be of great interest to investigate whether mammalian SREBPs are regulated by hypoxia.

So far, the analysis of the regulation of cell growth by the PI3K pathway has mainly focused on the PI3K effectors Akt, mTOR and S6K. mTOR and S6K positively regulate translation, ribosome biogenesis and protein biosynthesis. However, in addition to protein biogenesis, cholesterol and fatty acids are required for *de novo* membrane synthesis during cell growth. The SREBP family of transcription factors regulate expression of enzymes involved in cholesterol and fatty acid synthesis. SREBP activity is tightly controlled and involves sterol-regulated processing regulated by the ER proteins INSIG and SCAP. Transcriptional activity of nuclear SREBP is regulated by post-translational modifications as well as interactions with different co-activators.

Cell growth and proliferation require *de novo* synthesis of proteins and lipids as well as metabolites required for the synthesis of nucleic acids. The Akt/mTOR pathway mediates a cell growth response by integrating cell-intrinsic information such as nutrient availability and energy status in conjunction with extrinsic growth factor stimuli. Activation of SREBP by the PI3K/Akt/mTOR pathway could be involved in the induction of lipid biosynthesis required for the generation of biological membranes (Figure 7-2). This provides all essential resources for the cell to grow in size. The regulation of cell growth and its role in protection from apoptosis makes Akt a potent transforming factor during tumourigenesis. The work described in this thesis shows the complexity of metabolic regulation and demonstrates the importance of cross-talk between the RAS/PI3K/TOR signalling pathways and lipid metabolism. It also underlines the role of metabolism in various human diseases such as type 2 diabetes, obesity and cancer.

Figure 7-1 Model of regulation of lipid biosynthesis by Akt

Akt can regulate lipid biosynthesis on several levels. Activation of glucose uptake and induction of glycolysis is required for the generation of mitochondrial citrate. Phosphorylation and activation of ATP-citrate lyase (ACL) increases the production of cytoplasmic Acetyl-CoA, which is the substrate for Acetyl-CoA carboxylase (ACC) and fatty acid synthase (FAS). Activation of SREBP by Akt induces the expression of a number of enzymes involved in lipid biosynthesis, including ACL, FAS and ACC. Inactivation of PGCα by direct phosphorylation by Akt inhibits β-oxidation of fatty acids in the mitochondria.

Figure 7-1

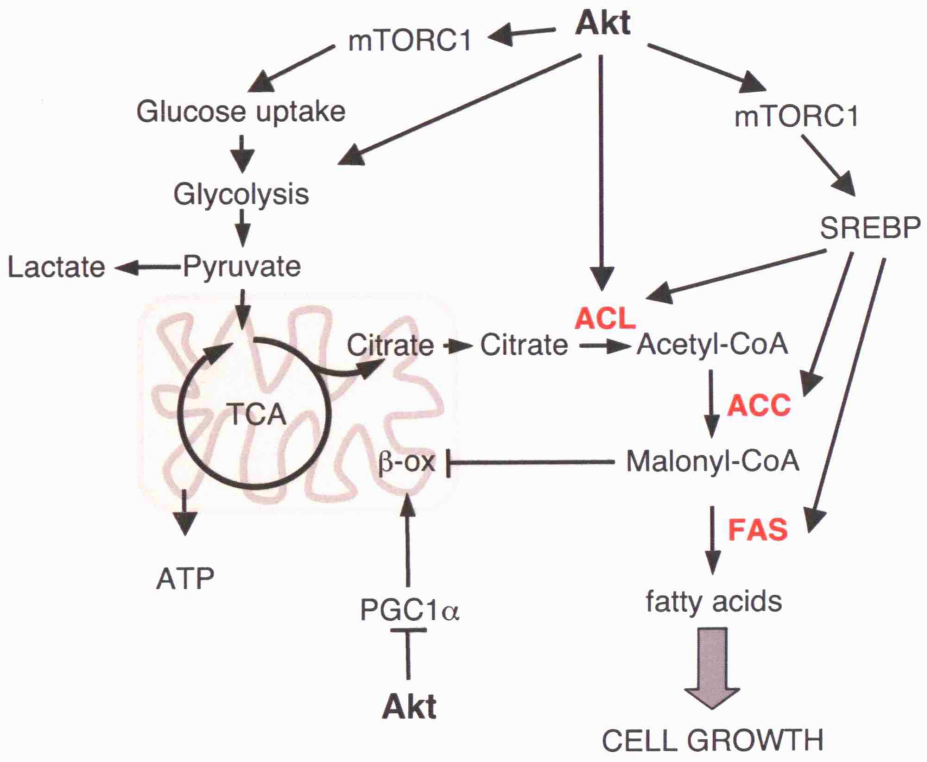
Akt
mTORC1
Glucose uptake
Glycolysis
Lactate
Pyruvate
mTORC1
SREBP
ACL
Citrate
Citrate
Acetyl-CoA
TCA
ACC
β-ox
Malonyl-CoA
FAS
ATP
PGC1α
fatty acids
Akt
CELL GROWTH

Figure 7-2 Regulation of cell growth by nutrients and mitogens

Cell growth and proliferation require *de novo* synthesis of proteins and lipids as well as metabolites required for the synthesis of nucleic acids. The Akt/mTOR pathway senses availability of nutrients as well as activation of mitogenic signalling pathways to regulate cell growth. Activation of SREBP by the Akt/mTOR pathway could be involved in the induction of lipid biosynthesis required for the generation of biological membranes.

Figure 7-2

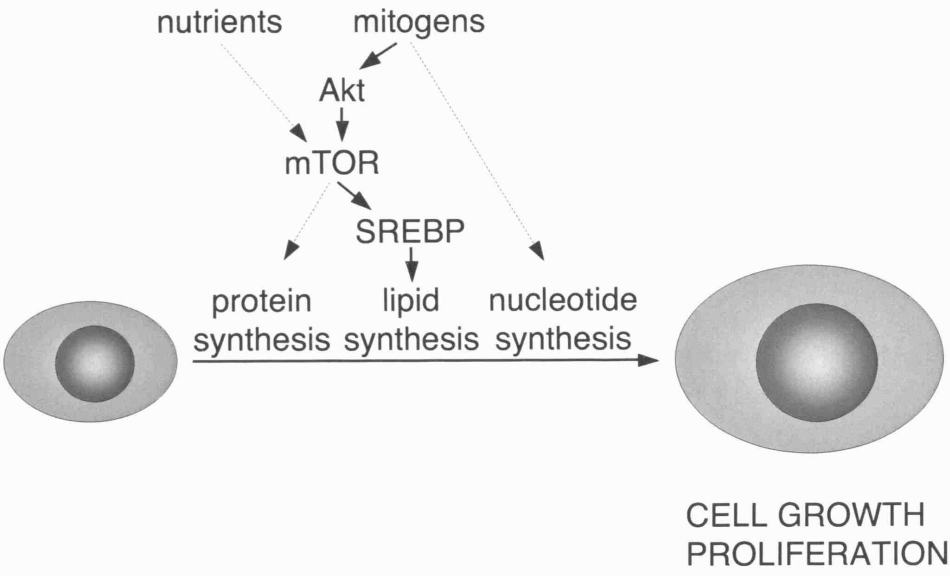
nutrients
mitogens
Akt
mTOR
SREBP
protein synthesis
lipid synthesis
nucleotide synthesis
CELL GROWTH
PROLIFERATION

8 References

Accili, D., and Arden, K.C. (2004). FoxOs at the crossroads of cellular metabolism, differentiation, and transformation. Cell *117*, 421-426.

Ahmed, N.N., Franke, T.F., Bellacosa, A., Datta, K., Gonzalez-Portal, M.E., Taguchi, T., Testa, J.R., and Tsichlis, P.N. (1993). The proteins encoded by c-akt and v-akt differ in post-translational modification, subcellular localization and oncogenic potential. Oncogene *8*, 1957-1963.

Alessi, D.R., Andjelkovic, M., Caudwell, B., Cron, P., Morrice, N., Cohen, P., and Hemmings, B.A. (1996). Mechanism of activation of protein kinase B by insulin and IGF-1. Embo J *15*, 6541-6551.

Alessi, D.R., James, S.R., Downes, C.P., Holmes, A.B., Gaffney, P.R., Reese, C.B., and Cohen, P. (1997). Characterization of a 3-phosphoinositide-dependent protein kinase which phosphorylates and activates protein kinase Balpha. Curr Biol *7*, 261-269.

Ali, I.U., Schriml, L.M., and Dean, M. (1999). Mutational spectra of PTEN/MMAC1 gene: a tumor suppressor with lipid phosphatase activity. J Natl Cancer Inst *91*, 1922-1932.

Allayee, H., Laffitte, B.A., and Lusis, A.J. (2000). Biochemistry. An absorbing study of cholesterol. Science *290*, 1709-1711.

Alo, P.L., Visca, P., Marci, A., Mangoni, A., Botti, C., and Di Tondo, U. (1996). Expression of fatty acid synthase (FAS) as a predictor of recurrence in stage I breast carcinoma patients. Cancer *77*, 474-482.

Amemiya-Kudo, M., Shimano, H., Hasty, A.H., Yahagi, N., Yoshikawa, T., Matsuzaka, T., Okazaki, H., Tamura, Y., Iizuka, Y., Ohashi, K., *et al.* (2002). Transcriptional activities of nuclear SREBP-1a, -1c, and -2 to different target promoters of lipogenic and cholesterogenic genes. J Lipid Res *43*, 1220-1235.

Amemiya-Kudo, M., Shimano, H., Yoshikawa, T., Yahagi, N., Hasty, A.H., Okazaki, H., Tamura, Y., Shionoiri, F., Iizuka, Y., Ohashi, K., *et al.* (2000). Promoter analysis of the mouse sterol regulatory element-binding protein-1c gene. J Biol Chem *275*, 31078-31085.

Andjelkovic, M., Alessi, D.R., Meier, R., Fernandez, A., Lamb, N.J., Frech, M., Cron, P., Cohen, P., Lucocq, J.M., and Hemmings, B.A. (1997). Role of translocation in the activation and function of protein kinase B. J Biol Chem *272*, 31515-31524.

Aplin, A.E., Howe, A.K., and Juliano, R.L. (1999). Cell adhesion molecules, signal transduction and cell growth. Curr Opin Cell Biol *11*, 737-744.

Arcaro, A., Khanzada, U.K., Vanhaesebroeck, B., Tetley, T.D., Waterfield, M.D., and Seckl, M.J. (2002). Two distinct phosphoinositide 3-kinases mediate polypeptide growth factor-stimulated PKB activation. Embo J *21*, 5097-5108.

Arvidsson, A.K., Rupp, E., Nanberg, E., Downward, J., Ronnstrand, L., Wennstrom, S., Schlessinger, J., Heldin, C.H., and Claesson-Welsh, L. (1994). Tyr-716 in the platelet-derived growth factor beta-receptor kinase insert is involved in GRB2 binding and Ras activation. Mol Cell Biol *14*, 6715-6726.

Attie, A.D. (2004). Insig: a significant integrator of nutrient and hormonal signals. J Clin Invest *113*, 1112-1114.

Attwell, S., Roskelley, C., and Dedhar, S. (2000). The integrin-linked kinase (ILK) suppresses anoikis. Oncogene *19*, 3811-3815.

Azzout-Marniche, D., Becard, D., Guichard, C., Foretz, M., Ferre, P., and Foufelle, F. (2000). Insulin effects on sterol regulatory-element-binding protein-1c (SREBP-1c) transcriptional activity in rat hepatocytes. Biochem J *350 Pt 2*, 389-393.

Bader, A.G., Kang, S., Zhao, L., and Vogt, P.K. (2005). Oncogenic PI3K deregulates transcription and translation. Nat Rev Cancer *5*, 921-929.

Bandyopadhyay, G., Standaert, M.L., Sajan, M.P., Kanoh, Y., Miura, A., Braun, U., Kruse, F., Leitges, M., and Farese, R.V. (2004). Protein kinase C-lambda knockout in embryonic stem cells and adipocytes impairs insulin-stimulated glucose transport. Mol Endocrinol *18*, 373-383.

Bandyopadhyay, G., Standaert, M.L., Zhao, L., Yu, B., Avignon, A., Galloway, L., Karnam, P., Moscat, J., and Farese, R.V. (1997). Activation of protein kinase C (alpha, beta, and zeta) by insulin in 3T3/L1 cells. Transfection studies suggest a role for PKC-zeta in glucose transport. J Biol Chem *272*, 2551-2558.

Banker, D.E., Mayer, S.J., Li, H.Y., Willman, C.L., Appelbaum, F.R., and Zager, R.A. (2004). Cholesterol synthesis and import contribute to protective cholesterol increments in acute myeloid leukemia cells. Blood *104*, 1816-1824.

Bao, S., and Cagan, R. (2006). Fast cloning inverted repeats for RNA interference. Rna *12*, 2020-2024.

Baron, A., Migita, T., Tang, D., and Loda, M. (2004). Fatty acid synthase: a metabolic oncogene in prostate cancer? J Cell Biochem *91*, 47-53.

Barthel, A., and Schmoll, D. (2003). Novel concepts in insulin regulation of hepatic gluconeogenesis. Am J Physiol Endocrinol Metab *285*, E685-692.

Basso, A.D., Kirschmeier, P., and Bishop, W.R. (2006). Lipid posttranslational modifications. Farnesyl transferase inhibitors. J Lipid Res *47*, 15-31.

Basu, S., Totty, N.F., Irwin, M.S., Sudol, M., and Downward, J. (2003). Akt phosphorylates the Yes-associated protein, YAP, to induce interaction with 14-3-3 and attenuation of p73-mediated apoptosis. Mol Cell *11*, 11-23.

Basu, T., Warne, P.H., and Downward, J. (1994). Role of Shc in the activation of Ras in response to epidermal growth factor and nerve growth factor. Oncogene *9*, 3483-3491.

Bauer, D.E., Hatzivassiliou, G., Zhao, F., Andreadis, C., and Thompson, C.B. (2005). ATP citrate lyase is an important component of cell growth and transformation. Oncogene *24*, 6314-6322.

Becard, D., Hainault, I., Azzout-Marniche, D., Bertry-Coussot, L., Ferre, P., and Foufelle, F. (2001). Adenovirus-mediated overexpression of sterol regulatory element binding protein-1c mimics insulin effects on hepatic gene expression and glucose homeostasis in diabetic mice. Diabetes *50*, 2425-2430.

Bellacosa, A., Chan, T.O., Ahmed, N.N., Datta, K., Malstrom, S., Stokoe, D., McCormick, F., Feng, J., and Tsichlis, P. (1998). Akt activation by growth factors is a multiple-step process: the role of the PH domain. Oncogene *17*, 313-325.

Bellacosa, A., Testa, J.R., Staal, S.P., and Tsichlis, P.N. (1991). A retroviral oncogene, akt, encoding a serine-threonine kinase containing an SH2-like region. Science *254*, 274-277.

Bengoechea-Alonso, M.T., and Ericsson, J. (2007). SREBP in signal transduction: cholesterol metabolism and beyond. Curr Opin Cell Biol *19*, 215-222.

Bennett, M.K., Lopez, J.M., Sanchez, H.B., and Osborne, T.F. (1995). Sterol regulation of fatty acid synthase promoter. Coordinate feedback regulation of two major lipid pathways. J Biol Chem *270*, 25578-25583.

Bennett, M.K., Toth, J.I., and Osborne, T.F. (2004). Selective association of sterol regulatory element-binding protein isoforms with target promoters in vivo. J Biol Chem *279*, 37360-37367.

Berwick, D.C., Hers, I., Heesom, K.J., Moule, S.K., and Tavare, J.M. (2002). The identification of ATP-citrate lyase as a protein kinase B (Akt) substrate in primary adipocytes. J Biol Chem *277*, 33895-33900.

Beuvink, I., Boulay, A., Fumagalli, S., Zilbermann, F., Ruetz, S., O'Reilly, T., Natt, F., Hall, J., Lane, H.A., and Thomas, G. (2005). The mTOR inhibitor RAD001 sensitizes tumor cells to DNA-damaged induced apoptosis through inhibition of p21 translation. Cell *120*, 747-759.

Bhaskar, P.T., and Hay, N. (2007). The two TORCs and Akt. Dev Cell *12*, 487-502.

Bittman, R. (1997). Has nature designed the cholesterol side chain for optimal interaction with phospholipids? Subcell Biochem *28*, 145-171.

Blaikie, P., Immanuel, D., Wu, J., Li, N., Yajnik, V., and Margolis, B. (1994). A region in Shc distinct from the SH2 domain can bind tyrosine-phosphorylated growth factor receptors. J Biol Chem *269*, 32031-32034.

Bobard, A., Hainault, I., Ferre, P., Foufelle, F., and Bossard, P. (2005). Differential regulation of sterol regulatory element-binding protein 1c transcriptional activity by insulin and liver X receptor during liver development. J Biol Chem *280*, 199-206.

Bodnar, A.G., Ouellette, M., Frolkis, M., Holt, S.E., Chiu, C.P., Morin, G.B., Harley, C.B., Shay, J.W., Lichtsteiner, S., and Wright, W.E. (1998). Extension of life-span by introduction of telomerase into normal human cells. Science *279*, 349-352.

Boehmer, C., Embark, H.M., Bauer, A., Palmada, M., Yun, C.H., Weinman, E.J., Endou, H., Cohen, P., Lahme, S., Bichler, K.H., *et al.* (2004). Stimulation of renal Na+ dicarboxylate cotransporter 1 by Na+/H+ exchanger regulating factor 2, serum and glucocorticoid inducible kinase isoforms, and protein kinase B. Biochem Biophys Res Commun *313*, 998-1003.

Boehmer, C., Okur, F., Setiawan, I., Broer, S., and Lang, F. (2003). Properties and regulation of glutamine transporter SN1 by protein kinases SGK and PKB. Biochem Biophys Res Commun *306*, 156-162.

Bohni, R., Riesgo-Escovar, J., Oldham, S., Brogiolo, W., Stocker, H., Andruss, B.F., Beckingham, K., and Hafen, E. (1999). Autonomous control of cell and organ size by CHICO, a Drosophila homolog of vertebrate IRS1-4. Cell *97*, 865-875.

Boriack-Sjodin, P.A., Margarit, S.M., Bar-Sagi, D., and Kuriyan, J. (1998). The structural basis of the activation of Ras by Sos. Nature *394*, 337-343.

Brand, A.H., and Perrimon, N. (1993). Targeted gene expression as a means of altering cell fates and generating dominant phenotypes. Development *118*, 401-415.

Brauweiler, A., Lorick, K.L., Lee, J.P., Tsai, Y.C., Chan, D., Weissman, A.M., Drabkin, H.A., and Gemmill, R.M. (2007). RING-dependent tumor suppression and G2/M arrest induced by the TRC8 hereditary kidney cancer gene. Oncogene *26*, 2263-2271.

Brazil, D.P., and Hemmings, B.A. (2001). Ten years of protein kinase B signalling: a hard Akt to follow. Trends Biochem Sci *26*, 657-664.

Britton, J.S., Lockwood, W.K., Li, L., Cohen, S.M., and Edgar, B.A. (2002). Drosophila's insulin/PI3-kinase pathway coordinates cellular metabolism with nutritional conditions. Dev Cell *2*, 239-249.

Brogiolo, W., Stocker, H., Ikeya, T., Rintelen, F., Fernandez, R., and Hafen, E. (2001). An evolutionarily conserved function of the Drosophila insulin receptor and insulin-like peptides in growth control. Curr Biol *11*, 213-221.

Brognard, J., Sierecki, E., Gao, T., and Newton, A.C. (2007). PHLPP and a Second Isoform, PHLPP2, Differentially Attenuate the Amplitude of Akt Signaling by Regulating Distinct Akt Isoforms. Mol Cell *25*, 917-931.

Broughton, S.J., Piper, M.D., Ikeya, T., Bass, T.M., Jacobson, J., Driege, Y., Martinez, P., Hafen, E., Withers, D.J., Leevers, S.J., *et al.* (2005). Longer lifespan, altered metabolism, and stress resistance in Drosophila from ablation of cells making insulin-like ligands. Proc Natl Acad Sci U S A *102*, 3105-3110.

Brower, V. (2003). Of cancer and cholesterol: studies elucidate anticancer mechanisms of statins. J Natl Cancer Inst *95*, 844-846.

Brown, A.J., Sun, L., Feramisco, J.D., Brown, M.S., and Goldstein, J.L. (2002). Cholesterol addition to ER membranes alters conformation of SCAP, the SREBP escort protein that regulates cholesterol metabolism. Mol Cell *10*, 237-245.

Brown, M.S., and Goldstein, J.L. (1997). The SREBP pathway: regulation of cholesterol metabolism by proteolysis of a membrane-bound transcription factor. Cell *89*, 331-340.

Brown, M.S., and Goldstein, J.L. (1999). A proteolytic pathway that controls the cholesterol content of membranes, cells, and blood. Proc Natl Acad Sci U S A *96*, 11041-11048.

Brugarolas, J., Lei, K., Hurley, R.L., Manning, B.D., Reiling, J.H., Hafen, E., Witters, L.A., Ellisen, L.W., and Kaelin, W.G., Jr. (2004). Regulation of mTOR function in response to hypoxia by REDD1 and the TSC1/TSC2 tumor suppressor complex. Genes Dev *18*, 2893-2904.

Brugge, J., Hung, M.C., and Mills, G.B. (2007). A new mutational AKTivation in the PI3K pathway. Cancer Cell *12*, 104-107.

Brunet, A., Bonni, A., Zigmond, M.J., Lin, M.Z., Juo, P., Hu, L.S., Anderson, M.J., Arden, K.C., Blenis, J., and Greenberg, M.E. (1999). Akt promotes cell survival by phosphorylating and inhibiting a Forkhead transcription factor. Cell *96*, 857-868.

Brunet, A., Datta, S.R., and Greenberg, M.E. (2001a). Transcription-dependent and -independent control of neuronal survival by the PI3K-Akt signaling pathway. Curr Opin Neurobiol *11*, 297-305.

Brunet, A., Park, J., Tran, H., Hu, L.S., Hemmings, B.A., and Greenberg, M.E. (2001b). Protein kinase SGK mediates survival signals by phosphorylating the forkhead transcription factor FKHRL1 (FOXO3a). Mol Cell Biol *21*, 952-965.

Bryant, P.J., and Simpson, P. (1984). Intrinsic and extrinsic control of growth in developing organs. Q Rev Biol *59*, 387-415.

Buday, L., and Downward, J. (1993). Epidermal growth factor regulates p21ras through the formation of a complex of receptor, Grb2 adapter protein, and Sos nucleotide exchange factor. Cell *73*, 611-620.

Buerger, C., DeVries, B., and Stambolic, V. (2006). Localization of Rheb to the endomembrane is critical for its signaling function. Biochem Biophys Res Commun *344*, 869-880.

Bui, T., and Thompson, C.B. (2006). Cancer's sweet tooth. Cancer Cell *9*, 419-420.

Burgering, B.M., and Kops, G.J. (2002). Cell cycle and death control: long live Forkheads. Trends Biochem Sci *27*, 352-360.

Burgering, B.M., Medema, R.H., Maassen, J.A., van de Wetering, M.L., van der Eb, A.J., McCormick, F., and Bos, J.L. (1991). Insulin stimulation of gene expression mediated by p21ras activation. Embo J *10*, 1103-1109.

Byfield, M.P., Murray, J.T., and Backer, J.M. (2005). hVps34 is a nutrient-regulated lipid kinase required for activation of p70 S6 kinase. J Biol Chem *280*, 33076-33082.

Cagen, L.M., Deng, X., Wilcox, H.G., Park, E.A., Raghow, R., and Elam, M.B. (2005). Insulin activates the rat sterol-regulatory-element-binding protein 1c (SREBP-1c) promoter through the

combinatorial actions of SREBP, LXR, Sp-1 and NF-Y cis-acting elements. Biochem J *385*, 207-216.

Calera, M.R., Martinez, C., Liu, H., Jack, A.K., Birnbaum, M.J., and Pilch, P.F. (1998). Insulin increases the association of Akt-2 with Glut4-containing vesicles. J Biol Chem *273*, 7201-7204.

Cantley, L.C. (2002). The phosphoinositide 3-kinase pathway. Science *296*, 1655-1657.

Cantley, L.C., and Neel, B.G. (1999). New insights into tumor suppression: PTEN suppresses tumor formation by restraining the phosphoinositide 3-kinase/AKT pathway. Proc Natl Acad Sci U S A *96*, 4240-4245.

Capdevila, J., and Guerrero, I. (1994). Targeted expression of the signaling molecule decapentaplegic induces pattern duplications and growth alterations in Drosophila wings. Embo J *13*, 4459-4468.

Cardone, M.H., Roy, N., Stennicke, H.R., Salvesen, G.S., Franke, T.F., Stanbridge, E., Frisch, S., and Reed, J.C. (1998). Regulation of cell death protease caspase-9 by phosphorylation. Science *282*, 1318-1321.

Carpten, J.D., Faber, A.L., Horn, C., Donoho, G.P., Briggs, S.L., Robbins, C.M., Hostetter, G., Boguslawski, S., Moses, T.Y., Savage, S., *et al.* (2007). A transforming mutation in the pleckstrin homology domain of AKT1 in cancer. Nature.

Castro, A.F., Rebhun, J.F., Clark, G.J., and Quilliam, L.A. (2003). Rheb binds tuberous sclerosis complex 2 (TSC2) and promotes S6 kinase activation in a rapamycin- and farnesylation-dependent manner. J Biol Chem *278*, 32493-32496.

Chakravarty, K., Leahy, P., Becard, D., Hakimi, P., Foretz, M., Ferre, P., Foufelle, F., and Hanson, R.W. (2001). Sterol regulatory element-binding protein-1c mimics the negative effect of insulin on phosphoenolpyruvate carboxykinase (GTP) gene transcription. J Biol Chem *276*, 34816-34823.

Chan, S. (2004). Targeting the mammalian target of rapamycin (mTOR): a new approach to treating cancer. Br J Cancer *91*, 1420-1424.

Chan, S., Scheulen, M.E., Johnston, S., Mross, K., Cardoso, F., Dittrich, C., Eiermann, W., Hess, D., Morant, R., Semiglazov, V., *et al.* (2005). Phase II study of temsirolimus (CCI-779), a novel inhibitor of mTOR, in heavily pretreated patients with locally advanced or metastatic breast cancer. J Clin Oncol *23*, 5314-5322.

Chan, T.O., Rittenhouse, S.E., and Tsichlis, P.N. (1999). AKT/PKB and other D3 phosphoinositide-regulated kinases: kinase activation by phosphoinositide-dependent phosphorylation. Annu Rev Biochem *68*, 965-1014.

Chen, C., Jack, J., and Garofalo, R.S. (1996). The Drosophila insulin receptor is required for normal growth. Endocrinology *137*, 846-856.

Chen, G., Liang, G., Ou, J., Goldstein, J.L., and Brown, M.S. (2004). Central role for liver X receptor in insulin-mediated activation of Srebp-1c transcription and stimulation of fatty acid synthesis in liver. Proc Natl Acad Sci U S A *101*, 11245-11250.

Chi, M.M., Pusateri, M.E., Carter, J.G., Norris, B.J., McDougal, D.B., Jr., and Lowry, O.H. (1987). Enzymatic assays for 2-deoxyglucose and 2-deoxyglucose 6-phosphate. Anal Biochem *161*, 508-513.

Chirala, S.S., Chang, H., Matzuk, M., Abu-Elheiga, L., Mao, J., Mahon, K., Finegold, M., and Wakil, S.J. (2003). Fatty acid synthesis is essential in embryonic development: fatty acid synthase null mutants and most of the heterozygotes die in utero. Proc Natl Acad Sci U S A *100*, 6358-6363.

Church, R.B., and Robertson, F.W. (1966). Biochemical analysis of genetic differences in the growth of Drosophila. Genet Res *7*, 383-407.

Coffer, P.J., and Woodgett, J.R. (1991). Molecular cloning and characterisation of a novel putative protein-serine kinase related to the cAMP-dependent and protein kinase C families. European journal of biochemistry / FEBS *201*, 475-481.

Cohen, P., and Frame, S. (2001). The renaissance of GSK3. Nat Rev Mol Cell Biol *2*, 769-776.

Cohen, S., Bate, M., and Martinez-Arias, A. (1993). "Imaginal disc development" The Development of Drosophila melanogaster. Cold Spring Harbor Laboratory Press, Cold Spring Harbor, 747-842.

Colombani, J., Raisin, S., Pantalacci, S., Radimerski, T., Montagne, J., and Leopold, P. (2003). A nutrient sensor mechanism controls Drosophila growth. Cell *114*, 739-749.

Crackower, M.A., Oudit, G.Y., Kozieradzki, I., Sarao, R., Sun, H., Sasaki, T., Hirsch, E., Suzuki, A., Shioi, T., Irie-Sasaki, J., *et al.* (2002). Regulation of myocardial contractility and cell size by distinct PI3K-PTEN signaling pathways. Cell *110*, 737-749.

Cross, D.A., Alessi, D.R., Cohen, P., Andjelkovich, M., and Hemmings, B.A. (1995). Inhibition of glycogen synthase kinase-3 by insulin mediated by protein kinase B. Nature *378*, 785-789.

Crozatier, M., Glise, B., and Vincent, A. (2004). Patterns in evolution: veins of the Drosophila wing. Trends Genet *20*, 498-505.

Cumming, G., Fidler, F., and Vaux, D.L. (2007). Error bars in experimental biology. J Cell Biol *177*, 7-11.

Darzynkiewicz, Z., and Bedner, E. (2000). Analysis of apoptotic cells by flow and laser scanning cytometry. Methods in enzymology *322*, 18-39.

Datta, S., and Osborne, T.F. (2005). Activation domains from both monomers contribute to transcriptional stimulation by sterol regulatory element-binding protein dimers. J Biol Chem *280*, 3338-3345.

Datta, S.R., Dudek, H., Tao, X., Masters, S., Fu, H., Gotoh, Y., and Greenberg, M.E. (1997). Akt phosphorylation of BAD couples survival signals to the cell-intrinsic death machinery. Cell *91*, 231-241.

Datta, S.R., Katsov, A., Hu, L., Petros, A., Fesik, S.W., Yaffe, M.B., and Greenberg, M.E. (2000). 14-3-3 proteins and survival kinases cooperate to inactivate BAD by BH3 domain phosphorylation. Mol Cell *6*, 41-51.

Day, S.J., and Lawrence, P.A. (2000). Measuring dimensions: the regulation of size and shape. Development *127*, 2977-2987.

De Virgilio, C., and Loewith, R. (2006). Cell growth control: little eukaryotes make big contributions. Oncogene *25*, 6392-6415.

DeBose-Boyd, R.A., Ou, J., Goldstein, J.L., and Brown, M.S. (2001). Expression of sterol regulatory element-binding protein 1c (SREBP-1c) mRNA in rat hepatoma cells requires endogenous LXR ligands. Proc Natl Acad Sci U S A *98*, 1477-1482.

del Peso, L., Gonzalez-Garcia, M., Page, C., Herrera, R., and Nunez, G. (1997). Interleukin-3-induced phosphorylation of BAD through the protein kinase Akt. Science *278*, 687-689.

Demierre, M.F., Higgins, P.D., Gruber, S.B., Hawk, E., and Lippman, S.M. (2005). Statins and cancer prevention. Nat Rev Cancer *5*, 930-942.

Deng, X., Cagen, L.M., Wilcox, H.G., Park, E.A., Raghow, R., and Elam, M.B. (2002). Regulation of the rat SREBP-1c promoter in primary rat hepatocytes. Biochem Biophys Res Commun *290*, 256-262.

Deng, X., Yellaturu, C., Cagen, L., Wilcox, H.G., Park, E.A., Raghow, R., and Elam, M.B. (2007). Expression of the rat sterol regulatory element binding protein-1c gene in response to insulin is mediated by increased transactivating capacity of specificity protein 1 (Sp1). J Biol Chem.

Dennis, P.B., Jaeschke, A., Saitoh, M., Fowler, B., Kozma, S.C., and Thomas, G. (2001). Mammalian TOR: a homeostatic ATP sensor. Science *294*, 1102-1105.

Desai, B.N., Myers, B.R., and Schreiber, S.L. (2002). FKBP12-rapamycin-associated protein associates with mitochondria and senses osmotic stress via mitochondrial dysfunction. Proc Natl Acad Sci U S A *99*, 4319-4324.

Devasahayam, G., Ritz, D., Helliwell, S.B., Burke, D.J., and Sturgill, T.W. (2006). Pmr1, a Golgi Ca2+/Mn2+-ATPase, is a regulator of the target of rapamycin (TOR) signaling pathway in yeast. Proc Natl Acad Sci U S A *103*, 17840-17845.

Di Cristofano, A., Pesce, B., Cordon-Cardo, C., and Pandolfi, P.P. (1998). Pten is essential for embryonic development and tumour suppression. Nat Genet *19*, 348-355.

Diehl, J.A., Cheng, M., Roussel, M.F., and Sherr, C.J. (1998). Glycogen synthase kinase-3beta regulates cyclin D1 proteolysis and subcellular localization. Genes Dev *12*, 3499-3511.

Dignam, J.D., Martin, P.L., Shastry, B.S., and Roeder, R.G. (1983). Eukaryotic gene transcription with purified components. Methods in enzymology *101*, 582-598.

Dijkers, P.F., Birkenkamp, K.U., Lam, E.W., Thomas, N.S., Lammers, J.W., Koenderman, L., and Coffer, P.J. (2002). FKHR-L1 can act as a critical effector of cell death induced by cytokine withdrawal: protein kinase B-enhanced cell survival through maintenance of mitochondrial integrity. J Cell Biol *156*, 531-542.

Dobrosotskaya, I.Y., Seegmiller, A.C., Brown, M.S., Goldstein, J.L., and Rawson, R.B. (2002). Regulation of SREBP processing and membrane lipid production by phospholipids in Drosophila. Science *296*, 879-883.

Domin, J., Pages, F., Volinia, S., Rittenhouse, S.E., Zvelebil, M.J., Stein, R.C., and Waterfield, M.D. (1997). Cloning of a human phosphoinositide 3-kinase with a C2 domain that displays reduced sensitivity to the inhibitor wortmannin. Biochem J *326 (Pt 1)*, 139-147.

Dong, J., and Pan, D. (2004). Tsc2 is not a critical target of Akt during normal Drosophila development. Genes Dev *18*, 2479-2484.

Downward, J. (2004). PI 3-kinase, Akt and cell survival. Semin Cell Dev Biol *15*, 177-182.

Drenan, R.M., Liu, X., Bertram, P.G., and Zheng, X.F. (2004). FKBP12-rapamycin-associated protein or mammalian target of rapamycin (FRAP/mTOR) localization in the endoplasmic reticulum and the Golgi apparatus. J Biol Chem *279*, 772-778.

Du, K., Herzig, S., Kulkarni, R.N., and Montminy, M. (2003). TRB3: a tribbles homolog that inhibits Akt/PKB activation by insulin in liver. Science *300*, 1574-1577.

Du, X., Kristiana, I., Wong, J., and Brown, A.J. (2006). Involvement of Akt in ER-to-Golgi Transport of SCAP/SREBP: A Link between a Key Cell Proliferative Pathway and Membrane Synthesis. Mol Biol Cell.

Duffy, J.B. (2002). GAL4 system in Drosophila: a fly geneticist's Swiss army knife. Genesis *34*, 1-15.

Dummler, B., and Hemmings, B.A. (2007). Physiological roles of PKB/Akt isoforms in development and disease. Biochem Soc Trans *35*, 231-235.

Durr, G., Strayle, J., Plemper, R., Elbs, S., Klee, S.K., Catty, P., Wolf, D.H., and Rudolph, H.K. (1998). The medial-Golgi ion pump Pmr1 supplies the yeast secretory pathway with Ca2+ and Mn2+ required for glycosylation, sorting, and endoplasmic reticulum-associated protein degradation. Mol Biol Cell *9*, 1149-1162.

Eberle, D., Hegarty, B., Bossard, P., Ferre, P., and Foufelle, F. (2004). SREBP transcription factors: master regulators of lipid homeostasis. Biochimie *86*, 839-848.

Edgar, B.A. (2006). How flies get their size: genetics meets physiology. Nat Rev Genet *7*, 907-916.

Edinger, A.L. (2007). Controlling cell growth and survival through regulated nutrient transporter expression. Biochem J *406*, 1-12.

Edinger, A.L., and Thompson, C.B. (2002). Akt maintains cell size and survival by increasing mTOR-dependent nutrient uptake. Mol Biol Cell *13*, 2276-2288.

Eguez, L., Lee, A., Chavez, J.A., Miinea, C.P., Kane, S., Lienhard, G.E., and McGraw, T.E. (2005). Full intracellular retention of GLUT4 requires AS160 Rab GTPase activating protein. Cell Metab *2*, 263-272.

Engelman, J.A., Luo, J., and Cantley, L.C. (2006). The evolution of phosphatidylinositol 3-kinases as regulators of growth and metabolism. Nat Rev Genet *7*, 606-619.

Eskelinen, E.L., Prescott, A.R., Cooper, J., Brachmann, S.M., Wang, L., Tang, X., Backer, J.M., and Lucocq, J.M. (2002). Inhibition of autophagy in mitotic animal cells. Traffic *3*, 878-893.

Ettinger, S.L., Sobel, R., Whitmore, T.G., Akbari, M., Bradley, D.R., Gleave, M.E., and Nelson, C.C. (2004). Dysregulation of sterol response element-binding proteins and downstream effectors in prostate cancer during progression to androgen independence. Cancer Res *64*, 2212-2221.

Faridi, J., Fawcett, J., Wang, L., and Roth, R.A. (2003). Akt promotes increased mammalian cell size by stimulating protein synthesis and inhibiting protein degradation. Am J Physiol Endocrinol Metab *285*, E964-972.

Fingar, D.C., Salama, S., Tsou, C., Harlow, E., and Blenis, J. (2002). Mammalian cell size is controlled by mTOR and its downstream targets S6K1 and 4EBP1/eIF4E. Genes Dev *16*, 1472-1487.

Fleischmann, M., and Iynedjian, P.B. (2000). Regulation of sterol regulatory-element binding protein 1 gene expression in liver: role of insulin and protein kinase B/cAkt. Biochem J *349*, 13-17.

Fonseca, B.D., Smith, E.M., Lee, V.H., Mackintosh, C., and Proud, C.G. (2007). PRAS40 is a target for mammalian target of rapamycin complex 1 and is required for signaling downstream of this complex. J Biol Chem.

Foretz, M., Guichard, C., Ferre, P., and Foufelle, F. (1999a). Sterol regulatory element binding protein-1c is a major mediator of insulin action on the hepatic expression of glucokinase and lipogenesis-related genes. Proc Natl Acad Sci U S A *96*, 12737-12742.

Foretz, M., Pacot, C., Dugail, I., Lemarchand, P., Guichard, C., Le Liepvre, X., Berthelier-Lubrano, C., Spiegelman, B., Kim, J.B., Ferre, P., *et al.* (1999b). ADD1/SREBP-1c is required in the activation of hepatic lipogenic gene expression by glucose. Mol Cell Biol *19*, 3760-3768.

Frisch, S.M., and Screaton, R.A. (2001). Anoikis mechanisms. Curr Opin Cell Biol *13*, 555-562.

Fulton, D., Gratton, J.P., McCabe, T.J., Fontana, J., Fujio, Y., Walsh, K., Franke, T.F., Papapetropoulos, A., and Sessa, W.C. (1999). Regulation of endothelium-derived nitric oxide production by the protein kinase Akt. Nature *399*, 597-601.

Gaidarov, I., Smith, M.E., Domin, J., and Keen, J.H. (2001). The class II phosphoinositide 3-kinase C2alpha is activated by clathrin and regulates clathrin-mediated membrane trafficking. Mol Cell *7*, 443-449.

Gao, T., Furnari, F., and Newton, A.C. (2005). PHLPP: a phosphatase that directly dephosphorylates Akt, promotes apoptosis, and suppresses tumor growth. Mol Cell *18*, 13-24.

Gao, X., and Pan, D. (2001). TSC1 and TSC2 tumor suppressors antagonize insulin signaling in cell growth. Genes Dev *15*, 1383-1392.

Garami, A., Zwartkruis, F.J., Nobukuni, T., Joaquin, M., Roccio, M., Stocker, H., Kozma, S.C., Hafen, E., Bos, J.L., and Thomas, G. (2003). Insulin activation of Rheb, a mediator of mTOR/S6K/4E-BP signaling, is inhibited by TSC1 and 2. Mol Cell *11*, 1457-1466.

Giancotti, F.G., and Ruoslahti, E. (1999). Integrin signaling. Science *285*, 1028-1032.

Goberdhan, D.C., Paricio, N., Goodman, E.C., Mlodzik, M., and Wilson, C. (1999). Drosophila tumor suppressor PTEN controls cell size and number by antagonizing the Chico/PI3-kinase signaling pathway. Genes Dev *13*, 3244-3258.

Goldstein, J.L., and Brown, M.S. (1990). Regulation of the mevalonate pathway. Nature *343*, 425-430.

Goldstein, J.L., Rawson, R.B., and Brown, M.S. (2002). Mutant mammalian cells as tools to delineate the sterol regulatory element-binding protein pathway for feedback regulation of lipid synthesis. Arch Biochem Biophys *397*, 139-148.

Gong, Y., Lee, J.N., Lee, P.C., Goldstein, J.L., Brown, M.S., and Ye, J. (2006). Sterol-regulated ubiquitination and degradation of Insig-1 creates a convergent mechanism for feedback control of cholesterol synthesis and uptake. Cell Metab *3*, 15-24.

Gottlob, K., Majewski, N., Kennedy, S., Kandel, E., Robey, R.B., and Hay, N. (2001). Inhibition of early apoptotic events by Akt/PKB is dependent on the first committed step of glycolysis and mitochondrial hexokinase. Genes Dev *15*, 1406-1418.

Graff, J.R., Konicek, B.W., McNulty, A.M., Wang, Z., Houck, K., Allen, S., Paul, J.D., Hbaiu, A., Goode, R.G., Sandusky, G.E., *et al.* (2000). Increased AKT activity contributes to prostate cancer progression by dramatically accelerating prostate tumor growth and diminishing p27Kip1 expression. J Biol Chem *275*, 24500-24505.

Graziani, A., Gramaglia, D., dalla Zonca, P., and Comoglio, P.M. (1993). Hepatocyte growth factor/scatter factor stimulates the Ras-guanine nucleotide exchanger. J Biol Chem *268*, 9165-9168.

Gu, H., Maeda, H., Moon, J.J., Lord, J.D., Yoakim, M., Nelson, B.H., and Neel, B.G. (2000). New role for Shc in activation of the phosphatidylinositol 3-kinase/Akt pathway. Mol Cell Biol *20*, 7109-7120.

Gu, J., Tamura, M., Pankov, R., Danen, E.H., Takino, T., Matsumoto, K., and Yamada, K.M. (1999). Shc and FAK differentially regulate cell motility and directionality modulated by PTEN. J Cell Biol *146*, 389-403.

Gual, P., Gremeaux, T., Gonzalez, T., Le Marchand-Brustel, Y., and Tanti, J.F. (2003). MAP kinases and mTOR mediate insulin-induced phosphorylation of insulin receptor substrate-1 on serine residues 307, 612 and 632. Diabetologia *46*, 1532-1542.

Guan, K.L., Figueroa, C., Brtva, T.R., Zhu, T., Taylor, J., Barber, T.D., and Vojtek, A.B. (2000). Negative regulation of the serine/threonine kinase B-Raf by Akt. J Biol Chem *275*, 27354-27359.

Guarente, L., and Kenyon, C. (2000). Genetic pathways that regulate ageing in model organisms. Nature *408*, 255-262.

Guillet-Deniau, I., Pichard, A.L., Kone, A., Esnous, C., Nieruchalski, M., Girard, J., and Prip-Buus, C. (2004). Glucose induces de novo lipogenesis in rat muscle satellite cells through a sterol-regulatory-element-binding-protein-1c-dependent pathway. J Cell Sci *117*, 1937-1944.

Gupta, S., Ramjaun, A.R., Haiko, P., Wang, Y., Warne, P.H., Nicke, B., Nye, E., Stamp, G., Alitalo, K., and Downward, J. (2007). Binding of ras to phosphoinositide 3-kinase p110alpha is required for ras-driven tumorigenesis in mice. Cell *129*, 957-968.

Gutierrez, E., Wiggins, D., Fielding, B., and Gould, A.P. (2007). Specialized hepatocyte-like cells regulate Drosophila lipid metabolism. Nature *445*, 275-280.

Haas-Kogan, D., Shalev, N., Wong, M., Mills, G., Yount, G., and Stokoe, D. (1998). Protein kinase B (PKB/Akt) activity is elevated in glioblastoma cells due to mutation of the tumor suppressor PTEN/MMAC. Curr Biol *8*, 1195-1198.

Hager, M.H., Solomon, K.R., and Freeman, M.R. (2006). The role of cholesterol in prostate cancer. Curr Opin Clin Nutr Metab Care *9*, 379-385.

Hahn-Windgassen, A., Nogueira, V., Chen, C.C., Skeen, J.E., Sonenberg, N., and Hay, N. (2005). Akt activates the mammalian target of rapamycin by regulating cellular ATP level and AMPK activity. J Biol Chem *280*, 32081-32089.

Hall, D.J., Grewal, S.S., de la Cruz, A.F., and Edgar, B.A. (2007). Rheb-TOR signaling promotes protein synthesis, but not glucose or amino acid import, in Drosophila. BMC Biol *5*, 10.

Han, J., Luby-Phelps, K., Das, B., Shu, X., Xia, Y., Mosteller, R.D., Krishna, U.M., Falck, J.R., White, M.A., and Broek, D. (1998). Role of substrates and products of PI 3-kinase in regulating activation of Rac-related guanosine triphosphatases by Vav. Science *279*, 558-560.

Hancock, J.F., Magee, A.I., Childs, J.E., and Marshall, C.J. (1989). All ras proteins are polyisoprenylated but only some are palmitoylated. Cell *57*, 1167-1177.

Hannah, V.C., Ou, J., Luong, A., Goldstein, J.L., and Brown, M.S. (2001). Unsaturated fatty acids down-regulate srebp isoforms 1a and 1c by two mechanisms in HEK-293 cells. J Biol Chem *276*, 4365-4372.

Hanzal-Bayer, M.F., and Hancock, J.F. (2007). Lipid rafts and membrane traffic. FEBS Lett *581*, 2098-2104.

Hardie, D.G. (2005). New roles for the LKB1-->AMPK pathway. Curr Opin Cell Biol *17*, 167-173.

Harmer, S.L., and DeFranco, A.L. (1997). Shc contains two Grb2 binding sites needed for efficient formation of complexes with SOS in B lymphocytes. Mol Cell Biol *17*, 4087-4095.

Harrington, L.S., Findlay, G.M., Gray, A., Tolkacheva, T., Wigfield, S., Rebholz, H., Barnett, J., Leslie, N.R., Cheng, S., Shepherd, P.R., *et al.* (2004). The TSC1-2 tumor suppressor controls insulin-PI3K signaling via regulation of IRS proteins. J Cell Biol *166*, 213-223.

Harrington, L.S., Findlay, G.M., and Lamb, R.F. (2005). Restraining PI3K: mTOR signalling goes back to the membrane. Trends Biochem Sci *30*, 35-42.

Hatzivassiliou, G., Zhao, F., Bauer, D.E., Andreadis, C., Shaw, A.N., Dhanak, D., Hingorani, S.R., Tuveson, D.A., and Thompson, C.B. (2005). ATP citrate lyase inhibition can suppress tumor cell growth. Cancer Cell *8*, 311-321.

Hay, N., and Sonenberg, N. (2004). Upstream and downstream of mTOR. Genes Dev *18*, 1926-1945.

Heemers, H., Maes, B., Foufelle, F., Heyns, W., Verhoeven, G., and Swinnen, J.V. (2001). Androgens stimulate lipogenic gene expression in prostate cancer cells by activation of the sterol regulatory element-binding protein cleavage activating protein/sterol regulatory element-binding protein pathway. Mol Endocrinol *15*, 1817-1828.

Hegarty, B.D., Bobard, A., Hainault, I., Ferre, P., Bossard, P., and Foufelle, F. (2005). Distinct roles of insulin and liver X receptor in the induction and cleavage of sterol regulatory element-binding protein-1c. Proc Natl Acad Sci U S A *102*, 791-796.

Hemminki, A., Markie, D., Tomlinson, I., Avizienyte, E., Roth, S., Loukola, A., Bignell, G., Warren, W., Aminoff, M., Hoglund, P., *et al.* (1998). A serine/threonine kinase gene defective in Peutz-Jeghers syndrome. Nature *391*, 184-187.

Hietakangas, V., and Cohen, S.M. (2007). Re-evaluating AKT regulation: role of TOR complex 2 in tissue growth. Genes Dev *21*, 632-637.

Hirano, Y., Yoshida, M., Shimizu, M., and Sato, R. (2001). Direct demonstration of rapid degradation of nuclear sterol regulatory element-binding proteins by the ubiquitin-proteasome pathway. J Biol Chem *276*, 36431-36437.

Horton, J.D. (2002). Sterol regulatory element-binding proteins: transcriptional activators of lipid synthesis. Biochem Soc Trans *30*, 1091-1095.

Horton, J.D., Bashmakov, Y., Shimomura, I., and Shimano, H. (1998). Regulation of sterol regulatory element binding proteins in livers of fasted and refed mice. Proc Natl Acad Sci U S A *95*, 5987-5992.

Horton, J.D., Goldstein, J.L., and Brown, M.S. (2002). SREBPs: activators of the complete program of cholesterol and fatty acid synthesis in the liver. J Clin Invest *109*, 1125-1131.

Horton, J.D., Shah, N.A., Warrington, J.A., Anderson, N.N., Park, S.W., Brown, M.S., and Goldstein, J.L. (2003). Combined analysis of oligonucleotide microarray data from transgenic and knockout mice identifies direct SREBP target genes. Proc Natl Acad Sci U S A *100*, 12027-12032.

Hresko, R.C., and Mueckler, M. (2005). mTOR.RICTOR is the Ser473 kinase for Akt/protein kinase B in 3T3-L1 adipocytes. J Biol Chem *280*, 40406-40416.

Hua, X., Sakai, J., Ho, Y.K., Goldstein, J.L., and Brown, M.S. (1995). Hairpin orientation of sterol regulatory element-binding protein-2 in cell membranes as determined by protease protection. J Biol Chem *270*, 29422-29427.

Hughes, A.L., Todd, B.L., and Espenshade, P.J. (2005). SREBP pathway responds to sterols and functions as an oxygen sensor in fission yeast. Cell *120*, 831-842.

Hutti, J.E., Jarrell, E.T., Chang, J.D., Abbott, D.W., Storz, P., Toker, A., Cantley, L.C., and Turk, B.E. (2004). A rapid method for determining protein kinase phosphorylation specificity. Nat Methods *1*, 27-29.

Ikeya, T., Galic, M., Belawat, P., Nairz, K., and Hafen, E. (2002). Nutrient-dependent expression of insulin-like peptides from neuroendocrine cells in the CNS contributes to growth regulation in Drosophila. Curr Biol *12*, 1293-1300.

Inoki, K., Li, Y., Xu, T., and Guan, K.L. (2003a). Rheb GTPase is a direct target of TSC2 GAP activity and regulates mTOR signaling. Genes Dev *17*, 1829-1834.

Inoki, K., Li, Y., Zhu, T., Wu, J., and Guan, K.L. (2002). TSC2 is phosphorylated and inhibited by Akt and suppresses mTOR signalling. Nat Cell Biol *4*, 648-657.

Inoki, K., Ouyang, H., Zhu, T., Lindvall, C., Wang, Y., Zhang, X., Yang, Q., Bennett, C., Harada, Y., Stankunas, K., *et al.* (2006). TSC2 integrates Wnt and energy signals via a coordinated phosphorylation by AMPK and GSK3 to regulate cell growth. Cell *126*, 955-968.

Inoki, K., Zhu, T., and Guan, K.L. (2003b). TSC2 mediates cellular energy response to control cell growth and survival. Cell *115*, 577-590.

Inoue, N., Shimano, H., Nakakuki, M., Matsuzaka, T., Nakagawa, Y., Yamamoto, T., Sato, R., Takahashi, A., Sone, H., Yahagi, N., *et al.* (2005). Lipid synthetic transcription factor SREBP-1a activates p21WAF1/CIP1, a universal cyclin-dependent kinase inhibitor. Mol Cell Biol *25*, 8938-8947.

Jacinto, E., Facchinetti, V., Liu, D., Soto, N., Wei, S., Jung, S.Y., Huang, Q., Qin, J., and Su, B. (2006). SIN1/MIP1 Maintains rictor-mTOR Complex Integrity and Regulates Akt Phosphorylation and Substrate Specificity. Cell.

Janowski, B.A., Grogan, M.J., Jones, S.A., Wisely, G.B., Kliewer, S.A., Corey, E.J., and Mangelsdorf, D.J. (1999). Structural requirements of ligands for the oxysterol liver X receptors LXRalpha and LXRbeta. Proc Natl Acad Sci U S A *96*, 266-271.

Jiang, K., Zhong, B., Gilvary, D.L., Corliss, B.C., Hong-Geller, E., Wei, S., and Djeu, J.Y. (2000). Pivotal role of phosphoinositide-3 kinase in regulation of cytotoxicity in natural killer cells. Nat Immunol *1*, 419-425.

Jimenez, C., Jones, D.R., Rodriguez-Viciana, P., Gonzalez-Garcia, A., Leonardo, E., Wennstrom, S., von Kobbe, C., Toran, J.L., L, R.B., Calvo, V., *et al.* (1998). Identification and

characterization of a new oncogene derived from the regulatory subunit of phosphoinositide 3-kinase. Embo J *17*, 743-753.

Jimenez, C., Portela, R.A., Mellado, M., Rodriguez-Frade, J.M., Collard, J., Serrano, A., Martinez, A.C., Avila, J., and Carrera, A.C. (2000). Role of the PI3K regulatory subunit in the control of actin organization and cell migration. J Cell Biol *151*, 249-262.

Jin, S., DiPaola, R.S., Mathew, R., and White, E. (2007). Metabolic catastrophe as a means to cancer cell death. J Cell Sci *120*, 379-383.

Johnston, L.A., Prober, D.A., Edgar, B.A., Eisenman, R.N., and Gallant, P. (1999). Drosophila myc regulates cellular growth during development. Cell *98*, 779-790.

Jones, K.A., Jiang, X., Yamamoto, Y., and Yeung, R.S. (2004). Tuberin is a component of lipid rafts and mediates caveolin-1 localization: role of TSC2 in post-Golgi transport. Experimental cell research *295*, 512-524.

Jones, P.F., Jakubowicz, T., Pitossi, F.J., Maurer, F., and Hemmings, B.A. (1991). Molecular cloning and identification of a serine/threonine protein kinase of the second-messenger subfamily. Proc Natl Acad Sci U S A *88*, 4171-4175.

Joseph, S.B., Laffitte, B.A., Patel, P.H., Watson, M.A., Matsukuma, K.E., Walczak, R., Collins, J.L., Osborne, T.F., and Tontonoz, P. (2002). Direct and indirect mechanisms for regulation of fatty acid synthase gene expression by liver X receptors. J Biol Chem *277*, 11019-11025.

Junger, M.A., Rintelen, F., Stocker, H., Wasserman, J.D., Vegh, M., Radimerski, T., Greenberg, M.E., and Hafen, E. (2003). The Drosophila forkhead transcription factor FOXO mediates the reduction in cell number associated with reduced insulin signaling. J Biol *2*, 20.

Kallin, A., Johannessen, L.E., Cani, P.D., Marbehant, C.Y., Essaghir, A., Foufelle, F., Ferre, P., Heldin, C.H., Delzenne, N.M., and Demoulin, J.B. (2007). SREBP1 regulates the expression of heme oxygenase 1 and the phosphatidylinositol-3 kinase regulatory subunit p55gamma. J Lipid Res.

Katso, R., Okkenhaug, K., Ahmadi, K., White, S., Timms, J., and Waterfield, M.D. (2001). Cellular function of phosphoinositide 3-kinases: implications for development, homeostasis, and cancer. Annu Rev Cell Dev Biol *17*, 615-675.

Khwaja, A., Rodriguez-Viciana, P., Wennstrom, S., Warne, P.H., and Downward, J. (1997). Matrix adhesion and Ras transformation both activate a phosphoinositide 3-OH kinase and protein kinase B/Akt cellular survival pathway. Embo J *16*, 2783-2793.

Kihara, A., Noda, T., Ishihara, N., and Ohsumi, Y. (2001). Two distinct Vps34 phosphatidylinositol 3-kinase complexes function in autophagy and carboxypeptidase Y sorting in Saccharomyces cerevisiae. J Cell Biol *152*, 519-530.

Kim, D.H., Sarbassov, D.D., Ali, S.M., King, J.E., Latek, R.R., Erdjument-Bromage, H., Tempst, P., and Sabatini, D.M. (2002). mTOR interacts with raptor to form a nutrient-sensitive complex that signals to the cell growth machinery. Cell *110*, 163-175.

Kim, J.B., Sarraf, P., Wright, M., Yao, K.M., Mueller, E., Solanes, G., Lowell, B.B., and Spiegelman, B.M. (1998). Nutritional and insulin regulation of fatty acid synthetase and leptin gene expression through ADD1/SREBP1. J Clin Invest *101*, 1-9.

Kim, J.B., and Spiegelman, B.M. (1996). ADD1/SREBP1 promotes adipocyte differentiation and gene expression linked to fatty acid metabolism. Genes Dev *10*, 1096-1107.

Kim, J.B., Spotts, G.D., Halvorsen, Y.D., Shih, H.M., Ellenberger, T., Towle, H.C., and Spiegelman, B.M. (1995). Dual DNA binding specificity of ADD1/SREBP1 controlled by a single amino acid in the basic helix-loop-helix domain. Mol Cell Biol *15*, 2582-2588.

Kim, J.E., and Chen, J. (2000). Cytoplasmic-nuclear shuttling of FKBP12-rapamycin-associated protein is involved in rapamycin-sensitive signaling and translation initiation. Proc Natl Acad Sci U S A *97*, 14340-14345.

Kim, J.E., and Chen, J. (2004). regulation of peroxisome proliferator-activated receptor-gamma activity by mammalian target of rapamycin and amino acids in adipogenesis. Diabetes *53*, 2748-2756.

Kim, K.H., Song, M.J., Yoo, E.J., Choe, S.S., Park, S.D., and Kim, J.B. (2004). Regulatory role of glycogen synthase kinase 3 for transcriptional activity of ADD1/SREBP1c. J Biol Chem *279*, 51999-52006.

Kiyokawa, E., Hashimoto, Y., Kurata, T., Sugimura, H., and Matsuda, M. (1998). Evidence that DOCK180 up-regulates signals from the CrkII-p130(Cas) complex. J Biol Chem *273*, 24479-24484.

Klausner, R.D., Donaldson, J.G., and Lippincott-Schwartz, J. (1992). Brefeldin A: insights into the control of membrane traffic and organelle structure. J Cell Biol *116*, 1071-1080.

Kohn, A.D., Barthel, A., Kovacina, K.S., Boge, A., Wallach, B., Summers, S.A., Birnbaum, M.J., Scott, P.H., Lawrence, J.C., Jr., and Roth, R.A. (1998). Construction and characterization of a conditionally active version of the serine/threonine kinase Akt. J Biol Chem *273*, 11937-11943.

Kohn, A.D., Summers, S.A., Birnbaum, M.J., and Roth, R.A. (1996). Expression of a constitutively active Akt Ser/Thr kinase in 3T3-L1 adipocytes stimulates glucose uptake and glucose transporter 4 translocation. J Biol Chem *271*, 31372-31378.

Kolch, W. (2000). Meaningful relationships: the regulation of the Ras/Raf/MEK/ERK pathway by protein interactions. Biochem J *351 Pt 2*, 289-305.

Kops, G.J., de Ruiter, N.D., De Vries-Smits, A.M., Powell, D.R., Bos, J.L., and Burgering, B.M. (1999). Direct control of the Forkhead transcription factor AFX by protein kinase B. Nature *398*, 630-634.

Kops, G.J., Medema, R.H., Glassford, J., Essers, M.A., Dijkers, P.F., Coffer, P.J., Lam, E.W., and Burgering, B.M. (2002). Control of cell cycle exit and entry by protein kinase B-regulated forkhead transcription factors. Mol Cell Biol *22*, 2025-2036.

Kotani, K., Ogawa, W., Matsumoto, M., Kitamura, T., Sakaue, H., Hino, Y., Miyake, K., Sano, W., Akimoto, K., Ohno, S., *et al.* (1998). Requirement of atypical protein kinase clambda for insulin stimulation of glucose uptake but not for Akt activation in 3T3-L1 adipocytes. Mol Cell Biol *18*, 6971-6982.

Kotzka, J., Muller-Wieland, D., Koponen, A., Njamen, D., Kremer, L., Roth, G., Munck, M., Knebel, B., and Krone, W. (1998). ADD1/SREBP-1c mediates insulin-induced gene expression linked to the MAP kinase pathway. Biochem Biophys Res Commun *249*, 375-379.

Kotzka, J., Muller-Wieland, D., Roth, G., Kremer, L., Munck, M., Schurmann, S., Knebel, B., and Krone, W. (2000). Sterol regulatory element binding proteins (SREBP)-1a and SREBP-2 are linked to the MAP-kinase cascade. J Lipid Res *41*, 99-108.

Kozma, S.C., and Thomas, G. (2002). Regulation of cell size in growth, development and human disease: PI3K, PKB and S6K. Bioessays *24*, 65-71.

Kuhajda, F.P. (2000). Fatty-acid synthase and human cancer: new perspectives on its role in tumor biology. Nutrition *16*, 202-208.

Kuhajda, F.P., Pizer, E.S., Li, J.N., Mani, N.S., Frehywot, G.L., and Townsend, C.A. (2000). Synthesis and antitumor activity of an inhibitor of fatty acid synthase. Proc Natl Acad Sci U S A *97*, 3450-3454.

Kulkarni, M.M., Booker, M., Silver, S.J., Friedman, A., Hong, P., Perrimon, N., and Mathey-Prevot, B. (2006). Evidence of off-target effects associated with long dsRNAs in Drosophila melanogaster cell-based assays. Nat Methods *3*, 833-838.

Kunte, A.S., Matthews, K.A., and Rawson, R.B. (2006). Fatty acid auxotrophy in Drosophila larvae lacking SREBP. Cell Metab *3*, 439-448.

Kurlawalla-Martinez, C., Stiles, B., Wang, Y., Devaskar, S.U., Kahn, B.B., and Wu, H. (2005). Insulin hypersensitivity and resistance to streptozotocin-induced diabetes in mice lacking PTEN in adipose tissue. Mol Cell Biol *25*, 2498-2510.

Kwiatkowski, D.J. (2003). Rhebbing up mTOR: new insights on TSC1 and TSC2, and the pathogenesis of tuberous sclerosis. Cancer Biol Ther *2*, 471-476.

Kwon, J., Lee, S.R., Yang, K.S., Ahn, Y., Kim, Y.J., Stadtman, E.R., and Rhee, S.G. (2004). Reversible oxidation and inactivation of the tumor suppressor PTEN in cells stimulated with peptide growth factors. Proc Natl Acad Sci U S A *101*, 16419-16424.

Lacasa, D., Le Liepvre, X., Ferre, P., and Dugail, I. (2001). Progesterone stimulates adipocyte determination and differentiation 1/sterol regulatory element-binding protein 1c gene expression. potential mechanism for the lipogenic effect of progesterone in adipose tissue. J Biol Chem *276*, 11512-11516.

Land, S.C., and Tee, A.R. (2007). Hypoxia inducible factor 1alpha is regulated by the mammalian target of rapamycin (mTOR) via an mTOR-signalling motif. J Biol Chem.

Latasa, M.J., Griffin, M.J., Moon, Y.S., Kang, C., and Sul, H.S. (2003). Occupancy and function of the -150 sterol regulatory element and -65 E-box in nutritional regulation of the fatty acid synthase gene in living animals. Mol Cell Biol *23*, 5896-5907.

Latasa, M.J., Moon, Y.S., Kim, K.H., and Sul, H.S. (2000). Nutritional regulation of the fatty acid synthase promoter in vivo: sterol regulatory element binding protein functions through an upstream region containing a sterol regulatory element. Proc Natl Acad Sci U S A *97*, 10619-10624.

Lee, G., and Chung, J. (2007). Discrete functions of rictor and raptor in cell growth regulation in Drosophila. Biochem Biophys Res Commun *357*, 1154-1159.

Lee, Y.S., and Carthew, R.W. (2003). Making a better RNAi vector for Drosophila: use of intron spacers. Methods (San Diego, Calif *30*, 322-329.

Leevers, S.J., and Hafen, E. (2004). Growth Regulation by Insulin and TOR Signaling in Drosophila. Cold Spring Harbor Laboratory Press, 167-192.

Leevers, S.J., and McNeill, H. (2005). Controlling the size of organs and organisms. Curr Opin Cell Biol *17*, 604-609.

Leevers, S.J., Weinkove, D., MacDougall, L.K., Hafen, E., and Waterfield, M.D. (1996). The Drosophila phosphoinositide 3-kinase Dp110 promotes cell growth. Embo J *15*, 6584-6594.

Li, N., Batzer, A., Daly, R., Yajnik, V., Skolnik, E., Chardin, P., Bar-Sagi, D., Margolis, B., and Schlessinger, J. (1993). Guanine-nucleotide-releasing factor hSos1 binds to Grb2 and links receptor tyrosine kinases to Ras signalling. Nature *363*, 85-88.

Li, X., Monks, B., Ge, Q., and Birnbaum, M.J. (2007). Akt/PKB regulates hepatic metabolism by directly inhibiting PGC-1alpha transcription coactivator. Nature *447*, 1012-1016.

Li, Y., Corradetti, M.N., Inoki, K., and Guan, K.L. (2004). TSC2: filling the GAP in the mTOR signaling pathway. Trends Biochem Sci *29*, 32-38.

Li, Y., Inoki, K., Vacratsis, P., and Guan, K.L. (2003). The p38 and MK2 kinase cascade phosphorylates tuberin, the tuberous sclerosis 2 gene product, and enhances its interaction with 14-3-3. J Biol Chem *278*, 13663-13671.

Liliental, J., Moon, S.Y., Lesche, R., Mamillapalli, R., Li, D., Zheng, Y., Sun, H., and Wu, H. (2000). Genetic deletion of the Pten tumor suppressor gene promotes cell motility by activation of Rac1 and Cdc42 GTPases. Curr Biol *10*, 401-404.

Lim, K.H., Baines, A.T., Fiordalisi, J.J., Shipitsin, M., Feig, L.A., Cox, A.D., Der, C.J., and Counter, C.M. (2005). Activation of RalA is critical for Ras-induced tumorigenesis of human cells. Cancer Cell *7*, 533-545.

Lin, J., Puigserver, P., Donovan, J., Tarr, P., and Spiegelman, B.M. (2002). Peroxisome proliferator-activated receptor gamma coactivator 1beta (PGC-1beta), a novel PGC-1-related transcription coactivator associated with host cell factor. J Biol Chem *277*, 1645-1648.

Lin, J., Yang, R., Tarr, P.T., Wu, P.H., Handschin, C., Li, S., Yang, W., Pei, L., Uldry, M., Tontonoz, P., *et al.* (2005). Hyperlipidemic effects of dietary saturated fats mediated through PGC-1beta coactivation of SREBP. Cell *120*, 261-273.

Littlewood, T.D., Hancock, D.C., Danielian, P.S., Parker, M.G., and Evan, G.I. (1995). A modified oestrogen receptor ligand-binding domain as an improved switch for the regulation of heterologous proteins. Nucleic Acids Res *23*, 1686-1690.

Liu, L., Cash, T.P., Jones, R.G., Keith, B., Thompson, C.B., and Simon, M.C. (2006). Hypoxia-induced energy stress regulates mRNA translation and cell growth. Mol Cell *21*, 521-531.

Liu, X., and Zheng, X.F. (2007). Endoplasmic reticulum and Golgi localization sequences for mammalian target of rapamycin. Mol Biol Cell *18*, 1073-1082.

Livak, K.J., and Schmittgen, T.D. (2001). Analysis of relative gene expression data using real-time quantitative PCR and the 2(-Delta Delta C(T)) Method. Methods (San Diego, Calif *25*, 402-408.

Lizcano, J.M., Alrubaie, S., Kieloch, A., Deak, M., Leevers, S.J., and Alessi, D.R. (2003). Insulin-induced Drosophila S6 kinase activation requires phosphoinositide 3-kinase and protein kinase B. Biochem J *374*, 297-306.

Loewith, R., Jacinto, E., Wullschleger, S., Lorberg, A., Crespo, J.L., Bonenfant, D., Oppliger, W., Jenoe, P., and Hall, M.N. (2002). Two TOR complexes, only one of which is rapamycin sensitive, have distinct roles in cell growth control. Mol Cell *10*, 457-468.

Lowy, D.R., and Willumsen, B.M. (1993). Function and regulation of ras. Annu Rev Biochem *62*, 851-891.

Lu, M., and Shyy, J.Y. (2005). Sterol Regulatory Element-Binding Protein 1 Is Negatively Modulated by Protein Kinase A Phosphorylation. Am J Physiol Cell Physiol.

Lum, J.J., Bui, T., Gruber, M., Gordan, J.D., DeBerardinis, R.J., Covello, K.L., Simon, M.C., and Thompson, C.B. (2007). The transcription factor HIF-1alpha plays a critical role in the growth factor-dependent regulation of both aerobic and anaerobic glycolysis. Genes Dev *21*, 1037-1049.

Luo, J., Manning, B.D., and Cantley, L.C. (2003). Targeting the PI3K-Akt pathway in human cancer: rationale and promise. Cancer Cell *4*, 257-262.

Luo, J., Sobkiw, C.L., Hirshman, M.F., Logsdon, M.N., Li, T.Q., Goodyear, L.J., and Cantley, L.C. (2006). Loss of class I(A) PI3K signaling in muscle leads to impaired muscle growth, insulin response, and hyperlipidemia. Cell Metab *3*, 355-366.

Luong, N., Davies, C.R., Wessells, R.J., Graham, S.M., King, M.T., Veech, R., Bodmer, R., and Oldham, S.M. (2006). Activated FOXO-mediated insulin resistance is blocked by reduction of TOR activity. Cell Metab *4*, 133-142.

Ma, D., Nutt, C.L., Shanehsaz, P., Peng, X., Louis, D.N., and Kaetzel, D.M. (2005a). Autocrine platelet-derived growth factor-dependent gene expression in glioblastoma cells is mediated largely by activation of the transcription factor sterol regulatory element binding protein and is

associated with altered genotype and patient survival in human brain tumors. Cancer Res *65*, 5523-5534.

Ma, L., Chen, Z., Erdjument-Bromage, H., Tempst, P., and Pandolfi, P.P. (2005b). Phosphorylation and functional inactivation of TSC2 by Erk implications for tuberous sclerosis and cancer pathogenesis. Cell *121*, 179-193.

Ma, Y.Y., Wei, S.J., Lin, Y.C., Lung, J.C., Chang, T.C., Whang-Peng, J., Liu, J.M., Yang, D.M., Yang, W.K., and Shen, C.Y. (2000). PIK3CA as an oncogene in cervical cancer. Oncogene *19*, 2739-2744.

Maehama, T., and Dixon, J.E. (1998). The tumor suppressor, PTEN/MMAC1, dephosphorylates the lipid second messenger, phosphatidylinositol 3,4,5-trisphosphate. J Biol Chem *273*, 13375-13378.

Magana, M.M., and Osborne, T.F. (1996). Two tandem binding sites for sterol regulatory element binding proteins are required for sterol regulation of fatty-acid synthase promoter. J Biol Chem *271*, 32689-32694.

Maira, S.M., Galetic, I., Brazil, D.P., Kaech, S., Ingley, E., Thelen, M., and Hemmings, B.A. (2001). Carboxyl-terminal modulator protein (CTMP), a negative regulator of PKB/Akt and v-Akt at the plasma membrane. Science *294*, 374-380.

Majewski, N., Nogueira, V., Bhaskar, P., Coy, P.E., Skeen, J.E., Gottlob, K., Chandel, N.S., Thompson, C.B., Robey, R.B., and Hay, N. (2004). Hexokinase-mitochondria interaction mediated by Akt is required to inhibit apoptosis in the presence or absence of Bax and Bak. Mol Cell *16*, 819-830.

Malumbres, M., and Barbacid, M. (2003). RAS oncogenes: the first 30 years. Nat Rev Cancer *3*, 459-465.

Manning, B.D., and Cantley, L.C. (2003). Rheb fills a GAP between TSC and TOR. Trends Biochem Sci *28*, 573-576.

Manning, B.D., and Cantley, L.C. (2007). AKT/PKB Signaling: Navigating Downstream. Cell *129*, 1261-1274.

Margarit, S.M., Sondermann, H., Hall, B.E., Nagar, B., Hoelz, A., Pirruccello, M., Bar-Sagi, D., and Kuriyan, J. (2003). Structural evidence for feedback activation by Ras.GTP of the Ras-specific nucleotide exchange factor SOS. Cell *112*, 685-695.

Marquez, D.C., Chen, H.W., Curran, E.M., Welshons, W.V., and Pietras, R.J. (2006). Estrogen receptors in membrane lipid rafts and signal transduction in breast cancer. Mol Cell Endocrinol *246*, 91-100.

Martel, P.M., Bingham, C.M., McGraw, C.J., Baker, C.L., Morganelli, P.M., Meng, M.L., Armstrong, J.M., Moncur, J.T., and Kinlaw, W.B. (2006). S14 protein in breast cancer cells: direct evidence of regulation by SREBP-1c, superinduction with progestin, and effects on cell growth. Experimental cell research *312*, 278-288.

Martin, G.A., Viskochil, D., Bollag, G., McCabe, P.C., Crosier, W.J., Haubruck, H., Conroy, L., Clark, R., O'Connell, P., Cawthon, R.M., *et al.* (1990). The GAP-related domain of the neurofibromatosis type 1 gene product interacts with ras p21. Cell *63*, 843-849.

Massion, P.P., Kuo, W.L., Stokoe, D., Olshen, A.B., Treseler, P.A., Chin, K., Chen, C., Polikoff, D., Jain, A.N., Pinkel, D., *et al.* (2002). Genomic copy number analysis of non-small cell lung cancer using array comparative genomic hybridization: implications of the phosphatidylinositol 3-kinase pathway. Cancer Res *62*, 3636-3640.

Mastick, C.C., Brady, M.J., and Saltiel, A.R. (1995). Insulin stimulates the tyrosine phosphorylation of caveolin. J Cell Biol *129*, 1523-1531.

Matsumoto, M., Ogawa, W., Akimoto, K., Inoue, H., Miyake, K., Furukawa, K., Hayashi, Y., Iguchi, H., Matsuki, Y., Hiramatsu, R., *et al.* (2003). PKClambda in liver mediates insulin-induced SREBP-1c expression and determines both hepatic lipid content and overall insulin sensitivity. J Clin Invest *112*, 935-944.

Maurer, U., Charvet, C., Wagman, A.S., Dejardin, E., and Green, D.R. (2006). Glycogen Synthase Kinase-3 Regulates Mitochondrial Outer Membrane Permeabilization and Apoptosis by Destabilization of MCL-1. Mol Cell *21*, 749-760.

Mayer, C., and Grummt, I. (2006). Ribosome biogenesis and cell growth: mTOR coordinates transcription by all three classes of nuclear RNA polymerases. Oncogene *25*, 6384-6391.

Mayo, L.D., and Donner, D.B. (2001). A phosphatidylinositol 3-kinase/Akt pathway promotes translocation of Mdm2 from the cytoplasm to the nucleus. Proc Natl Acad Sci U S A *98*, 11598-11603.

McKay, R.M., McKay, J.P., Avery, L., and Graff, J.M. (2003). C elegans: a model for exploring the genetics of fat storage. Dev Cell *4*, 131-142.

McMullen, J.R., Shioi, T., Huang, W.Y., Zhang, L., Tarnavski, O., Bisping, E., Schinke, M., Kong, S., Sherwood, M.C., Brown, J., *et al.* (2004). The insulin-like growth factor 1 receptor induces physiological heart growth via the phosphoinositide 3-kinase(p110alpha) pathway. J Biol Chem *279*, 4782-4793.

Medema, R.H., Kops, G.J., Bos, J.L., and Burgering, B.M. (2000). AFX-like Forkhead transcription factors mediate cell-cycle regulation by Ras and PKB through p27kip1. Nature *404*, 782-787.

Menendez, J.A., and Lupu, R. (2004). Fatty acid synthase-catalyzed de novo fatty acid biosynthesis: from anabolic-energy-storage pathway in normal tissues to jack-of-all-trades in cancer cells. Arch Immunol Ther Exp (Warsz) *52*, 414-426.

Menendez, J.A., and Lupu, R. (2006). Oncogenic properties of the endogenous fatty acid metabolism: molecular pathology of fatty acid synthase in cancer cells. Curr Opin Clin Nutr Metab Care *9*, 346-357.

Miljan, E.A., and Bremer, E.G. (2002). Regulation of growth factor receptors by gangliosides. Sci STKE *2002*, RE15.

Mirza, A.M., Kohn, A.D., Roth, R.A., and McMahon, M. (2000). Oncogenic transformation of cells by a conditionally active form of the protein kinase Akt/PKB. Cell Growth Differ *11*, 279-292.

Mitin, N., Rossman, K.L., and Der, C.J. (2005). Signaling interplay in Ras superfamily function. Curr Biol *15*, R563-574.

Mitro, N., Mak, P.A., Vargas, L., Godio, C., Hampton, E., Molteni, V., Kreusch, A., and Saez, E. (2007). The nuclear receptor LXR is a glucose sensor. Nature *445*, 219-223.

Montagne, J., Stewart, M.J., Stocker, H., Hafen, E., Kozma, S.C., and Thomas, G. (1999). Drosophila S6 kinase: a regulator of cell size. Science *285*, 2126-2129.

Moscatello, D.K., Holgado-Madruga, M., Emlet, D.R., Montgomery, R.B., and Wong, A.J. (1998). Constitutive activation of phosphatidylinositol 3-kinase by a naturally occurring mutant epidermal growth factor receptor. J Biol Chem *273*, 200-206.

Myers, M.P., Pass, I., Batty, I.H., Van der Kaay, J., Stolarov, J.P., Hemmings, B.A., Wigler, M.H., Downes, C.P., and Tonks, N.K. (1998). The lipid phosphatase activity of PTEN is critical for its tumor supressor function. Proc Natl Acad Sci U S A *95*, 13513-13518.

Nadeau, K.J., Leitner, J.W., Gurerich, I., and Draznin, B. (2004). Insulin regulation of sterol regulatory element-binding protein-1 expression in L-6 muscle cells and 3T3 L1 adipocytes. J Biol Chem *279*, 34380-34387.

Nagai, H., Noguchi, T., Takeda, K., and Ichijo, H. (2007). Pathophysiological roles of ASK1-MAP kinase signaling pathways. J Biochem Mol Biol *40*, 1-6.

Nateri, A.S., Riera-Sans, L., Da Costa, C., and Behrens, A. (2004). The ubiquitin ligase SCFFbw7 antagonizes apoptotic JNK signaling. Science *303*, 1374-1378.

Nebenfuhr, A., Ritzenthaler, C., and Robinson, D.G. (2002). Brefeldin A: deciphering an enigmatic inhibitor of secretion. Plant Physiol *130*, 1102-1108.

Neufeld, T.P. (2007). TOR Regulation: Sorting out the Answers. Cell Metab *5*, 3-5.

Neufeld, T.P., de la Cruz, A.F., Johnston, L.A., and Edgar, B.A. (1998). Coordination of growth and cell division in the Drosophila wing. Cell *93*, 1183-1193.

Nobukuni, T., Joaquin, M., Roccio, M., Dann, S.G., Kim, S.Y., Gulati, P., Byfield, M.P., Backer, J.M., Natt, F., Bos, J.L., *et al.* (2005). Amino acids mediate mTOR/raptor signaling through activation of class 3 phosphatidylinositol 3OH-kinase. Proc Natl Acad Sci U S A *102*, 14238-14243.

Nojima, H., Tokunaga, C., Eguchi, S., Oshiro, N., Hidayat, S., Yoshino, K., Hara, K., Tanaka, N., Avruch, J., and Yonezawa, K. (2003). The mammalian target of rapamycin (mTOR) partner, raptor, binds the mTOR substrates p70 S6 kinase and 4E-BP1 through their TOR signaling (TOS) motif. J Biol Chem *278*, 15461-15464.

O'Reilly, K.E., Rojo, F., She, Q.B., Solit, D., Mills, G.B., Smith, D., Lane, H., Hofmann, F., Hicklin, D.J., Ludwig, D.L., *et al.* (2006). mTOR inhibition induces upstream receptor tyrosine kinase signaling and activates Akt. Cancer Res *66*, 1500-1508.

Obata, T., Yaffe, M.B., Leparc, G.G., Piro, E.T., Maegawa, H., Kashiwagi, A., Kikkawa, R., and Cantley, L.C. (2000). Peptide and protein library screening defines optimal substrate motifs for AKT/PKB. J Biol Chem *275*, 36108-36115.

Ohanna, M., Sobering, A.K., Lapointe, T., Lorenzo, L., Praud, C., Petroulakis, E., Sonenberg, N., Kelly, P.A., Sotiropoulos, A., and Pende, M. (2005). Atrophy of S6K1(-/-) skeletal muscle cells reveals distinct mTOR effectors for cell cycle and size control. Nat Cell Biol *7*, 286-294.

Oldham, S., and Hafen, E. (2003). Insulin/IGF and target of rapamycin signaling: a TOR de force in growth control. Trends Cell Biol *13*, 79-85.

Oldham, S., Montagne, J., Radimerski, T., Thomas, G., and Hafen, E. (2000). Genetic and biochemical characterization of dTOR, the Drosophila homolog of the target of rapamycin. Genes Dev *14*, 2689-2694.

Ono, F., Nakagawa, T., Saito, S., Owada, Y., Sakagami, H., Goto, K., Suzuki, M., Matsuno, S., and Kondo, H. (1998). A novel class II phosphoinositide 3-kinase predominantly expressed in the liver and its enhanced expression during liver regeneration. J Biol Chem *273*, 7731-7736.

Ono, H., Shimano, H., Katagiri, H., Yahagi, N., Sakoda, H., Onishi, Y., Anai, M., Ogihara, T., Fujishiro, M., Viana, A.Y., *et al.* (2003). Hepatic Akt activation induces marked hypoglycemia, hepatomegaly, and hypertriglyceridemia with sterol regulatory element binding protein involvement. Diabetes *52*, 2905-2913.

Oshiro, N., Takahashi, R., Yoshino, K.I., Tanimura, K., Nakashima, A., Eguchi, S., Miyamoto, T., Hara, K., Takehana, K., Avruch, J., *et al.* (2007). The proline-Rich Akt substrate of 40 kDa (PRAS40) is a physiological substrate of mTOR complex 1. J Biol Chem.

Ou, J., Tu, H., Shan, B., Luk, A., DeBose-Boyd, R.A., Bashmakov, Y., Goldstein, J.L., and Brown, M.S. (2001). Unsaturated fatty acids inhibit transcription of the sterol regulatory element-binding protein-1c (SREBP-1c) gene by antagonizing ligand-dependent activation of the LXR. Proc Natl Acad Sci U S A *98*, 6027-6032.

Ozes, O.N., Mayo, L.D., Gustin, J.A., Pfeffer, S.R., Pfeffer, L.M., and Donner, D.B. (1999). NF-kappaB activation by tumour necrosis factor requires the Akt serine-threonine kinase. Nature *401*, 82-85.

Pai, J.T., Brown, M.S., and Goldstein, J.L. (1996). Purification and cDNA cloning of a second apoptosis-related cysteine protease that cleaves and activates sterol regulatory element binding proteins. Proc Natl Acad Sci U S A *93*, 5437-5442.

Palmada, M., Speil, A., Jeyaraj, S., Bohmer, C., and Lang, F. (2005). The serine/threonine kinases SGK1, 3 and PKB stimulate the amino acid transporter ASCT2. Biochem Biophys Res Commun *331*, 272-277.

Park, J., Leong, M.L., Buse, P., Maiyar, A.C., Firestone, G.L., and Hemmings, B.A. (1999). Serum and glucocorticoid-inducible kinase (SGK) is a target of the PI 3-kinase-stimulated signaling pathway. Embo J *18*, 3024-3033.

Parton, R.G., and Simons, K. (2007). The multiple faces of caveolae. Nat Rev Mol Cell Biol *8*, 185-194.

Patel, P.H., Thapar, N., Guo, L., Martinez, M., Maris, J., Gau, C.L., Lengyel, J.A., and Tamanoi, F. (2003). Drosophila Rheb GTPase is required for cell cycle progression and cell growth. J Cell Sci *116*, 3601-3610.

Pawson, T., and Nash, P. (2003). Assembly of cell regulatory systems through protein interaction domains. Science *300*, 445-452.

Pearl, L.H., and Barford, D. (2002). Regulation of protein kinases in insulin, growth factor and Wnt signalling. Curr Opin Struct Biol *12*, 761-767.

Pende, M., Kozma, S.C., Jaquet, M., Oorschot, V., Burcelin, R., Le Marchand-Brustel, Y., Klumperman, J., Thorens, B., and Thomas, G. (2000). Hypoinsulinaemia, glucose intolerance and diminished beta-cell size in S6K1-deficient mice. Nature *408*, 994-997.

Pende, M., Um, S.H., Mieulet, V., Sticker, M., Goss, V.L., Mestan, J., Mueller, M., Fumagalli, S., Kozma, S.C., and Thomas, G. (2004). S6K1(-/-)/S6K2(-/-) mice exhibit perinatal lethality and rapamycin-sensitive 5'-terminal oligopyrimidine mRNA translation and reveal a mitogen-activated protein kinase-dependent S6 kinase pathway. Mol Cell Biol *24*, 3112-3124.

Peng, T., Golub, T.R., and Sabatini, D.M. (2002). The immunosuppressant rapamycin mimics a starvation-like signal distinct from amino acid and glucose deprivation. Mol Cell Biol *22*, 5575-5584.

Peng, X.D., Xu, P.Z., Chen, M.L., Hahn-Windgassen, A., Skeen, J., Jacobs, J., Sundararajan, D., Chen, W.S., Crawford, S.E., Coleman, K.G., *et al.* (2003). Dwarfism, impaired skin development, skeletal muscle atrophy, delayed bone development, and impeded adipogenesis in mice lacking Akt1 and Akt2. Genes Dev *17*, 1352-1365.

Perez-Sala, D. (2007). Protein isoprenylation in biology and disease: general overview and perspectives from studies with genetically engineered animals. Front Biosci *12*, 4456-4472.

Persad, S., Attwell, S., Gray, V., Delcommenne, M., Troussard, A., Sanghera, J., and Dedhar, S. (2000). Inhibition of integrin-linked kinase (ILK) suppresses activation of protein kinase B/Akt and induces cell cycle arrest and apoptosis of PTEN-mutant prostate cancer cells. Proc Natl Acad Sci U S A *97*, 3207-3212.

Philp, A.J., Campbell, I.G., Leet, C., Vincan, E., Rockman, S.P., Whitehead, R.H., Thomas, R.J., and Phillips, W.A. (2001). The phosphatidylinositol 3'-kinase p85alpha gene is an oncogene in human ovarian and colon tumors. Cancer Res *61*, 7426-7429.

Pizer, E.S., Lax, S.F., Kuhajda, F.P., Pasternack, G.R., and Kurman, R.J. (1998). Fatty acid synthase expression in endometrial carcinoma: correlation with cell proliferation and hormone receptors. Cancer *83*, 528-537.

Pizer, E.S., Thupari, J., Han, W.F., Pinn, M.L., Chrest, F.J., Frehywot, G.L., Townsend, C.A., and Kuhajda, F.P. (2000). Malonyl-coenzyme-A is a potential mediator of cytotoxicity induced by fatty-acid synthase inhibition in human breast cancer cells and xenografts. Cancer Res *60*, 213-218.

Plas, D.R., and Thompson, C.B. (2005). Akt-dependent transformation: there is more to growth than just surviving. Oncogene *24*, 7435-7442.

Pore, N., Liu, S., Shu, H.K., Li, B., Haas-Kogan, D., Stokoe, D., Milanini-Mongiat, J., Pages, G., O'Rourke, D.M., Bernhard, E., *et al.* (2004). Sp1 is involved in Akt-mediated induction of VEGF expression through an HIF-1-independent mechanism. Mol Biol Cell *15*, 4841-4853.

Porstmann, T., Griffiths, B., Chung, Y.L., Delpuech, O., Griffiths, J.R., Downward, J., and Schulze, A. (2005). PKB/Akt induces transcription of enzymes involved in cholesterol and fatty acid biosynthesis via activation of SREBP. Oncogene *24*, 6465-6481.

Potter, C.J., Huang, H., and Xu, T. (2001). Drosophila Tsc1 functions with Tsc2 to antagonize insulin signaling in regulating cell growth, cell proliferation, and organ size. Cell *105*, 357-368.

Potter, C.J., Pedraza, L.G., and Xu, T. (2002). Akt regulates growth by directly phosphorylating Tsc2. Nat Cell Biol *4*, 658-665.

Prober, D.A., and Edgar, B.A. (2000). Ras1 promotes cellular growth in the Drosophila wing. Cell *100*, 435-446.

Pruitt, K., and Der, C.J. (2001). Ras and Rho regulation of the cell cycle and oncogenesis. Cancer Lett *171*, 1-10.

Pugazhenthi, S., Boras, T., O'Connor, D., Meintzer, M.K., Heidenreich, K.A., and Reusch, J.E. (1999). Insulin-like growth factor I-mediated activation of the transcription factor cAMP response element-binding protein in PC12 cells. Involvement of p38 mitogen-activated protein kinase-mediated pathway. J Biol Chem *274*, 2829-2837.

Puigserver, P. (2005). Tissue-specific regulation of metabolic pathways through the transcriptional coactivator PGC1-alpha. Int J Obes (Lond) *29 Suppl 1*, S5-9.

Puigserver, P., Rhee, J., Donovan, J., Walkey, C.J., Yoon, J.C., Oriente, F., Kitamura, Y., Altomonte, J., Dong, H., Accili, D., *et al.* (2003). Insulin-regulated hepatic gluconeogenesis through FOXO1-PGC-1alpha interaction. Nature *423*, 550-555.

Punga, T., Bengoechea-Alonso, M.T., and Ericsson, J. (2006). Phosphorylation and ubiquitination of the transcription factor sterol regulatory element-binding protein-1 in response to DNA binding. J Biol Chem.

Radhakrishnan, A., Ikeda, Y., Kwon, H.J., Brown, M.S., and Goldstein, J.L. (2007). Sterol-regulated transport of SREBPs from endoplasmic reticulum to Golgi: Oxysterols block transport by binding to Insig. Proc Natl Acad Sci U S A *104*, 6511-6518.

Radimerski, T., Montagne, J., Hemmings-Mieszczak, M., and Thomas, G. (2002a). Lethality of Drosophila lacking TSC tumor suppressor function rescued by reducing dS6K signaling. Genes Dev *16*, 2627-2632.

Radimerski, T., Montagne, J., Rintelen, F., Stocker, H., van der Kaay, J., Downes, C.P., Hafen, E., and Thomas, G. (2002b). dS6K-regulated cell growth is dPKB/dPI(3)K-independent, but requires dPDK1. Nat Cell Biol *4*, 251-255.

Rashid, A., Pizer, E.S., Moga, M., Milgraum, L.Z., Zahurak, M., Pasternack, G.R., Kuhajda, F.P., and Hamilton, S.R. (1997). Elevated expression of fatty acid synthase and fatty acid synthetic activity in colorectal neoplasia. Am J Pathol *150*, 201-208.

Rawson, R.B. (2003). The SREBP pathway--insights from Insigs and insects. Nat Rev Mol Cell Biol *4*, 631-640.

Reiling, J.H., and Hafen, E. (2004). The hypoxia-induced paralogs Scylla and Charybdis inhibit growth by down-regulating S6K activity upstream of TSC in Drosophila. Genes Dev *18*, 2879-2892.

Repa, J.J., Berge, K.E., Pomajzl, C., Richardson, J.A., Hobbs, H., and Mangelsdorf, D.J. (2002). Regulation of ATP-binding cassette sterol transporters ABCG5 and ABCG8 by the liver X receptors alpha and beta. J Biol Chem *277*, 18793-18800.

Repa, J.J., Liang, G., Ou, J., Bashmakov, Y., Lobaccaro, J.M., Shimomura, I., Shan, B., Brown, M.S., Goldstein, J.L., and Mangelsdorf, D.J. (2000). Regulation of mouse sterol regulatory element-binding protein-1c gene (SREBP-1c) by oxysterol receptors, LXRalpha and LXRbeta. Genes Dev *14*, 2819-2830.

Repasky, G.A., Chenette, E.J., and Der, C.J. (2004). Renewing the conspiracy theory debate: does Raf function alone to mediate Ras oncogenesis? Trends Cell Biol *14*, 639-647.

Resh, M.D. (1999). Fatty acylation of proteins: new insights into membrane targeting of myristoylated and palmitoylated proteins. Biochim Biophys Acta *1451*, 1-16.

Ribaux, P.G., and Iynedjian, P.B. (2003). Analysis of the role of protein kinase B (cAKT) in insulin-dependent induction of glucokinase and sterol regulatory element-binding protein 1 (SREBP1) mRNAs in hepatocytes. Biochem J *376*, 697-705.

Rishi, V., Gal, J., Krylov, D., Fridriksson, J., Boysen, M.S., Mandrup, S., and Vinson, C. (2004). SREBP-1 dimerization specificity maps to both the helix-loop-helix and leucine zipper domains: use of a dominant negative. J Biol Chem *279*, 11863-11874.

Robey, R.B., and Hay, N. (2006). Mitochondrial hexokinases, novel mediators of the antiapoptotic effects of growth factors and Akt. Oncogene *25*, 4683-4696.

Rodriguez-Viciana, P., Warne, P.H., Dhand, R., Vanhaesebroeck, B., Gout, I., Fry, M.J., Waterfield, M.D., and Downward, J. (1994). Phosphatidylinositol-3-OH kinase as a direct target of Ras. Nature *370*, 527-532.

Romashkova, J.A., and Makarov, S.S. (1999). NF-kappaB is a target of AKT in anti-apoptotic PDGF signalling. Nature *401*, 86-90.

Roth, G., Kotzka, J., Kremer, L., Lehr, S., Lohaus, C., Meyer, H.E., Krone, W., and Muller-Wieland, D. (2000). MAP kinases Erk1/2 phosphorylate sterol regulatory element-binding protein (SREBP)-1a at serine 117 in vitro. J Biol Chem *275*, 33302-33307.

Roux, P.P., Ballif, B.A., Anjum, R., Gygi, S.P., and Blenis, J. (2004). Tumor-promoting phorbol esters and activated Ras inactivate the tuberous sclerosis tumor suppressor complex via p90 ribosomal S6 kinase. Proc Natl Acad Sci U S A *101*, 13489-13494.

Roy, S., Luetterforst, R., Harding, A., Apolloni, A., Etheridge, M., Stang, E., Rolls, B., Hancock, J.F., and Parton, R.G. (1999). Dominant-negative caveolin inhibits H-Ras function by disrupting cholesterol-rich plasma membrane domains. Nat Cell Biol *1*, 98-105.

Rozycka, M., Lu, Y.J., Brown, R.A., Lau, M.R., Shipley, J.M., and Fry, M.J. (1998). cDNA cloning of a third human C2-domain-containing class II phosphoinositide 3-kinase, PI3K-C2gamma, and chromosomal assignment of this gene (PIK3C2G) to 12p12. Genomics *54*, 569-574.

Rubin, G.M., and Spradling, A.C. (1982). Genetic transformation of Drosophila with transposable element vectors. Science *218*, 348-353.

Rubio, I., Wittig, U., Meyer, C., Heinze, R., Kadereit, D., Waldmann, H., Downward, J., and Wetzker, R. (1999). Farnesylation of Ras is important for the interaction with phosphoinositide 3-kinase gamma. European journal of biochemistry / FEBS *266*, 70-82.

Rudolph, H.K., Antebi, A., Fink, G.R., Buckley, C.M., Dorman, T.E., LeVitre, J., Davidow, L.S., Mao, J.I., and Moir, D.T. (1989). The yeast secretory pathway is perturbed by mutations in PMR1, a member of a Ca2+ ATPase family. Cell *58*, 133-145.

Rulifson, E.J., Kim, S.K., and Nusse, R. (2002). Ablation of insulin-producing neurons in flies: growth and diabetic phenotypes. Science *296*, 1118-1120.

Ruvinsky, I., and Meyuhas, O. (2006). Ribosomal protein S6 phosphorylation: from protein synthesis to cell size. Trends Biochem Sci *31*, 342-348.

Ruvinsky, I., Sharon, N., Lerer, T., Cohen, H., Stolovich-Rain, M., Nir, T., Dor, Y., Zisman, P., and Meyuhas, O. (2005). Ribosomal protein S6 phosphorylation is a determinant of cell size and glucose homeostasis. Genes Dev *19*, 2199-2211.

Ryder, S.P., Frater, L.A., Abramovitz, D.L., Goodwin, E.B., and Williamson, J.R. (2004). RNA target specificity of the STAR/GSG domain post-transcriptional regulatory protein GLD-1. Nat Struct Mol Biol *11*, 20-28.

Sakai, J., Nohturfft, A., Cheng, D., Ho, Y.K., Brown, M.S., and Goldstein, J.L. (1997). Identification of complexes between the COOH-terminal domains of sterol regulatory element-binding proteins (SREBPs) and SREBP cleavage-activating protein. J Biol Chem *272*, 20213-20221.

Saltiel, A.R., and Kahn, C.R. (2001). Insulin signalling and the regulation of glucose and lipid metabolism. Nature *414*, 799-806.

Sancak, Y., Thoreen, C.C., Peterson, T.R., Lindquist, R.A., Kang, S.A., Spooner, E., Carr, S.A., and Sabatini, D.M. (2007). PRAS40 Is an Insulin-Regulated Inhibitor of the mTORC1 Protein Kinase. Mol Cell *25*, 903-915.

Sanchez-Cespedes, M., Parrella, P., Esteller, M., Nomoto, S., Trink, B., Engles, J.M., Westra, W.H., Herman, J.G., and Sidransky, D. (2002). Inactivation of LKB1/STK11 is a common event in adenocarcinomas of the lung. Cancer Res *62*, 3659-3662.

Sarbassov, D.D., Guertin, D.A., Ali, S.M., and Sabatini, D.M. (2005). Phosphorylation and regulation of Akt/PKB by the rictor-mTOR complex. Science *307*, 1098-1101.

Sarbassov dos, D., Ali, S.M., Sengupta, S., Sheen, J.H., Hsu, P.P., Bagley, A.F., Markhard, A.L., and Sabatini, D.M. (2006). Prolonged rapamycin treatment inhibits mTORC2 assembly and Akt/PKB. Mol Cell *22*, 159-168.

Sasaoka, T., Langlois, W.J., Leitner, J.W., Draznin, B., and Olefsky, J.M. (1994). The signaling pathway coupling epidermal growth factor receptors to activation of p21ras. J Biol Chem *269*, 32621-32625.

Sato, R., Inoue, J., Kawabe, Y., Kodama, T., Takano, T., and Maeda, M. (1996). Sterol-dependent transcriptional regulation of sterol regulatory element-binding protein-2. J Biol Chem *271*, 26461-26464.

Sato, R., Yang, J., Wang, X., Evans, M.J., Ho, Y.K., Goldstein, J.L., and Brown, M.S. (1994). Assignment of the membrane attachment, DNA binding, and transcriptional activation domains of sterol regulatory element-binding protein-1 (SREBP-1). J Biol Chem *269*, 17267-17273.

Schalm, S.S., Fingar, D.C., Sabatini, D.M., and Blenis, J. (2003). TOS motif-mediated raptor binding regulates 4E-BP1 multisite phosphorylation and function. Curr Biol *13*, 797-806.

Scheffzek, K., Ahmadian, M.R., Kabsch, W., Wiesmuller, L., Lautwein, A., Schmitz, F., and Wittinghofer, A. (1997). The Ras-RasGAP complex: structural basis for GTPase activation and its loss in oncogenic Ras mutants. Science *277*, 333-338.

Schmelzle, T., Beck, T., Martin, D.E., and Hall, M.N. (2004). Activation of the RAS/cyclic AMP pathway suppresses a TOR deficiency in yeast. Mol Cell Biol *24*, 338-351.

Schmidt, M., Fernandez de Mattos, S., van der Horst, A., Klompmaker, R., Kops, G.J., Lam, E.W., Burgering, B.M., and Medema, R.H. (2002). Cell cycle inhibition by FoxO forkhead transcription factors involves downregulation of cyclin D. Mol Cell Biol *22*, 7842-7852.

Schubbert, S., Shannon, K., and Bollag, G. (2007). Hyperactive Ras in developmental disorders and cancer. Nat Rev Cancer *7*, 295-308.

Schultz, J.R., Tu, H., Luk, A., Repa, J.J., Medina, J.C., Li, L., Schwendner, S., Wang, S., Thoolen, M., Mangelsdorf, D.J., *et al.* (2000). Role of LXRs in control of lipogenesis. Genes Dev *14*, 2831-2838.

Sebti, S.M. (2003). Blocked pathways: FTIs shut down oncogene signals. Oncologist *8 Suppl 3*, 30-38.

Seegmiller, A.C., Dobrosotskaya, I., Goldstein, J.L., Ho, Y.K., Brown, M.S., and Rawson, R.B. (2002). The SREBP pathway in Drosophila: regulation by palmitate, not sterols. Dev Cell *2*, 229-238.

Sekimoto, T., Fukumoto, M., and Yoneda, Y. (2004). 14-3-3 suppresses the nuclear localization of threonine 157-phosphorylated p27(Kip1). Embo J *23*, 1934-1942.

Semenza, G.L., Jiang, B.H., Leung, S.W., Passantino, R., Concordet, J.P., Maire, P., and Giallongo, A. (1996). Hypoxia response elements in the aldolase A, enolase 1, and lactate dehydrogenase A gene promoters contain essential binding sites for hypoxia-inducible factor 1. J Biol Chem *271*, 32529-32537.

Shaw, R.J., and Cantley, L.C. (2006). Ras, PI(3)K and mTOR signalling controls tumour cell growth. Nature *441*, 424-430.

Shayesteh, L., Lu, Y., Kuo, W.L., Baldocchi, R., Godfrey, T., Collins, C., Pinkel, D., Powell, B., Mills, G.B., and Gray, J.W. (1999). PIK3CA is implicated as an oncogene in ovarian cancer. Nat Genet *21*, 99-102.

Shimano, H., Horton, J.D., Hammer, R.E., Shimomura, I., Brown, M.S., and Goldstein, J.L. (1996). Overproduction of cholesterol and fatty acids causes massive liver enlargement in transgenic mice expressing truncated SREBP-1a. J Clin Invest *98*, 1575-1584.

Shimano, H., Horton, J.D., Shimomura, I., Hammer, R.E., Brown, M.S., and Goldstein, J.L. (1997a). Isoform 1c of sterol regulatory element binding protein is less active than isoform 1a in livers of transgenic mice and in cultured cells. J Clin Invest *99*, 846-854.

Shimano, H., Shimomura, I., Hammer, R.E., Herz, J., Goldstein, J.L., Brown, M.S., and Horton, J.D. (1997b). Elevated levels of SREBP-2 and cholesterol synthesis in livers of mice homozygous for a targeted disruption of the SREBP-1 gene. J Clin Invest *100*, 2115-2124.

Shimomura, I., Bashmakov, Y., Shimano, H., Horton, J.D., Goldstein, J.L., and Brown, M.S. (1997a). Cholesterol feeding reduces nuclear forms of sterol regulatory element binding proteins in hamster liver. Proc Natl Acad Sci U S A *94*, 12354-12359.

Shimomura, I., Hammer, R.E., Ikemoto, S., Brown, M.S., and Goldstein, J.L. (1999). Leptin reverses insulin resistance and diabetes mellitus in mice with congenital lipodystrophy. Nature *401*, 73-76.

Shimomura, I., Shimano, H., Horton, J.D., Goldstein, J.L., and Brown, M.S. (1997b). Differential expression of exons 1a and 1c in mRNAs for sterol regulatory element binding protein-1 in human and mouse organs and cultured cells. J Clin Invest *99*, 838-845.

Shin, I., Yakes, F.M., Rojo, F., Shin, N.Y., Bakin, A.V., Baselga, J., and Arteaga, C.L. (2002). PKB/Akt mediates cell-cycle progression by phosphorylation of p27(Kip1) at threonine 157 and modulation of its cellular localization. Nat Med *8*, 1145-1152.

Shingleton, A.W., Das, J., Vinicius, L., and Stern, D.L. (2005). The temporal requirements for insulin signaling during development in Drosophila. PLoS Biol *3*, e289.

Shioi, T., McMullen, J.R., Kang, P.M., Douglas, P.S., Obata, T., Franke, T.F., Cantley, L.C., and Izumo, S. (2002). Akt/protein kinase B promotes organ growth in transgenic mice. Mol Cell Biol *22*, 2799-2809.

Shiota, C., Woo, J.T., Lindner, J., Shelton, K.D., and Magnuson, M.A. (2006). Multiallelic disruption of the rictor gene in mice reveals that mTOR complex 2 is essential for fetal growth and viability. Dev Cell *11*, 583-589.

Shoshani, T., Faerman, A., Mett, I., Zelin, E., Tenne, T., Gorodin, S., Moshel, Y., Elbaz, S., Budanov, A., Chajut, A., *et al.* (2002). Identification of a novel hypoxia-inducible factor 1-responsive gene, RTP801, involved in apoptosis. Mol Cell Biol *22*, 2283-2293.

Simons, K., and Ikonen, E. (2000). How cells handle cholesterol. Science *290*, 1721-1726.

Simons, K., and Vaz, W.L. (2004). Model systems, lipid rafts, and cell membranes. Annu Rev Biophys Biomol Struct *33*, 269-295.

Simonsen, A., Wurmser, A.E., Emr, S.D., and Stenmark, H. (2001). The role of phosphoinositides in membrane transport. Curr Opin Cell Biol *13*, 485-492.

Smith, E.M., Finn, S.G., Tee, A.R., Browne, G.J., and Proud, C.G. (2005). The tuberous sclerosis protein TSC2 is not required for the regulation of the mammalian target of rapamycin by amino acids and certain cellular stresses. J Biol Chem *280*, 18717-18727.

Sofer, A., Lei, K., Johannessen, C.M., and Ellisen, L.W. (2005). Regulation of mTOR and cell growth in response to energy stress by REDD1. Mol Cell Biol *25*, 5834-5845.

Sonoda, Y., Matsumoto, Y., Funakoshi, M., Yamamoto, D., Hanks, S.K., and Kasahara, T. (2000). Anti-apoptotic role of focal adhesion kinase (FAK). Induction of inhibitor-of-apoptosis proteins and apoptosis suppression by the overexpression of FAK in a human leukemic cell line, HL-60. J Biol Chem *275*, 16309-16315.

Souto, R.P., Vallega, G., Wharton, J., Vinten, J., Tranum-Jensen, J., and Pilch, P.F. (2003). Immunopurification and characterization of rat adipocyte caveolae suggest their dissociation from insulin signaling. J Biol Chem *278*, 18321-18329.

Staal, S.P. (1987). Molecular cloning of the akt oncogene and its human homologues AKT1 and AKT2: amplification of AKT1 in a primary human gastric adenocarcinoma. Proc Natl Acad Sci U S A *84*, 5034-5037.

Stambolic, V., Suzuki, A., de la Pompa, J.L., Brothers, G.M., Mirtsos, C., Sasaki, T., Ruland, J., Penninger, J.M., Siderovski, D.P., and Mak, T.W. (1998). Negative regulation of PKB/Akt-dependent cell survival by the tumor suppressor PTEN. Cell *95*, 29-39.

Standaert, M.L., Bandyopadhyay, G., Kanoh, Y., Sajan, M.P., and Farese, R.V. (2001). Insulin and PIP3 activate PKC-zeta by mechanisms that are both dependent and independent of phosphorylation of activation loop (T410) and autophosphorylation (T560) sites. Biochemistry *40*, 249-255.

Steffensen, K.R., and Gustafsson, J.A. (2004). Putative metabolic effects of the liver X receptor (LXR). Diabetes *53 Suppl 1*, S36-42.

Stein, R.C. (2001). Prospects for phosphoinositide 3-kinase inhibition as a cancer treatment. Endocr Relat Cancer *8*, 237-248.

Stephens, L., Anderson, K., Stokoe, D., Erdjument-Bromage, H., Painter, G.F., Holmes, A.B., Gaffney, P.R., Reese, C.B., McCormick, F., Tempst, P., *et al.* (1998). Protein kinase B kinases that mediate phosphatidylinositol 3,4,5-trisphosphate-dependent activation of protein kinase B. Science *279*, 710-714.

Stocker, H., and Hafen, E. (2000). Genetic control of cell size. Curr Opin Genet Dev *10*, 529-535.

Stocker, H., Radimerski, T., Schindelholz, B., Wittwer, F., Belawat, P., Daram, P., Breuer, S., Thomas, G., and Hafen, E. (2003). Rheb is an essential regulator of S6K in controlling cell growth in Drosophila. Nat Cell Biol *5*, 559-565.

Suire, S., Coadwell, J., Ferguson, G.J., Davidson, K., Hawkins, P., and Stephens, L. (2005). p84, a new Gbetagamma-activated regulatory subunit of the type IB phosphoinositide 3-kinase p110gamma. Curr Biol *15*, 566-570.

Suire, S., Hawkins, P., and Stephens, L. (2002). Activation of phosphoinositide 3-kinase gamma by Ras. Curr Biol *12*, 1068-1075.

Sul, H.S., Latasa, M.J., Moon, Y., and Kim, K.H. (2000). Regulation of the fatty acid synthase promoter by insulin. J Nutr *130*, 315S-320S.

Sun, L.P., Li, L., Goldstein, J.L., and Brown, M.S. (2005). Insig required for sterol-mediated inhibition of Scap/SREBP binding to COPII proteins in vitro. J Biol Chem *280*, 26483-26490.

Sun, L.P., Seemann, J., Goldstein, J.L., and Brown, M.S. (2007). Sterol-regulated transport of SREBPs from endoplasmic reticulum to Golgi: Insig renders sorting signal in Scap inaccessible to COPII proteins. Proc Natl Acad Sci U S A *104*, 6519-6526.

Sun, M., Wang, G., Paciga, J.E., Feldman, R.I., Yuan, Z.Q., Ma, X.L., Shelley, S.A., Jove, R., Tsichlis, P.N., Nicosia, S.V., *et al.* (2001). AKT1/PKBalpha kinase is frequently elevated in human cancers and its constitutive activation is required for oncogenic transformation in NIH3T3 cells. Am J Pathol *159*, 431-437.

Sundqvist, A., Bengoechea-Alonso, M.T., Ye, X., Lukiyanchuk, V., Jin, J., Harper, J.W., and Ericsson, J. (2005). Control of lipid metabolism by phosphorylation-dependent degradation of the SREBP family of transcription factors by SCF(Fbw7). Cell Metab *1*, 379-391.

Sweeney, G., Somwar, R., Ramlal, T., Volchuk, A., Ueyama, A., and Klip, A. (1999). An inhibitor of p38 mitogen-activated protein kinase prevents insulin-stimulated glucose transport but not glucose transporter translocation in 3T3-L1 adipocytes and L6 myotubes. J Biol Chem *274*, 10071-10078.

Swinnen, J.V., Brusselmans, K., and Verhoeven, G. (2006). Increased lipogenesis in cancer cells: new players, novel targets. Curr Opin Clin Nutr Metab Care *9*, 358-365.

Swinnen, J.V., Heemers, H., de Sande, T.V., De Schrijver, E., Brusselmans, K., Heyns, W., and Verhoeven, G. (2004). Androgens, lipogenesis and prostate cancer. J Steroid Biochem Mol Biol *92*, 273-279.

Swinnen, J.V., Heemers, H., Deboel, L., Foufelle, F., Heyns, W., and Verhoeven, G. (2000). Stimulation of tumor-associated fatty acid synthase expression by growth factor activation of the sterol regulatory element-binding protein pathway. Oncogene *19*, 5173-5181.

Swinnen, J.V., Roskams, T., Joniau, S., Van Poppel, H., Oyen, R., Baert, L., Heyns, W., and Verhoeven, G. (2002). Overexpression of fatty acid synthase is an early and common event in the development of prostate cancer. Int J Cancer *98*, 19-22.

Sze, D.Y., and Jardetzky, O. (1990). Characterization of lipid composition in stimulated human lymphocytes by 1H-NMR. Biochim Biophys Acta *1054*, 198-206.

Takai, Y., Sasaki, T., and Matozaki, T. (2001). Small GTP-binding proteins. Physiol Rev *81*, 153-208.

Takaishi, H., Konishi, H., Matsuzaki, H., Ono, Y., Shirai, Y., Saito, N., Kitamura, T., Ogawa, W., Kasuga, M., Kikkawa, U., *et al.* (1999). Regulation of nuclear translocation of forkhead transcription factor AFX by protein kinase B. Proc Natl Acad Sci U S A *96*, 11836-11841.

Tamura, M., Gu, J., Matsumoto, K., Aota, S., Parsons, R., and Yamada, K.M. (1998). Inhibition of cell migration, spreading, and focal adhesions by tumor suppressor PTEN. Science *280*, 1614-1617.

Taniguchi, C.M., Kondo, T., Sajan, M., Luo, J., Bronson, R., Asano, T., Farese, R., Cantley, L.C., and Kahn, C.R. (2006). Divergent regulation of hepatic glucose and lipid metabolism by phosphoinositide 3-kinase via Akt and PKClambda/zeta. Cell Metab *3*, 343-353.

Tapon, N., Ito, N., Dickson, B.J., Treisman, J.E., and Hariharan, I.K. (2001). The Drosophila tuberous sclerosis complex gene homologs restrict cell growth and cell proliferation. Cell *105*, 345-355.

Tarling, E., Salter, A., and Bennett, A. (2004). Transcriptional regulation of human SREBP-1c (sterol-regulatory-element-binding protein-1c): a key regulator of lipogenesis. Biochem Soc Trans *32*, 107-109.

Tee, A.R., and Blenis, J. (2005). mTOR, translational control and human disease. Semin Cell Dev Biol *16*, 29-37.

Tee, A.R., Tee, J.A., and Blenis, J. (2004). Characterizing the interaction of the mammalian eIF4E-related protein 4EHP with 4E-BP1. FEBS Lett *564*, 58-62.

Teleman, A.A., Chen, Y.W., and Cohen, S.M. (2005). Drosophila Melted modulates FOXO and TOR activity. Dev Cell *9*, 271-281.

Theopold, U., Ekengren, S., and Hultmark, D. (1996). HLH106, a Drosophila transcription factor with similarity to the vertebrate sterol responsive element binding protein. Proc Natl Acad Sci U S A *93*, 1195-1199.

Thong, F.S., Dugani, C.B., and Klip, A. (2005). Turning signals on and off: GLUT4 traffic in the insulin-signaling highway. Physiology (Bethesda) *20*, 271-284.

Todd, B.L., Stewart, E.V., Burg, J.S., Hughes, A.L., and Espenshade, P.J. (2006). Sterol regulatory element binding protein is a principal regulator of anaerobic gene expression in fission yeast. Mol Cell Biol *26*, 2817-2831.

Toth, J.I., Datta, S., Athanikar, J.N., Freedman, L.P., and Osborne, T.F. (2004). Selective coactivator interactions in gene activation by SREBP-1a and -1c. Mol Cell Biol *24*, 8288-8300.

Tran, H., Brunet, A., Griffith, E.C., and Greenberg, M.E. (2003). The many forks in FOXO's road. Sci STKE *2003*, RE5.

Treisman, R. (1996). Regulation of transcription by MAP kinase cascades. Curr Opin Cell Biol *8*, 205-215.

Trotman, L.C., Niki, M., Dotan, Z.A., Koutcher, J.A., Di Cristofano, A., Xiao, A., Khoo, A.S., Roy-Burman, P., Greenberg, N.M., Van Dyke, T., *et al.* (2003). Pten dose dictates cancer progression in the prostate. PLoS Biol *1*, E59.

Turyn, J., Schlichtholz, B., Dettlaff-Pokora, A., Presler, M., Goyke, E., Matuszewski, M., Kmiec, Z., Krajka, K., and Swierczynski, J. (2003). Increased activity of glycerol 3-phosphate dehydrogenase and other lipogenic enzymes in human bladder cancer. Horm Metab Res *35*, 565-569.

Tzatsos, A., and Tsichlis, P.N. (2007). Energy depletion inhibits phosphatidylinositol 3-kinase/Akt signaling and induces apoptosis via AMP-activated protein kinase-dependent phosphorylation of IRS-1 at Ser794. J Biol Chem.

Um, S.H., Frigerio, F., Watanabe, M., Picard, F., Joaquin, M., Sticker, M., Fumagalli, S., Allegrini, P.R., Kozma, S.C., Auwerx, J., *et al.* (2004). Absence of S6K1 protects against age- and diet-induced obesity while enhancing insulin sensitivity. Nature *431*, 200-205.

van der Horst, A., and Burgering, B.M. (2007). Stressing the role of FoxO proteins in lifespan and disease. Nat Rev Mol Cell Biol *8*, 440-450.

Van Haastert, P.J., and Devreotes, P.N. (2004). Chemotaxis: signalling the way forward. Nat Rev Mol Cell Biol *5*, 626-634.

Vander Haar, E., Lee, S.I., Bandhakavi, S., Griffin, T.J., and Kim, D.H. (2007). Insulin signalling to mTOR mediated by the Akt/PKB substrate PRAS40. Nat Cell Biol *9*, 316-323.

Vanhaesebroeck, B., and Alessi, D.R. (2000). The PI3K-PDK1 connection: more than just a road to PKB. Biochem J *346 Pt 3*, 561-576.

Verdu, J., Buratovich, M.A., Wilder, E.L., and Birnbaum, M.J. (1999). Cell-autonomous regulation of cell and organ growth in Drosophila by Akt/PKB. Nat Cell Biol *1*, 500-506.

Vereshchagina, N., and Wilson, C. (2006). Cytoplasmic activated protein kinase Akt regulates lipid-droplet accumulation in Drosophila nurse cells. Development *133*, 4731-4735.

Villunger, A., Michalak, E.M., Coultas, L., Mullauer, F., Bock, G., Ausserlechner, M.J., Adams, J.M., and Strasser, A. (2003). p53- and drug-induced apoptotic responses mediated by BH3-only proteins puma and noxa. Science *302*, 1036-1038.

Vivanco, I., and Sawyers, C.L. (2002). The phosphatidylinositol 3-Kinase AKT pathway in human cancer. Nat Rev Cancer *2*, 489-501.

Voigt, P., Dorner, M.B., and Schaefer, M. (2006). Characterization of p87PIKAP, a novel regulatory subunit of phosphoinositide 3-kinase gamma that is highly expressed in heart and interacts with PDE3B. J Biol Chem *281*, 9977-9986.

Wang, C.Y., Guttridge, D.C., Mayo, M.W., and Baldwin, A.S., Jr. (1999). NF-kappaB induces expression of the Bcl-2 homologue A1/Bfl-1 to preferentially suppress chemotherapy-induced apoptosis. Mol Cell Biol *19*, 5923-5929.

Wang, C.Y., Mayo, M.W., Korneluk, R.G., Goeddel, D.V., and Baldwin, A.S., Jr. (1998). NF-kappaB antiapoptosis: induction of TRAF1 and TRAF2 and c-IAP1 and c-IAP2 to suppress caspase-8 activation. Science *281*, 1680-1683.

Wang, D., and Sul, H.S. (1998). Insulin stimulation of the fatty acid synthase promoter is mediated by the phosphatidylinositol 3-kinase pathway. Involvement of protein kinase B/Akt. J Biol Chem *273*, 25420-25426.

Wang, H., Maechler, P., Antinozzi, P.A., Herrero, L., Hagenfeldt-Johansson, K.A., Bjorklund, A., and Wollheim, C.B. (2003). The Transcription Factor SREBP-1c Is Instrumental in the Development of beta -Cell Dysfunction. J Biol Chem *278*, 16622-16629.

Wang, H.Q., Altomare, D.A., Skele, K.L., Poulikakos, P.I., Kuhajda, F.P., Di Cristofano, A., and Testa, J.R. (2005). Positive feedback regulation between AKT activation and fatty acid synthase expression in ovarian carcinoma cells. Oncogene *24*, 3574-3582.

Wang, L., Rhodes, C.J., and Lawrence, J.C., Jr. (2006). Activation of mammalian target of rapamycin (mTOR) by insulin is associated with stimulation of 4EBP1 binding to dimeric mTOR complex 1. J Biol Chem *281*, 24293-24303.

Wang, X., Sato, R., Brown, M.S., Hua, X., and Goldstein, J.L. (1994). SREBP-1, a membrane-bound transcription factor released by sterol-regulated proteolysis. Cell *77*, 53-62.

Warburg, O. (1956). On the origin of cancer cells. Science *123*, 309-314.

Waugh, M.G., Lawson, D., and Hsuan, J.J. (1999). Epidermal growth factor receptor activation is localized within low-buoyant density, non-caveolar membrane domains. Biochem J *337 (Pt 3)*, 591-597.

Weber, W.A., and Wieder, H. (2006). Monitoring chemotherapy and radiotherapy of solid tumors. Eur J Nucl Med Mol Imaging *33 Suppl 1*, 27-37.

Wei, W., Jin, J., Schlisio, S., Harper, J.W., and Kaelin, W.G., Jr. (2005). The v-Jun point mutation allows c-Jun to escape GSK3-dependent recognition and destruction by the Fbw7 ubiquitin ligase. Cancer Cell *8*, 25-33.

Weinkove, D., and Leevers, S.J. (2000). The genetic control of organ growth: insights from Drosophila. Curr Opin Genet Dev *10*, 75-80.

Weinkove, D., Neufeld, T.P., Twardzik, T., Waterfield, M.D., and Leevers, S.J. (1999). Regulation of imaginal disc cell size, cell number and organ size by Drosophila class I(A) phosphoinositide 3-kinase and its adaptor. Curr Biol *9*, 1019-1029.

Weiss, L., Hoffmann, G.E., Schreiber, R., Andres, H., Fuchs, E., Korber, E., and Kolb, H.J. (1986). Fatty-acid biosynthesis in man, a pathway of minor importance. Purification, optimal assay conditions, and organ distribution of fatty-acid synthase. Biol Chem Hoppe Seyler *367*, 905-912.

Welch, H., Eguinoa, A., Stephens, L.R., and Hawkins, P.T. (1998). Protein kinase B and rac are activated in parallel within a phosphatidylinositide 3OH-kinase-controlled signaling pathway. J Biol Chem *273*, 11248-11256.

Welch, H.C., Coadwell, W.J., Ellson, C.D., Ferguson, G.J., Andrews, S.R., Erdjument-Bromage, H., Tempst, P., Hawkins, P.T., and Stephens, L.R. (2002). P-Rex1, a PtdIns(3,4,5)P3- and Gbetagamma-regulated guanine-nucleotide exchange factor for Rac. Cell *108*, 809-821.

Welsh, G.I., Hers, I., Berwick, D.C., Dell, G., Wherlock, M., Birkin, R., Leney, S., and Tavare, J.M. (2005). Role of protein kinase B in insulin-regulated glucose uptake. Biochem Soc Trans *33*, 346-349.

Wienecke, R., Maize, J.C., Jr., Shoarinejad, F., Vass, W.C., Reed, J., Bonifacino, J.S., Resau, J.H., de Gunzburg, J., Yeung, R.S., and DeClue, J.E. (1996). Co-localization of the TSC2 product tuberin with its target Rap1 in the Golgi apparatus. Oncogene *13*, 913-923.

Williams, M.R., Arthur, J.S., Balendran, A., van der Kaay, J., Poli, V., Cohen, P., and Alessi, D.R. (2000). The role of 3-phosphoinositide-dependent protein kinase 1 in activating AGC kinases defined in embryonic stem cells. Curr Biol *10*, 439-448.

Wolfrum, C., Asilmaz, E., Luca, E., Friedman, J.M., and Stoffel, M. (2004). Foxa2 regulates lipid metabolism and ketogenesis in the liver during fasting and in diabetes. Nature *432*, 1027-1032.

Woodgett, J.R. (2005). Recent advances in the protein kinase B signaling pathway. Curr Opin Cell Biol *17*, 150-157.

Woods, A., Johnstone, S.R., Dickerson, K., Leiper, F.C., Fryer, L.G., Neumann, D., Schlattner, U., Wallimann, T., Carlson, M., and Carling, D. (2003). LKB1 is the upstream kinase in the AMP-activated protein kinase cascade. Curr Biol *13*, 2004-2008.

Wu, X., Senechal, K., Neshat, M.S., Whang, Y.E., and Sawyers, C.L. (1998). The PTEN/MMAC1 tumor suppressor phosphatase functions as a negative regulator of the phosphoinositide 3-kinase/Akt pathway. Proc Natl Acad Sci U S A *95*, 15587-15591.

Wullschleger, S., Loewith, R., and Hall, M.N. (2006). TOR signaling in growth and metabolism. Cell *124*, 471-484.

Wullschleger, S., Loewith, R., Oppliger, W., and Hall, M.N. (2005). Molecular organization of target of rapamycin complex 2. J Biol Chem *280*, 30697-30704.

Xiang, X., Saha, A.K., Wen, R., Ruderman, N.B., and Luo, Z. (2004). AMP-activated protein kinase activators can inhibit the growth of prostate cancer cells by multiple mechanisms. Biochem Biophys Res Commun *321*, 161-167.

Yabe, D., Komuro, R., Liang, G., Goldstein, J.L., and Brown, M.S. (2003). Liver-specific mRNA for Insig-2 down-regulated by insulin: implications for fatty acid synthesis. Proc Natl Acad Sci U S A *100*, 3155-3160.

Yabe, D., Xia, Z.P., Adams, C.M., and Rawson, R.B. (2002). Three mutations in sterol-sensing domain of SCAP block interaction with insig and render SREBP cleavage insensitive to sterols. Proc Natl Acad Sci U S A *99*, 16672-16677.

Yahagi, N., Shimano, H., Hasegawa, K., Ohashi, K., Matsuzaka, T., Najima, Y., Sekiya, M., Tomita, S., Okazaki, H., Tamura, Y., *et al.* (2005). Co-ordinate activation of lipogenic enzymes in hepatocellular carcinoma. Eur J Cancer *41*, 1316-1322.

Yang, C., McDonald, J.G., Patel, A., Zhang, Y., Umetani, M., Xu, F., Westover, E.J., Covey, D.F., Mangelsdorf, D.J., Cohen, J.C., *et al.* (2006a). Sterol intermediates from cholesterol biosynthetic pathway as liver X receptor ligands. J Biol Chem *281*, 27816-27826.

Yang, F., Vought, B.W., Satterlee, J.S., Walker, A.K., Jim Sun, Z.Y., Watts, J.L., Debeaumont, R., Mako Saito, R., Hyberts, S.G., Yang, S., *et al.* (2006b). An ARC/Mediator subunit required for SREBP control of cholesterol and lipid homeostasis. Nature.

Yang, T., Espenshade, P.J., Wright, M.E., Yabe, D., Gong, Y., Aebersold, R., Goldstein, J.L., and Brown, M.S. (2002a). Crucial step in cholesterol homeostasis: sterols promote binding of SCAP to INSIG-1, a membrane protein that facilitates retention of SREBPs in ER. Cell *110*, 489-500.

Yang, Y.A., Han, W.F., Morin, P.J., Chrest, F.J., and Pizer, E.S. (2002b). Activation of fatty acid synthesis during neoplastic transformation: role of mitogen-activated protein kinase and phosphatidylinositol 3-kinase. Experimental cell research *279*, 80-90.

Yang, Y.A., Morin, P.J., Han, W.F., Chen, T., Bornman, D.M., Gabrielson, E.W., and Pizer, E.S. (2003). Regulation of fatty acid synthase expression in breast cancer by sterol regulatory element binding protein-1c. Experimental cell research *282*, 132-137.

Yeh, E., Cunningham, M., Arnold, H., Chasse, D., Monteith, T., Ivaldi, G., Hahn, W.C., Stukenberg, P.T., Shenolikar, S., Uchida, T., *et al.* (2004). A signalling pathway controlling c-Myc degradation that impacts oncogenic transformation of human cells. Nat Cell Biol *6*, 308-318.

Yellaturu, C.R., Deng, X., Cagen, L.M., Wilcox, H.G., Park, E.A., Raghow, R., and Elam, M.B. (2005). Posttranslational processing of SREBP-1 in rat hepatocytes is regulated by insulin and cAMP. Biochem Biophys Res Commun *332*, 174-180.

Yokoyama, C., Wang, X., Briggs, M.R., Admon, A., Wu, J., Hua, X., Goldstein, J.L., and Brown, M.S. (1993). SREBP-1, a basic-helix-loop-helix-leucine zipper protein that controls transcription of the low density lipoprotein receptor gene. Cell *75*, 187-197.

Yoon, S., Lee, M.Y., Park, S.W., Moon, J.S., Koh, Y.K., Ahn, Y.H., Park, B.W., and Kim, K.S. (2007). Up-regulation of Acetyl-CoA Carboxylase {alpha} and Fatty Acid Synthase by Human Epidermal Growth Factor Receptor 2 at the Translational Level in Breast Cancer Cells. J Biol Chem *282*, 26122-26131.

Yoshikawa, T., Shimano, H., Yahagi, N., Ide, T., Amemiya-Kudo, M., Matsuzaka, T., Nakakuki, M., Tomita, S., Okazaki, H., Tamura, Y., *et al.* (2002). Polyunsaturated fatty acids suppress sterol regulatory element-binding protein 1c promoter activity by inhibition of liver X receptor (LXR) binding to LXR response elements. J Biol Chem *277*, 1705-1711.

Yu, J., Zhang, Y., McIlroy, J., Rordorf-Nikolic, T., Orr, G.A., and Backer, J.M. (1998). Regulation of the p85/p110 phosphatidylinositol 3'-kinase: stabilization and inhibition of the p110alpha catalytic subunit by the p85 regulatory subunit. Mol Cell Biol *18*, 1379-1387.

Zhang, C., Shin, D.J., and Osborne, T.F. (2005). A simple promoter containing two Sp1 sites controls the expression of sterol-regulatory-element-binding protein 1a (SREBP-1a). Biochem J *386*, 161-168.

Zhang, H., Stallock, J.P., Ng, J.C., Reinhard, C., and Neufeld, T.P. (2000). Regulation of cellular growth by the Drosophila target of rapamycin dTOR. Genes Dev *14*, 2712-2724.

Zhang, X., Shu, L., Hosoi, H., Murti, K.G., and Houghton, P.J. (2002). Predominant nuclear localization of mammalian target of rapamycin in normal and malignant cells in culture. J Biol Chem *277*, 28127-28134.

Zhang, Y., Billington, C.J., Jr., Pan, D., and Neufeld, T.P. (2006). Drosophila target of rapamycin kinase functions as a multimer. Genetics *172*, 355-362.

Zhou, B.P., Liao, Y., Xia, W., Spohn, B., Lee, M.H., and Hung, M.C. (2001a). Cytoplasmic localization of p21Cip1/WAF1 by Akt-induced phosphorylation in HER-2/neu-overexpressing cells. Nat Cell Biol *3*, 245-252.

Zhou, B.P., Liao, Y., Xia, W., Zou, Y., Spohn, B., and Hung, M.C. (2001b). HER-2/neu induces p53 ubiquitination via Akt-mediated MDM2 phosphorylation. Nat Cell Biol *3*, 973-982.

Zhou, G., Myers, R., Li, Y., Chen, Y., Shen, X., Fenyk-Melody, J., Wu, M., Ventre, J., Doebber, T., Fujii, N., *et al.* (2001c). Role of AMP-activated protein kinase in mechanism of metformin action. J Clin Invest *108*, 1167-1174.

Zhuang, L., Lin, J., Lu, M.L., Solomon, K.R., and Freeman, M.R. (2002). Cholesterol-rich lipid rafts mediate akt-regulated survival in prostate cancer cells. Cancer Res *62*, 2227-2231.

Zimmermann, S., and Moelling, K. (1999). Phosphorylation and regulation of Raf by Akt (protein kinase B). Science *286*, 1741-1744.